Neural Encoding of Local vs. Global Space:

From Structure to Function

Han Yin Cheng

Institute of Behavioural Neuroscience, UCL

supervised by

Professor Kate Jeffery

Submitted in partial fulfilment of the requirements

for the degree of Doctor of Philosophy in Neuroscience at

University College London

September 2020

Declaration

I, Han Yin Cheng, confirm that the work presented in this thesis is my own. Where information has been derived from other sources, I confirm that this has been indicated in the thesis.

_____

Han Yin Cheng

September 2020

Acknowledgements

The work done in this thesis is not possible without the supports of many people whom I am eternally grateful for. First and foremost, I am most grateful to Kate Jeffery who has provided me with unparalleled support over the years. Thanks for the guidance over the years, for stopping me when you feel that I have gone down a rabbit hole too deep, for all the opportunities you have given me in presenting my work to the external world and for being there to listen when I had problems in my life. Your insight, discussions and patience have definitely shaped me as a scientist, and I hope to do you proud one day.

To the IBN in general: Thank you for being my home away from home. I cannot emphasize how happy I am to have the opportunity to work in a place where people are friendly, helpful and supportive. Thanks for the experiences: good or bad. Special thanks to James Street who had gone through this journey with me: I will miss those evenings where we scribbled down analysis and hypotheses on paper towels and had extremely intense discussions about science. To Marta, Stefano, Jo and Karolina: Thanks for keeping me sane during the pandemic lockdown. It has been an extremely stressful period and I would not have tide through it without you all. To Zita and Will: Thanks for the best two (?) years of my life. I will never have enough gratitude to show for the positive impacts you have brought to my life. To Gioia: I will never forget the moment when you asked me to grab a drink with you. It is because of you that I felt integrated into the social IBN. And to Kate's lab – past and present: Thanks for all the guidance and advice. Kate's lab will always hold a special place in my heart.

Last but not least, to Rini: Even though we are far apart, you have provided me with far more emotional support than you know. To Miranda: we have had our difficult moments, but I cannot imagine any other person I would stick London out with. To Jonny: You have been a great friend for the past few years, and thanks for always dishing out solid scientific advice. To my family, especially my dad: This thesis is truly for you. I would not be who I am or where I am without you, and I am thankful every day for having the most supportive dad ever. I have always regretted that you had to sacrifice your own dreams when you had us, but I hope I have made you proud. And to my rats: this thesis would not have been possible without each and every one of you.

Abstract

The retrosplenial cortex may be important for navigating visually similar compartmentalised spaces by conjunctively encoding both local and global environments. Previously, a novel directional signal that encodes local spaces was found in the dysgranular retrosplenial cortex (dRSC) while global head direction encoding was found in both dRSC and granular retrosplenial cortex (gRSC; Jacob *et al*., 2017). This thesis addresses two questions arising from this finding: (i) how does the local directional signal arise? and (ii) do the downstream place cells (cells that display spatially constrained firing) display local or global encoding?

The first question was explored by retrogradely labelling the neuronal inputs into the two retrosplenial regions under the hypothesis that the differences in directional encoding are due to differences in their inputs. Particularly, gRSC was found to receive more inputs from anterodorsal thalamus, which was previously shown to display global encoding (Jacob *et al.,* 2017). In addition, gRSC, but not dRSC, received inputs from dorsal subiculum which is the main output structure of hippocampus. It is however unclear if place cell in hippocampus displayed local or global place encoding.

The second question thus arises: Do place cells display local or global place encoding? As hippocampus is strongly coupled with gRSC, place cells were predicted to show a global representation similar to that in gRSC. Extracellular recording of place cells in an environment with two differentially scented, visually rotated compartments showed that no place cells that are sensitive to the local visual scene were found. Thus, place cells displayed global encoding.

Together, these findings indicate that global encoding in gRSC may be a consequence of its stronger coupling with vestibular-directional nuclei and the hippocampal system, both of which displayed global encoding. In contrast, the local encoding observed in dRSC may reflect its structural disconnect from the global spatial network.

Impact Statement

The impact of the work done in this thesis can be divided into those specific to our field as well as more general impacts applicable to the society. Starting with the former, within the context of this thesis, we have specifically examined how the two directional encodings (local vs. global encoding) could arise in the brain and how they are interpreted by the downstream spatial system. In the first experiment, the retrograde tracing data had replicated previous results, but also highlighted differences that can arise as a consequence of the retrograde tracers and the rat strains used. This thus underscores the importance of taking precautions when drawing conclusions between rat strains and between different experimental designs. More importantly, the data obtained in the retrograde tracing experiment could be used to guide future inactivation experiments, which would help prove causality of the projections in generating the bidirectional and/or head direction signal.

In addition, we have shown how the place cell system represents compartmentalised spaces that are visually similar. This work, together with the previous experiment, contributes to our understanding of how reference frames are integrated and/or resolved within the brain. Particularly, the finding that place cells could disambiguate the visually identical compartments suggests that information about the local and global reference frames is integrated upstream of hippocampal CA1 but possibly downstream of medial entorhinal cortex (see Chapter 6). This hypothesis could be tested in the future by placing tetrodes in areas like dentate gyrus and hippocampal CA3, which are situated in between the two regions.

More generally, the work done in this thesis contributes to the ever-expanding literature on how the brain helps us navigate. Although the work carried out here is considered to be part of ‘basic’ science (i.e. understanding the basic mechanism of how our brains navigate), the knowledge contributed by the field could be clinically relevant as impairments in the ability to navigate has been described in patients with Alzheimer’s disease. Thus, further understanding of how our brains navigate could be used to guide therapeutic interventions that may slow down or stop the progression of the disease.

Last but not least, much of the work in the navigation field has been used to guide algorithms that can help robots navigate. This work could thus be used to guide studies that will

allow robots to better navigate in multi-compartment spaces (e.g. offices in buildings). Consequently, this could lead to development of robots that are more efficient in rescue missions such as those that can better navigate collapsed buildings.

Abbreviations

Anatomical axis abbreviation	
AP	Anterior-posterior
ML	Medial-lateral
DV	Dorsal-ventral
Anatomical structures abbreviation	
ADN	Anterodorsal thalamus
dRSC	Dysgranular retrosplenial cortex
DTN	Dorsal tegmental nucleus
MEC	Medial entorhinal cortex
gRSCa	Granular retrosplenial cortex area A
gRSCb	Granular retrosplenial cortex area B
gRSCc	Granular retrosplenial cortex area C
LDN	Laterodorsal thalamus
LMN	Lateral mammillary nucleus
PoS	Postsubiculum
RSC	Retrosplenial cortex
SC	Superior colliculus
V1	Primary visual cortex
V2	Secondary visual cortex
V2L	Lateral secondary visual cortex
V2M	Medial secondary visual cortex
Cells	
BD	Bi-directional cells
HD	Head direction cells
Technical abbreviation	
AF488	Alexa Fluor 488
AF594	Alexa Fluor 594
CTB	Cholera toxin subunit B
GFP	Green Fluorescent Protein
PFD	Preferred firing direction
PV	Population vector
ROI	Region of Interest
TxCx	Tetrode *x* Cluster *x*

Table of Contents

Table of Figures

Table of Tables

Chapter 1.

General Introduction to Navigation

One of the common requirements across all motile animals for survival is the need to search for food and mates, escape from predators and find their way home. To perform these essential behaviours, animals must navigate through environments that are constantly changing. How do the brains of these animals help them navigate? Tolman (1948) suggests that animals form an internal representation of the external environment to help guide navigation. This 'cognitive map', as he described, encodes the relationships between external stimuli and is useful for guiding flexible navigational behaviours including shortcut and detour behaviours.

This thesis is primarily concerned with how the cognitive map in the rat brain constructs an internal representation of complex environments, especially those that have ambiguous sensory information. As will be explored later, the cognitive map relies on both visual and self-motion cues (Poucet, 1993; Etienne and Jeffery, 2004) and the two types of cues interact with each other in the brain to provide a coherent representation of the environment. The overarching question pertinent to this thesis is: How does the cognitive map represents a complex environment with multiple visually similar local spaces (e.g. offices within a building; flats within an apartment building)? In particular, the work done in this thesis is an extension of the study by Jacob et al. (2017) who described a novel directional signal in the dysgranular retrosplenial cortex (dRSC) that is more sensitive to the local visual scene, in addition to the classical global directional signal. In the following chapters, this thesis addresses the following two questions: (1) How do the two distinct directional signals arise in the retrosplenial cortex? (2) Could information about location in global space be used to resolve ambiguities in the local perceptual scene?

Before we answer the two questions, it is essential to understand our current state of knowledge with regards to neural encoding of visually similar multi-compartmental spaces. In the first chapter, we will review our current understanding of the neural substrates underlying the cognitive map so as to provide the fundamental knowledge required for understanding the content of this thesis. In the second chapter, we will review our current understanding of how the cognitive map encodes visually similar compartmental spaces, including a detailed review of the

retrosplenial cortex which conjunctively encodes both local visual and global directional signals. We will then dive into the experiments at hand in the subsequent chapters.

1.1 The cognitive map

Tolman's cognitive map is arguably one of the most important theory in describing complex navigational behaviours seen in animals and humans. Particularly, during navigational behaviour, the spatial relationships between salient features in the external environment are believed to be stored in the brain forming an abstract representation (a 'cognitive map'). This internal representation is often metaphorically described as a 'map control room', indicating the possible routes (hence responses) the animals could take (Tolman, 1948).

In his seminal theoretical paper, Tolman (1948) described several behavioural evidence from his work in support of the cognitive map – the most famous of which is the sunburst experiment (Fig 1; Tolman *et al.*, 1946). The sunburst experiment was designed to examine if rats can take a novel shortcut when a familiar path to the goal is blocked. The animals were first trained to follow a path using the apparatus in Figure 1.1A, which involved multiple systematic turns (i.e. left-right-right). Post-training, the animals were placed in a similar apparatus with the same

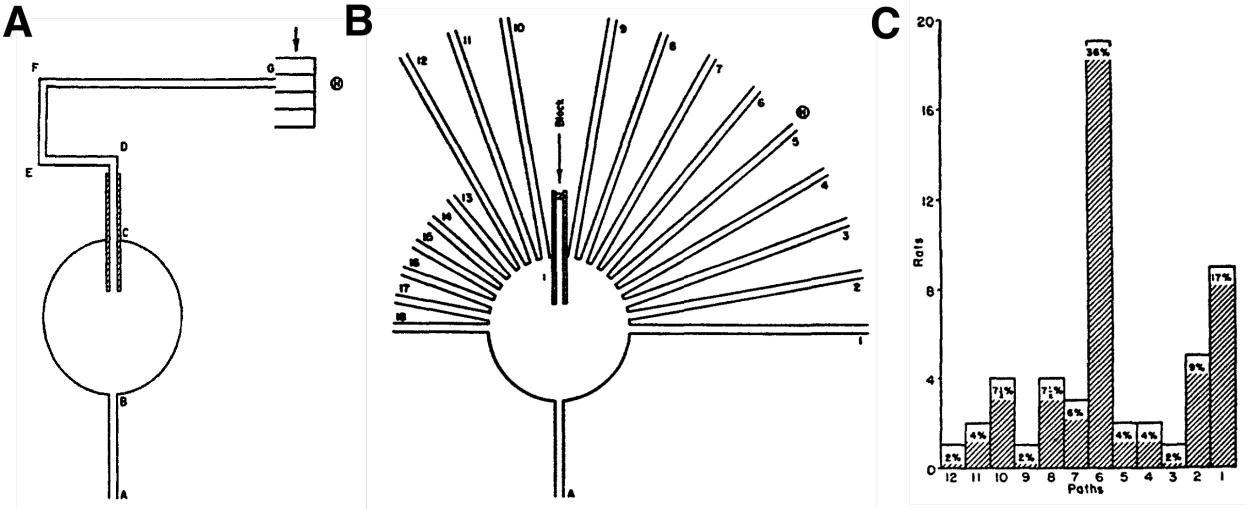

Figure 1.1: Tolman's sunburst experiment (A) The apparatus used to familiarize the animals. Animals were trained progressively to run down the apparatus starting from A (bottom) to G (top). A desk lamp was placed at H and was the only light source in the room. **(B)** Post-training, animals were placed in the sunburst maze. The sunburst apparatus has the same starting path (AB) and circular platform as the training apparatus. However, the familiar path is now blocked off, and the rats were instead offered multiple alternative paths arranged radially at 10° separation. **(C)** Most rats ran down path 6, the shortest path to the trained goal. *Adapted from Tolman et al., 1946*.

starting platform but with the trained path (CD) blocked and several radially arranged paths attached to the circular platform ('Sunburst'; Figure 1.1B). The authors reasoned that if the animals cannot compute shortcut and strictly follow a stimulus-response approach, it will choose the two arms closer to the trained path (arm 9 and 10). However, if the animals can compute shortcut (and hence have a cognitive map), the animals would take the path with the shortest Euclidean distance to the goal. In support of the presence of a cognitive map, most animals chose the shortest path (Figure 1.1C). However, the Tolman's sunburst experiment has a significant caveat - a desk lamp was used as an external cue (O'Keefe and Nadel, 1978). As such, the animals could be using the light source as a 'beacon' and were instead navigating towards the light (movement towards a familiar external stimulus; Bennett, 1996).

Since then, attempts to replicate Tolman's experiment in rodents have produced mixed results. Gentry *et al.* (1947) repeated the original experiment but instead of replicating the results, showed that animals did not have a preference for the shortest path as described by Tolman *et al.* (1946). Particularly, they observed a clustering of path choices around the trained blocked path (path CD; Figure 1B) and demonstrated that visual and/or tactile features of the trained path may have influenced path choices during the test trial. Similarly, Muir and Taube (2004) repeated the sunburst experiment (with less paths and without any obvious external cues) and found that only one (out of four) animals took the novel shortcut. On the contrary, Singer *et al*. (2006) demonstrated an ability for rats to take novel shortcut, but only if distinct intramaze cues for each path are available during training. How these intramaze cues promote the formation of a cognitive map however remained unclear, especially since rats did not have access to the cues in the probe trial. In addition, some studies have suggested that rats are unable to take a novel shortcut unless they have experienced the shortcuts (Grieves and Dudchenko, 2013; Roberts *et al*., 2007). After experiencing the shortcut, the animals use the shortcut more – akin to learning a new route in the pre-existing environment. This is evident in experiment 2 of Roberts *et al*. (2007) during which animals did not display preference for the novel peripheral alley leading to the reward in the first two testing trials, but quickly learn the shorter route after.

Nonetheless, there is now substantial evidence for shortcut and detour behaviour in rodents. Using a M-runway maze with panels of wall removed to generate shortcuts, Alvernhe *et al*. (2008) reported that "rats immediately and consistently used the newly available shortcuts". The same group further showed that rats can take detours using a Tolman detour maze and would

choose to take the shorter detour path, if privy to reward (Alvernhe *et al.*, 2011). Specifically, rats were trained to run between two ends of a linear track with no restriction along three possible paths – a straight direct path, a shorter detour path and a longer detour path. During testing, a barrier is then placed on the track in a manner such that 1) only the long detour path or 2) either detour paths can lead to the reward. In both conditions, rats were able to optimize their path choices (i.e. choose the only available path in condition 1 or choose the shorter detour path in condition 2). Interestingly, on first exposure to the barrier session in condition 2, only half the rats chose the shorter detour path. Their performance however increases over time, reminiscent of learning a new shorter route when the direct path was blocked. Detour behaviours in rats were also observed in three-dimensional environments (e.g. pegboard and lattice maze), although the preference for the shorter or longer detour routes is less direct and is influenced by an animal's preference for the horizontal motion (Jovalekic *et al.*, 2011). Similar detour behaviours were also observed in mice using barriers in a water maze task. Most mice adopted an optimized path (i.e. swimming directly to the end of the barrier instead of along the barrier) as training progresses, thus demonstrating an ability to compute a shorter route to the hidden platform (Juszczak and Miller, 2016).

Hence, even if the cognitive map may not exist in rodents in the form Tolman (1948) envisioned, there is no doubt that rodents can navigate flexibly to guide ethologically relevant behaviours. It may be worthwhile to note that in recent years, the cognitive map is also thought to be the underlying principle for cognition in the non-spatial domain, in addition to navigation and spatial memory. Specifically, the cognitive map may encode the relative relationship between abstract concepts (Behrens *et al.*, 2018). However, the current work will focus on the spatial aspect of the cognitive map.

The question then arises as to where in the brain could such a flexible and adaptive system exist and a rat race for the search of a neural substrate commenced in the post-Tolman era.

1.2 The 'Positioning System' in the Brain

The first physiological indication of a map-like system in the rodents' brains comes from the findings of O'Keefe and Dostrovsky (1971) who recorded neurons in the hippocampus of freely moving rats. They found neurons that displayed spatially constrained firing patterns (Figure 1.2). These neurons, which are now known as *place cells*, are thought to underlie the cognitive map,

encoding information about the local space and providing the 'where' information in our memory (O'Keefe and Nadel, 1978).

Since then, a wide range of other functionally defined cell types was found in other related brain regions that seemingly contribute to the cognitive map. The three other main spatial cell types (besides place cells) are *head direction cells*, which do not display spatially constrained firing patterns but instead have spiking activities modulated by the heading direction of the animals' head (Figure 1.2; Taube *et al.*, 1990a; 1990b), *grid cells* which display multiple regularly spaced, spatially constrained firing fields (Figure 1.2; Fyhn *et al.*, 2004; Hafting *et al.*, 2005) and *border/boundary vector cells* which spike when the animal is close to a wall in a specific allocentric ("world-centred"; external environment reference frame) direction (Figure 1.2; Solstad *et al.*, 2008; Lever *et al.*, 2009). These four cells are believed to form the neural basis of a cognitive map required for navigation with place cells providing 'location' information, head direction cells acting as a 'compass', grid cells providing 'metric' information and border/boundary vector cells providing information about edges and boundaries in the environment.

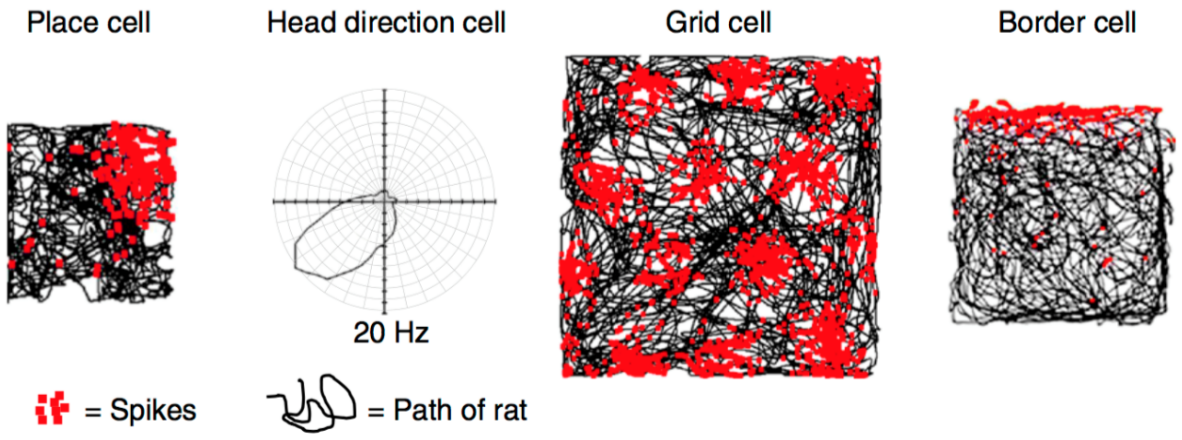

Figure 1.2: The four main cell types related to navigation and spatial memory. Place cells spike within a location in the environment and is believed to provide information about the location. Head direction cells do not display spatially constrained firing, but instead spike when the animal's head faces a specific direction in allocentric space (e.g. a HD cell spiking when the animal faces southwest). Grid cells showed regularly spaced hexagonal firing pattern in the environment and may provide metric information. Border/boundary vector cells fire in response to a boundary (e.g. wall, drop edges) in a specific allocentric direction. *For place, grid and boundary vector cells, red dots represent neuronal spikes while the black lines represent the path took by the animals. For head direction cells, the angular displacement in the circular polar plot indicates the preferred firing direction, while the radius indicates the firing rate. Adapted from Marozzi and Jeffery (2012).*

The above four cell types form the foundation of spatial navigation and will be discussed in further detail. However, it is important to note that other spatially relevant cell types exist in the

brain including but not limited to *egocentric boundary cells* (Hinman *et al*., 2019; Alexander *et al*., 2020) which respond to boundaries in egocentric (self-centred) coordinates (i.e. relative to the animal's body), and *center-bearing* and *center-distance cells* which encode the egocentric bearing of the center and the absolute distance to the center of the environment respectively (LaChance *et al*., 2019). A recent and useful discussion of cell types in the brain that represent space can also be found in this extensive review by Grieves and Jeffery (2017). This section will focus on reviewing the four main spatial cells, the properties of which are crucial for understanding how they encode space. See section 1.3 of this thesis for a more detailed review of the neuroanatomical structures where these spatial signals are found and how they interact with each other to form a coherent spatial representation.

1.2.1 Place cells

Place cells, which were the first spatial cell to be discovered, fire when an animal traverses a specific location in the environment (Figure 1.2; O'Keefe and Dostrovsky, 1971). The location at which a place cell fire is known as a "place field". Place cells are described in the pyramidal cell layer of hippocampus and have been observed in all sub-regions of hippocampus (Jung *et al*., 1994; O'Keefe and Dostrovsky, 1971; Jung and McNaughton, 1993; Mankin *et al*., 2015; Muller *et al*., 1987).

1.2.1.1 General properties of place cells

Hippocampal place cells are pyramidal cells that displayed low background firing rate when the animal is outside the place fields but showed increased firing rate as the animal enters the place fields. These neurons have complex spiking activities, defined by bursting activity of 2 to 11 spikes with reducing amplitudes and inter-spike intervals of between 1.6 to 6ms (Fox and Ranck, 1975; Muller *et al*., 1987). In a typical open field recording arena, most place cells were observed to have only one place field. However, in larger environments, the number of place fields per cell increases and a place cell could have more than one place field (Fenton *et al*., 2008; Park *et al*., 2011; Rich *et al*., 2014). Previously silent pyramidal cells can also be recruited to become place cells (Lee *et* al., 2012; McKenzie *et al*., BioRxiv 2019; Rich *et al*., 2014). In a foraging task, the place representation of an environment tends to be homogenous with place fields mapping the whole arena evenly (Muller *et al*., 1987; Fenton *et al*., 2000), although a slight

tendency for place fields to cluster close to walls and cues has also been described (Hetherington and Shapiro, 1997).

In line with the hypothesis that place cells encode long-term spatial memory, the place representation observed in place cells is stable (if the environment does not change) and can be recorded over multiple days or weeks (Muller *et al.*, 1987; Thompson and Best, 1990). However, a more recent study investigating the stability of hundreds of place cells over days using calcium imaging suggests that not all place cells are active over days (Ziv *et al.*, 2013). In fact, only a subset of place cells is recruited each day and the recruitment of place cells across days are uncorrelated. Nonetheless, if recruited, the place fields are spatially invariant (i.e. in the same location as previously seen). Across any two sessions, only 15-25% of active cells overlap and the commonality is sufficient to decode an animal's position on the track across days. It is however important to note that the latter study was done in mice, and it is still not known if rats exhibit the same dynamic place code.

Given that place cells tile the environment evenly and are stable over days, one could speculate that the place code in the hippocampus might be topographically organized (i.e. place cells with place fields that are physically close to each other are also close to each other anatomically). Multiple studies have sought to examine if such a spatially correlated topographical organization of place cells exists in the hippocampus, though with mixed results. Some studies demonstrated possible topography (Eichenbaum *et al.,* 1989; Hampson *et al.*, 1999; Nakamura *et al.*, 2010) while others showed no obvious topography (O'Keefe *et* al., 1998; Redish *et al.*, 2001; Dombeck *et al.*, 2010). It remains unclear why topography was only observed in some studies, but it may reflect an interaction between task engagements and recording techniques. Nonetheless, it is clear that place cells with distant place fields can be recorded on the same electrode or tetrode (O'Keefe 1976; O'Keefe and Speakman, 1987; O'Keefe *et al.*, 1998), suggesting that a simple topographic organization of place cells is likely to be absent.

Although it remains inconclusive if place cells are organized topographically via the spatial locations of their place fields, recordings across the longitudinal axis of the hippocampus (septal-temporal axis; or dorsal-ventral axis) have revealed topography based on place field size. Place cells tend to have larger place fields as recordings progress from dorsal to ventral hippocampus (Jung *et al.*, 1994; Kjelstrup *et al.*, 2008).

1.2.1.2 Multi-modality of place cells

If place cells truly encode information about the current location, they must be able to process and integrate sensory information about the external environment so as to provide an accurate estimate of the animal's current location. To investigate the role of sensory information in modulating place activities, O'Keefe (1976) examined place cell firing in the dark and observed a sudden loss in firing in a subpopulation of place cells on first exposure, which gradually recovered on subsequent trials. The conclusion of this experiment is twofold. First, some place cells are sensitive to the visual scene (i.e. they receive visual inputs). Secondly, the sudden loss and subsequent recovery in place activities reflect a switch from utilizing visual information to some other sensory modalities. This section will expand upon the findings by O'Keefe (1976) and review our current understanding of the sensory inputs into the place cell system.

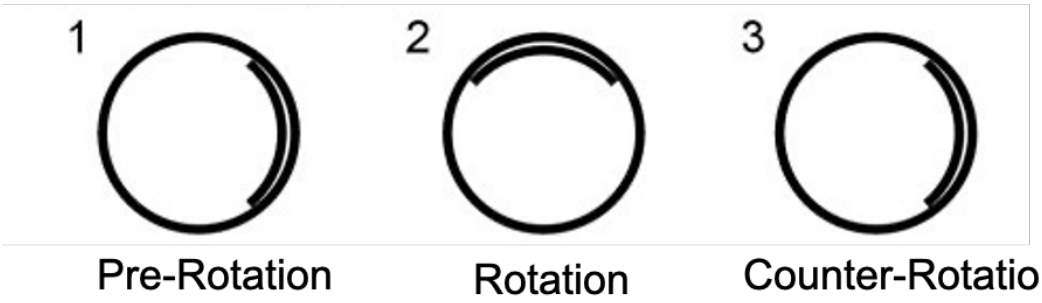

Figure 1.3: Cue rotation experiments. Cue rotation experiments are classic experiments used to test the influences of visual information and other sensory modalities on spatial cells. *Adapted from Calton et al.* (2003).

The influences of the visual scene on place cell activity are relatively well understood, mostly from studies that involve manipulations of the visual environment. Place cells tend to fire in relation to the visual scene and rotate when the visual scene (or visual landmark) is rotated (Figure 1.3; O'Keefe and Conway, 1978; O'Keefe and Speakman, 1987; Muller and Kubie, 1987; Fenton *et al*., 2000). Furthermore, place cells are sensitive to both proximal and distal visual cues and rotate accordingly with both type of visual cues (Scaplen *et al*., 2014). Muller and Kubie (1987) went on to show that place cells were not anchoring to local features of the cue card (e.g. texture) but instead relied on the visual aspect of the cue. Interestingly, place cells are unlikely to be responding to visual cues individually but instead perceive the visual environment as an entire visual panorama. As demonstrated by Fenton *et al.* (2000), the centroids of place fields systematically reorganized when the distance between two visual cues was changed (i.e. the cues were moved closer together or further apart). This systematic reorganization suggests that

place cells are integrating information about the distance between the two visual cues, instead of relying on a single landmark. Nonetheless, when one of the two visual cues was removed, place cells remained stable and demonstrate an ability to recognize the environment (i.e. pattern completion).

There is also clear evidence for the use of other sensory modalities beside visual information. When visual information is made unavailable (e.g. lights off conditions, no discerning visual cues) while the animals were still in the environment, place cells continued to fire and did not display markedly different properties (Muller and Kubie, 1987. Quirk *et al.*, 1990; Jeffery *et al.*, 1997). Intact place cells were also observed upon first exposure to the environment in blindfolded (Hill and Best, 1981) and surgically blind animals (Save *et al.*, 1998). In addition, the place cells found in visually impaired animals rotate coherently with the local environment, thus indicating a dependency on local, non-visual cues. What could these non-visual cues be? Place cells were observed to be sensitive to and rotate coherently (if cue control experiments were carried out) with tactile cues (Gener *et al.*, 2013) and olfactory cues (Save *et al.*, 2000; Zhang and Manahan-Vaughan, 2015). Place cells were also observed to be sensitive to the geometry/walls of the environment such that place fields scale with changes in the length of the wall in the same axis, occasionally developing a second peak in the process (O'Keefe and Burgess, 1996; Barry *et al.*, 2006). Furthermore, place cells, on occasion, displayed random rotations in their place maps according to the rotational symmetry of the recording arenas (Keinath *et al.*, 2017; Kinsky *et al.*, 2018). Geometry/boundary inputs appear to be distinct from other sensory inputs as changing the walls (hence changing the local textures, odours and/or colours) did not change the place fields (O'Keefe and Burgess, 1996; Barry *et al.*, 2006). Information about the boundary and/or geometry is likely to be provided by a unique class of cells, the boundary vector cells (see Section 1.2.4; Lever *et al.*, 2009), which provide allocentric boundary information.

In addition to external sensory information, animals can also use internal self-motion cues (e.g. motor efference, vestibular and proprioceptive information; idiothetic cues) to keep track of its location in the environment. This process, known as path integration (Mittelstaedt and Mittelstaedt, 1980), can be used to maintain place cell firing, although it can be difficult to prove that the animals are not using any external cues (Etienne and Jeffery, 2004). Nonetheless, there is some evidence showing an influence of path integration on place cell firings. For example, Hill and Best (1981) demonstrated that a subpopulation of place cells in blindfolded deaf rats did not

rotate with the intramaze cues when the rats were not disoriented, suggesting that these place cells were using vestibular information to guide their spatial firing (Best and Thompson, 1989). Jeffery *et al*. (1997) provide further support for the use of internal self-motion cues by slowly rotating rats in the dark and showed that place cells tend to rotate in concordance with the rotation of the rats. In addition, Stackman *et al*. (2002) showed disruptions of place fields when the vestibular apparatus was temporarily inactivated using tetrodotoxin. This finding was also corroborated by Russell *et al*. (2003), who also showed disrupted place cell activity when the vestibular apparatus was permanently lesioned.

Path integration is thought to be useful for estimating one's location when external cues are not available or unstable. Because path integration is a continuous and cumulative process, it is prone to accumulating errors. External cues are then useful to help reset the movement (and direction) vectors (Etienne and Jeffery, 2004). Save *et al.* (1998) provide support for such interactions between external cues and path integrator using blind rats, which are presumed to rely mainly on path integration. Particularly, place cells in blind rats were observed to fire only after they have made contact with at least one intramaze cue. In addition, blind rats contacted intramaze cues more frequently than sighted rats, presumably to update their path integrators.

Given the multitude of modalities that can influence place cell activities, it is then logical to question if there are any hierarchical organizations in the modalities employed. Cue conflict experiments are traditionally employed to help address this question. When the visual scene is placed in conflict with an animal's path integrator, visual information was found to predominate over self-motion cues (Jeffery and O'Keefe, 1999; Jayakumar *et al*., 2019). In contrast, geometry information appears to dominate over visual information as place cells were occasionally found to ignore the polarized visual environment and rotate randomly according to the rotational symmetry of the environment (Keinath *et al*., 2017; Kinsky *et al*., 2018). However, mixed responses were observed when proximal cues (multimodal in nature – tactile, olfaction and/or visual) were placed in conflict with distal cues (visual in nature). Some place cells rotate with proximal cues while others rotate with distal cues (Tanila *et al.* 1997; Shapiro *et al*., 1997; Knierim, 2002; Lee *et al*., 2004; Renaudineau *et al*., 2007). Thus, place cells encode both proximal and distal cues regardless of their modalities. Interestingly, place cells are able to switch between different sensory modalities depending on the stability of the cues present. For example, Jeffery and O'Keefe (1999) showed that place cells switched to using self-motion cues to guide firing

when visual cues were made unreliable. Similarly, Shapiro *et al*. (1997) showed that place cells switched between using distal cues and local cues when local cues and distal cues were scrambled respectively. Thus, it is likely that place cells weigh the available cues and sensory information available and use the most salient and stable information to guide firing.

1.2.1.3 Remapping

As described in the previous section, place cells are multi-modal and can switch between using different modalities to guide spatial firing depending on the saliency and stability of the available cues ('pattern completion'). However, when the environment changes or when the animals are placed in two distinct environments, place cells can also undergo a process known as 'remapping', first described by Muller and Kubie (1987). In that experiment, Muller and Kubie (1987) recorded the same place cells in both cylindrical and rectangular environments and noticed that their place fields are uncorrelated, stating 'it is impossible to predict the nature of a firing field in a cylinder from a knowledge of the cell's field in a rectangle and vice versa'. Since then, multiple studies have investigated the process of remapping – which is usually described to manifest in three distinct forms (Figure 1.4):

1. ***Global* remapping** describes changes in place representations when all co-recorded place cells changed their firing activity concomitantly. However, the observed changes within the population are not identical and can vary from cell to cell. Some cells may change the locations of their place fields while others may stop firing. Previously silent cells in one environment can also start firing and developed a field in another environment (Figure 1.4A).

   Global remapping generally happens when there are drastic changes in the environment (e.g. cylindrical and rectangular environment) and may be involved in 'pattern separation' such that each unique combination of place cell patterns for each environment represents the spatial memory trace for that environment. Place representations are more orthogonal in CA3 than CA1 even in environments with common features, implicating a role for CA3 in pattern separation (Leutgeb *et al*., 2004). Interestingly, CA3 has a large capacity for the number of orthogonal maps it can store with dissimilar maps observed for up to 11 environments with identical geometry (Alme *et al*., 2014).

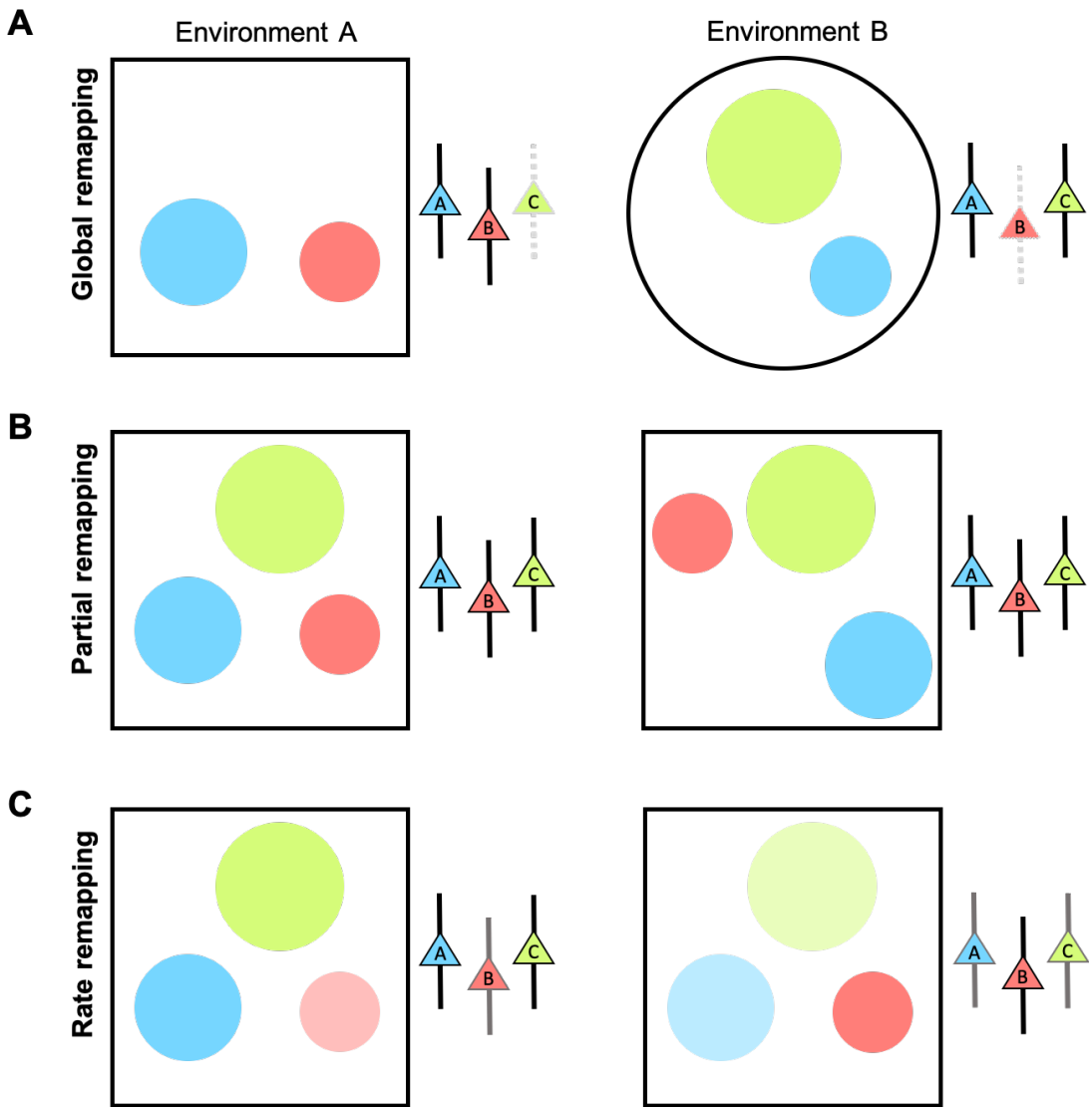

Figure 1.4: Three types of remapping have been described experimentally. (A) Place cells can undergo *global remapping* when the environments are significantly different. Cells can become silent (red cell in cylindrical environment), start firing (green cell in cylindrical environment), or have shifted place fields (blue cell). **(B)** In *partial remapping*, some place cells remain stable (green cell) while others have changes in their firing activities, which could include a shift in the locations of their place fields (blue and red cells). **(C)** For *rate remapping*, place cells have place fields in the same locations, but their firing rates are altered. Some place cells can have increased firing rates (red cell) while others can have a reduction in firing rates (blue and green cells).

2. ***Partial* remapping** describes changes in place representations when a subset of cells remained stable across environments, while a distinct subset changed their firing activity. As such, the place representations between the two environments are distinct but not orthogonal.

Partial remapping generally happens when a subset of the available cues (especially local cues) in a familiar environment is altered. A clear example of partial remapping can be observed in Anderson and Jeffery (2003) who recorded place cells in the same arena using either black or white walls with lemon or vanilla scented flooring and walls. This setup give rise to four possible combinations of the same arena – black walls with lemon odour, black walls with vanilla odour, white walls with lemon odour and white walls with vanilla odour. A small subset of place cells showed consistent place fields across all four arenas (Figure 1.5D) but most place cells exhibited partial remapping and are sensitive to either odours (Figure 1.5A), colours (Figure 1.5B) or a combination of both (Figure

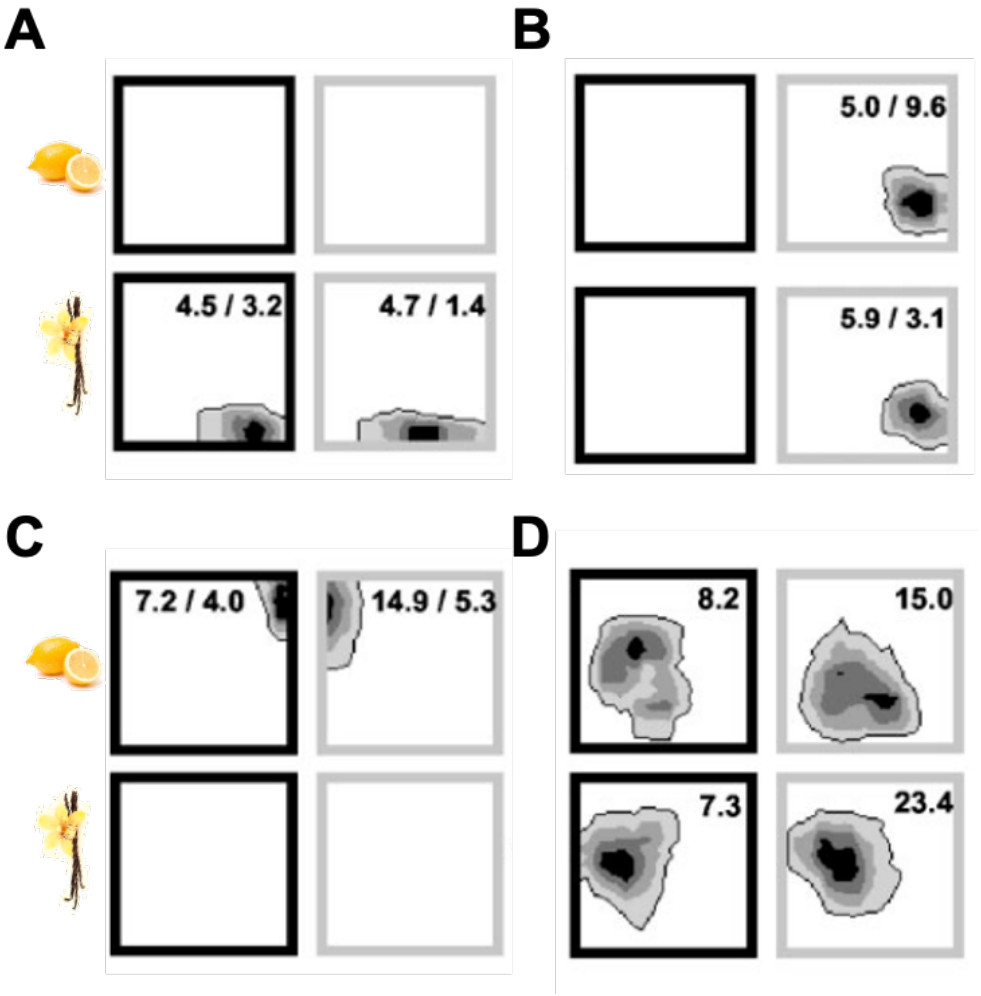

Figure 1.5: Partial remapping in familiar environment with different contexts. (A) An example place cell which have the same fields in vanilla scented environments but remapped in the lemon environments. **(B)** This place cell fires in the white wall environments but remapped in the black wall arenas. **(C)** An example place cell that likely receives complex contextual inputs and displayed different place fields in the lemon scented environment but did not display any fields in the vanilla scented environment **(D)** A place cell that has the same place field in all four arenas. *Adapted from Anderson and Jeffery, 2003*.

1.5C). This observation suggests that each place cell receives information about the contexts (odours/colours) that seemingly regulate or select the metric (grid cells) inputs to form place fields ('contextual gating model'; Anderson and Jeffery, 2003; Jeffery, 2007; Hayman and Jeffery, 2008; Jeffery, 2011).

In addition to colours and odours, partial remapping was also observed when barriers were inserted into an environment and/or when the local structure of the environment was changed (Alvernhe *et al*., 2008, 2011; Spiers *et al*., 2015). However, such changes generally affect place cells close to the manipulations and cells with place fields far from the manipulations are often not affected (except in CA3 when shortcuts are made available; Alvernhe *et al*., 2008). This is also described as local remapping.

3. ***Rate* remapping** describes changes in the firing rates of place cells without any changes in the locations of the place fields. Rate remapping is believed to be a mechanism by which place cells encode subtle changes in the environment.

An example of rate remapping was clearly described in Hayman *et al*. (2003) where the place cells found in one rat were found to fire in the same relative positions between two non-connecting compartments of an environment, instead of remapping to a different position. Detailed examination of the place fields in the respective compartments revealed a consistent difference in the firing rates of the two place fields, as if the place cells received a stronger drive in only one of the compartments. Leutgeb *et al*. (2005) further showed that it is likely that non-spatial features of the environment are encoded in the firing rates of place cells while spatial location is encoded by the location of the firing fields. To separate non-spatial features from spatial location, they recorded place cells in two conditions – in different boxes in the same room (variable cues-constant place) and in the same box in different room (variable place-constant cues). Interestingly, they found that place cells fire in the same place but with different firing rates (rate remapped) in the variable cues-constant place condition but globally remapped in the variable place-constant cues condition. Rate remapping were observed (though to different extent) when both the geometry and wall colours were changed – indicating that information about both geometry and wall colours are encoded in the firing rates of place cells.

1.2.1.4 Attractor dynamics

An interesting property of place cells is the ability for the population to coherently switch between spatial representations when changes to the environments are significant and unambiguous. Place cells rotate coherently when the entire visual scene is rotated (see Section 1.2.1.2) and globally remap when there are drastic changes to the environment (see Section 1.2.1.3). The coherent firing activities of place cells are often thought to be the result of an attractor network dynamic, a process where synaptically connected neurons collectively gravitates toward stable firing states. Networks with attractor dynamics are thought to underlie autoassociative memory, akin to how place cells stably fire when only a subset of cues is available and/or stable (Fenton et al., 2000; Jeffery and O'Keefe, 1999; Shapiro et al., 1997).

Attractor dynamics can be broadly classified into two forms – one with discrete states, and one with continuous states (Figure 1.6; Jeffery, 2011). In a discrete attractor, stable states can be visualized as low-energy states in which the network tend to gravitate to. With a discrete attractor, place representations are stable and are resistant to small changes but will switch between discrete representations if sufficient 'energy' (i.e. changes to the environment) is provided into the network. In contrast, continuous attractors do not have discrete states and the network moves between states that are in a continuum (i.e. gradual changes in place representation).

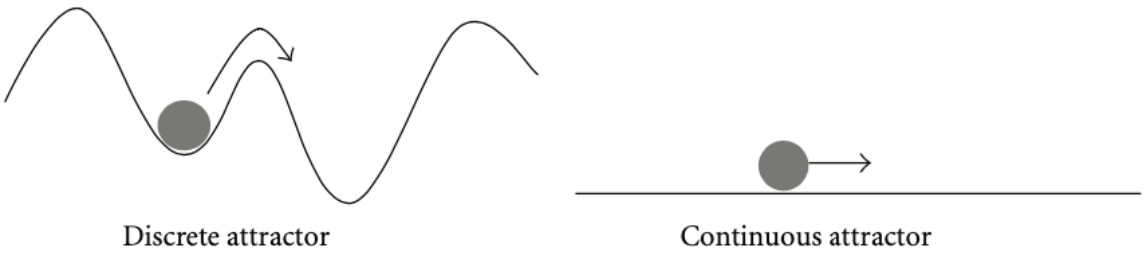

Figure 1.6: Schematic diagram of the two forms of attractor dynamics. *Left,* in a discrete attractor, the energy landscape resembles crests and troughs with the network preferring low energy states (troughs). The network (grey ball) is resistant to small changes and significant energy is needed to change between states. *Right*, in a continuous attractor, the energy landscape can be visualized as flat and progression between states is gradual. *Adapted from Jeffery (2011).*

Even though global remapping and coherent rotation of place cells provide some evidence for discrete attractors in the place cell network, it was not until 2005 that Wills *et al*. (2005) provided direct evidence for a discrete attractor network in how spatial representations are stored

in the hippocampus. In the study, rats were trained to distinguish between two environments with distinct geometry (circle and square) which induced global remapping. They then examined the place representations when the shape of the environment was morphed to one of several intermediary shapes. Interestingly, they observed that place representations in the intermediatry shapes tend to be either circle-like or square-like, and all place cells abruptly and coherently switched between the two distinct place representations. This finding suggests that a discrete attractor state is present for each geometry, and the place cell network collectively represents the ambiguous intermediary environments using one of the two attractor states from the two familiar geometry (Wills *et al*., 2005).

Surprisingly, Leutgeb *et al*. (2005) did a similar experiment and showed gradual changes in place representations across intemediary shapes, instead of the abrupt changes observed in Will *et al*. (2005). The difference in observations can be explained by several differences in the protocol but is likely due to the fact that changes in geometry from circle to square (and vice versa) were done in slow incremental steps in Leutgeb *et al*. (2005) but in a semi-random manner in Wills *et al*. (2005). This thus suggests that the energy landscape of the attractor dynamics in the place cell network and the subsequent place representations can be influenced by the experience of the animals (Plitt and Giocomo, BioRxiv 2019). Therefore, attractor dynamics of a more continuous nature may exist when changes to the environment are gradual and continuous.

1.2.2 Head direction Cells

Head direction (HD) cells are cells that fire when the head of an animal faces a specific direction. Unlike place cells, HD cells do not display place fields but instead display preferred firing directions (PFDs; Figure 1.2). First discovered in postsubiculum (Taube *et* al., 1990a, 1990b), HD cells have since been found in multiple brain regions including dorsal tegmental nucleus (Sharp *et al*., 2001), lateral mammillary nucleus (Stackman and Taube, 1998), anterodorsal thalamus (Taube, 1995), laterodorsal thalamus (Mizumori and Williams, 1993), retrosplenial cortex (Chen *et al*., 1994; Cho and Sharp, 2001) and entorhinal cortex (Sargolini *et al*., 2006; Giocomo *et al*., 2014). Although the functional significance of having direction coding across multiple regions remains unknown, there are indications that the HD signals across the regions are not redundant and may help incorporate different sensory information at different levels of the pathway. This section will be dedicated to understanding the functional properties of

HD cells. The interactions of HD signals across different brain structures will be further discussed in Section 1.3.2.

1.2.2.1 General properties of head direction cells

HD cells display low background firing when the heading direction of the animal is outside its PFDs but display increased firing activity when the animals' head enters its PFD. The PFDs of HD cells can be visualized using a polar plot (Figure 1.2) and was first reported to have an average tuning width of 83.4° (in postsubiculum; Taube *et* al., 1990a), although subsequent studies have reported slightly different values in postsubiculum and across different brain regions (Lozano *et al*., 2017; see Table 3 of Cho and Sharp, 2001). Similar to place cells, HD cells are stable in familiar environments and maintain the same PFDs over days (Taube *et al*., 1990a). Likewise, the PFDs of HD cells are unbiased and are evenly distributed across all head directions (Taube *et al*., 1990a; Giocomo *et al*., 2014).

Also similar to place cells, there is no evidence of a topographic organization in the PFDs of HD cells in rats. This means that HD cells with different PFDs can be co-recorded (Taube *et al*., 1990b), and HD cells with similar PFDs are not clustered together anatomically. Although there is no topography organized by PFDs, a different form of topography has been described in the medial entorhinal cortex. Specifically, a gradual dorsal-to-ventral decrease in directional tunings of HD cells was observed in layer III of medial entorhinal cortex (Giocomo *et al*., 2014). The functional implication of the topography remains unknown, but may be related to the dorsal-to-ventral increase in grid scales (see Section 1.2.3.1)

1.2.2.2 Sensory inputs into head direction cells

Like place cells, HD cells are also able to integrate sensory information about the external environment so as to provide an accurate estimate of the animals' heading direction. Particularly, HD cells have been shown to be sensitive to the visual environment and rotate their PFDs coherently when a visual landmark is rotated (Figure 1.3; Taube *et al*., 1990b, Taube, 1995). When presented with two distinct visual cues, HD cells were also able to discriminate between them, thus suggesting a reliance on the visual features of the visual cues in guiding HD cell firings (Lozano *et al*., 2017).

However, HD cells do not just rely on visual information and they continue firing when visual cues are removed (Taube *et al*., 1990b; Goodridge and Taube, 1995), when lights are switched off (Mizumori and Williams, 1993) and when animals are blindfolded (Goodridge *et al*., 1998). Although HD cells continue firing in the absence of visual information, the PFDs of HD cells were observed to drift and accumulate errors with time (Goodridge *et al*., 1998; Mizumori and Williams, 1993; Goodridge and Taube, 1995; Taube *et al*., 1990b). Interestingly, when the familiar visual cue was returned to the environment, HD cells restored their originally established PFDs relative to the visual cue (Goodridge and Taube, 1995). This finding suggests that visual information likely provides a more precise estimate of an animal's heading direction and thus exerts a stronger influence on the HD system as compared to other sensory information.

The dominant influence of visual information is corroborated by Goodridge *et al*. (1998), who systematically examined the roles of other external sensory information on HD cell firing. Using a set of cue control experiments (Figure 1.3), HD cells were found to be weakly coupled to olfactory information and systematically under-rotate when odours (in the form of peppermint scented Q-tips) were rotated. The same under-rotations were also observed in blindfolded rats when the whole environment (cylinder and floor; tactile and odour constellation) was rotated. Unlike olfactory cues, auditory cues did not exert any influence and rotations of auditory cues led to seemingly random rotations in the PFDs of HD cells (Goodridge *et al*., 1998). Geometric cues also have a weak influence and HD cells do not rotate their PFDs in geometrically polarized environments unless the animals have been disoriented (Knight *et al*., 2011; Clark *et al*. 2010). This finding thus suggests that geometric cues are only utilized in the absence of a reliable path integrator (i.e. when disrupted by disorientation).

The influences of path integration on HD cell firing are well-established. As mentioned, HD cells drift when visual information is not available (Goodridge *et al*., 1998; Mizumori and Williams, 1993; Goodridge and Taube, 1995; Taube *et al*., 1990b), which likely reflects the errors accumulated as a consequence of path integration. In addition, HD cells maintained their PFDs when animals actively moved from a familiar compartment to a novel compartment that was geometrically and visually dissimilar (Taube and Burton, 1995). The maintenance of PFDs across the compartments can however be abolished when lights are turned off (i.e. removing optic flow information; moderate, non-significant effect) and/or when the animals are passively transported (i.e. removing motor efference and proprioceptive information; Stackman *et al*., 2003). Passive

rotations of animals through the PFDs of HD cells also reduced the peak firing rates of HD cells (Taube *et al*., 1990b, Knierim *et al*, 1995, Taube, 1995, Zugaro *et al*., 2001), although these findings were not replicated in a subsequent study (Shinder and Taube, 2011). More substantially, genetic or chemical ablations of the vestibular system in mice or rats disrupt HD cell activity in anterodorsal thalamus (Valerio and Taube, 2016; Stackman and Taube, 1997). Similarly, temporary inactivation of the vestibular apparatus via transtympanic injection of tetrodotoxin also temporarily disrupts HD cell activity in postsubiculum (Stackman *et al*., 2002).

Unlike place cells, when proximal (multimodal) cues are placed in conflict with distal (visual) cues, HD cells behave as an ensemble and tend to rotate coherently with distal cues (Zugaro *et al*., 2001; Yoganarashimha *et al*., 2006). HD cells thus have a preference for distal visual cues over proximal multimodal cues.

1.2.2.3 Attractor dynamics

An interesting property of HD cells is their ability to behave coherently as a population. For example, simultaneously co-recorded HD cells behave coherently and shift their PFDs by approximately the same angle (Taube *et* al., 1990b; Goodridge and Taube, 1995; Taube and Burton, 1995; Yoganarashimha *et al*., 2006). As such, HD cells are believed to exist in a one-dimensional continuous attractor network (see Figure 1.6; Figure 1.7; Skaggs *et al*., 1995; Zhang, 1996; Redish *et al*., 1996; Goodridge and Touretzky, 2000) with head direction encoded as a continuous variable.

For simplicity, HD cells can be conceptually envisioned as existing in a ring organized by their preferred directions (Figure 1.7). It should however be noted that no such ring topography is found in rodents (see Section 1.2.2.1), although a ring structure encoding direction information have been described in the central complex of the fruit fly *Drosophila melanogaster* (Seelig and Jayaraman, 2015). Each cell in the ring is strongly connected, via excitatory connections, with its neighbours which have similar PFDs and the strength of the excitatory connections decreases with distance between their PFDs. Cells are also connected by inhibitory synapses. In this model, an activity bump arises spontaneously and will indicate the current heading of the animal.

The activity bump is then believed to be moved around the ring via inputs from an intermediate ring of cells, which conjunctively encode the current heading direction and the

angular head velocity of the animals. Cells that encode angular head velocity have been found in the dorsal tegmental nucleus (Bassett and Taube, 2001; Sharp *et al.*, 2001) and likely provide the information required to move the activity bump. The intermediate ring of cells moves the bump by projecting asymmetrically to the ring of HD cells with conjunctive cells that receive clockwise angular information projecting to the right and cells that receive anti-clockwise angular information projecting to the left (Figure 1.7). Information about external landmarks are then fed into the model to correct for errors that could result from inaccurate estimation of angular velocity, thus helping to anchor the activity bump to the external world (Skaggs *et al.*, 1995; Zhang, 1996; Goodridge and Touretzky, 2000; Knierim and Zhang, 2012; McNaughton *et al.*, 2006).

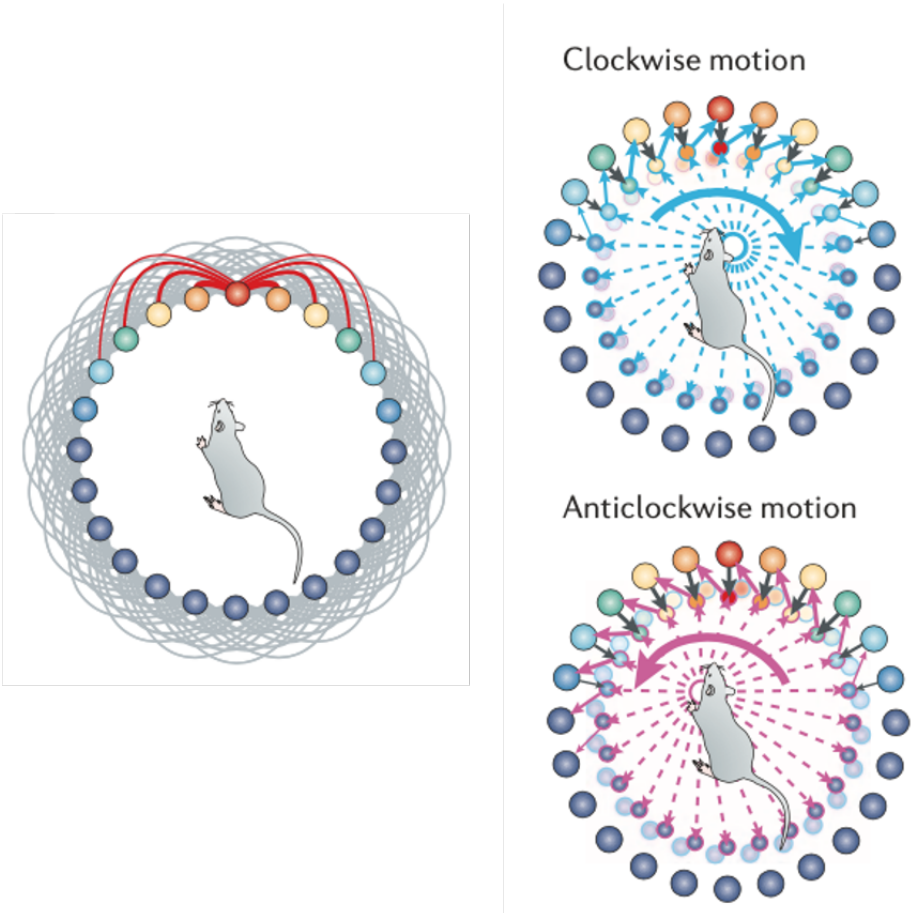

Figure 1.7: Continuous attractor network of HD cells. Head direction cells could be envisioned as a ring-like attractor connected by excitatory synapses that decrease with strength with increased differences in PFDs. The resulting activity bump can be moved around the ring via an intermediate ring of cells that conjunctively encode the current heading direction and the angular head velocity. The conjunctive cells project asymmetrically to the left and right for anti-clockwise and clockwise turns respectively. *Adapted from McNaughton et al. (2006).*

Although the model has been useful in accounting for the coherent activity of HD cells, it is inconsistent neuroanatomically as the projections from dorsal tegmental nucleus (where angular head velocity cells are found) to laterally mammillary nucleus (the next node in the HD network; see Section 1.3.2.1; Figure 1.11) are predominantly GABAergic (Allen and Hopkins, 1989; Wirtshafter and Stratford, 1993; Liu *et al.*, 1984). As such, it is unlikely that the rotational shift of the activity bump in the attractor network is mediated by excitatory connections. A subsequent model by Song and Wang (2005) resolved this inconsistency by showing that the activity bump can also be generated and moved around the attractor by having two populations of inhibitory neurons projecting asymmetrically to a population of excitatory cells. In this model, cells in the excitatory head direction population do not need to be recurrently connected with each other to generate the activity bump.

No matter which mechanisms were employed to generate the continuous attractor network, the continuous attractor network model can explain many of the properties seen in the HD network. Because the activity bump is primarily driven by the vestibular system (i.e. angular velocity), it can explain for the persistence and drifting of PFDs in the dark (Goodridge *et al.*, 1998; Mizumori and Williams, 1993; Goodridge and Taube, 1995; Taube *et al.*, 1990b). In addition, given that self-motion cues are the primary drivers of the attractor network, disruption of the vestibular system should lead to degradation of the HD network which was also observed experimentally (Valerio and Taube, 2016; Stackman and Taube, 1997; Stackman *et al.*, 2002).

1.2.3 Grid cells

Grid cells are spatially modulated cells that have multiple, regularly spaced firing fields arranged in a hexagonal pattern (Figure 1.2). They are thought to provide metric information for path integration and are found in the medial entorhinal cortex (Fyhn *et al.*, 2004; Hafting *et al.*, 2005).

1.2.3.1 General properties of grid cells

The regular firing patterns of grid cells can be described using three features - grid scale, grid orientation and grid phase (Figure 1.8; Hafting *et al.,* 2005; Moser *et al.*, 2014), which measures the distance between fields, the degree of rotation of the grid axes and the x-y coordinate translation of the grid fields respectively. Similar to the other spatial cells, grid cells are

stable and exhibit the same scale, orientation and phase in a familiar environment over days (Hafting *et al.*, 2005; Fyhn *et al.*, 2007; Barry *et al.*, 2012).

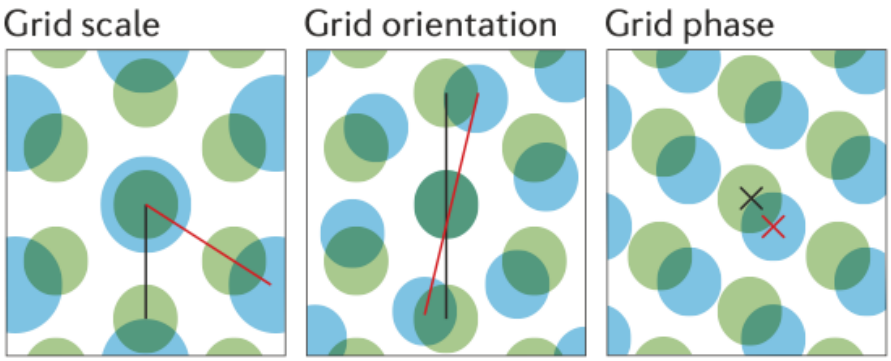

Figure 1.8: Features describing grid cells. Grid cells can be described primarily via three properties - *grid scale* which examines the distance between neighbouring firing fields, *grid orientation* which describes the orientation of the grid fields and *grid phase* which describes the x-y translation of the firing fields. *Adapted from Moser et al. (2014).*

Unlike place cells and HD cells, grid cells were found to be organized topographically into grid modules. Different grid modules have different grid scales and orientations, but grid cells within the same module have similar grid scales and orientations. Grid scales were also found to increase along the dorsal-ventral axis of medial entorhinal cortex, though not steadily, but instead in discrete steps (Stensola *et al.*, 2012). The same dorsal-ventral topographic organization was not observed for grid phase, and neighbouring grid cells have slightly offset phases such that a small number of grid cells would have sufficient firing fields to tesselate the entire arena. Grid phases appear to be randomly distributed and firing fields of neighbouring cells do not tend to overlap more than distant cells (Hafting *et al.*, 2005).

1.2.3.2 Sensory inputs into grid cells

The periodic firing patterns of grid cells suggest that grid cells may be an ideal neural substrate for path integration, allowing the brain to track the distance travelled. Consistent with this, grid cells are relatively stable (except for a slight decrease in spatial coherence) and continue firing in the dark (Hafting *et al.*, 2005). Disruption of grid cell firing via removal of N-methyl-D-aspartate receptors (NMDARs) was also found to disrupt path integration (Gil *et al.*, 2018), suggesting that grid cells are necessary for path integration.

However, a path integrator tends to accumulate errors and external landmarks are required to correct for this error. As such, grid cells should also be sensitive to the external environment. In line with this, grid cells rotate when visual cues are rotated (Hafting *et al*., 2005), showing sensitivity to the visual scene. In addition, grid cells are sensitive to boundaries and rescale parametrically to systematic changes to the geometry of an environment (via movements of walls; Barry *et al*., 2007; Stensola *et al*., 2012). Interestingly, the rescaling was not coherent across grid modules, and each grid module appears to respond independently to the wall translocations. Grid cells within the same grid modules however always respond coherently. Modules with smaller grid scale were observed to be more resistant to rescaling while grid modules with larger grid scale rescale completely (Stensola *et al*., 2012). This finding suggests that grid modules may function independently with grid cells within the same modules connected strongly while grid cells across modules connected weakly.

1.2.3.3 Realignment in grid cells

Grid cells were also found to reorganize their firing patterns when the environments were changed, akin to the remapping process observed in place cells (see Section 1.2.1.3). The reorganization, however, does not manifest as appearance or disappearance of place fields (as seen in global and partial remapping; see Section 1.2.1.3), but instead is observed as translation and/or rotation of firing fields between two distinct environments (Fyhn *et al*., 2007; Barry *et al*., 2012; Marozzi *et al*., 2015). The types of realignment (translation and/or rotation) observed may be dependent on the types of changes made to the environment as changes in non-spatial contextual cues (e.g. colours and odours of walls and flooring) resulted in translation but not rotation of grid fields (Marozzi *et al*., 2015).

Fyhn *et al*. (2007) further examined how grid cells and place cells 'co-remapped' by co-recording hippocampal place cells and layer II grid cells. Interestingly, realignments of grid cells were observed only when place cells globally remapped but not when they rate remapped, suggesting that grid cells and place cells coherently change the positions of their firing fields. This is in line with theoretical models of layer II grid cells, which are upstream of place cells (Witter *et al*., 2014), generating place fields via convergence in synaptic connections from grid modules of different spatial scales (McNaughton *et al*., 2006; Solstad *et al*., 2006).

The realignment of grid cells is also corroborated by Barry *et al*., (2012), who recorded grid cells when an animal was exposed to a novel environment. In addition to realignment, grid cells were also observed to expand when the animals were first placed in the environment. The expansion in grid scale, unlike grid realignment, disappeared over days as animals became more familiar with the environment and is thus believed to signal for environmental novelty.

1.2.4 Boundary vector cells

Boundary vector cells are cells that fire when an animal is in close proximity to a boundary in a specific allocentric direction (Figure 1.2). They have been reported in medial entorhinal cortex and dorsal subiculum (Solstad *et al*., 2008; Lever *et al*., 2009).

Compared to place, HD and grid cells, less is known about boundary vector cells. Nonetheless, boundary vector cells were found to be stable in the dark, suggesting that visual input is not necessary for their firing activity (Lever *et al*., 2009). In addition, they were found to respond similarly to different boundaries that require different sensory representations (e.g. walls versus drop-edge), thus indicating that boundary vector cells are not defined by a single sensory modality (Solstad *et al*., 2008; Lever *et al*., 2009; Stewart *et al*., 2014).

1.2.4.1 Boundary vector cell model for place field generation

Boundary vector cells represent an interesting population of cells whose existence and firing properties were predicted by the boundary vector cell model (O'Keefe and Burgess, 1996; Barry *et al*., 2006) before they were eventually discovered (Solstad *et al*., 2008; Lever *et al*., 2009). The model was first conceived based on the observation that place cells are sensitive to the walls (hence boundaries) in an environment and place fields were seemingly scaled in environments with different shape and sizes such that the fields were stretched along the axes that were 'moved' (O'Keefe and Burgess, 1996).

In the model, O'Keefe and Burgess (1996) posited that place fields in an environment can be generated via a population of cells that have spatially constrained firing fields defined by a specific boundary in an allocentric direction (i.e. boundary vector cells; see Figure 1.9A). These cells have gaussian tuning curves with firing activity that peaked at a preferred distance from a wall in a preferred allocentric direction. Convergence and thresholded sum of these boundary

vector inputs could then generate place fields (Figure 1.9B). The discovery of boundary vector cells thus corroborated the model. In concordance with the model (O'Keefe and Burgess, 1996; Barry *et al.*, 2006), these cells exhibited additional firing fields in the same allocentric direction when additional walls ere added, or when drop edges were created (Solstad *et al.*, 2008; Lever *et al.*, 2009; Stewart *et al.*, 2014).

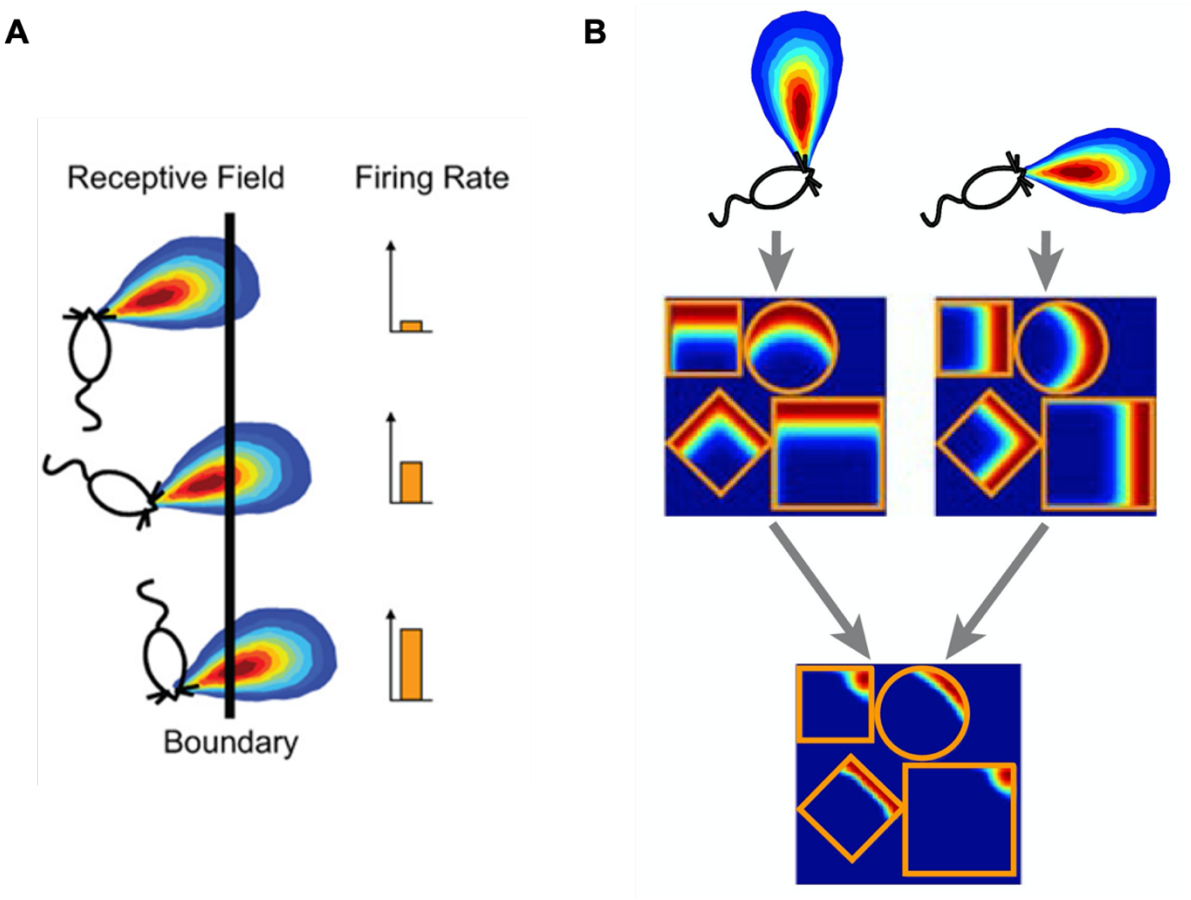

Figure 1.9: Boundary vector cell model. (A) Boundary vector cells were modelled as cells that have receptive fields sensitive to a boundary in a specific allocentric direction. They fire optimally at a specific distance away from the boundary. For instance, the example modelled cell is sensitive to a boundary in the east location, and fire optimally when the animal is close to the boundary. *Adapted from Lever et al. (2009).* **(B)** Convergence and thresholded sum of multiple boundary vector cells with different preferred firing directions and distances can generate place fields, similar to those seen in place cells. *Adapted from Bush et al. (2014).*

It is however surprising that boundary vector cells were primarily described in dorsal subiculum, the main hippocampal output structure (see Section 1.3.1; van Strien *et al.*, 2009; O'Mara, 2005). Interestingly, recent studies have shown that dorsal subiculum back-projects to CA1 (Sun *et al.*, 2014; Sun *et al.*, 2018; Sun *et al.*, 2019) and deep layers of medial entorhinal cortex (Winter *et al.*, 2014; Roy *et al.*, 2017), and these back-projections are ideal candidates for

propagation of boundary information from dorsal subiculum to CA1 and medial entorhinal cortex respectively. However, temporary inactivation of the dorsal subiculum → CA1 projections using chemogenetics did not disrupt or modify the spatial selectivity of CA1 place cells (Sun *et al*., 2019), suggesting that the role of these back-projections in generating place fields may be limited. Thus, the role of boundary vector cells in generating place fields has yet to be clarified experimentally and it remains likely that boundary information from dorsal subiculum may reach hippocampal place cells via medial entorhinal cortex.

1.3 Neuroanatomical organization of the spatial signals

In the previous section, we have explored the properties of the major spatial cell types and their roles in spatial memory and cognition. However, these cell types do not exist independently and interact extensively in the brain so as to generate a coherent representation of the environment. In this section, we will examine the brain structures in which these spatial cells are found as well as the connectivity between them, so as to better understand how these seemingly different spatial signals can come together to form an internal representation of the environment.

1.3.1 Place and boundary vector cells in hippocampal formation

The hippocampus, where place cells were first discovered, first came into prominence due to patient Henry Molaison (best known as patient H.M.), who after bilateral surgical removal of hippocampus and neighbouring medial temporal lobe structures, suffered from severe anterograde amnesia (i.e. inability to form new memories). This observation, together with observations from other patients, led to the seminal conclusion that hippocampus is critical for memory (Scoville and Milner, 1957).

In rats, the hippocampus formation (HF) consists of the hippocampus proper (which includes CA1, CA2 and CA3), dentate gyrus and subiculum. As mentioned, place cells are found in the hippocampus proper and dentate gyrus, while boundary vector cells are found in the subiculum. Unlike the rest of the cortex, the HF only has three layers instead of six –a deep layer composed of afferent and efferent fibres and interneurons; a cell layer with principal neurons and

interneurons; and a superficial layer. In the hippocampus proper, the deep layer is known as stratum oriens, the cell layer is known as the stratum pyramidale (pyramidal cell layer) and the superficial layer is further divided into two layers: stratum radiatum and stratum lacunosum-moleculare. The apical dendrites of pyramidal neurons and apical tufts of the apical dendrites are located in the stratum radiatum and stratum lacunosum-moleculare respectively. CA3 has an additional layer in the superficial layer known as stratum lucidum which receives inputs from dentate gyrus (Figure 1.10A; van Strien *et al*., 2009).

Classically, the anatomical connections within hippocampus are described to exist in a 'trisynaptic loop'. As the name suggests, the loop involves three sequential synaptic connections (Figure 1.10B) starting from entorhinal cortex, the major cortical structure providing inputs into hippocampus. Entorhinal cortex projects mainly to the dentate gyrus (synapse 1), which in turn projects to CA3 (synapse 2). CA3 then projects to CA1 (synapse 3) which outputs back to subiculum and entorhinal cortex (Andersen *et al*., 1971; Knierim, 2015).

It is however now generally accepted that the anatomical connectivity within the hippocampus is more complicated than a serially connected circuit (more details in Figure 1.10C). For example, medial entorhinal cortex is now known to project to all sub-regions of hippocampus proper with layer II projecting to dentate gyrus and CA3 (input site for the trisynaptic loop), and layer III projecting directly to CA1 and subiculum. CA1 in turn projects back to deep layers of entorhinal cortex, either directly or indirectly via subiculum (Witter *et al*., 2014). The direct medial entorhinal cortex layer III → CA1 projections appear to be sufficient for maintaining place cell activity in CA1 as lesioning dentate gyrus or removal of CA3 inputs did not disrupt place fields in CA1 (McNaughton *et al*., 1989; Brun *et al*., 2002). In support of this, selective lesions in layer III of medial entorhinal cortex impaired place cells in CA1, but not in CA3, such that the place fields in CA1 were observed to be larger and more diffuse (Brun *et al*., 2008).

In addition, back-projections are known to exist between all sub-regions (not shown in Figure 1.10C; van Strien *et al*., 2009) including CA3 back-projecting to dentate gyrus (Li *et al*., 1994; Scharfman, 1994), CA1 back-projecting to CA3 (Sik *et al*., 1994; Sik *et al*., 1995) and subiculum back-projecting to CA1 (Sun *et al*., 2014; Sun *et al*., 2018; Sun *et al*., 2019). The projections from subiculum to CA1 may have a limited role in propagating boundary information from boundary vector cells to place cells (see Section 1.2.4.1).

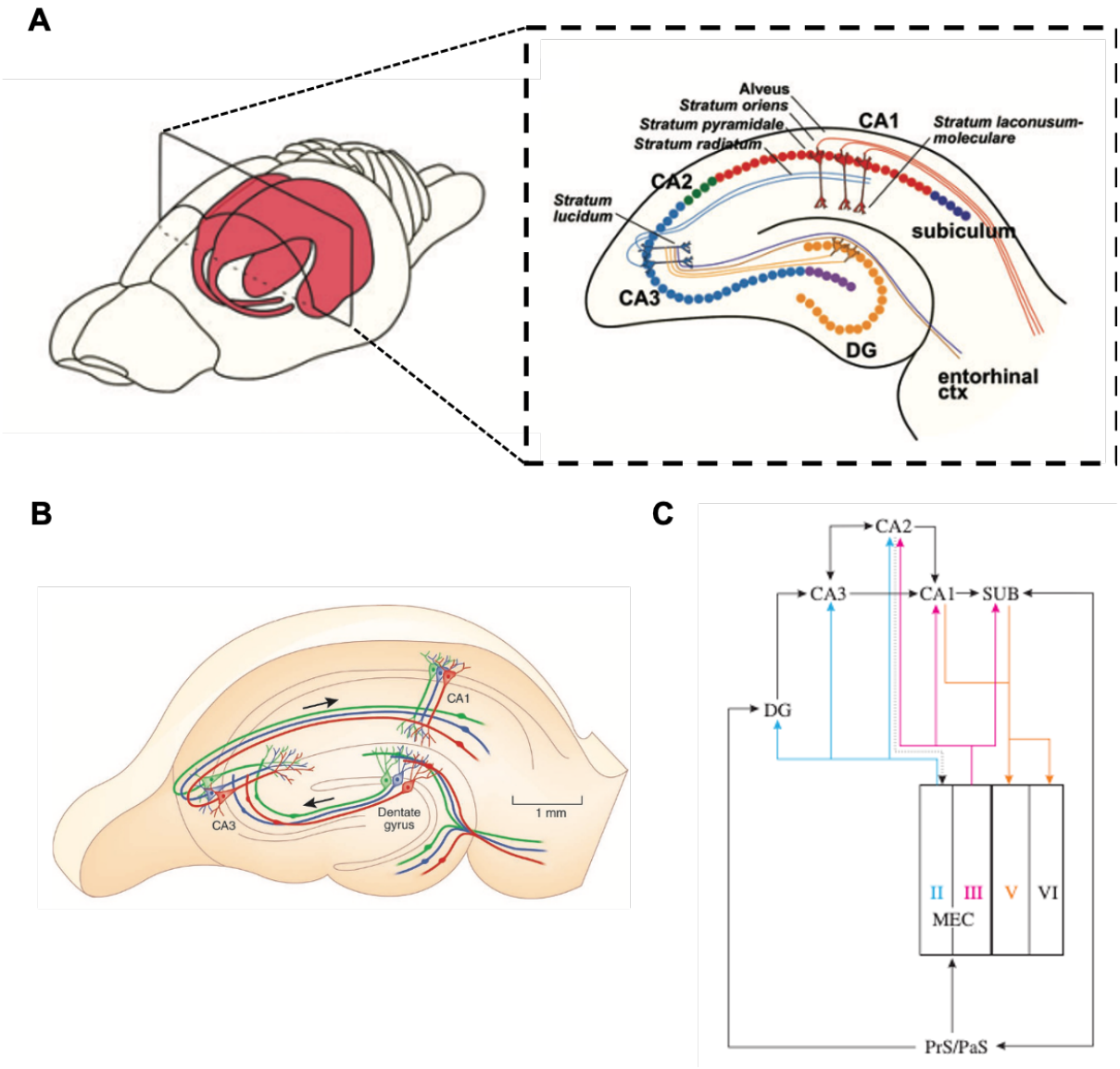

Figure 1.10: Hippocampus structure and circuitry. (A) The hippocampal formation in the rat brain shown in red on the *left*. A coronal slice through the rat hippocampus formation shows the different sub-regions of the hippocampus formation including the dentate gyrus (DG; orange), CA3 (light blue), CA2 (green), CA1 (red) and subiculum (dark blue). *Adapted from Temido-Ferreira et al. (2019).* **(B)** The classical trisynaptic loop with inputs into hippocampus coming primarily from entorhinal cortex to dentate gyrus. Dentate gyrus then projects to CA3, which in turn projects to CA1. CA1 then project to the subiculum and entorhinal cortex. *Adapted from Moser (2011).* **(C)** An updated view of the connections within the hippocampus formation, and its interaction with medial entorhinal cortex. Specifically, layer II and III of medial entorhinal cortex projects to all sub-regions of hippocampus, unlike the serial connections described in the trisynaptic loop. CA1 and subiculum also project back to deep layer of medial entorhinal cortex. *DG: dentate gyrus; SUB: subiculum; MEC: medial entorhinal cortex; PrS: Presubiculum; PaS: Parasubiculum. Adapted from Witter et al. (2014).*

Although grid cells are generally thought to be upstream of place cells (via medial entorhinal cortex layer II/III → CA1/CA3; McNaughton *et al.*, 2006; Solstad *et al.*, 2006), it is likely that place cells also project to grid cells (via CA1/subiculum → medial entorhinal cortex layer V)

as grid cells have also been described in deeper layers of medial entorhinal cortex (Sargolini *et al*., 2006). These 'back-projections' were thought to help reduce errors accumulated during path integration by propagating sensory information from the place cell network to the grid cell network (Bush *et al*., 2014). However, instead of observing drifts in the grid patterns (as would be expected if place cells are truly only required to 'anchor' grid cells to the external environment), disruption of grid patterns were observed when hippocampus was inactivated. This finding suggests that the back-projections are likely to play a more integral role in grid cell activity (Bonnevie *et al*., 2013). Interestingly, hippocampus disruptions (either temporarily via muscimol or permanently via lesion) were found to increase directional tuning in grid cells that were previously non-directional or weakly directional, suggesting an independence of HD cell inputs from place cell inputs (Bonnevie *et al*., 2013; Fyhn *et al*., 2004). This is in line with findings showing that hippocampal lesions did not affect properties of HD cells in postsubiculum and anterior thalamus, and their PFDs remained largely stable across days (Golob and Taube, 1997; Golob and Taube, 1999).

1.3.2 Head direction cells and the Papez circuit

The connectivity within the HD system is arguably more complicated than the other spatial systems and HD cells have been found in multiple brain regions previously implicated in the classical Papez circuit including dorsal tegmental nucleus (Sharp *et al*., 2001), anterodorsal thalamus (Taube, 1995), postsubiculum (Taube *et* al., 1990a, 1990b), lateral mammillary nucleus (Stackman and Taube, 1998) and entorhinal cortex (Sargolini *et al*., 2006; Giocomo *et al*., 2014). In addition, HD cells have been described in laterodorsal thalamus (Mizumori and Williams, 1993) and retrosplenial cortex (Chen *et al*., 1994; Cho and Sharp, 2011).

Why are there redundancy in the head direction system? Although the functional significance of the redundancy remains unclear, there are indications that the different brain regions may reflect steps in integration of sensory information into the HD network. This section will be dedicated to exploring interactions within the HD networks, before examining its position within the entire spatial network.

1.3.2.1 Hierarchy in the HD network

An interesting property of the HD network comes fundamentally from lesion studies suggesting that the different HD regions may be organized hierarchically with directional

information flowing through the network from dorsal tegmental nucleus → lateral mammillary nucleus → anterodorsal thalamus → the cortical regions (Figure 1.11). Specifically, bilateral lesions of dorsal tegmental nucleus or lateral mammillary nucleus were found to disrupt HD cells in anterodorsal thalamus (Blair *et al*., 1998; Blair *et al*., 1999; Bassett *et al*., 2007), postsubiculum and medial entorhinal cortex (Sharp and Koeste, 2008). Similarly, bilateral lesions of anterodorsal

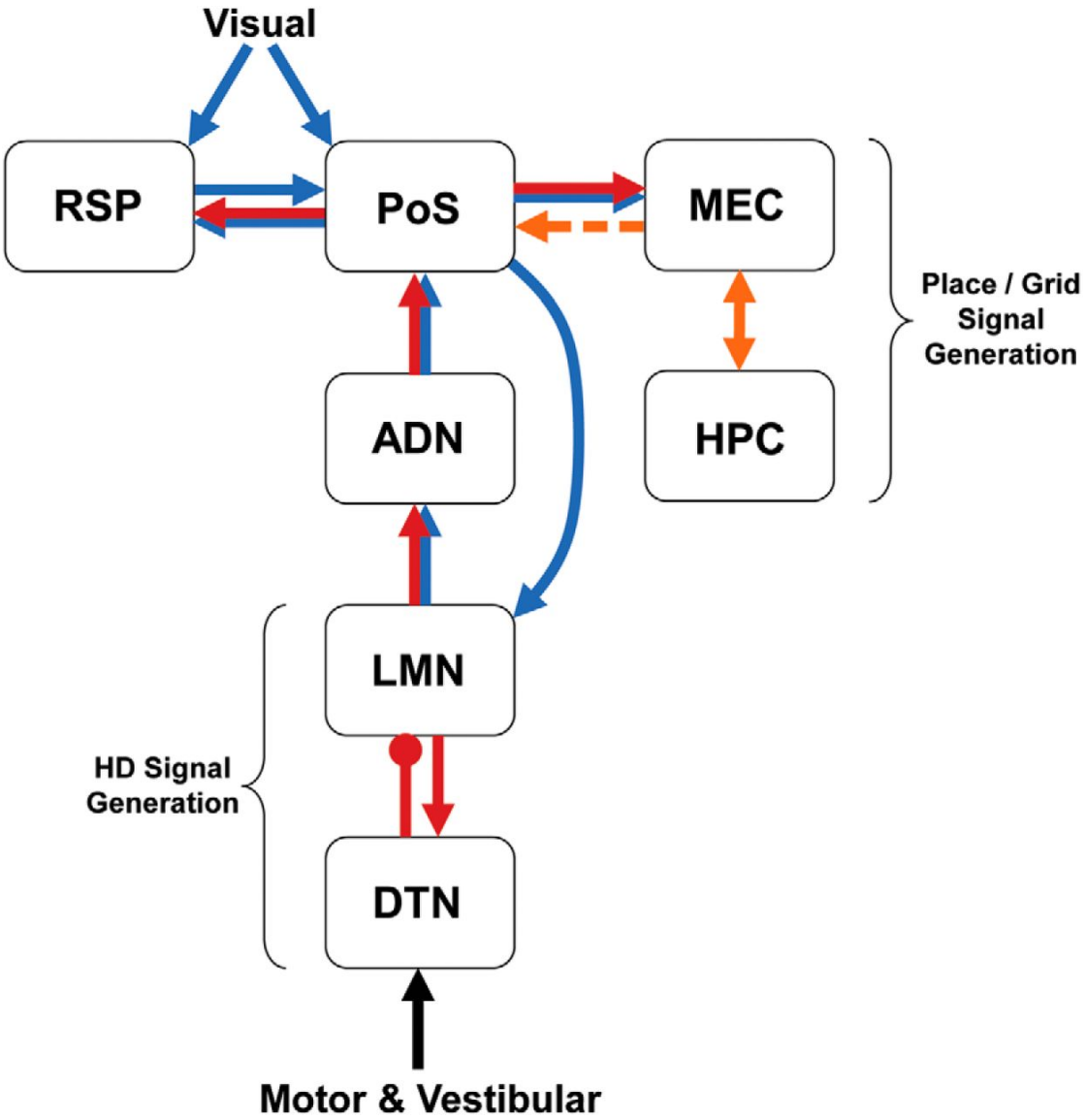

Figure 1.11: Schematic diagram of the HD network and its interactions with the grid and place cell network. The HD network is believed to be organized hierarchically with motor and vestibular information being integrated via dorsal tegmental nucleus (DTN) or lateral mammillary nucleus (LMN). The vestibular and motor information then ascend through the network (red arrows) from LMN to anterodorsal thalamus (ADN) to postsubiculum and eventually the medial entorhinal cortex (MEC). Meanwhile, visual (and landmark) information is fed into the network via retrosplenial cortex (RSP) and/or postsubiculum (PoS) and is propagated to MEC. At the same time, the visual information is feedback to LMN (blue arrows). Place and grid cells may provide additional spatial information back to the HD network via MEC connections with the postsubiculum (orange arrows). *Adapted from Yoder et al., 2015*.

thalamus were found to disrupt HD cells in postsubiculum (Goodridge and Taube, 1997) and medial entorhinal cortex (Winter *et al.*, 2015). The contrasting effect however was not observed, that is lesions of either postsubiculum, retrosplenial cortex or medial entorhinal cortex did not disrupt HD signals in anterodorsal thalamus (Goodridge and Taube, 1997; Clark *et al.*, 2010; Clark *et al.*, 2011) or lateral mammillary nuclei (Yoder *et al.*, 2015). Lesions of laterodorsal thalamus did not disrupt HD cells in postsubiculum (Golob *et al.*, 1998), which suggests that laterodorsal thalamus, unlike anterodorsal thalamus, is not necessary for HD cells in postsubiculum to function.

In addition to lesion studies, investigations of the relative timing of the peak firing direction of HD cells with the current heading of the animals (also known as 'anticipatory time interval') also tell a similar story. Particularly, HD cells in the lateral mammillary nucleus lead that of current heading by approximately 40-60ms and that of anterior thalamus by 15-20ms (Stackman and Taube, 1998; Blairs *et al.*, 1998). The HD cells in the anterior thalamus in turn lead that of current heading by approximately 20s (Blair and Sharp, 1995; Blairs *et al.*, 1997; Taube and Muller, 1998). Meanwhile, HD cells in postsubiculum do not fire ahead of the current heading direction and seemingly encode the present heading of the animal (Blair and Sharp, 1995; Taube and Muller, 1998). Interestingly, unlike postsubiculum HD cells, retrosplenial HD cells were also found to anticipate present heading by approximately 25-50ms (Cho and Sharp, 2001; Lozano *et al.*, 2017). Thus, HD cells in retrosplenial cortex may be upstream of those in postsubiculum.

The hierarchical nature of the HD network, suggested by lesions and anticipatory time interval studies, is also in line with neuroanatomical connectivity studies: dorsal tegmental nucleus is known to project to lateral mammillary nucleus (via GABAaergic projections; Allen and Hopkins, 1989; Wirtshafter and Stratford, 1993; Liu *et al.*, 1984), which in turn project to anterodorsal thalamus (Shibata, 1992). Anterodorsal thalamus is also known to project to retrosplenial cortex (van Groen and Wyss, 1990a; van Groen and Wyss, 1992; van Groen and Wyss, 1995; van Groen and Wyss, 2003) and postsubiculum (van Groen and Wyss, 1990b; van Groen and Wyss, 1995), the latter of which projects to hippocampus via medial entorhinal cortex (Figure 1.10; van Groen and Wyss, 1990b, Caballero-Bleda and Witter, 1993; Huang *et al.*, 2017; Preston-Ferrer *et al.*, 2016).

In addition to the feed-forward hierarchically organized connections, there are multiple feedback and reciprocal connections within the HD network, which suggest a more complex

interaction between the different HD regions in contrast to a simple feedforward circuit. For example, postsubiculum and retrosplenial cortex are reciprocally connected to each other (van Groen and Wyss, 1990a; van Groen and Wyss, 1990b; van Groen and Wyss, 1992; van Groen and Wyss, 2003; Preston-Ferrer *et al*., 2016; Kononenko and Witter, 2012). Back-projections were also observed with postsubiculum projecting back to anterodorsal thalamus (van Groen and Wyss, 1990b; Wright *et al*., 2010; Yoder and Taube, 2011; Huang *et al*., 2017), retrosplenial cortex to anterodorsal thalamus (Wright *et al*., 2010; van Groen and Wyss, 2003) and laterally mamillary nucleus to dorsal tegmental nucleus (Hayakawa and Zyo, 1990; Allen and Hopkins, 1989; Liu *et al*., 1984). Postsubiculum was also found to project back to lateral mammillary nucleus (van Groen and Wyss, 1990b; Allen and Hopkins, 1989; Huang *et al.,* 2017; Yoder and Taube, 2011; Shibata, 1989).

What could then be the reason behind the hierarchical organization in the HD circuit? It seems likely that the different steps in the network could reflect steps in integrating sensory information into the HD network. For example, vestibular information is believed to be integrated into the HD network via dorsal tegmental nucleus. This is supported by neuroanatomical studies showing that dorsal tegmental nucleus receives direct projections from medial vestibular nucleus (Liu *et al*., 1984) which in turn receives projections from the horizontal semi-circular canals (Khan and Chan, 2013), an organ within the inner ear that detects rotational acceleration. However, the former projections (medial vestibular nuclei → dorsal tegmental nuclei) have not been replicated in a recent study (Biazoli Jr *et al*., 2006) and it seems more likely that vestibular information reaches the dorsal tegmental nucleus indirectly via supragenual nucleus and nucleus prepositus. Both supragenual nucleus and nucleus prepositus receive projections from the medial vestibular nuclei (Biazoli Jr. *et al*., 2006; Iwasaki *et al*., 1999) and project to dorsal tegmental nucleus (Liu *et al*., 1984; Biazoli Jr *et al*., 2006), making them ideal candidates in the pathway for propagating vestibular information to the HD network. The neuroanatomy is corroborated by lesion studies showing that HD cells in anterodorsal thalamus were disrupted when supragenual nucleus and nucleus prepositus were bilaterally lesioned (Clark *et al*., 2012; Butler and Taube, 2015).

In addition to vestibular information, motor information is also believed to be propagated to the HD network at the level of dorsal tegmental nucleus via the interpeduncular nucleus-lateral habenula circuit (Taube, 2007). Specifically, lateral habenula receives inputs from the entopeduncular nucleus (also known as globus pallidus, pars interna; Wallace *et al.,* 2017; van

der Kooy and Carter, 1981), a subcortical structure known to be involved in motor control (Nelson and Kreitzer, 2014). Lateral habenula is known to project to interpeduncular nucleus (Contestabile and Flumerfelt, 1981), and both structures project to dorsal tegmental nucleus (Liu *et al*., 1984; Contestabile and Flumerfelt, 1981). Thus, they are ideally situated for integrating motor information from the basal ganglia to the HD network. Motor information may however play a smaller role than vestibular information as lesioning the interpenduncular nucleus did not disrupt HD cells in anterodorsal thalamus, although the HD cells had altered firing properties including reduced peak firing, larger PFD widths, longer anticipatory time interval, and were less sensitive to visual landmarks (Clark *et al*., 2009).

In contrast, visual information is believed to be integrated into the head direction network via retrosplenial cortex and/or postsubiculum. Both structures have reciprocal connections with visual cortex and with each other (van Groen and Wyss, 1992; van Groen and Wyss, 1990b; van Groen and Wyss, 2003; Vogt and Miller, 1983). Lesions in both structures did not disrupt HD signals in either anterodorsal thalamus or lateral mammillary nucleus but impaired landmark anchoring (Goodridge and Taube, 1997; Clark *et al*., 2010; Yoder *et al*., 2015), corroborating their roles in visual processing. Additionally, directional cells that are sensitive to the local visual scene have been found in the retrosplenial cortex, which may be important for integrating visual information into the HD network (see Section 2.3.1 for a detailed description of these cells; Jacob *et al*., 2017). Recent two-photon imaging studies in head-fixed mice have also found visually evoked responses (Powell *et al*., 2020) as well as visual landmark-aligned signals (Fischer *et al*., 2020) in the retrosplenial cortex. Interestingly, these visual neurons were also modulated by locomotion (Powell *et al*., 2020; Fischer *et al*., 2020) although the motor inputs did not contribute to the spatial tunings of the neurons (Fischer *et al*., 2020).

1.3.2.2 HD network and the other spatial networks

The HD network does not function independently and is coupled to the place and grid cell network via the projections from postsubiculum to medial entorhinal cortex (Figure 1.11; van Groen and Wyss, 1990b, Caballero-Bleda and Witter, 1993; Huang *et al*., 2017; Preston-Ferrer *et al*., 2016). In line with the anatomical connections, conjunctive grid and head direction cells have been reported in the medial entorhinal cortex – many of which are located in layer III and V (Sargolini *et al*., 2006).

What happens to grid and place cell representations when structures within the HD network are disrupted? Temporary inactivation or lesion of the anterior thalamus disrupted the spatial periodicity of grid cells in medial entorhinal cortex and parasubiculum, suggesting that anterior thalamus is necessary for the generation of grid fields (Winter *et al*., 2015). Unexpectedly, given that grid cells were thought to be involved in the generation of place fields, the same effect was not observed for place cells. Lesions of lateral mammillary nucleus, anterodorsal thalamus or postsubiculum did not disrupt place cell activity, although the place fields are noisier (Calton *et al*., 2003; Sharp and Koester, 2008; Harland *et al*., 2017). Interestingly, place cells rotated their place fields unpredictably between sessions in animals with postsubiculum lesions but not in animals with anterodorsal thalamus lesions, further supporting a visual role for postsubiculum in the spatial network (Calton *et al*., 2003).

It is however surprising that anterodorsal thalamus lesions did not disrupt landmark anchoring of place cells between sessions given that anterodorsal thalamus lesion is known to disrupt HD cells in postsubiculum (Goodridge and Taube, 1997). The discrepancy can be accounted via two non-mutually exclusive explanations. Firstly, visual information may not be solely propagated to grid and place cells via HD cells and there may be a parallel, HD independent visual information propagating neural circuit from postsubiculum to hippocampus. Alternatively, it remains unclear if anterodorsal thalamus lesions disrupt HD cells in retrosplenial cortex. As such, HD cells in retrosplenial cortex may persist after anterodorsal thalamus lesions and may hence function as a second pathway for visual information to reach place cells (Figure 1.11). A visual role for retrosplenial cortex is corroborated by Cooper and Mizumori (2001), who temporarily inactivated retrosplenial cortex and recorded place cells while the animals performed a spatial memory task on a radial maze. Similar to Calton *et al*. (2003), place cell properties were mostly unaltered, but place fields were found to be unstable and partially remapped upon inactivation of retrosplenial cortex (Cooper and Mizumori, 2001).

1.3.3 Grid cells in medial entorhinal cortex

As observed in the previous sections, the medial entorhinal cortex (and hence the grid cell network) is located at the intersection of the spatial system (Figure 1.10; Figure 1.11). The HD network provides HD inputs via the projections from postsubiculum (van Groen and Wyss, 1990b; Caballero-Bleda and Witter, 1993; Huang *et al*., 2017; Preston-Ferrer *et al*., 2016) while the

medial entorhinal cortex is reciprocally connected with hippocampus (and hence, the place cell network; see Section 1.3.1). As such, the medial entorhinal cortex is often thought to be an important node for cortico-hippocampal interactions and may serve to integrate the spatial signals. In line with this, conjunctive HD and grid cells have been observed in medial entorhinal cortex (Sargolini *et al*., 2006), which may represent a step in the integration of HD signals into the grid cell network.

In concordance with a downstream position of medial entorhinal cortex relative to the HD network, lesioning medial entorhinal cortex did not abolish or affect HD signals in anterodorsal thalamus (Clark *et al*., 2011). In contrast to the HD network, grid cells were observed to be disrupted when hippocampus was lesioned (see Section 1.3.1; Bonnevie *et al*., 2013), suggesting an essential role for the projections from hippocampus to medial entorhinal cortex in generating grid cell activity. This finding was surprising as grid cells were often thought to be upstream of place cells (instead of the other way around) and may generate place fields through linear summation of grids with different scales (McNaughton *et al*., 2006; Solstad *et al*., 2006). Thus, the interactions between grid cells in medial entorhinal cortex and place cells in hippocampus may be more complex than previously conceived.

In agreement with a more complex interaction rather than a unidirectional flow of grid information into place cells, lesions and inactivation of medial entorhinal cortex did not disrupt formation of place fields although place fields were found to be less stable (Miller and Best, 1980; Hales *et al*., 2014; van Cauter *et al*., 2008; Brun *et al*., 2008; Ormond and McNaughton, 2015; Miao *et al*., 2015; Navawongse and Eichenbaum, 2013; Rueckemann *et al*., 2016). Interestingly, changes in place cell properties were found to differ between studies upon inactivation or lesions of medial entorhinal cortex. For example, some studies reported a broadening of place fields (Hales *et al*., 2014; Brun *et al*., 2008; Ormond and McNaughton, 2015) while others reported no change (Miao *et al*., 2015; Rueckemann *et al*., 2016) or reduction in place field size (van Cauter *et al*., 2008). The differences may be a consequence of the lesion extent (e.g. van Cauter *et al*. (2008) lesioned lateral entorhinal cortex, in addition to medial entorhinal cortex) or the temporal and spatial specificity of inactivation (e.g. Reukemann *et al*. (2016) and Miao *et al*. (2015) used chemogenetics and/or optogenetics to inactivate medial entorhinal cortex). Nonetheless, it is clear that place cells are still present when medial entorhinal cortex is disrupted, providing evidence against a unidirectional generative role of grid cells in forming place fields.

1.4 Summary

In this chapter, we have explored the neural substrates that underlie the cognitive map – the four main components being place cells, grid cells, head direction cells and boundary vector cells. Each component of the spatial system plays a crucial role in navigation by providing location, metric, directional and boundary information respectively. They interact extensively in the brain (see Section 1.3) with the medial entorhinal cortex (and by extension, the grid cell system) being positioned at the intersection of the spatial system and seemingly integrating the different spatial signals such that the spatial representation of an environment is coherent.

How then does the spatial system represents more complex environments? In their natural environment, humans do not live in open environments and/or linear tracks - environments which are commonly used in the laboratory. Instead, we often live in complex environments which are compartmentalised (e.g. offices within a building; flats within an apartment block; hotels and their rooms), of which some compartments can look remarkably similar. How then do we localize ourselves within such environment? Can our brain discriminate such compartmentalised, visually similar local spaces that are embedded within a global environment? The next chapter would be dedicated to discussing the spatial representations in such environments, before we dive into the experiments at hand.

Chapter 2.

Navigation in Visually Similar Compartmentalised Environments

In the previous chapter, we have examined the neural substrates underlying navigation and reviewed the properties of the different spatial cells. However, much of our understanding of these cells comes from studies which were done in relatively simple environments such as open-field environments and/or linear tracks. Humans and animals, however, do not live in simplistic environments and often interact and navigate through compartmentalised spaces that may look visually similar. For example, many of us live in apartment buildings, stay in hotels with similar looking rooms when we travel, and work in office buildings with multiple visually similar offices. Animals also navigate through compartmental spaces with the most prominent example coming from burrowing animals such as the naked mole rats. Specifically, naked mole rats (and other

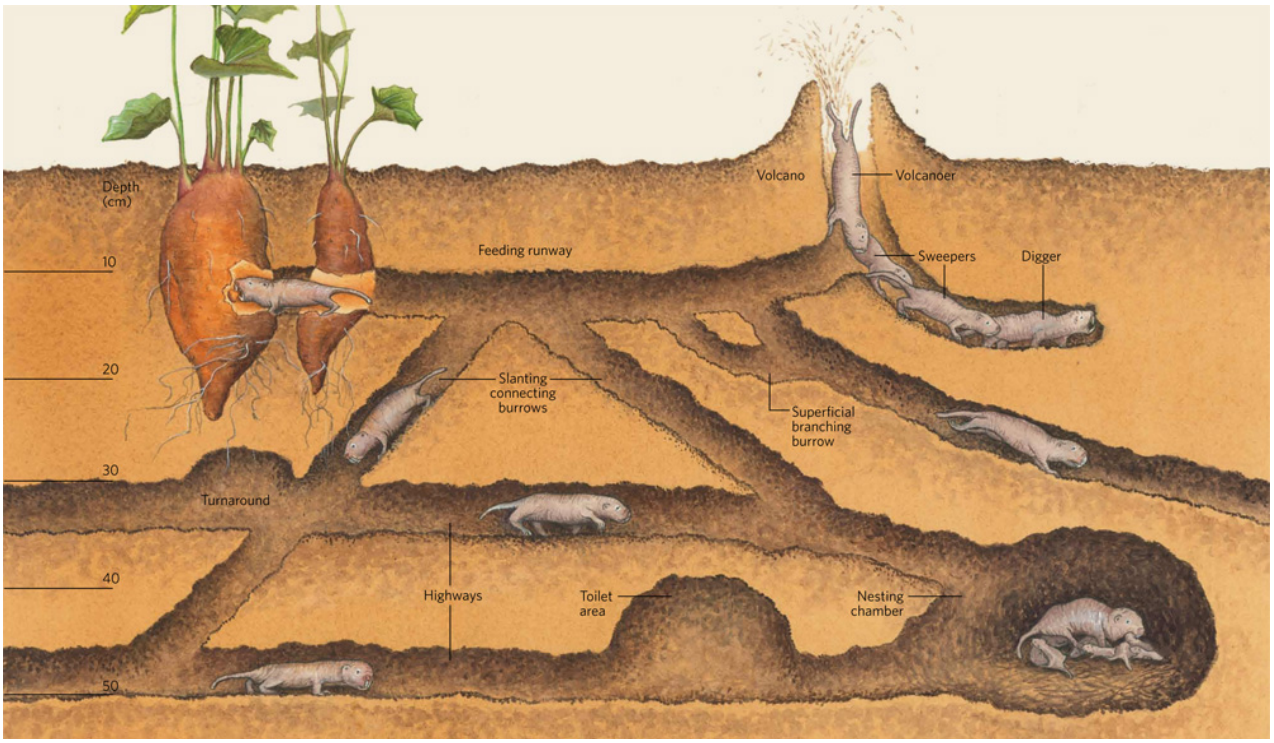

Figure 2.1: Underground tunnels and chambers in the lives of the naked mole rats. Naked mole rats live in intricate subterranean tunnels and chambers, through which they would have to navigate. *Adapted with permission. Illustration by Logan Parsons Illustration from: www.parsonsillustration.com.*

burrowing animals) often build extensive underground tunnels with chambers (Buffenstein *et al*., 2012; Figure 2.1) through which they would have to navigate.

The question then arises as to how the brains of animals and humans represent these local spaces and if they can distinguish these visually similar compartmentalised spaces? This chapter is thus dedicated to reviewing our current understanding of how the different spatial cells represent local compartmental spaces, focusing especially on the findings from Jacob *et al*. (2017) which inspired the experiments in this thesis.

2.1 Place cells in visually similar compartmentalised spaces

Several studies have examined how place cells represent visually similar compartments, with most studies concurring that a proportion of place cells displayed repeating fields if the compartments were aligned and oriented in the same direction (Figure 2.2A; Skaggs and McNaughton, 1998; Spiers *et al*., 2015; Grieves *et al*., 2016; Fuhs *et al*., 2005). The same repetition of place fields can also be observed in alleyway mazes (Derdikman *et al*., 2009, Singer *et al*., 2010) with place fields seemingly only repeating in alleys that were consistent with the animals' running directions (e.g. a place cell firing only in alleys when the animal is running north; Derdikman *et al*., 2009). Interestingly, these repeating place cells did not disappear with experience in the experiments by Spiers *et al*. (2015) and Grieves *et al*. (2016), and behaved as if they cannot distinguish the compartments even though the animals were able to travel freely between the two compartments (except in Skaggs and McNaughton (1998) and Fuhs *et al*. (2005) where they limited the animals' movements).

Do these findings then suggest that place cells are not privy to linear self-motion cues for updating their place representations in multi-compartments spaces? This is highly unlikely as Skaggs and McNaughton (1998) did a probe trial in which they started the rats in the opposing compartment rather than its usual starting compartment. Interestingly, they observed map shifting in some of their non-repeating place cells such that the place map usually observed in the starting compartment was now observed in the opposing compartment (the new starting compartment; Figure 2.2B, trial 2a). However, when the animals were subsequently allowed to move between the two compartments, the place representation updated accordingly and the place representation now reverted back to its original location prior to the probe trial (Figure 2.2B, trial 2b). Thus, linear self-motion information appears to be available to place cells which can be used to update the

place representations accordingly. Likewise, Grieves *et al*. (2016) showed that similarity in place maps tend to decrease as distances between the compartments increase, potentially implicating an influence of linear distances (and by extension, linear self-motion cues) on place cells.

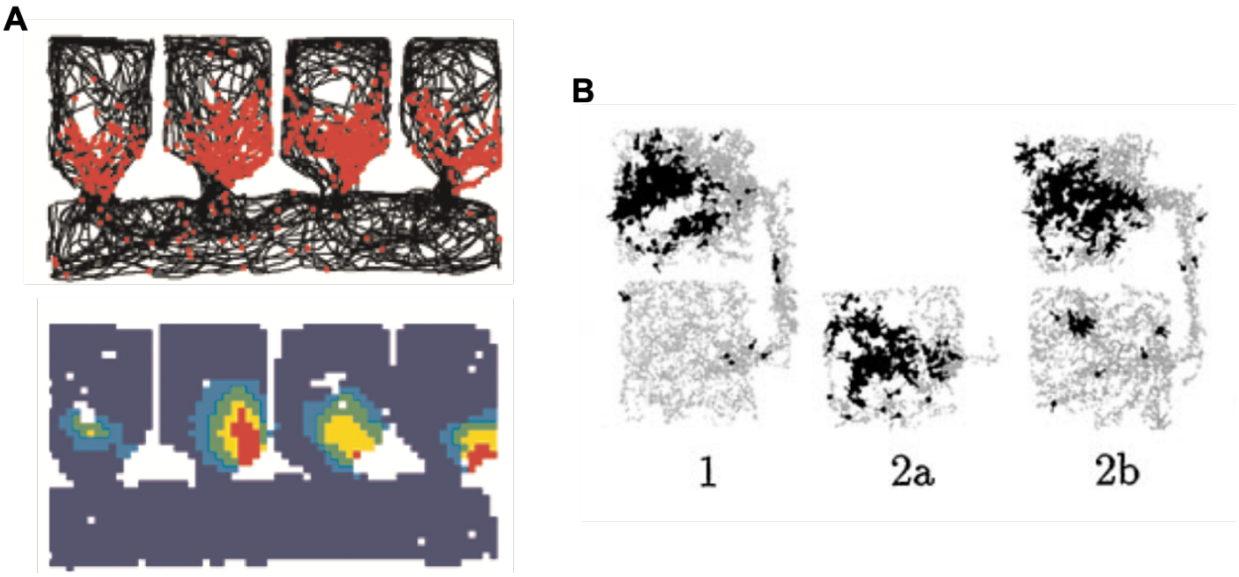

Figure 2.2: Place field repetitions in visually similar multi-compartment environments (A) Place cells have repeating place fields in multi-compartment spaces if the compartments are parallel and oriented in the same direction. *Adapted from Spiers et al. (2015).* **(B)** Place field repetition is unlikely to be due to a lack of linear self-motion inputs. This is evident in the above cell from Skaggs and McNaughton (1998) which had a single field in the north compartment where the animal was consistently started in (see 1). In the probe trial when the animal was started in the south instead, the place field initially found in the north compartment was now found in the south compartment (2A). However, when the animals were allowed to move freely between the two compartments, the place representation updated accordingly (2B) such that the place field reverted back to its original position in the north compartment. This suggests that linear self-motion cues were available to the cell which is then used to update its place representation. *Adapted from Skaggs and McNaughton (1998).*

If linear self-motion cues are likely to be available to place cells, why are place field repetitions then observed? A possible explanation would be that place cells are more sensitive to the local space such that locally derived sensory information (e.g. visual, olfactory, tactile, boundary) dominates over linear self-motion cues. In support, Spiers *et al*. (2015) observed local remapping when either small local changes (e.g. changing the wall colour in one compartment) or large global changes (e.g. changing the global structure by merging three compartments and leaving one compartment intact) were made to the environment. The local remapping observed was mainly restricted to compartments that were changed and firing patterns remained undisturbed in unchanged compartments. In line with these observations, Grieves *et al*. (2018) modelled place cells in multi-compartment environment using the boundary vector cell model and

showed that repeating place fields can be generated via boundary inputs. They however argued that place repetitions can be explained almost entirely by boundary vector inputs. This is unlikely as local remapping was observed when the colour of the walls in a compartment was changed (Spiers *et al*., 2015), thus indicating an interaction between boundary and contextual inputs (such as visual inputs). Hence, a model that could account for the influences of contexts on boundary inputs (such as the earlier version of contextual gating model; Anderson and Jeffery, 2003) may be more relevant.

Although linear self-motion cues play a less important role than local sensory information, directional cues appear to have a dominant effect on place representations in compartmentalised spaces. Particularly, place field repetitions were not observed when compartments were oriented in different directions (Figure 2.3; 60° separation in Grieves *et al*., 2016; 180° separation in Fuhs *et al*., 2005) and/or when the rat need to rotate (and hence had angular self-motion information) when it moved between the compartmental spaces (Fuhs *et al*., 2005; Tanila *et al*., 1999; Derdikman *et al*, 2009). The lack of place field repetitions observed thus suggests that place cells could disambiguate the compartments if differentiating directional cues are made available. Because directional information is thought to be provided by the head direction system, Harland *et al*. (2017) bilaterally lesioned lateral mammillary nucleus and examined place cell activity in the radially arranged multi-compartment environment. In support for an involvement of the HD system, lesions of the lateral mammillary nuclei induced place field repetitions in radially arranged

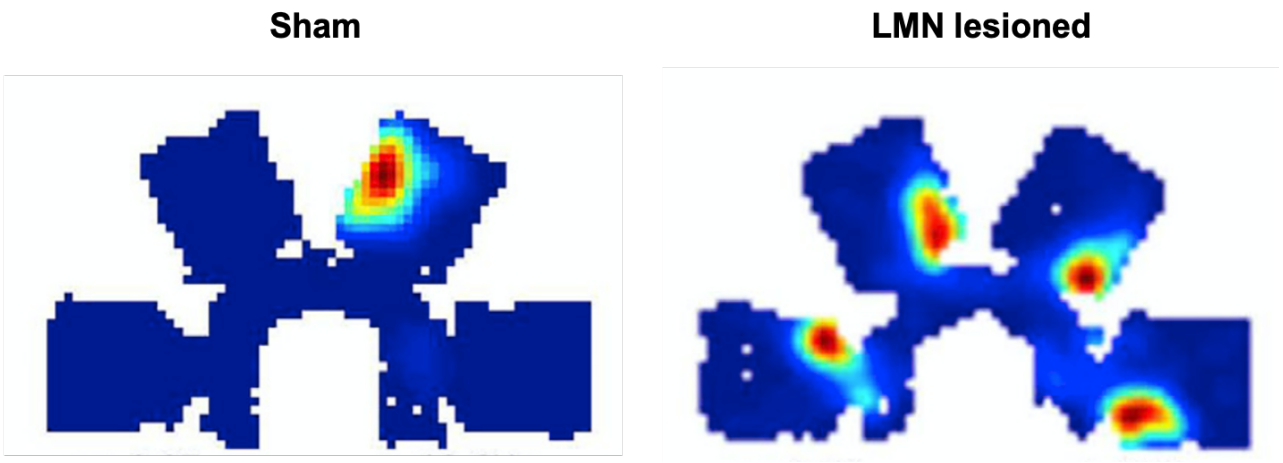

Figure 2.3: The HD system is necessary for disambiguation of visually similar, radially arranged compartments. *Left*: In sham lesioned animals, place cells do not display repeating fields between radially arranged compartments. This suggests that place cells are able to disambiguate compartments when differentiating angular information is available. *Right:* However, when the lateral mammillary nuclei were lesioned, place cells displayed repeating fields similar to those seen when the compartments were arranged in parallel. Thus, the HD system is necessary for disambiguating radially arranged compartments, likely by providing differentiating angular information. *Adapted from Harland et al. (2017)*.

compartments such that the place representations in radially arranged compartments now resemble that of parallel compartments (Figure 2.3). Thus, it is likely that HD cells provide angular information to place cells, which in turn allows place cells to discriminate the compartments when radially arranged.

The ability of place cells in discriminating radially arranged compartments but not parallel compartments implies that animals, by extension, can readily discriminate radially arranged compartments but would be unable to discriminate parallel compartments. To test this hypothesis, Grieves *et al*. (2016) trained animals on an odour-location task and found that learning of the task was significantly impaired in the parallel compartments but not the radially arranged compartments. Surprisingly, animals that first learnt the task in the radially arranged compartments can subsequently better learn the task in parallel compartments, suggesting that animals (and place cells) could possibly disambiguate the parallel compartments after extensive experience. Nonetheless, the same impairment in learning was observed in the radially arranged compartments when lateral mammillary nuclei was lesioned, providing further support for a role of the HD system in providing differentiating angular information (Smith *et al*., 2019). Thus, the behaviours of the animals concur with that of place cells in the multi-compartment environment – both of which are unable to discriminate the multi-compartment environment if differentiating directional cues are not available (i.e. in parallel compartments or when the head direction system is lesioned).

2.2 Grid cells in visually similar compartmentalised spaces

Similar to place cells, grid cells displayed similar fields at the same relative locations between compartments or alleys oriented in the same direction (Figure 2.4; Carpenter *et al*., 2015; Derdikman *et al*., 2009). This suggests that the grid map is also primarily determined by the local visual environment. Although not explicitly tested in the same manner as in place cells, it is also likely that angular self-motion cues play an important role in grid field repetitions. This is evident in the hairpin maze where the locations of grid fields are highly correlated between alleys in which the animals ran in the same direction, but comparatively different between alleys in which the running directions were opposite (Figure 2.4B; Derdikman *et al*., 2009).

Surprisingly, unlike place cells, grid field repetitions disappeared with more experience in the environment and the grid cells gradually formed an unified representation (Figure 2.4A;

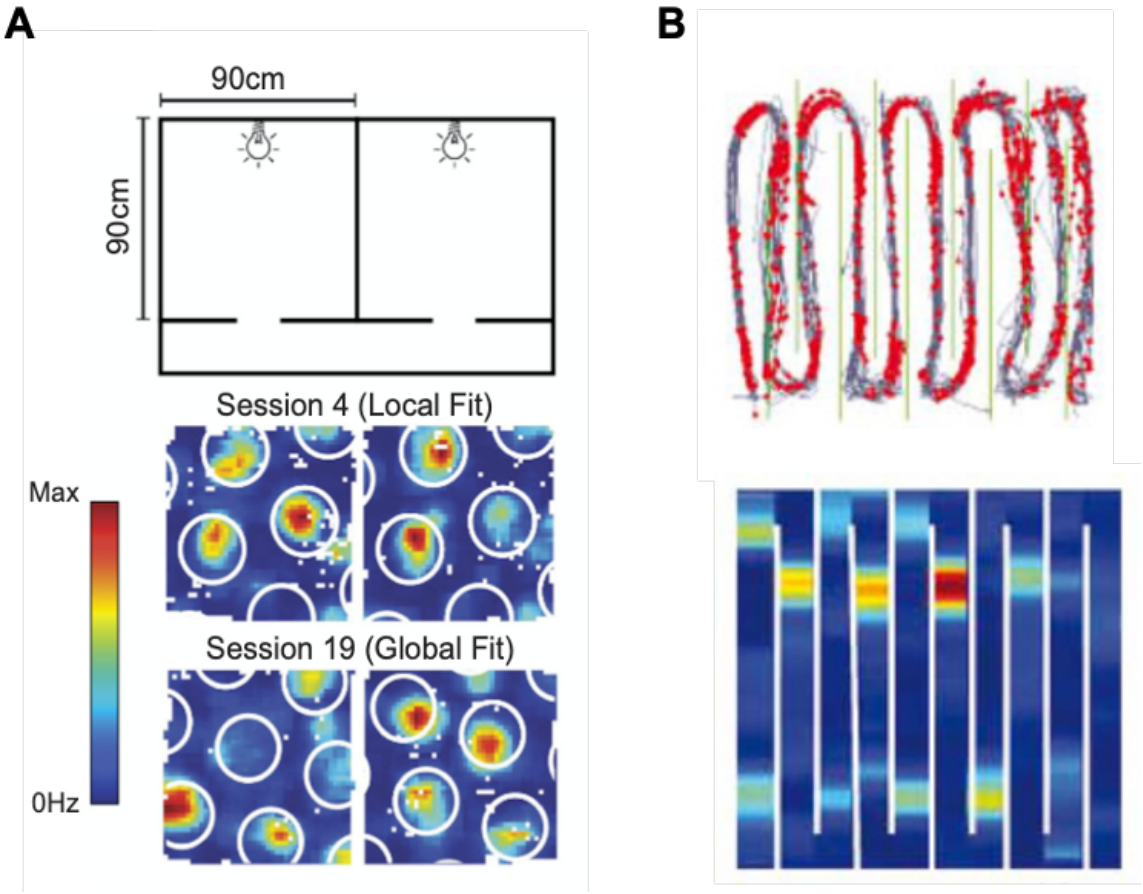

Figure 2.4: Grid field repetitions in visually similar compartmentalised spaces. (A) In a two-compartment environment, grid cells initially showed similar firing patterns between the compartments (Session 4). However, with experience, grid cells repeated less and formed an unified representation of the entire environment (Session 19). *Adapted from Grieves et al. (2017).* **(B)** In the hairpin maze, grid field repetitions were only observed between alleys in which the animals ran in the same direction (e.g. similar grid fields between even alleys). This suggests that angular self-motion cues control grid cell firings in alleys (and compartments), similar to that in place cells. *Adapted from Derdikman et al. (2009)*

Carpenter *et al*., 2015). This finding indicates a gradual switch in grid cells from using local sensory information to using self-motion cues. Using a model that allows for dynamic interactions between entorhinal grid cells and hippocampal place cells, Li *et al*. (2020) suggest that the gradual switch in local grid maps to a global grid map likely reflects a weakening of visual influence on grid cells via the back-projections from place cells as the animals learn the environment (see Section 1.3.1 and 1.3.3). Because grid cells project back to place cells, the weakening of visual influence would eventually propagate back to place cells such that most place cells (with the exception of visual place cells in their model) would eventually disambiguate the environment. However, as described in the previous section, place field repetitions in parallel compartments seemingly do not reduce with experience (~two weeks; Spiers *et al*., 2015; Grieves *et al*., 2016).

Nonetheless, it is possible that if longer recordings were done (> two weeks), place cells may also switch from local place representations to that of a global representation (i.e. reduced field repetitions).

2.3 HD cells in visually similar compartmentalised spaces

As demonstrated by Harland *et al*. (2017), the HD system likely provides angular information so that place cells could discriminate radially arranged compartments (see Section 2.1; Figure 2.3). This finding would suggest that the HD system behaves as a global compass instead of several local compasses that reset every time the animals enter each compartment. In agreement, HD cells maintained their PFDs when animals moved from a familiar compartment to a novel compartment (Taube and Burton, 1995; Dudchenko and Zinyuk, 2005), indicating a contribution of path integration in stabilizing the PFDs of HD cells. However, the local visual environment can override path integration if the visual cues are salient and familiar to the animals. This is apparent in Dudchenko and Zinyuk (2005) where they attempt to examine the relative influence of the visual environment versus path integration by creating a conflict between them. Particularly, when animals were allowed to move between visually familiar compartments, HD cells were observed to switch its PFDs to reflect the PFDs previously observed when these compartments were experienced separately. Thus, visual landmarks can override path integration information and dominate HD cell activity if they are familiar to the animals.

Nonetheless, the above findings were done in compartments that were visually or geometrically dissimilar. How do HD cells then behave in visually similar compartments where the visual scene may be uninformative and unreliable? In the hairpin maze (Figure 2.4B), HD cells were found to be surprisingly stable even though grid and place cells repeated their firing fields across alleys (Whitlock and Derdikman, 2012). Likewise, recordings of HD cells from the anterodorsal thalamus and postsubiculum across two visually rotated, differently scented compartments revealed globally stable PFDs (Jacob *et al*., 2017; Figure 2.5). Thus, in visually ambiguous environment, HD cells mostly ignore the local visual scenes and rely on path integration. This is also consistent with a role for HD cells as a global compass, thus allowing place cells to disambiguate visually similar compartments when they are radially arranged (Harland *et al*., 2017; Grieves *et al*., 2016).

2.3.1 Bidirectionality in the HD network

In addition to global HD cells, there is now increasing evidence to suggest that the HD system may also encode visual information about the local environment. Using a two-compartment box that have visual cues on opposite end of each compartment and is differentially scented with either lemon or vanilla odour (visually rotated, differentially scented two-compartment context box), Jacob *et al*. (2017) observed a subpopulation of directional cells in the retrosplenial cortex that was distinct from global HD cells. Instead of maintaining their PFDs across compartments, these directional cells displayed PFDs that rotated 180° between the two compartments such that their PFDs seemingly followed the local visual scene (Figure 2.5). These directional cells, also known as 'bidirectional cells' (BD cells) to denote the bidirectionality of their PFDs (at least in this experiment), can be co-recorded with HD cells in the retrosplenial cortex, and likely reflect sensitivity to the local visual scene. Interestingly, bidirectional cells maintained their bidirectionality in the dark, suggesting that other sensory modalities (other than visual) can support the firing of bidirectional cells.

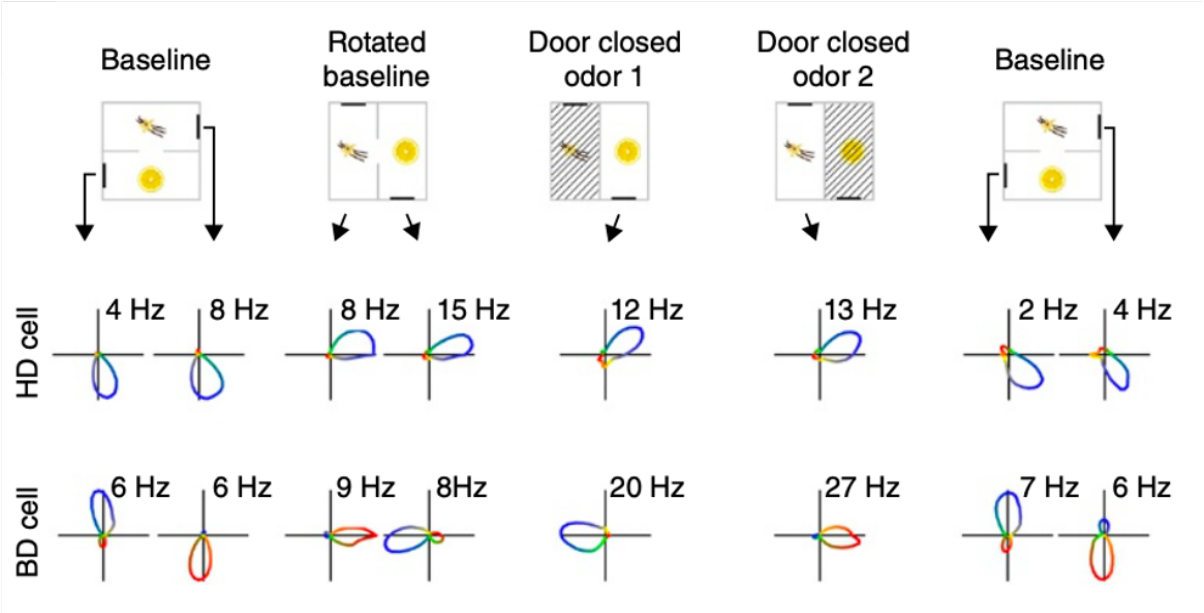

Figure 2.5: Bidirectional cells and head direction cells recorded in the two-compartment context box. Rats were recorded in a two-compartment context box where the compartments were 180° visually rotated, and differentially scented with either lemon or vanilla odour (*top row*). Head direction cells maintained their PFDs across compartments, suggesting a role in encoding global direction (*middle row*). Bidirectional cells however displayed 180° rotated PFDs between the two compartments, suggesting a sensitivity to the local visual scene (*bottom row*). Head direction cells can be co-recorded with bidirectional cells. *Adapted from Jacob et al. (2017).*

The presence of visually modulated directional cells in the HD system was further corroborated by Kornienko *et al*. (2018) who recorded parasubiculum and medial entorhinal cortex HD cells in an open field arena that fluctuates between two visual patterns. Interestingly, they saw a multitude of changes when the visual scene was manipulated, including HD cells that fluctuated between two PFDs and HD cells that became silent or had altered directionality in one of the two visual patterns. Surprisingly, they also observed bidirectional cells that may display bidirectionality in one or both of the visual pattern trials. Their finding thus suggests that a proportion of HD cells are visually driven. What is most interesting however is that the observed visually driven changes in firing activities were most apparent in HD cells that were not theta rhythmic (theta = oscillatory rhythm in the brain between 6-10 Hz) and unlike theta rhythmic cells, the changes induced by the visual manipulation were not coherent among non-theta rhythmic cell pairs or between non-theta and theta rhythmic cell pairs. This observation suggests that non-theta rhythmic cells, which are more visually driven, may exist outside the continuous attractor network that is typically postulated for HD cells (see Section 1.2.2.3).

Although it is unknown if the visually driven non-theta rhythmic cells found in Kornienko *et al*. (2018) relate to the bidirectional cells found by Jacob *et al.* (2017), it is nonetheless clear that there are two directional signals in the retrosplenial cortex - one locally (visually) tuned and one globally tuned. It is thus likely that retrosplenial cortex encodes local visual-centric directional information, in addition to global directional information. Why would the brain need two directional signals? Although it is not yet proven, it is likely that having a locally tuned directional signal would help individuals understand where they are facing in a local environment, while not losing their orientation in the global context (e.g. knowing where you are facing in the office, while still knowing where the nearest tube station is). In support of a local directional role, retrosplenial cortex activity was found to be remarkably similar when participants were asked to imagine the spatial view in the same relative direction and/or location in two geometrically similar but visually distinct local environments embedded in a global environment (museums within a park; Marchette *et al*., 2014). Thus, in humans, the same representation was elicited in the retrosplenial cortex within the two local environments even though they were globally separated.

2.3.2 Neuroanatomical segregation of bidirectional signals

An additional interesting finding stemming from Jacob *et al.* (2017) is the observation that the visually dominated, bidirectional signals seem to be localised only to the dysgranular retrosplenial cortex while head direction cells were found in all sub-regions of retrosplenial cortex (Figure 2.6; see Section 2.3.3 for a more detailed review of the different sub-regions of retrosplenial cortex). This finding is surprising as retrosplenial cortex (as a whole) is often considered to be a potential site for integration of visual information into the HD network (see Section 1.3.2.1; Figure 1.11). Instead, the functional and neuroanatomical segregation of a subpopulation of visually modulated directional cells in the retrosplenial cortex suggest otherwise, and it seems more likely that visual information is integrated into the HD network only via the dysgranular retrosplenial cortex. Additionally, it may suggest that bidirectional cells in the dysgranular retrosplenial cortex are not privy to self-motion cues, thus leading to the bidirectionality observed. It should be noted that these two possibilities are not mutually exclusive and will be addressed later on in the thesis (see Section 2.4; Chapter 4). Regardless of how bidirectionality could arise, it is now clear that heterogeneity exists within the HD network in retrosplenial cortex. As such, the role of retrosplenial cortex in the HD network should not be considered as single unit (as often done) but should be considered according to each sub-region.

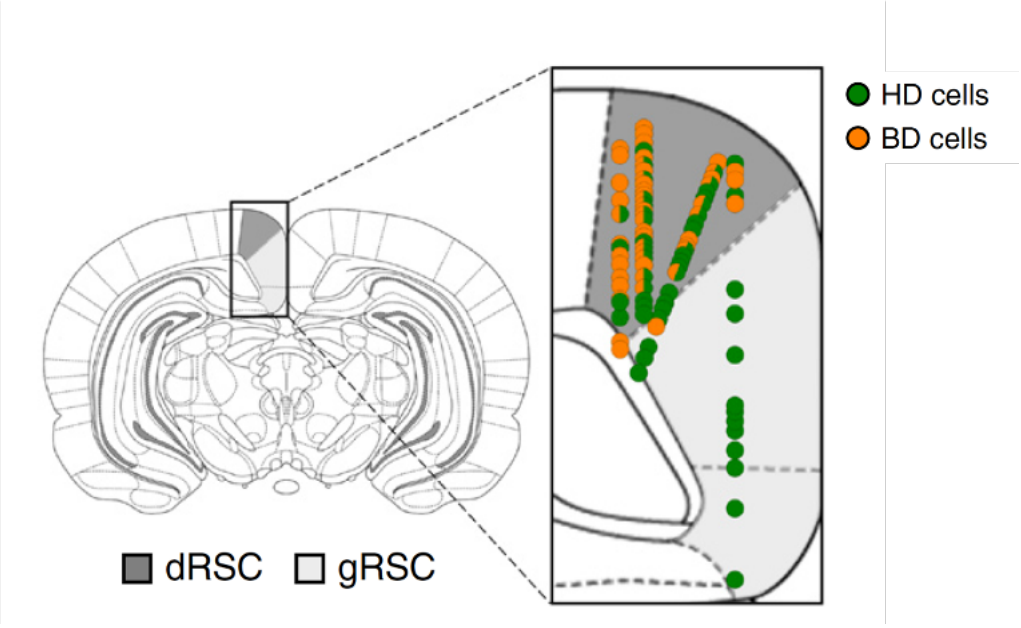

Figure 2.6: Neuroanatomical segregation of bidirectional signals in the retrosplenial cortex. Reconstruction of the sites where bidirectional and head direction cells were recorded revealed a segregation in the bidirectional cells. Although head direction cells can be found in all sub-regions of retrosplenial cortex, bidirectional cells were only found in dysgranular retrosplenial cortex. *Adapted from Jacob et al.* (2017).

Interestingly, Kornienko *et al*. (2018) also reported a possible neuroanatomical segregation between the visually driven, non-theta rhythmic cells and the theta rhythmic HD cells in the medial entorhinal cortex and parasubiculum. Particularly, they observed that they rarely co-record non-theta rhythmic cells with theta rhythmic cells, indicating a segregation between the two groups of HD cells. In addition, non-theta rhythmic cells tend to be recorded in earlier sessions, possibly suggesting that non-theta rhythmic cells may be either closer to the dorsal border or in deeper layers of medial entorhinal cortex and parasubiculum. The observation that visually driven directional cells may be segregated from the less visually driven directional cells in the medial entorhinal cortex thus imply that that the bidirectional and head direction signals in retrosplenial cortex may be propagated downstream via parallel streams to the medial entorhinal cortex (see Section 1.3.2.1; Figure 1.11). The question then arises as to if these signals are also propagated in parallel to the hippocampus (and hence place cells), which will be addressed in Chapter 5 of this thesis.

2.3.3 Retrosplenial cortex

As mentioned, retrosplenial cortex, together with postsubiculum, are often thought to be the sites of visual integration into the HD network. The discovery and segregation of bidirectional cells in a sub-region of retrosplenial cortex provides an opportunity to examine how visual information could be integrated into the HD network. Of particular interest to this thesis is the finding that bidirectionality is only observed in dysgranular retrosplenial cortex but not in the neighbouring granular retrosplenial cortex. This section hence aims to review our current knowledge of the retrosplenial cortex, focusing on the differences between the different sub-regions.

2.3.3.1 Neuroanatomy

The retrosplenial cortex is a cortical region first described in human and is traditionally denoted as Brodmann area 29 and 30 (Vann *et al*., 2009). In the rat, the retrosplenial cortex is defined cytoarchitecturally and can be found dorsomedially on the brain surface and extend along the anterior-posterior (AP) axis of the cerebrum (Vogt and Peter, 1981; Figure 2.7A). Based on the cytoarchitecture, the rat retrosplenial cortex can be divided into two main regions – the dysgranular retrosplenial cortex (dRSC; Brodmann area 30 – also previously referenced as

Brodmann area 29d) which is more similar with the neocortex and the granular retrosplenial cortex (gRSC; Brodmann area 29) which resembles the hippocampal archicortex more (Miller *et al*., 2014). The granular retrosplenial cortex can be further divided into two or three sub-regions depending on the literature referenced (Vogt and Peters, 1981; Van Groen and Wyss, 2003). For the purpose of this thesis, we adopt the divisions and nomenclatures defined in Van Groen and Wyss (2003) who divided gRSC into two sub-regions – gRSCa and gRSCb. We will focus predominantly on the differences between the neighbouring and more dorsally located gRSCb and dRSC as they were the main areas in which Jacob *et al*. (2017) recorded from (Figure 2.6).

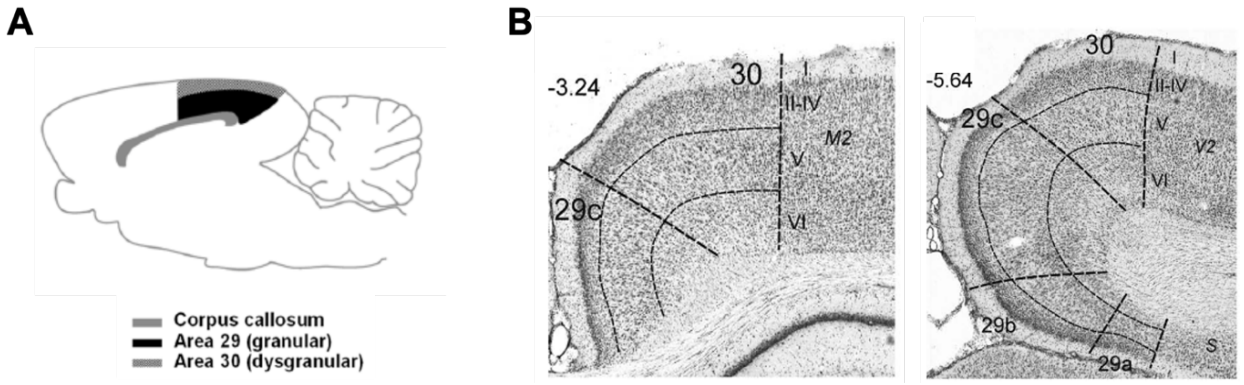

Figure 2.7: The dysgranular and granular retrosplenial cortex in the rat brain. (A) The retrosplenial cortex can be found on the dorsomedial surface of the rat brain. *Adapted from Mitchell et al. (2018).* **(B)** The retrosplenial cortex can be divided into two sub-regions. The dysgranular retrosplenial cortex (Brodmann area 30) is located more dorsally while the granular retrosplenial cortex (Brodmann area 29a-c) is located more medial and ventral. *Adapted from Malinowska et al. (2016)*.

The dRSC is more dorsally located and can be distinguished from the neighbouring gRSCb via several anatomical characteristics (Figure 2.7B). Specifically, layer II and III of dRSC is wider and more loosely packed than that of gRSCb. In contrast, gRSCb has darkly Nissl stained layer II cells that are more densely packed. Layer IV of dRSC is also wider and less densely packed than its counterpart. Last but not least, the cell bodies of neurons in layer V of dRSC tend to be larger (Vogt and Peters, 1981; Malinowska *et al*., 2016; Van Groen and Wyss, 1992). Along the anterior-posterior axis, both sub-regions of retrosplenial cortex extend to the caudal end of the cerebrum but are bordered by the anterior cingulate cortex anteriorly.

2.3.3.2 Connectivity

Multiple studies have systematically examined the afferent and efferent inputs into the different sub-regions of retrosplenial cortex (Van Groen and Wyss, 1990a; 1992; 2003). These studies typically used a combination of anterograde (*Phaseolus vulgaris* leukoagglutinin, mixture of [^{3}H] with proline and/or lysine, fluororuby and biotinylated dextran amine) and retrograde tracers (fast blue, fluorogold (FG), fluororuby) to map out the inputs and outputs across the different sub-regions. A summary of the connections from the hippocampal formation, sensory cortices and thalamus with the dRSC and gRSCb (based predominantly from the data by Van Groen and Wyss, 1992; 2003) is displayed in Figure 2.8.

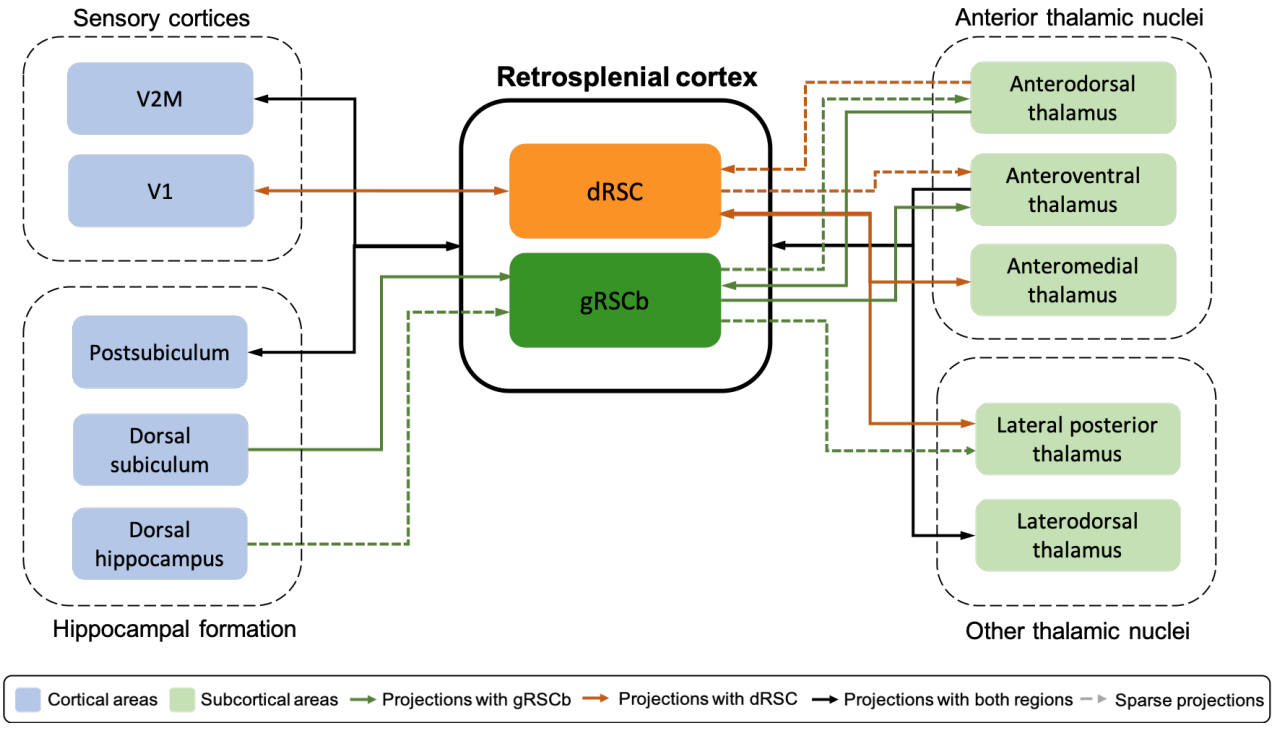

Figure 2.8: Connections of dRSC and gRSCb with sensory cortices, hippocampal formation and thalamic nuclei. The diagram is centered around dRSC, gRSCb, and other spatially relevant neuroanatomical structures. Green boxes represent subcortical structures, while blue boxes represent cortical structures. Black arrows indicate afferent projections to both regions. Orange arrows indicate connections with dRSC while green arrows indicate connections with gRSCb. Dotted arrows, regardless of colours, indicate sparse projections. Both sub-regions have extensive connections with the HD network (anterior thalamus, postsubiculum, laterodorsal thalamus) while only gRSCb receives additional information from other spatial rnetworks (e.g. dorsal hippocampus and dorsal subiculum). In contrast, dRSC is more interconnected with visual cortices as compared to gRSCb. Both sub-regions are also interconnected with each other (not shown). It should also be noted that the connectivity of dRSC and gRSCb varies qualitatively and quantitatively, depending if the injections were made rostrally or caudally.

Consistent for a role of retrosplenial cortex in the HD system, both dRSC and gRSCb are extensively connected with postsubiculum, laterodorsal thalamus and anterodorsal thalamus (Figure 2.8; Van Groen and Wyss, 1990b, 1992, 1995, 2003; Sripnidkulchai and Wyss, 1986; Kononenko and Witter, 2012). Interestingly, the anterodorsal thalamus (as well as the other thalamic nuclei) have quantitative difference in connectivity between the two retrosplenial sub-regions with gRSCb being more strongly connected with the anterodorsal thalamus than dRSC (Van Groen and Wyss, 1992, 2003; Sripanidkulchai and Wyss, 1986). Additionally, gRSCb receives unique inputs from dorsal subiculum and dorsal hippocampus (Van Groen and Wyss, 2003; Yamawaki *et al*., 2019; Cenquiza and Swanson, 2007; Miyashita and Rockland, 2007; Jinno *et al*., 2007). Thus, gRSCb, as compared to dRSC, may be more involved in the HD and spatial network.

In contrast, the dRSC may have more of a visual processing role that is in line with the visual integrative role of RSC in the HD network. Although both dRSC and gRSCb were found to be connected with extrastriate visual cortex V2M, only dRSC is reciprocally connected with the primary visual cortex (V1) and the lateral posterior thalamus (Van Groen and Wyss, 1992; 2003; Vogt and Miller, 1983), the latter of which is homologous to the primate pulvinar nucleus and has been implicated in visual processing (Zhou *et al*., 2017). Additionally, Vogt and Miller (1983) reported exclusive projections from V2L to dRSC (not shown). Thus, dRSC may receive qualitatively different visual inputs as compared to gRSCb and may be involved in visual processing.

Despite providing extensive knowledge about the connectivity between the different retrosplenial sub-regions, it should be noted that the studies by Van Groen and Wyss (1992; 2003) are limited in a couple of aspects. First and foremost, injection coordinates were not specified in their studies even though there were observations of differential labelling depending on the rostral-caudal axis in which the injections were made (Van Groen and Wyss, 1992; 2003). For example, Van Groen and Wyss (1992) found that the “most dorsal, septal part of the subiculum” was labelled when retrograde tracers were placed in the rostral part of gRSCb but the “dorsal part of the intermediate one-third of the subiculum“ was labelled when the retrograde tracers were placed in the caudal part of gRSCb. Likewise, in the dRSC, caudal injections of retrograde tracers resulted in more labelling in the visual cortical regions as compared to rostral injections (Van Groen and Wyss, 1992). Quantitative differences in the thalamic projections to both dRSC and

gRSCb were also observed depending on the rostral-caudal axis at which injections were made (Van Groen and Wyss, 1992; 2003). Thus, it is important to be aware of the approximate sites along the rostral-caudal axis in which the projections are studied.

In addition, many of the studies listed above (including Van Groen and Wyss, 1992; 2003) used Sprague-Dawley or Wistar rats in their studies. Sprague-Dawley and Wistar rats are albino rats that may be different from the pigmented Lister-hooded rats used in Jacob *et al.* (2017). For example, differences in visual acuity between pigmented and albino rats have been reported by Prusky *et al*. (2002). Although the report did not compare Lister-hooded rats with Sprague-Dawley and/or Wistar rats directly, Sprague-Dawley and Wistar rats were reported to have lower visual acuity than pigmented rats (Dark Agouti, Fisher-Norway and Long Evans rats). Thus, it is possible that some differences in connectivity (e.g. especially in visual cortices) may exist between non-pigmented and pigmented rat strains and any extrapolation of data between animal strains should be done with caution.

2.3.3.3 Behavioural relevance

The role of retrosplenial cortex in behaving animals on spatial tasks has been examined extensively, typically via lesion studies. Lesion studies are often difficult to interpret due to variability in lesion extent, but there is now a growing consensus that lesions of retrosplenial cortex impaired performances in various spatial memory tasks. In the morris water maze, animals with lesions in retrosplenial cortex were found to take longer and less direct paths to find a platform either in a fixed location or with changing locations. (Sutherland *et al*., 1988; Whishaw *et al*., 2001; Vann and Aggleton, 2002; Vann *et al.,* 2003; Harker and Whishaw, 2004; Cain *et al*., 2006). Likewise, in the working memory version of the radial arm maze, lesioned animals make more erroneous arm entries (Vann and Aggleton, 2002, 2004; Keene and Bucci, 2009). Additionally, retrosplenial cortex lesioned animals in a go/no-go discrimination task have impaired performance if they are required to rely on the visual scene to solve the task (Hindley *et al*., 2014). Impairments in these tasks are often attributed to an inability of the animals to use the allocentric environment (i.e. visual cues) to locate themselves. Because lesioned animals eventually do learn the tasks (but not to the asymptotic level seen in control animals), it is likely that the lesioned animals employed a different strategy that is less dependent on using allocentric cues to solve the task (Vann and Aggleton, 2004).

Interestingly, lesions in retrosplenial cortex were also associated with impairments in path integration so it is unlikely that lesioned animals switched to a strategy dependent on self-motion cues. Particularly, Cooper and Mizumori (1999; 2001) observed impairments in performances on the radial arm maze only in the dark when retrosplenial cortex was inactivated. In support, Whishaw *et al*. (2001) examined homing behaviour on a rotatable open table under infrared light (which is outside the rat visible range) and observed a similar deficit in lesioned animals to path integrate home. Using the same task, Elduayan and Save (2014) also observed an inability of lesioned animals to path integrate home in the dark. It should be noted that the findings by Cooper and Mizumori (1999; 2001) differ from that by Vann and Aggleton (2002; 2004), who found a deficit in the radial arm maze in the light. The discrepancy is likely to be due to differences in lesion and inactivation extent across the two studies as deficit in performance on the radial arm maze in the light sometimes did not manifest if lesions are incomplete (Vann *et al*., 2003; Vann and Aggleton, 2004).

In addition to allocentric and idiothetic cue processing, retrosplenial cortex lesions also impaired performances in an alternation task that was designed to tax the use of directional information (Pothuizen *et al*., 2008; Pothuizen *et al*., 2010). This is in line with the observation of head direction cells in the retrosplenial cortex (see Section 1.2.2; Chen *et al*., 1994; Cho and Sharp, 2011). Lesioned animals were also impaired in an object-in-place task and could not distinguish when familiar objects were displaced from their original locations even though the animals were able to discriminate novel objects (Vann and Aggleton, 2002; Parron and Save, 2004).

The retrosplenial cortex has been hypothesized to be part of a transformation circuit that mediates transformation between egocentric and allocentric place representation (Bryne *et al*., 2007). In support of the hypothesis but not necessarily limited to egocentric-allocentric transformation, there is now increasing evidence to suggest that the impairments observed across the wide range of spatial tasks may result from an inability of lesioned animals to mediate the switch between reference frames and/or use of different spatial cues (Vann *et al.,* 2009; Mitchell *et al*., 2017). For example, impairments in the radial arm maze were consistently observed when the maze was rotated in the middle of a training session, which created a conflict between extramaze and intramaze cues (Vann and Aggleton, 2002; Vann *et al*., 2003; Vann and Aggleton, 2004; Pothuizen *et al*., 2010). Likewise, lesioned animals were impaired in a place avoidance task

but only when distal and local cues were placed in conflict. These animals otherwise performed as well as control animals when cues were stable or when only one set of cues (distal or local) was available. These findings thus suggest that retrosplenial cortex is required for animals to flexibly switch between using distal and local cues (Wesierska *et al*., 2009).

Do the different sub-regions of retrosplenial cortex contribute differently to spatial behaviours? Although multiple studies have considered the roles of dRSC and gRSC in spatial behaviours, it is important to note that these studies did not directly compare the behaviours of dRSC and gRSC lesioned animals in the same study. Thus, interpretation and generalization of the findings across different studies can be difficult. Nonetheless, there is some evidence from these studies to suggest that dRSC and gRSC (and even within sub-regions of gRSC) may have different functional roles in spatial behaviours. For instance, even though selective dRSC and gRSC lesions were both found to disrupt performances in the radial arm maze (Vann and Aggleton, 2005; Pothuizen *et al*., 2010), only rats with dRSC lesions were found to employ a sequential choice behaviour (Vann and Aggleton, 2005). Particularly, the animals were found to turn consistently in one direction and enter sequential arms rather than relying on the allocentric visual environment. A visual role for dRSC was further corroborated by Hindley *et al*. (2014) who designed a go/no-go discrimination task that can only be solved if the animals used the visual scene (and hence the allocentric reference frame) to localize themselves. Interestingly, dRSC lesions were sufficient to disrupt the acquisition of the discrimination, suggesting that dRSC is required for the animals to effectively learn to use the visual cues to solve the task. Pothuizen *et al*. (2009) also found a role for dRSC in visual processing by using immediate-early gene activity (*c-fos* and *zif268*) to estimate neuronal activity. Specifically, dRSC was found to have increased *c-fos* activity on the radial arm maze but only in the light and not in the dark. This is in contrast to gRSC which has increased expressions in both conditions. Last but not least, studies using two-photon calcium imaging have also revealed visually responsive neurons (Powell *et al.,* 2020) and visual landmark aligned neurons (Fischer *et al*., 2020) in dysgranular retrosplenial cortex. It however remains unclear if these visually responsive neurons can be found in the granular retrosplenial cortex. Taken together, these findings seem to suggest that dRSC may play an important role in visual processing.

2.4 Summary

In this chapter, we have discussed how the different spatial cells encode visually similar multi-compartment spaces. Particularly, place cells were observed to have repeating fields in visually similar compartments but only when the local visual environments were similarly oriented (Skaggs and McNaughton, 1998; Spiers *et al.*, 2015; Grieves *et al.*, 2016; Singer *et al.*, 2010; Fuhs *et al.*, 2005; Tanila *et al.*, 1999; Derdikman *et al*, 2009). These findings thus suggest that directional information provided by the head direction system may be vital for disambiguation of visually similar local spaces. In support, the preferred firing directions of head direction cells are stable across multi-compartment spaces (Whitlock and Derdikman, 2012; Jacob *et al.*, 2017) indicating global encoding. In addition, bilateral lesions of lateral mamillary nucleus induced field repetitions between radially arranged compartments (Harland *et al.*, 2017).

Do head direction cells then not encode information about the local environment? A recent study by Jacob *et al.* (2017) suggests otherwise. Specifically, the authors found directional cells in the retrosplenial cortex that rotated their preferred firing directions by 180° as the animals moved across two 180° visually rotated, differentially scented compartments. These bidirectional cells appear to be sensitive to the local visual scene and may encode information about the local visual scene. Together with global head direction cells, the retrosplenial cortex may conjunctively encode information about the local and global environments. Interestingly, the bidirectional cells were only found in the dysgranular retrosplenial cortex while head direction cells were found in the entire retrosplenial cortex. This suggests that the bidirectional signal may be functionally segregated in the retrosplenial cortex, in line with the differences in neuroanatomy, connectivity and behavioural relevance observed across the different retrosplenial sub-regions (see Section 2.3.3).

2.4.1 Hypotheses and aims

The discovery of bidirectional signals in the dysgranular retrosplenial cortex (together with the findings by Kornienko *et al.*, 2018) provided the first evidence that the head direction cell population is not homogenous, and a distinct sub-population of visually modulated directional neurons exists within the head direction network. It is still unclear how the bidirectional signals could be involved in spatial navigation. In this thesis, we aim to address two questions that will

further our understanding of the bidirectional signals and its interactions with other spatial networks:

1) What are the differences in the inputs to gRSC and dRSC that could give rise to the distinct directional signals in the retrosplenial sub-regions?

   As mentioned, the anatomical segregation of bidirectional cells within a sub-region of the retrosplenial cortex provides an opportunity to examine the type of information that could be responsible for the bidirectionality. We hypothesized that dRSC and gRSC receive different inputs that give rise to the different directional signals observed. Although the connectivity of both dRSC and gRSC have been studied, the studies were limited in a couple of aspects. Particularly, the studies were done in albino rats which may have different connectivity from that of pigmented rats. In addition, there are rostral-caudal differences in projections and the studies by van Groen and Wyss (1992; 2003) did not specify the coordinates used (see Section 2.3.3.2 for a lengthier discussion on the limitations). As such, we decided to replicate the experiment, focusing on the inputs into the two sub-regions of retrosplenial cortex in Lister-Hooded rats at our implantation coordinate. In addition, we utilized a double retrograde tracing approach that could possibly provide additional information such as cells that project to both retrosplenial sub-regions and/or anatomical segregation of inputs from a specific brain region.

2) Do place cells behave like bidirectional cells or head direction cells?

   The observation of bidirectional cells in the visually rotated, two-compartment context box suggests that local visual directional signals could be available to place cells. In addition, given that gRSC is more strongly connected with the hippocampal spatial circuit (Chapter 4; Dorsal subiculum, dorsal hippocampus and anterodorsal thalamus), we hypothesized that place cells, the core of the hippocampal spatial circuit, would behave more like gRSC than dRSC. However, it is unclear if place cells do behave more like gRSC. As such, we decided to record place cells in the visually rotated, two-compartment context box and examine if their activity resembles that of bidirectional cells (local encoding) or head direction cells (global encoding).

Chapter 3.

Experimental Materials and Methods

3.1 Animals

Male Lister-Hooded rats were used for all experiments. The animals were housed individually post-surgery and maintained on a 12hr/12hr light/dark cycle. Animals used for retrograde tracing experiments were not food-restricted while animals used for recording were placed on food-restriction a week post-surgery and their body weights maintained at 90% of their free-feeding body weights throughout the experiments. All experiments were done in accordance with the national [Animals (Scientific Procedures) Act, 1986, United Kingdom] and the international [European Communities Council Directive of 24 November 1986 (86/609/EEC)] legislation governing the maintenance of laboratory animals and their use in scientific experiments.

3.2 Retrograde tracing experiment

3.2.1 Retrograde tracers

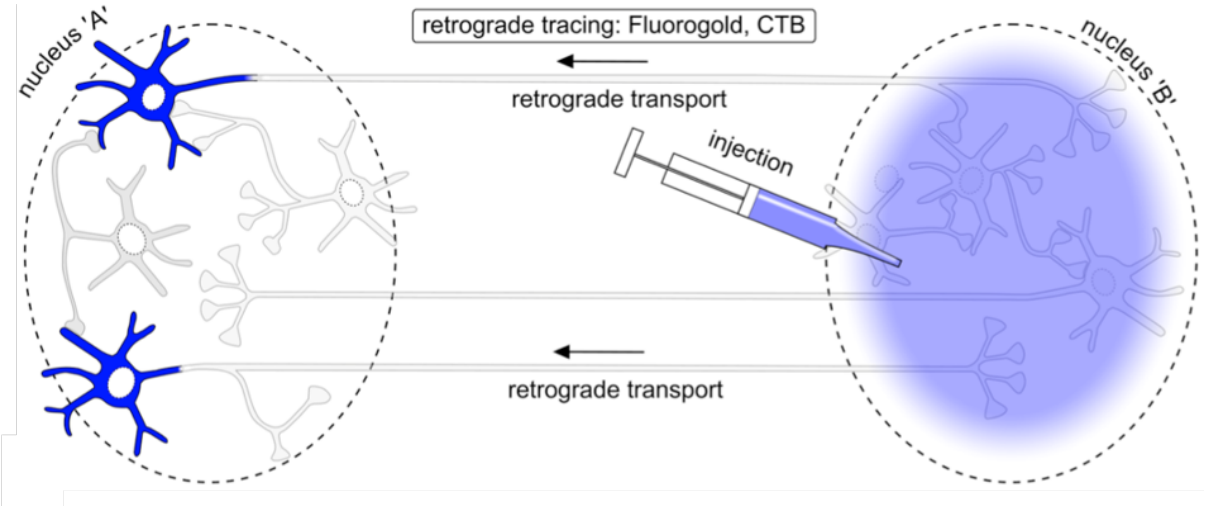

Figure 3.1: Principle underlying retrograde tracing. Retrograde tracers are taken up by axonal terminals (for instance in nucleus 'B') and is transported retrogradely back to the cell bodies (e.g. in nucleus 'A'), thus allowing one to study the inputs into a particular brain region. *Adapted from Lanciego and Wouterlood (2020).*

Retrograde tracers are taken up by the axonal terminals of neurons and transported back to the cell bodies, thus making them ideal for examining the inputs into the different retrosplenial sub-regions (Figure 3.1; Saleeba *et al*., 2019; Lanciego and Wouterlood, 2020). Three retrograde tracers were employed in this study – Fluorogold (FG; 4% in phosphate buffered saline (PBS); Fluorochrome Inc., Denver, CO, USA), Cholera toxin subunit B (CTB) conjugated with Alexa Fluor 594 (CTB-AF594; 1% in PBS; Molecular Probes, Invitrogen Inc.) and Cholera toxin subunit B conjugated with Alexa Fluor 488 (CTB-AF488; 1% in PBS; Molecular Probes, Invitrogen Inc.). The tracers were chosen such that their emission spectra do not overlap, and the tracers can be injected and visualized within the same animal via fluorescent microscopy without any fluorescence bleed-through. Fluorogold is an inorganic fluorescent dye that can be visualized directly in the blue wavelength spectrum while CTB-AF594 and CTB-AF488 are recombinant versions of subunit B of cholera toxin and can be visualized in the red and green wavelength spectrum respectively.

3.2.2 Tracer injections

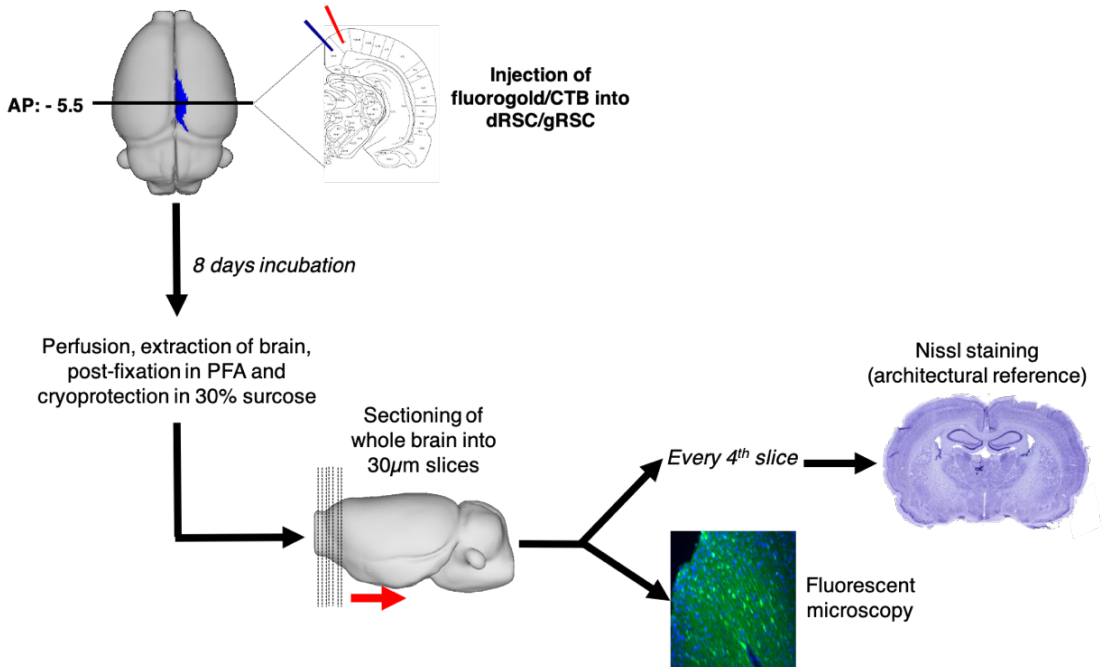

Figure 3.2: Schematic overview of the retrograde tracing protocol. A double retrograde tracing approach was utilized where fluorogold and CTB were injected into dRSC and gRSC in the same hemisphere in the same animal. The tracers were counterbalanced between the two retrosplenial sub-regions as much as possible. After a survival period of eight days, the animals were perfused, their brains extracted, processed and analysed for labelled cell bodies.

The tracers were injected in fourteen rats in one hemisphere. Specifically, anaesthesia was induced and maintained throughout surgery using isoflurane (1.5% to 3% isoflurane with an O_2 flowrate of 3L/min). Upon induction of anaesthesia, the animals were shaved and placed inside a stereotaxic frame. The skin above the dorsal surface of the skull was cleaned and an incision was made to expose the skull. The skin was then clamped down to the side using hemostats so as to expose the dorsal surface of the skull.

Under stereotaxic guidance, a craniotomy was made above gRSCb (AP: -5.5, ML: ±0.4 relative to bregma) and/or dRSC (AP: -5.5, ML: ±1.0 relative to bregma) using a 2.3mm trephine drill bit. A glass pipette (0.66μm diameter) filled with either fluorogold, CTB-AF594 or CTB-AF488 was lowered into either gRSCb (DV: 1.7 below pia) or dRSC (DV: 0.6 below pia) and 1μl of fluorogold, CTB-AF594 or CTB-AF488 was pressure injected at a flowrate of 0.1μl/min for 10min. The glass pipette was then left in place for 10min after injections to avoid reflux. Injections were counterbalanced across the two sub-regions in different animals (see Chapter 4, table 4.1 for the targeted injection sites).

After the injections, the craniotomy was cleaned and filled with sterile Vaseline. The skin above the craniotomy was then sutured and cleaned. The animals were then removed from the stereotaxic frame and placed in a heated box for recovery. After the animals have woken up, they were placed back into their cages and monitored daily for seven days. Carpofen (0.1ml of 10 v/v% per 100g animal weight; Pfizer Ltd, UK) was given pre-surgically while metacam was given post-surgically for three days, controlling for pain and inflammation.

3.2.3 Histology

To facilitate sufficient retrograde transport of tracers, a survival period of eight days was used (Conte *et al.*, 2009; Catapano *et al.*, 2008; Aparicio and Saldana, 2014). After eight days, the animals were perfused, and their brains extracted.

3.2.3.1 Perfusion and slide preparation

At the end of the survival period, the animals were deeply anaesthetised with isoflurane (3% isoflurane with an O_2 flowrate of 3L/min) and terminated via overdosing with sodium pentobarbital. The animals were then perfused transcardially with saline (0.9% sodium chloride

solution) and 10% formalin, and the brains removed and post-fixed in 4% paraformaldehyde for one or two days. The brains were cryo-protected in 30% sucrose solution for approximately two days, before being sliced coronally into 30μm slices using a cryostat (Leica CM1850 UV). The slices were then divided into two series: every fourth slice was separated for Nissl staining while the rest were mounted in Vectashield antifade mounting medium (Vectorlab, H-1000). Slides from animal R717 were mounted in Vectashield antifade mounting medium with propidium iodide (Vectorlab, H-1300) which stained the nucleus red, while slides from animal R878 and R879 were mounted in Vectashield antifade mounting medium with DAPI (Vectorlab, H-1200) which stained the nucleus blue. These slides were then fluorescence imaged with slices being imaged every 4 to 6 slices (every 120-180μm). All procedures upon extraction of the brains were carried out in the dark to avoid photo-bleaching.

3.2.3.2 Fluorescent microscopy

All images were captured using a Leica DMi8 fluorescent microscope installed with four filter cubes designed to view DAPI, GFP, YFP and Texas Red. The DAPI filter cube was used to examine for fluorogold and DAPI labelling. The Texas Red filter cube was used to examine for CTB-AF594 and propidium iodide labelling. The GFP filter cube was used to examine for CTB-AF488 labelling. For double tracing experiments, all images were acquired with a gain of 4.4 and an exposure time of 300ms and 450ms for fluorogold and fluorophore conjugated-CTB labelling respectively. The exposure time was however changed in some occasions to obtain suitably exposed images, especially in slices close to the injection sites. All such changes to exposure time were recorded. Whole-slice images were obtained by generating tile-scanned images which are stitched together with smoothed edges at 100x magnification. All images were saved in TIFF format for further analysis. For visualization purposes, all images were pseudo-coloured in grey and then inverted such that labelled neurons appeared as black on a greyscale background. For double-tracing images, the merged images were generated by merging the images from the different fluorescence channels. In these images, fluorogold labelled images were pseudo-coloured in cyan, CTB-AF594 in red and CTB-AF488 in green.

3.3 Single-unit recordings

3.3.1 Microdrives

Axona microdrives (Axona, UK) containing four drivable bundles of tetrodes were prepared for implantation in rats (see Figure 3.3). Each tetrode was made from four 25μm polyimide coated 90% platinum-10% iridium wires (California Fine Wire, Grover Beach, CA) twisted together and threaded through a 21G stainless steel cannula (Cooper's Needle Works Ltd, UK). If the impedance of the electrode tips was too high (> 300 kΩ), the electrode tips were gold plated (Neuralynx, MT) such that their impedances fell within the range of 180-300 kΩ (with a target impedance of 200 kΩ).

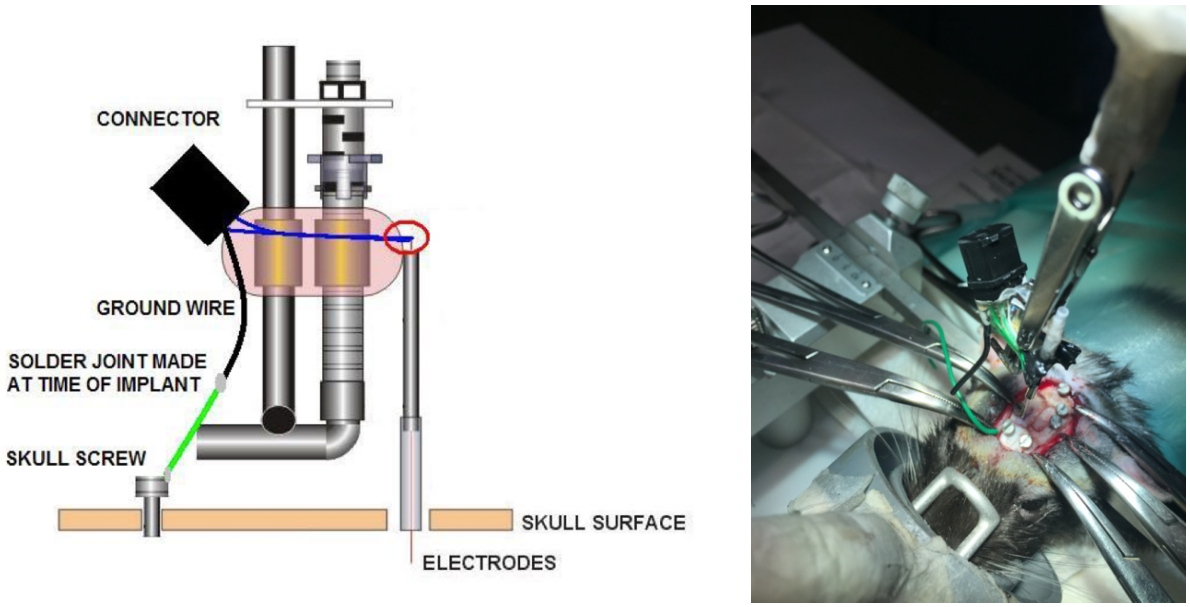

Figure 3.3: Axona microdrives used for single unit recordings. *Left*, a schematic diagram showing the mechanism used in Axona microdrives. The tetrodes are wired to the connectors, passed through a cannula and inserted into the animal's brain. The whole assembly is cemented to the screw mechanism, which allows the tetrodes to be lowered (or raised) as the screw is turned. A ground wire on the microdrive is soldered onto a skull screw during surgery to provide grounding. *Adapted from Axona microdrive user guide. Right*, a picture showing an Axona microdrive (slightly modified to house an optogenetic fibre) being implanted by the author during surgery.

3.3.2 Implantation surgery

Microdrives were implanted under standard stereotaxic procedure, similar to that described in Section 3.2.2. Specifically, the animals were induced and maintained under anaesthesia using isoflurane (2% to 3% isoflurane with O_2 flowrate of 2 to 3L/min). Following induction of anaesthesia, the animals were shaved, placed inside a stereotaxic frame and the skin above the dorsal surface of the skull was cleaned. An incision was made to expose the skull and the skin clamped down using hemostats.

Under stereotaxic guidance, a craniotomy was made above hippocampal CA1 (AP: -4.0, ML: ± 2.5 relative to bregma) using a 2.3mm trephine drill bit. In addition to the craniotomy, six additional holes were made using a 1.2mm burr drill bit, and jewellers' screws screwed into them to provide additional support. One screw is always situated on the contralateral side of the implanted hemisphere above the cerebellum and is soldered to a wire attached to the microdrive to serve as grounding. The tetrodes were then lowered into the craniotomy (DV: 1.5 below pia), and the whole assembly (microdrive and screws) cemented onto the skull using dental acrylic (Simplex Rapid ®, Kemdent, UK). The tetrodes were protected from the dental acrylic by an outer cannula that was lowered to the surface of the brain.

After the dental acrylic have dried, the screw on the microdrive was turned a quarter of a turn (~ 50μm) and the animals removed from the stereotaxic frame. The animals were then allowed to recover in a heated chamber, before being replaced into their cages. Carpofen (0.1ml of 10 v/v% per 100g animal weight; Pfizer Ltd, UK) was given pre-surgically while metacam was given post-surgically for three days, controlling for pain and inflammation. Animals were allowed 7 days of recovery before screenings and recordings begin.

3.3.3 Experimental apparatus

The animals were screened in a separate room distinct from the recording room. The screening room contained a square open box environment (120cm x 120cm) lifted off the floors by a chair in each corner of the arena (Figure 3.4). Strips of polypropylene sheets were mounted onto the walls of the environment to discourage the animals from climbing on and over the edge. Distal cues were available in the screening room.

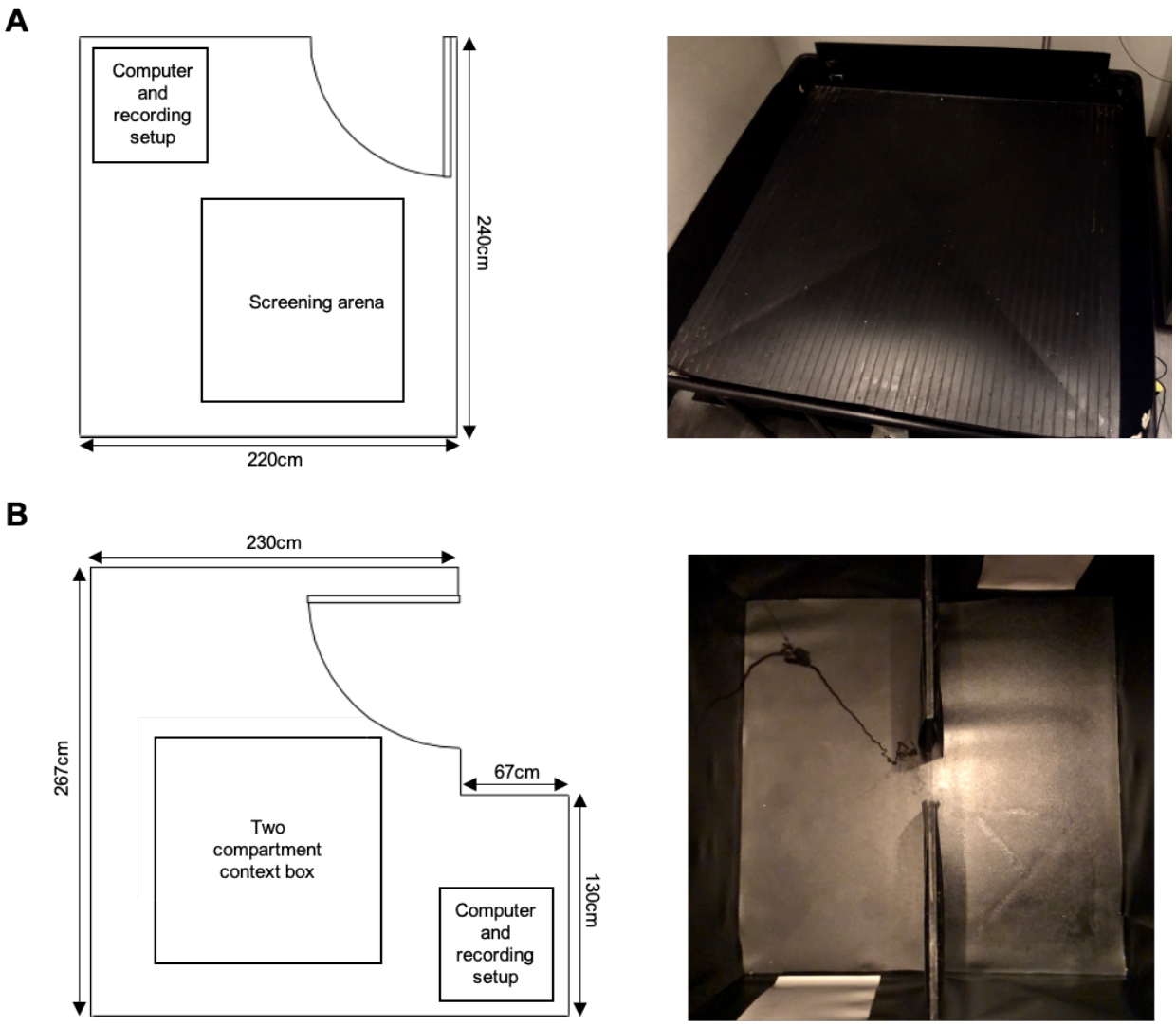

Figure 3.4: Experimental rooms and environments. (A) Schematic floorplan of the screening room (*left*) and a photo of the screening arena (*right*). **(B)** Schematic floorplan of the recording room (*left*) and a photo of the two-compartment context box (*right*). Note that there is a curtain around the two-compartment context box to help control for distal visual cues. The headstage is also shown in the photo.

The recording room contained the recording environment (two-compartment context box, Figure 3.4; see Section 2.3.1) surrounded by black curtains mounted on the ceiling. Thus, the animals were deprived of any distal cues. The two-compartment context box (120cm x 120cm x 50cm) was constructed from wood, painted black, lined with polypropylene sheets for the walls, and vinyl sheets for the floors. The floor of each compartment was scented with either vanilla (Dr Oetker, Germany) or lemon odours (Dr Oetker, Germany), and the scent identity for each compartment was kept constant throughout all recordings so as to avoid cross-contamination of odours between the two compartments. The doorway through which the animals used to move

between the two compartments is 18cm wide. Halogen lights were mounted onto the ceiling near each corner of the environment to provide homogenous lighting, and white noise was played on a portable speaker (SoundCore mini, Anker) mounted on the ceiling to eliminate any directional auditory cues.

3.3.4 Data acquisition

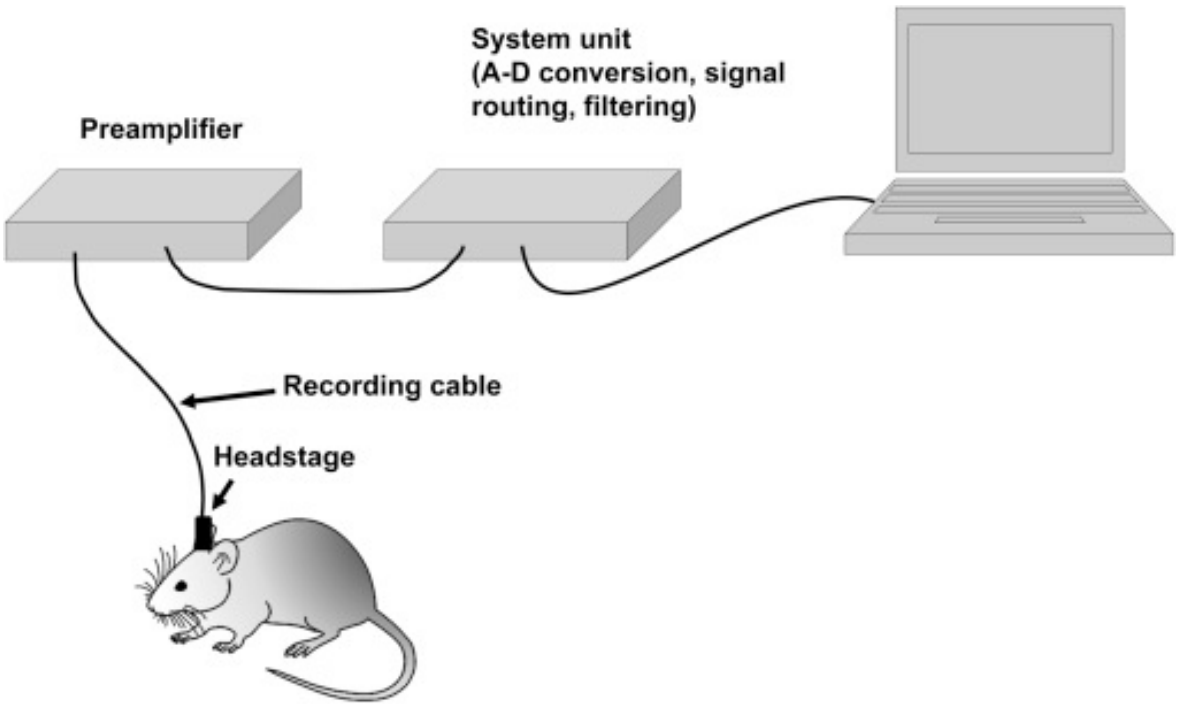

Figure 3.5: Schematic diagram of a typical recording setup. Electrical signals from the tips of the implanted tetrodes were propagated to the preamplifier via the headstage, amplified by the preamplifier and processed by the system unit before being visualized on a computer for analysis. *Adapted from Jeffery et al., 2018.*

For screening and recording, the connector on the microdrive was connected to a headstage with one LED, that is in turn connected to the dacqUSB preamplifier and recording system (Axona, UK; Figure 3.5). The signals acquired from the tetrodes were digitized (48 kHz), amplified between 10000 to 20000 times and high pass filtered. The digital signals were then assessed for deflections in voltage in any of the channels larger than the spike-triggered threshold set by the experimenter. These deflections were considered putative spikes and the voltages between 200μs pre-triggered to 800μs post-triggered were stored for spike sorting (see Section 3.3.5) and subsequent offline analysis in MATLAB (see Section 5.1.2). Local field potential signals were amplified 2000-3000 times and low pass filtered. The positions of the animals were tracked

via the single LED on the headstage using a camera (FCH-30C, Ganz) mounted on the ceiling (50 Hz sampling rate), and the tracked positions were synchronized with the digital signals by the recording system.

3.3.5 Spike sorting

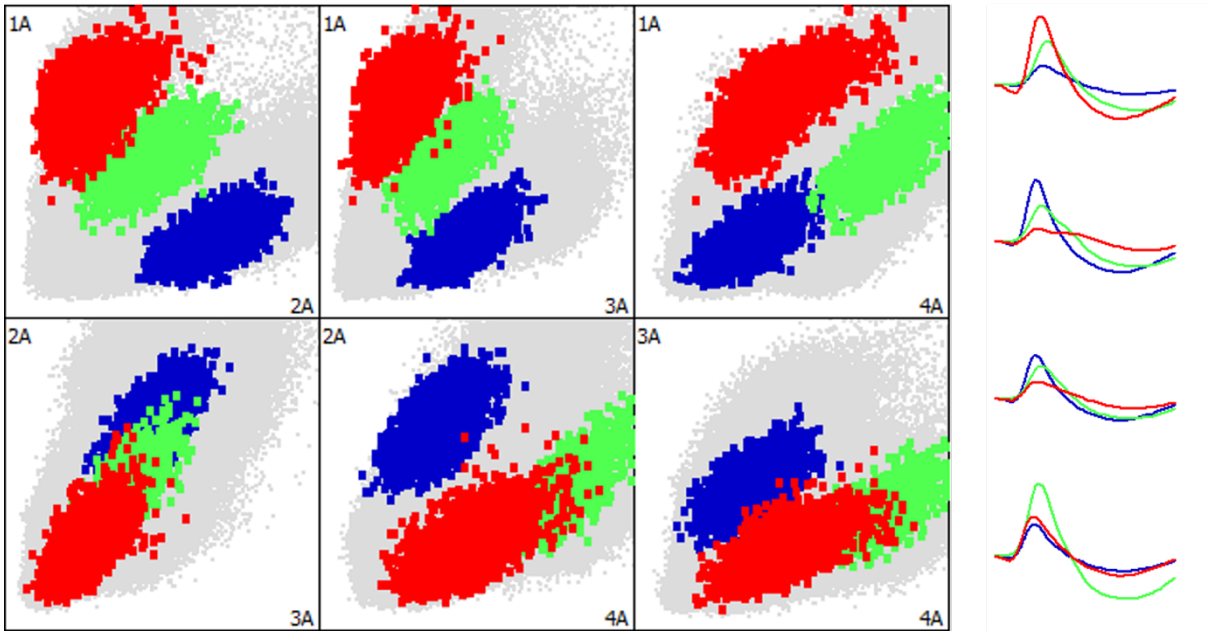

Figure 3.6: Example output of Tint. Using Klustakwik 3.0, spikes were automatically sorted into separate clusters and manually checked by the experimenter. An example output recorded by the author from Tint (Axona, UK) is showed above with three example place cells highlighted (more cells were recorded in this session). The *left* panel shows the spikes sorted in three clusters (unsorted spikes in grey) in a 4-dimension cluster space defined by the amplitudes of the spikes recorded across the four channels in a tetrode. The waveforms of the clusters are shown on the *right*. As observed, the three example cells occupied different locations within the cluster space and have qualitatively different waveforms across the four channels.

After recordings, neuronal spikes were sorted offline on the graphical clusters-cutting software Tint (Axona, UK; Figure 3.6) with the help of the clustering algorithm KlustaKwik 3.0 (Kadir *et al.*, 2014). Recording data obtained across trials but in the same session were loaded into Tint together and the resulting clustered units were manually compared with each other by examining their waveforms and their cross-correlogram (timing of firing activity with respect to each other). Clusters were grouped together if they occupied similar locations in the cluster space, had similar waveforms and did not spike within two seconds of each other. The sorted spikes were further analysed offline in MATLAB (see Section 5.1.3).

3.3.6 Histology

At the end of recordings (when place cells were no longer found during screening or if the tetrodes could not be lowered anymore), the animals were perfused. The brains were then extracted, processed and examined for the location of tetrode tracks. This will thus provide an estimation of where the place cells were recorded.

3.3.6.1 Perfusion and slide preparation

At the end of the experiments, the animals were deeply anaesthetised with isoflurane (3% isoflurane with an O_2 flowrate of 3L/min) and terminated via overdosing with sodium pentobarbital. The animals were then perfused transcardially with saline (0.9% sodium chloride solution) and 10% formalin. The tetrodes of the microdrives were then raised to the highest possible level so that aberrant tracks would not be made when the brains were extracted. The brains of the animals were then extracted and post-fixed in 4% paraformaldehyde for one or two days. They were then cryo-protected in 30% sucrose solution for approximately two days, before being sliced coronally into 40μm slices using a cryostat (Leica CM1850 UV). These slices were then mounted onto glass slides and Nissl-stained by immersing the slides in cresyl violet solution, washed in distilled water, dehydrated in increasing concentration of ethanol before being cleared in Histo-Clear (National Diagnostics, Scientific Laboratory Supplies). The slides were then coverslipped using DPX mounting media (Sigma Aldrich).

3.3.6.2 Imaging

All images were captured using a Leica DMi8 microscope under a bright-field setting. The images were acquired with a gain of 2.0 and an exposure time of 45ms. Whole-slice images were obtained by generating tile-scanned images which were stitched together with smoothed edges at 25x magnification. All images were saved in TIFF format.

Chapter 4.

Identifying the Inputs to the Different Retrosplenial Sub-regions

An interesting finding from Jacob *et al*. (2017) is the observation that bidirectionality is observed in the dysgranular retrosplenial cortex but not the granular retrosplenial cortex. This suggests that there are functional dissociations within the retrosplenial cortex, in line with the neuroanatomical, connectivity and behavioural differences we have described (see Section 2.3.3). Nonetheless, there are several limitations in the studies that have examined the differences between the two regions. For instance, even though a variety of behavioural tasks were employed, selective dRSC and gRSC lesions were never included as separate behavioural groups in the same lesion behavioural studies (see Section 2.3.3.3). As such, it remains unclear if the behavioural effects observed in each study were specific to that sub-region. Additionally, for studies that examined the inputs into the different retrosplenial sub-regions, they often used albino rats instead of pigmented rats and it may be inappropriate to extrapolate data between the two rat strains given that albino rats are known to have lower visual acuity (Prusky *et al*., 2002). The same studies also reported differential projections along the rostral-caudal axis of retrosplenial cortex, although they did not provide the coordinates in which they examined the projections (see Section 2.3.3.2 for more details).

In this experiment, we hypothesized that the differential directional information in dRSC and gRSC arises because of their inputs (i.e. information they receive). They can arise via two different but non-mutually exclusive means:

1. dRSC may receive exclusive inputs from visual cortical regions, which feed local visual information (i.e. visual cue cards that are 180° visually rotated between the two compartments) into bidirectional cells, hence generating 180° rotated PFDs.

2. gRSC may receive exclusive inputs that provide contextually relevant or vestibular related information that stabilises classical HD cells, thus enabling maintenance of PFDs across compartments.

Because of the limitations with existing connectivity studies (see above and Section 2.3.3.2), we decided to replicate the connectivity studies using Lister-Hooded rats at our implantation coordinates (Jacob *et al*., 2017; AP: - 5.5). To accomplish this, we decided to use a double retrograde tracing approach where tracers are injected at the same time in the two retrosplenial sub-regions (see Section 3.2.2; Schofield *et al*., 2007). This method offers several advantages including reducing variability between animals and surgeries, allowing for within-animal comparisons and allowing us to examine for axon collaterals (i.e. identifying common neurons that project to both retrosplenial sub-regions). The latter can be observed by examining for cells that are doubly labelled, which would suggest that they have axon terminals in both dRSC and gRSC. This method will also enable us to look for brain regions that could have anatomically segregated inputs into the different retrosplenial sub-regions. This chapter of the thesis will primarily focus on describing the qualitative differences between the inputs into the different retrosplenial sub-regions with specific focus placed on brain regions relevant to our hypothesis.

4.1 Methods

4.1.1 Animals

Fourteen male Lister Hooded rats were employed for the retrograde tracing experiments. After surgery, the animals were housed individually and maintained on a 12hr/12hr light/dark cycle. This experiment was done in accordance with the national [Animals (Scientific Procedures) Act, 1986, United Kingdom] and the international [European Communities Council Directive of 24 November 1986 (86/609/EEC)] legislation governing the maintenance of laboratory animals and their use in scientific experiments.

Out of fourteen animals, two animals were singly injected with just fluorogold ("single tracer") while the rest were injected with either fluorogold and CTB-AF594 or CTB-AF594 and CTB-AF488 ("double tracers"). The hemispheres and tracers were counterbalanced as much as possible, although occasionally the targeted hemisphere was changed during surgery if the superior sagittal sinus was found to cover a large extent of the craniotomy. In such cases, a craniotomy was made in the opposite hemisphere and the tracers were injected in that hemisphere. The tracers targeted to the respective retrosplenial sub-regions as well as the hemisphere in which the tracers were injected into are as follows:

Table 4.1: Tracers and their targeted injection sites and hemisphere.

ANIMAL	HEMISPHERE	DYSGRANULAR RSC	GRANULAR RSC
R699	Left	Fluorogold	
R717	Left	Fluorogold	
R681	Left	CTB-AF594	Fluorogold
R682	Left	Fluorogold	CTB-AF594
R685	Right	CTB-AF594	Fluorogold
R724	Right	CTB-AF594	Fluorogold
R729	Left	CTB-AF594	Fluorogold
R730	Left	CTB-AF594	Fluorogold
R731	Right	Fluorogold	CTB-AF594
R755	Right	CTB-AF594	Fluorogold
R756	Right	Fluorogold	CTB-AF594
R795	Right	Fluorogold	CTB-AF594
R878	Right	CTB-AF488	CTB-AF594
R879	Right	CTB-AF594	CTB-AF488

4.1.2 Data analysis

4.1.2.1 Qualitative identification

Qualitative identification of labelled structures represents the first parse in our data. All acquired images were post-processed in imageJ and manually cross-referenced to the atlas by Paxinos and Watson (6th Ed, 2007) to qualitatively identify retrogradely labelled structures. Identification of the labelled structures were done using several 'markers' – including the locations and size of ventricles, neighbouring structures and the closest Nissl-stained slices (see Section 3.2.3). Because there are variabilities in the injection sites and possible contamination to neighbouring structures (especially extrastriate visual cortex V2M; see Section 4.2.2), only consistently labelled neuroanatomical structures (across animals and slices) were considered to be projecting to either gRSCb or dRSC. We focus primarily on brain structures that are relevant to our discussion at hand. All anterior-posterior measurements are listed relative to bregma.

For visualization purposes, all images were pseudo-coloured in grey and then inverted such that labelled neurons appeared as black on a greyscale background. The animal identity, injection site and tracer identity are listed above each image. For double-tracing images, the merged images were generated by merging the images from the different fluorescence channels. In these images, fluorogold labelled images were pseudo-coloured in cyan, CTB-AF594 in red and CTB-AF488 in green. In addition, to make it consistent, images were flipped such that the injection sites are all on the right.

4.1.2.2 Quantitative analysis in the thalamus

For quantitative analysis, acquired images were post-processed and quantified in imageJ using a semi-automated cell counting workflow designed to remove observer's bias conducted as follows (Figure 4.1). The Tiff image was first opened in imageJ and the region of interest (ROI) selected and duplicated. The duplicated image was then adjusted to give the best contrast between labelled cells and the background via the use of an imageJ in-built local contrasting algorithm (Contrast Limited Adaptive Histogram Equalization (CLAHE); block size: 127, histogram bin: 256, max slope: 3), thus avoiding subjective adjustment of the contrast which would ultimately influence the efficiency of the thresholding algorithm. CLAHE functions by separating the image

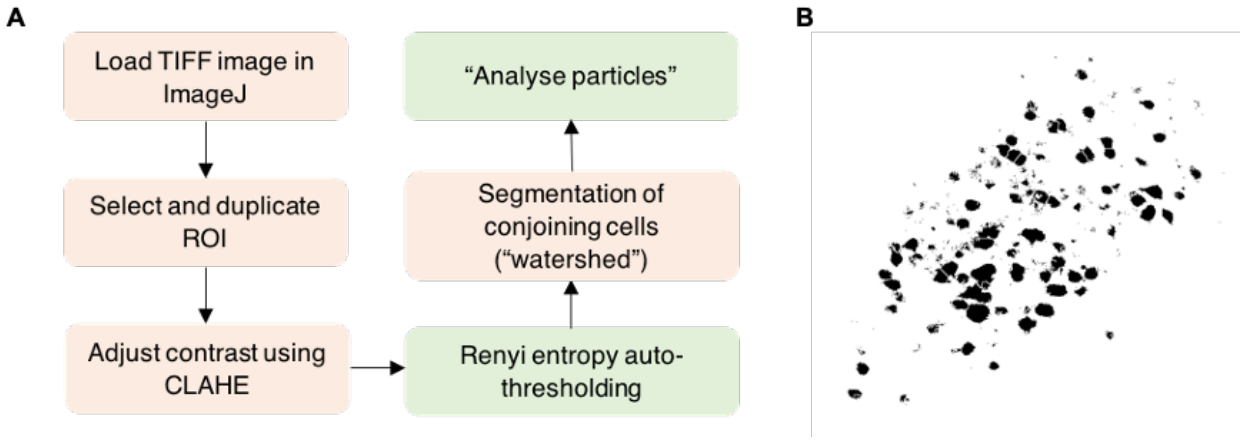

Figure 4.1: Semi-automated cell counting protocol. (A) The orange boxes indicate defined workflow while the green boxes indicate procedures that require some optimizations. Specifically, in selecting an appropriate auto-thresholding algorithm, several auto-thresholding algorithms were tested. Renyi entropy method gave the best contrast between cells and the background without over- or under-exposing the images. As for the 'analyse particle' plugin, the size to be used was determined by measuring the soma size of retrogradely labelled cells. The values obtained were similar to those that were reported in literature. **(B)** An example image from the anterodorsal thalamus showing the binary image generated after Renyi entropy thresholding. The semi-automated process worked relatively well for small structures like anterodorsal thalamus.

into blocks and equalizing the contrast histogram within each block (Lucas *et al*., 2013). The image was then thresholded using Renyi Entropy automated-thresholding algorithm and inverted to generate a binary image with labelled cells in black on a white background (Figure 4.1B). An automated segmentation plugin ("watershed") was used to separate conjoining cells and the number of cells were counted using the "analyse particles" plugin. To determine the appropriate size of the particles to be counted, random retrogradely labelled cells were selected from random images across two animals, and the size of the soma was measured and recorded. The average size was then used as the default value. For anterodorsal thalamus, fluorogold labelled cells have an average area of 204 ± 53.87 μm^2 (n = 32 cells) while CTB labelled cells have an average area of 166.19 ± 44.72 μm^2 (n = 21 cells). The measured sizes were similar to previous reports of soma sizes in the thalamus of male Holtzman rats (200 μm^2; Ling *et al*., 2012) and human thalamus (diameter of 15-25 μm, giving an area of approximately 173 μm^2 to 490 μm^2; van Buren and Borke, 1972). The slight difference in soma sizes seen between fluorogold and CTB labelled cells was likely due to the subcellular locations in which the tracers were localized – with fluorogold saturating the cytoplasm while CTB accumulated in discrete granules (endosomes) within the cells. The workflow was slightly altered for images from three animals (R682; CTB labelling, R699; fluorogold labelling and R878 double labelling) as the auto-thresholding algorithm over-exposed

the images. In the three animals, the images were not CLAHE-adjusted but undergo the thresholding algorithm directly.

For quantitative comparisons, the cell count for each slice was normalised against the area of the anterodorsal thalamus (or rather ROI for anterodorsal thalamus) in that slice, and the cell count per slice was expressed as labelled neurons per mm^2.

4.1.2.3 Statistics

The injections, even within the same animal, were treated as independent samples so as to allow us to combine data from animals that had only one working injection. The number of labelled neurons per mm^2 across slices was averaged within animals. Due to the resulting small sample sizes (especially for CTB samples, n = 4), the quantification was statistically tested using Wilcoxon rank sum test.

4.2 Results

The data presented in this section will be geared towards a qualitative description of the projections towards the two retrosplenial sub-regions instead of a quantitative description, similar to classical anatomical studies (such as van Groen and Wyss, 1992, 2003; Vogt and Miller, 1983). This is because large variation in retrograde labelling can be observed especially in cortical regions – likely as a consequence of interactions between several variable factors including: (i) differential extent of spread of tracers in the rostral-caudal axis (see Table 4.2) (ii) differential extent of spread of tracers along the dorsal-ventral axis (see Figure 4.2) and (iii) differential extent of spread between the tracers. As such, cautions were taken when interpreting the data and it will be unbefitting to make premature quantitative statements. Nonetheless, qualitative statements were made as when the data is convincing. Likewise, quantitative analysis was made only when the author has the confidence that it cannot be explain by the variations stated above.

4.2.1 Nomenclature

For the purpose of this thesis, we will adopt the divisions and nomenclatures defined in Van Groen and Wyss (2003) who divided gRSC into two sub-regions. Because we used the atlas by Paxinos and Watson (2007) as a point of reference in this thesis, the demarcations used by Van Groen and Wyss (2003) were applied to that of Paxinos and Watson (2007). Particularly, gRSCb and gRSCc in Paxinos and Watson (2007) were collapsed into a single area gRSCb while gRSCa was consistent between the atlas and Van Groen and Wyss (2003). The recording sites of Jacob *et al*. (2017) extended predominantly into gRSCb and dRSC (see Figure 2.6), which were where we targeted our injections. gRSCa is a small sub-region of retrosplenial cortex that is dorsal of postsubiculum, and only found caudally. As Jacob *et al*. (2017) mainly recorded from gRSCb, gRSCa was not targeted for injections.

In the atlas from Paxinos and Watson (2007), the RSC extended anterior-posteriorly from approximately -1.72mm to -9.36mm with dRSC extending through the entire length while gRSCb terminated at approximately -8.52mm. As such, our target injection site (AP: -5.5) is quite medial along the AP axis. At the injection site, the dRSC is bordered by gRSCb medially and V2M laterally. Meanwhile, gRSCb is bordered by dRSC dorsally and gRSCa ventrally (Figure 4.2).

4.2.2 Injection sites

We first examined the injection sites to ensure proper interpretation of data. Out of fourteen animals, we could not precisely define the injection sites for three animals – R681, R795 and R879 - and it seems likely that the tracers were not injected properly and had spread uncontrollably in the brain (not shown). As such, the three animals were removed from further analysis. Occasionally, the CTB-AF594 injections did not work (no fluorescence observed) and such injections were treated as single tracing animals (R724 and R756). The injection sites are shown schematically in Figure 4.2, while Table 4.2 shows the injections that were included for further analysis.

As observed, fluorogold injections tend to spread more than CTB (also shown in Yao *et al*., 2018) and as such have a tendency to contaminate the surrounding regions. Nonetheless, if placed in the right location, fluorogold gave a good labelling (and subsequent uptake) in the respective retrosplenial sub-regions. Within a slice, the diameter of fluorogold injection sites ranged from 1.074mm to 2.16mm while for CTB, it ranged from 0.447mm to 0.867mm along its largest extent. Pressure injections also occasionally damage some part of the brain causing lesions. These lesions were taken note of as CTB is known to be taken up by damaged fibres of passage and can be transported anterogradely (Conte *et al*., 2009). Nonetheless, for the purpose of this thesis, we only examined structures with clearly labelled cell bodies and labelled axonal terminals were ignored.

Examination of the injection sites resulted in several changes to the classification of animals within each injection group (dRSC vs gRSCb). The final classification of the animals according to their injection groups is summarized in Table 4.2. Because our comparison is between dRSC and gRSCb, we excluded injections that have extensive cross-contamination between the two sub-regions. Injections into dRSC occasionally resulted in tracers leaking into the extrastriate visual area V2M while injections into gRSCb occasionally resulted in leakage into the ventricle ventral of gRSCb, leading to contamination in the superficial layer of superior colliculus (SC). These animals were included unless the contamination was extensive, and the contamination taken note of. To make sure we are not including aberrantly labelled structures, only consistently labelled neuroanatomical structures (across animals and slices) were considered to be projecting to either gRSCb or dRSC.

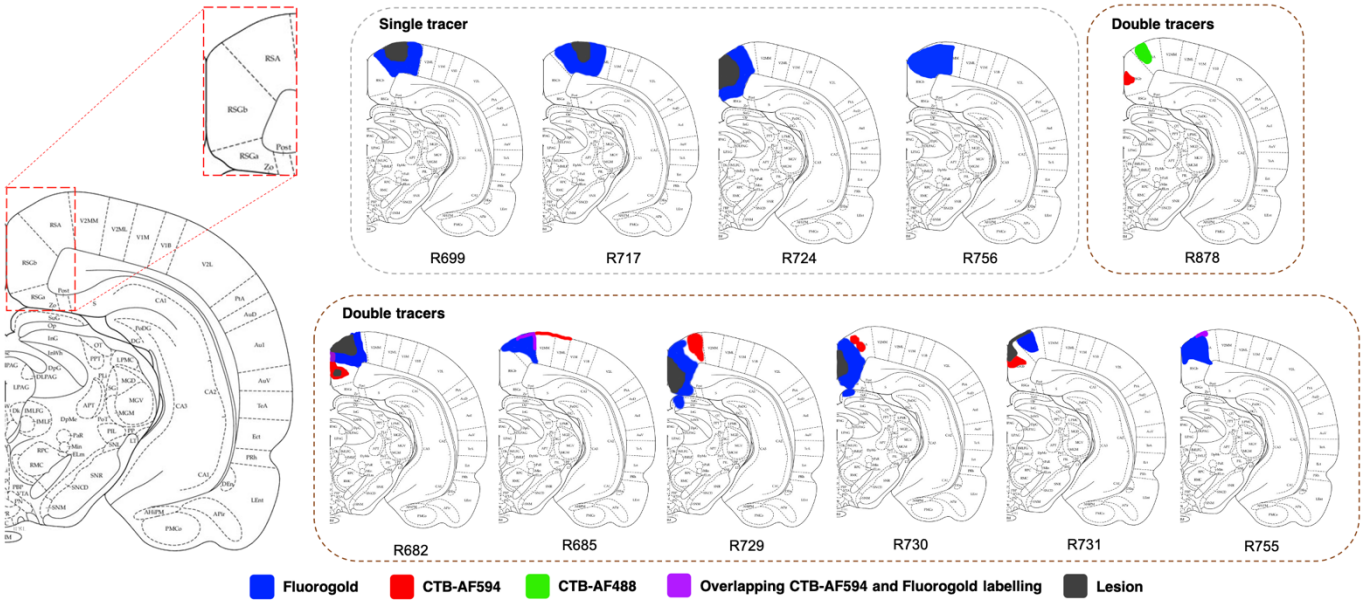

Figure 4.2: Schematic diagram of the injection sites at AP -5.5. The tracers were directed to either dRSC or gRSCb (*left*), and injected animals were classified as either single tracing or double tracing experiments. Occasionally, CTB labelling was not observed and these animals were treated as single tracing animal (R724 and R756). As observed, FG tend to spread extensively while CTB spreads are more localized. Examination of the injection sites is essential for interpretation of our data. The target injection sites for each animal are summarized in Table 4.1. The resulting classification of animals after examinations of the injection sites are summarized in Table 4.2. *Blue: Fluorogold; Red: CTB-AF594; Green: CTB-AF488; Magenta: Overlapping FG and CTB-AF594 labelling; Grey: Lesions caused by injections.*

In brief, several injections were discounted because the injection sites were found to be on the border of gRSCb and dRSC, and extensive contamination between the two sub-regions could be observed (e.g. R724 and R755 fluorogold injections targeted to gRSCb, and R682 and R756 fluorogold injections targeted to dRSC). The fluorogold injection in R685 originally targeted to gRSCb (see Table 4.1) was also reassigned as a dRSC injection after observation that the injection was more dorsolaterally located and had covered the extent of dRSC instead of gRSCb. However, the CTB injection for the same animal was removed as it appeared to have spread laterally on the surface of the brain (specifically above dRSC and V2M). The CTB injection for R755 was removed for the same reason as the injection was observed to be located superficially on the surface of dRSC (predominantly layer I). The fluorogold data for R729 was also removed as the tracer seems to have leaked into the ventricle, and the caudal extent of the brain was observed to be massively contaminated (i.e. contamination can be observed on the surface of superior colliculus as well as along the extent of postsubiculum).

Table 4.2: Summary of injections and whether they are included for further analysis

Animals	Dysgranular RSC					Granular RSC				
	Tracers	Possible Contamination? gRSCb	V2M	Included?	Rostral-Caudal Spread (mm)	Tracers	Possible Contamination? dRSC	Ventricle/SC	Included?	Rostral-Caudal Spread (mm)
R699	FG	Slight	✓	✓	-4.2 to -6.28					
R717	FG	×	✓	✓	-4.8 to -6.24					
R724						FG	✓	×	×	-
R756	FG	✓	✓	×	-					
R682	FG	✓	Slight	×	-	CTB-594	×	Slight	✓	-4.8 to -6.1
R685	FG	Slight	×	✓	-4.2 to -6.4					
R729	CTB-594	×	×	✓	-4.2 to -6.1	FG	Slight	✓	×	-
R730	CTB-594	×	×	✓	-5 to -6	FG	×	Slight	✓	-4.56 to -6.1
R731	FG	×	✓	✓	-4.2 to -6.36	CTB-594	×	×	✓	-4.8 to -6
R755	CTB-594	×	×	×	-	FG	✓	×	×	-
R878	CTB-488	×	×	✓	-4 to -5.6	CTB-594	×	×	✓	-4.2 to -5.6

FG = Fluorogold, CTB-594 = Choleratoxin subunit B conjugated with AF594, CTB-488 = Choleratoxin subunit B conjugated with AF488

Single injection animals or localized injection sites not found (read Section 4.2.2 for more details)

Because there are some differences in projections along the rostral-caudal axis (equivalent to the anterior-posterior axis in the rat brain) of retrosplenial cortex (Van Groen and Wyss, 1992; 2003), we also quantified the extent of spread of the injections along the rostral-caudal axis. Consistent with the wider spread of fluorogold within a slice, fluorogold also tends to spread further along the rostral-caudal axis although CTB also occasionally spread quite widely along the AP axis. CTB injections typically gave a clear injection locus, while fluorogold injections typically looked more diffuse. Nonetheless, the tracers spread between AP: -4 mm to – 6.4 mm (see Table 4.2).

4.2.3 Inputs from the head direction system

Because we are predominantly interested in how bidirectionality arises in the dRSC but not in the gRSC, we first examined inputs that retrosplenial cortex could receive from the head direction system. Particularly, both postsubiculum and anterodorsal thalamus were found to project to both sub-regions of retrosplenial cortex (Figure 4.3 and 4.4). For postsubiculum, labelled neurons were typically found in deeper layers (layer V and VI) when tracers were injected into both dRSC and gRSCb (Figure 4.3). This is consistent with Van Groen and Wyss (1992; 2003) who reported labelling in the deeper layers of postsubiculum. We occasionally observed superficial layer labelling when tracers were placed in dRSC, but this was not consistent and likely reflect contamination into the neighbouring V2M (see Figure 4.3, top row, left). Although labelled neurons were generally found in the same layers, doubly labelled cells in animals with valid double injections (see Table 4.2; R730, R731 and R878) were rarely observed. This could however be a consequence of the different size of the injections and/or our failure to have nice, clear injections that cover all layers of dRSC and gRSCb concomitantly in the same animals. Nonetheless, it is clear that deep layers of postsubiculum project to both retrosplenial sub-regions.

In contrast, significant differences in the projections from anterodorsal thalamus, the head direction thalamic nuclei, to the different retrosplenial sub-regions were observed. Particularly, injections in gRSCb consistently resulted in more labelled neurons in anterodorsal thalamus as compared to dRSC injections. (Figure 4.4A; unlike the variations often observed in cortical regions). The differences in the number of projections were observed throughout the entire rostral-caudal extent of anterodorsal thalamus. We hence decided to quantify the number of labelled neurons using a semi-automated protocol designed to remove observer's bias (see Section

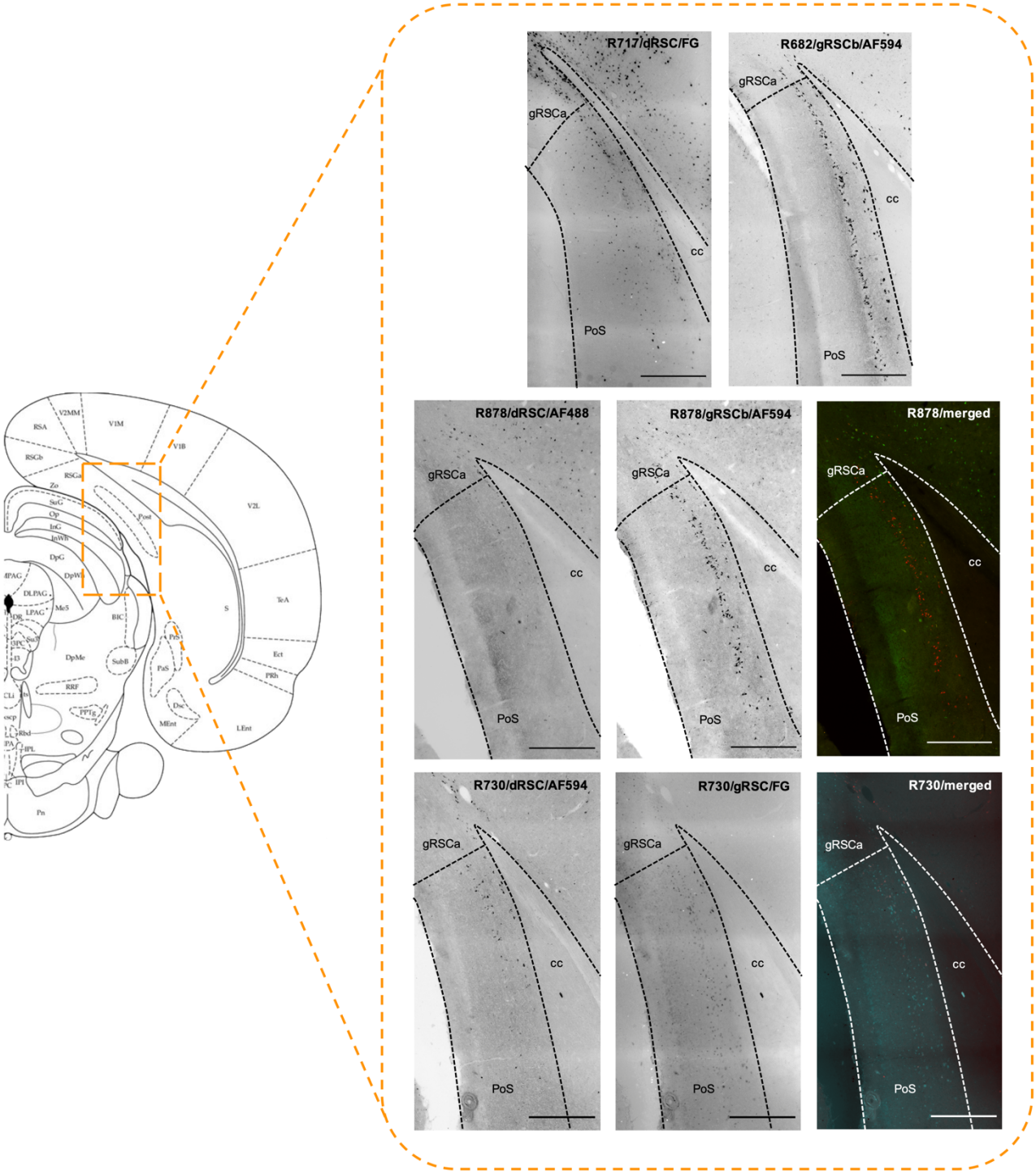

Figure 4.3: Retrograde labelling was observed in the postsubiculum when tracers were injected in both dRSC and gRSCb. *Top row*, two single tracing animals with injections either in the dRSC (*left*) or gRSCb (*right)*. *Middle and bottom row*, two double tracing animals with injections placed in both dRSC *(left)* and gRSCb *(middle)*. The third image of each row represents the composite image of the two previous images. As can be observed, labelled neurons were typically found in the deep layer of the postsubiculum (closer to the corpus callosum) in both injections. The animal identity, injection site and tracer used are listed at the top of each image. *AF488 = CTB-AF488; FG = fluorogold; AF594 = CTB-AF594.* Merged images were made by overlaying images pseudo-coloured as c*yan for fluorogold labelling, red for CTB-AF594 labelling and green for CTB-AF488 labelling. cc: corpus callosum. Scale bar: 500μm.*

4.1.2.2). Similar to the visual observation, the number of neurons per mm^2 was significantly lower when tracers were placed in dRSC than gRSCb (two-tailed Wilcoxon rank sum test, W = 28, *p = 0.006*). Fluorogold injections tend to give more labelled cells than CTB, consistent with the wider spread of the tracers (see Section 4.2.2). It is unlikely that the higher number of retrograde labelling observed in gRSCb is a consequence of a larger injection loci as significant retrograde labelling can be observed even within the animal that had one of the smallest injection locus in gRSCb (R878; see Figure 4.2; Figure 4.4, first row, second column). In summary, it is likely that anterodorsal thalamus projects differentially to the different retrosplenial sub-regions with gRSCb receiving more inputs than dRSC.

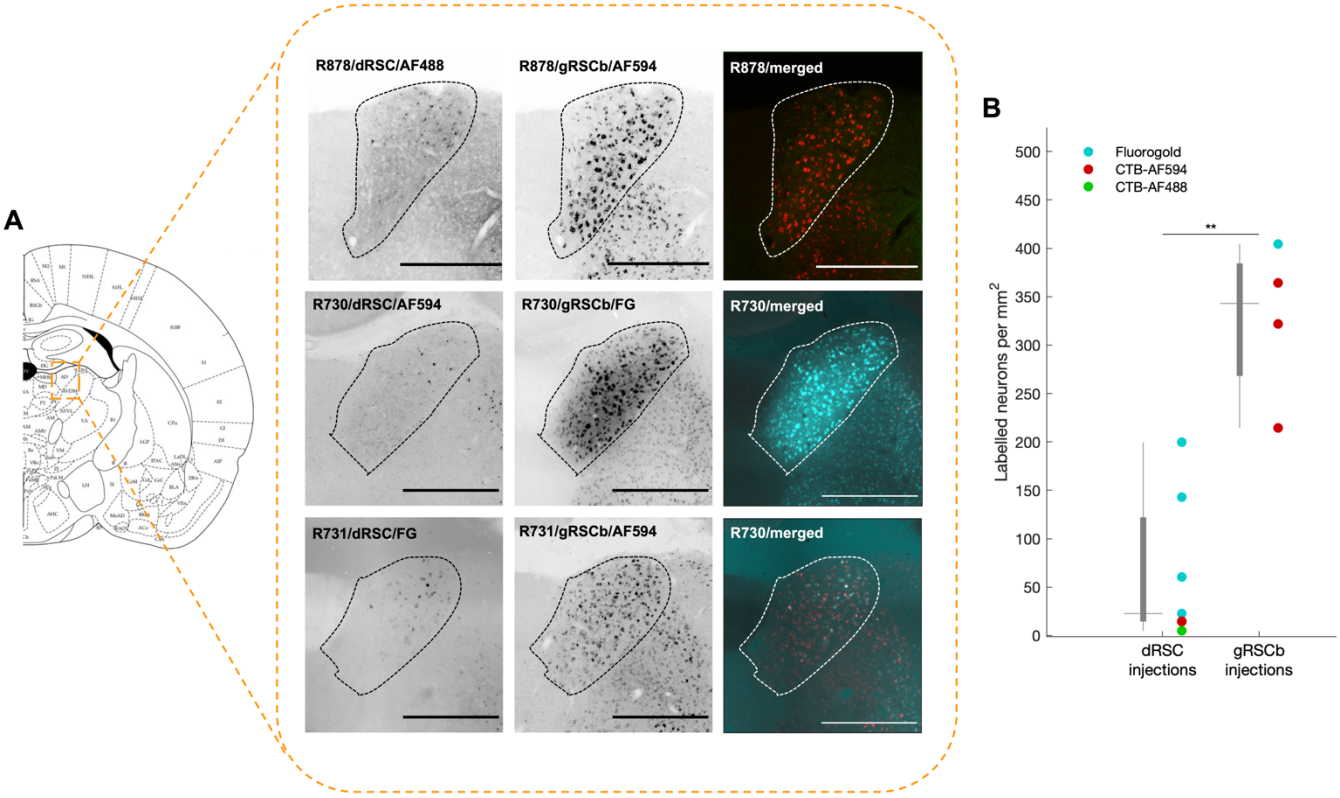

Figure 4.4: Anterodorsal thalamus is likely to project differentially to the two retrosplenial sub-regions (A) Double tracing animals showing consistent quantitative differences in the amount of retrograde labelling in anterodorsal thalamus when tracers were placed in dRSC and gRSCb. The quantitative differences observed were consistent regardless of tracers used. The animal identity, injection site and tracer used are listed at the top of each image. *AF488 = CTB-AF488; FG = fluorogold; AF594 = CTB-AF594.* Merged images were made by overlaying images pseudo-coloured as c*yan for fluorogold labelling, red for CTB-AF594 labelling and green for CTB-AF488 labelling. Scale bar: 500μm*. **(B)** Quantification of the number of labelled neurons per mm^2 when injections were placed in dRSC or gRSCb. Each marker represents the average number of labelled neurons per mm^2 across slices within an animal. Each animal thus contributed one data point except for successful double tracing animals (R730, R731 and R878) which contributed two data points each - one for each injection.

4.2.4 Inputs from other spatial systems

We next examine if the different retrosplenial sub-regions receive different inputs from the other spatial systems (i.e. place cells, border cells and grid cells). We thus shift our focus to the hippocampus, subiculum and entorhinal cortex respectively (see Section 1.3). We first examine the inputs from subiculum. Consistent with Van Groen and Wyss (1992, 2003), we observed labelled neurons in the dorsal part of subiculum but only when tracers were injected into gRSCb (Figure 4.5, middle column). No retrograde labelling in the dorsal subiculum was observed in

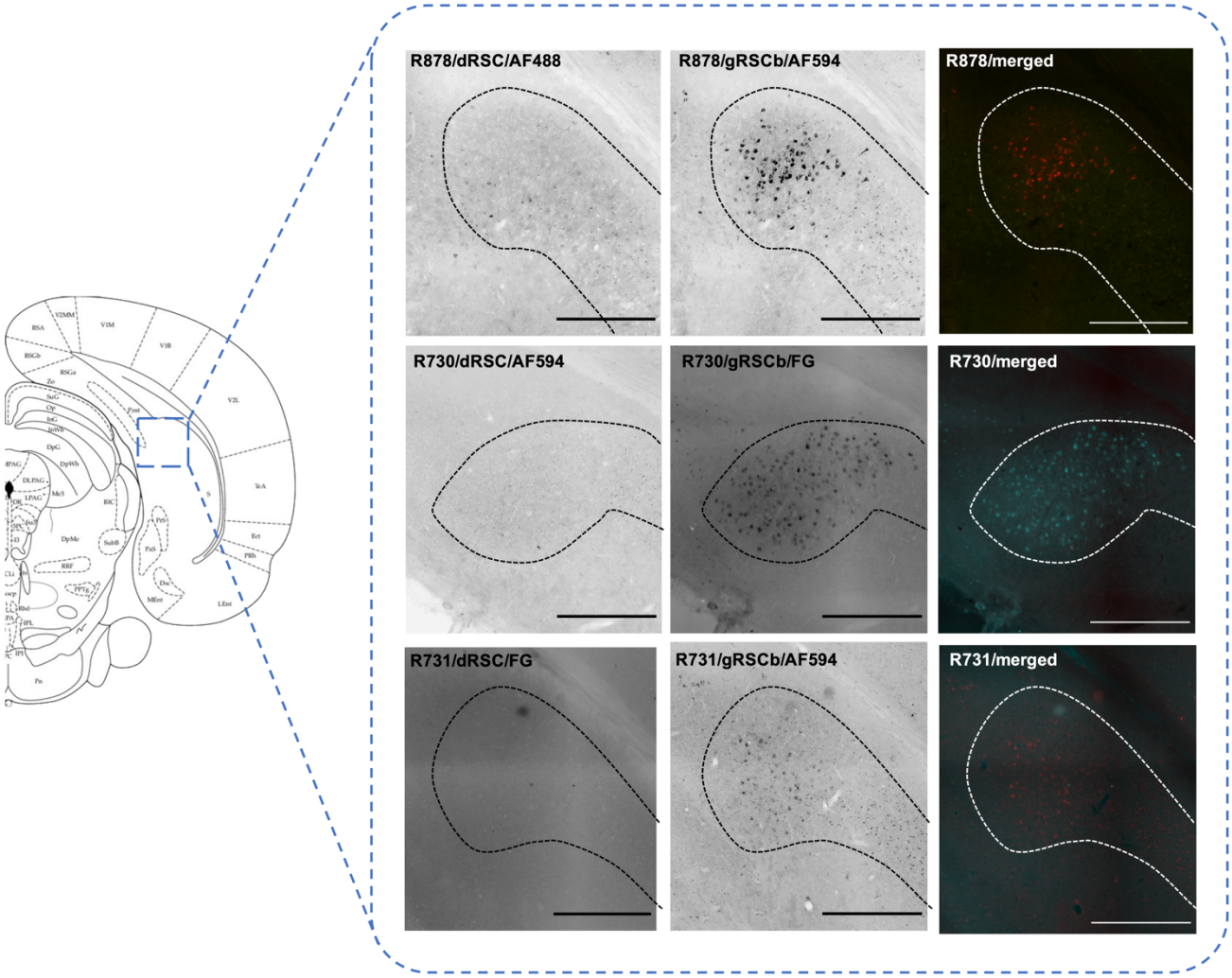

Figure 4.5: Dorsal subiculum projects only to gRSCb, but not dRSC. Each row shows each of the double tracing animals and the labelling in dorsal subiculum. As observed, labelled neurons were only observed when tracers were placed in gRSCb, but not dRSC. The labelled neurons were found in the most dorsal end of subiculum and were found throughout the rostral-caudal extent of subiculum. The animal identity, injection site and tracer used are listed at the top of each image. *AF488 = CTB-AF488; FG = fluorogold; AF594 = CTB-AF594.* Merged images were made by overlaying images pseudo-coloured as c*yan for fluorogold labelling, red for CTB-AF594 labelling and green for CTB-AF488 labelling. Scale bar: 500μm.*

dRSC injections (Figure 4.5, first column). The retrogradely labelled neurons in gRSCb injections were observed in the pyramidal layers at the most dorsal end of the subiculum (just ventral of postsubiculum) and were observed throughout the rostral-caudal extent of subiculum. Particularly, neurons that were labelled formed a cluster, akin to a nucleus found in the thalamus (Figure 4.5). These neurons could be glutaminergic in nature (Yamawaki *et al*., 2019). Thus, it is likely that dorsal subiculum projects exclusively to gRSCb.

In addition to dorsal subiculum, we also observed very sparse labelling in the CA1 subfield of dorsal hippocampus but also only when tracers were placed in gRSCb, consistent with Van Groen and Wyss (2003). Similar to dorsal subiculum, no retrograde labelling was observed when tracers were placed in dRSC. These retrograde labelling were minute and were not observed in every imaged slice. They were also typically found rostrally (around bregma -2.8 to -3.5) though some sparse caudal labelling can also be observed (not shown). Interestingly, we observed two patterns of labelling in CA1. Labelled neurons were found either in the pyramidal cell layer (Figure 4.6; R878, R730 and R682) or in the stratum lacunosum-moleculare layer (Figure 4.6; R731 and R682). The latter pattern of retrogradely labelled neurons has been extensively described with multiple studies showing that the labelled neurons found in stratum lacunosum-moleculare layers are long range GABAergic neurons projecting to layer I of gRSCb (Yamawaki *et al*., 2019; Jinno *et al*., 2007; Miyashita and Rockland, 2007). In contrast, there are only a few studies who have reported labelling in the pyramidal cell layer (Van Groen and Wyss, 1990c; Miyashita and Rockland, 2007) and it is less clear if these neurons are also long-range GABAergic neurons. It is also unclear why we see only one pattern of labelling in most animals (pyramidal cell layer in R878 and R730; stratum lacunosum-moleculare layer in R731) but this may reflect variability in the spread and uptake of tracers at the injection sites. Nonetheless, we did observe both patterns of labelling in one animal (R682; Figure 4.6, bottom row) and it is plausible that gRSCb, but not dRSC, receives projections from CA1 subfield of hippocampus.

We next examined for projections from the entorhinal cortex. We did not find any labelled neurons in the medial entorhinal cortex. Thus, it seems likely that both sub-regions do not receive inputs from the grid cell system. In contrast, we found retrogradely labelled neurons in dorsolateral entorhinal cortex (also more generally referred to as lateral entorhinal cortex) but only when CTB was injected into gRSCb (Figure 4.7, top three row: R682; R878; R731). Injections of fluorogold in gRSCb did not result in any visible retrograde labelling (Figure 4.7; last row). In addition, we

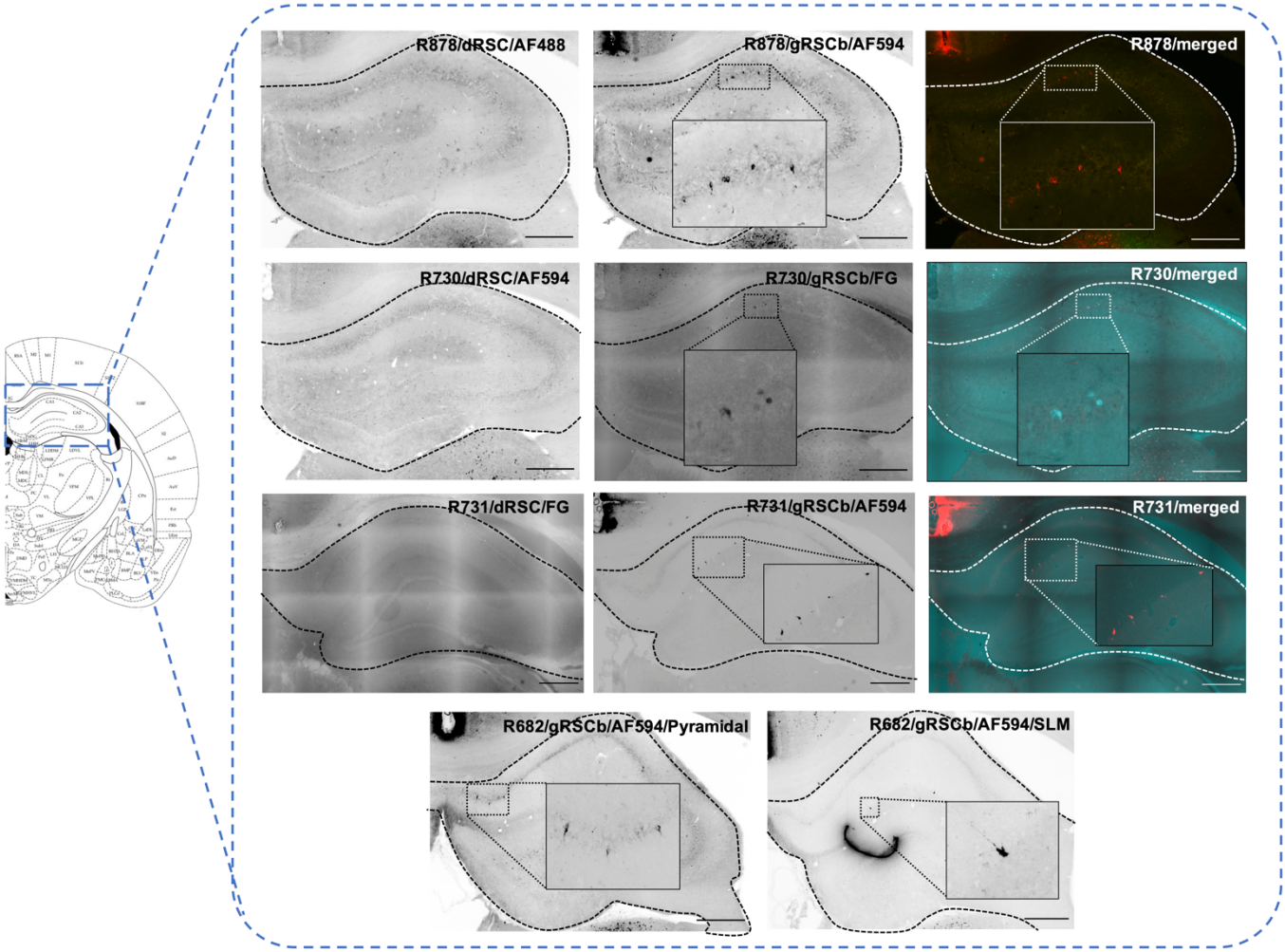

Figure 4.6: CA1 subfield of dorsal hippocampus likely projects only to gRSCb, but not dRSC. Two patterns of retrograde labelling were observed in dorsal hippocampus when tracers were placed in gRSCb. Labelled neurons were sometimes found in the pyramidal cell layer (top two rows, representative images from R878 and R730; bottom row, R682 left) or in the stratum lacunosum-moleculare layer (Second last row, representative images from R731; bottom row, R682 right). The large black strand seen in R682, SLM image (*bottom row, right*) is due to dirt on the slide. Insets are zoomed in images of the sparsely labelled hippocampal neurons. The animal identity, injection site and tracer used are listed at the top of each image. *AF488 = CTB-AF488; FG = fluorogold; AF594 = CTB-AF594.* Merged images were made by overlaying images pseudo-coloured as c*yan for fluorogold labelling, red for CTB-AF594 labelling and green for CTB-AF488 labelling. Scale bar: 500*μ*m.*

never observed labelling in the dorsolateral entorhinal cortex when tracers were placed in dRSC (regardless of tracer identity). This is surprising as projections from the superficial layer of dorsolateral entorhinal cortex to gRSCb have not been described in existing literature. Furthermore, the observation that retrogradely labelled neurons were only found in CTB-gRSCb injected animals but not in fluorogold-gRSCb injected animals suggests that there is an interaction between labelling efficiency and tracer identity, possibly a consequence of the different uptake mechanisms employed by fluorogold and CTB (further discussed in Section 4.3). Although there

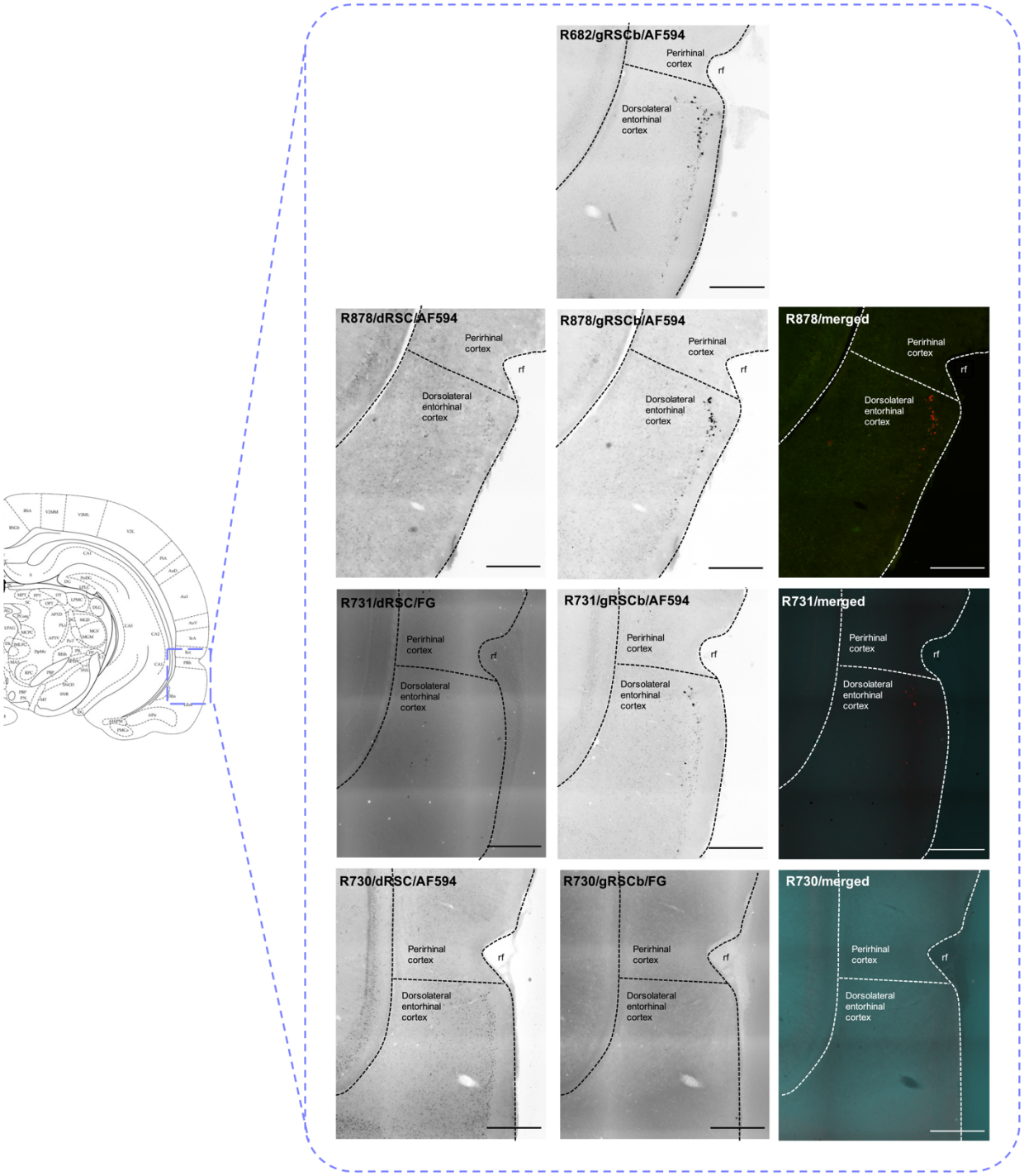

Figure 4.7: Retrogradely labelled neurons were found in dorsolateral entorhinal cortex but only when CTB was injected in gRSCb. *Top row*: single tracing data from R682 with CTB injected in gRSCb showing labelling in dorsolateral entorhinal cortex. *Second and third row*: double tracing data with CTB injected in gRSCb and either fluorogold (R731) or another variant of CTB (R878) injected in dRSC. Labelled neurons in dorsolateral entorhinal cortex were observed in both cases. *Fourth row*: A double tracing animal (R730) that receives fluorogold in gRSCb and CTB in dRSC. In contrast, labelled neurons were not observed in dorsolateral entorhinal cortex. The animal identity, injection site and tracer used are listed at the top of each image. *AF488 = CTB-AF488; FG = fluorogold; AF594 = CTB-AF594.* Merged images were made by overlaying images pseudo-coloured as c*yan for fluorogold labelling, red for CTB-AF594 labelling and green for CTB-AF488 labelling. rf: Rhinal fissure. Scale bar: 500*μ*m*.

is a possibility that the difference in observations across CTB and fluorogold injections could be a consequence of differently placed injections across animals, it is highly unlikely as fluorogold in R730 spread more extensively than any of the CTB injections (see Figure 4.2).

Nevertheless, the retrogradely labelled neurons observed in dorsolateral entorhinal cortex were typically found close to the border of perirhinal cortex. The labelling was remarkably consistent in the three animals we had with CTB in gRSCb, and they are observed as a band in layer II of dorsolateral entorhinal cortex. Thus, it is likely that gRSCb receives exclusive inputs from dorsolateral entorhinal cortex.

4.2.5 Visual cortical inputs

As described in Section 2.3.2, bidirectional cells are seemingly sensitive to the local visual environment as demonstrated by the 180° rotated PFDs when the animals crossed the doorway separating the two compartments (the only salient cue that has a 180° rotated symmetry is the visual scene). As such, it is possible that bidirectional cells (and by extension, dRSC) receive more visual inputs than HD cells (i.e. gRSCb). We thus examine for retrogradely labelled neurons in visual cortical areas – predominantly the striate (primary visual cortex V1; Brodmann area 17) and extrastriate visual cortex (V2; Brodmann area 18). The extrastriate V2 visual cortex is extremely complicated and has been previously subdivided into multiple smaller regions (Coogan and Burkhalter, 1993). For the purpose of this thesis, we will describe them simply as V2M and V2L (Brodmann area 18b and 18a respectively) as described in Paxinos and Watson (2007).

A complication from our injections stemmed from the occasional contamination of retrograde tracers into the neighbouring V2M when tracers were placed in dRSC (see Figure 4.2). As V2M receives inputs from both V1 and V2L (Coogan and Burkhalter, 1993), contamination into this region will give an inaccurate (and likely overestimation) of the number of labelled neurons in the different visual areas. In addition, fluorogold injection in gRSCb was also observed to contaminate the superficial layer of superior colliculus (see R730; Figure 4.2) which is known to receive inputs from visual cortical regions (Coogan and Burkhalter, 1993). As such, we decided to only examine cholera toxin injected animals, thus treating most animals (with the exception of R878) as single tracing animals. We thus have two dRSC-CTB animals (R729 and R730) and two gRSCb-CTB animals (R682 and R731), as well as one double tracing animal (R878).

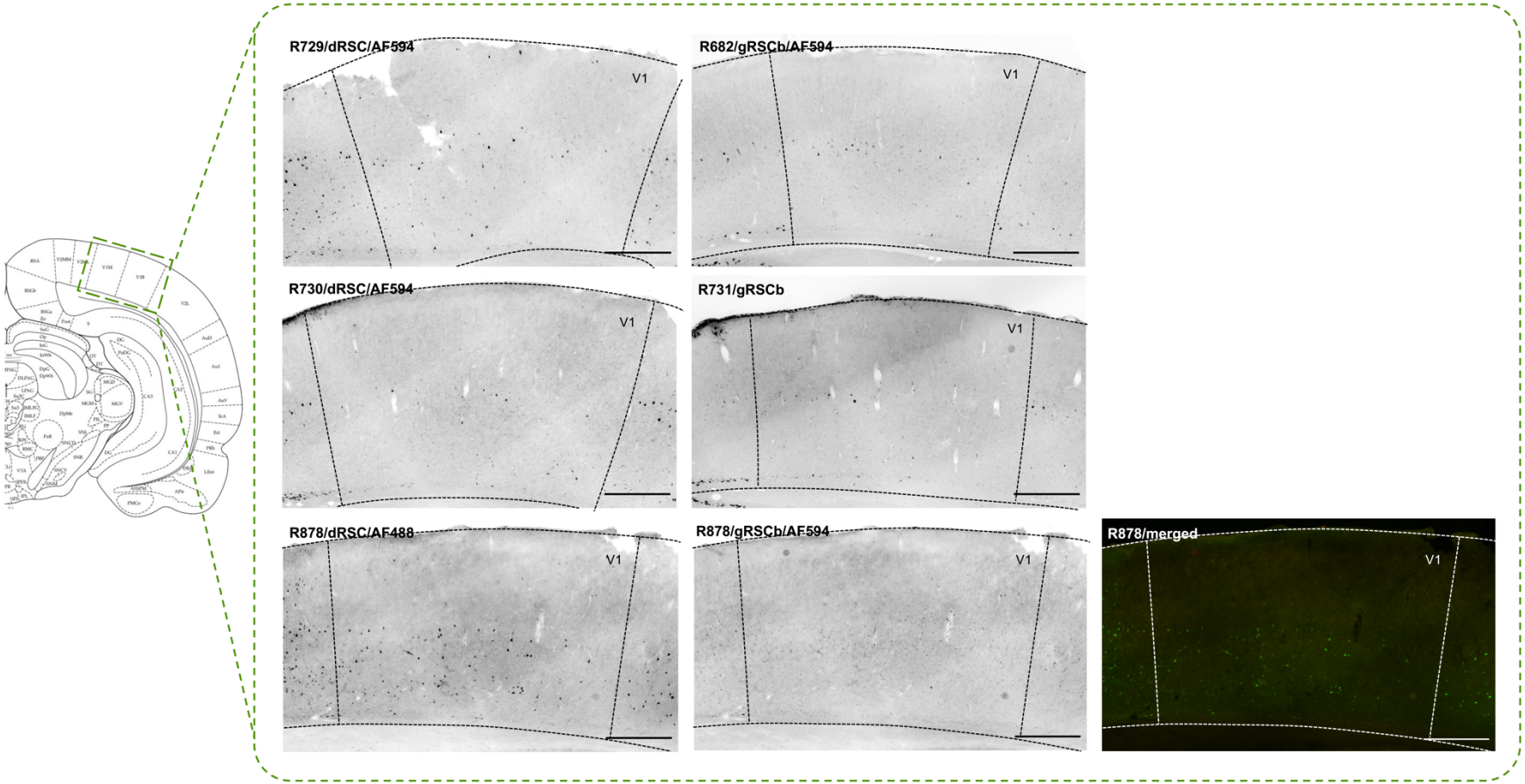

Figure 4.8: Representative images showing retrograde labelling in primary visual cortex. Retrograde labelling was observed in deeper layers of the primary visual cortex when tracers were placed in dRSC (l*eft most column*). Similarly, retrograde labelling can be observed in deeper layers of the primary visual cortex when tracers were placed in gRSCb, but only in two animals (*second column, first two rows; R682 and R731*). No labelling was observed in R878 when CTB was injected into gRSCb, but it is likely a consequence of differentially placed or smaller injection loci leading to insufficient axonal uptake. The animal identity, injection site and tracer used are listed at the top of each image. *AF488 = CTB-AF488; FG = fluorogold; AF594 = CTB-AF594.* Merged images were made by overlaying images pseudo-coloured as c*yan for fluorogold labelling, red for CTB-AF594 labelling and green for CTB-AF488 labelling. Scale bar: 500*μ*m*.

We first examine retrograde labelling in the primary visual cortex (V1), which Van Groen and Wyss (1992) previously reported projections only to dRSC. Consistent with van Groen and Wyss (1992), we observed retrograde labelling in V1 when retrograde tracers were placed in dRSC (Figure 4.8, column 1). The amount of retrograde labelling observed was quite variable (see second row R730, dRSC injection which had quite sparse neuronal labelling). Surprisingly, we also observed retrograde labelling in V1 in two (of three) animals when CTB were injected in gRSCb (Figure 4.8, column 2, row 1 and 2). These labelled neurons were also found predominantly in the deeper layers, and the patterns of labelling were not dissimilar to those observed for dRSC injections. Similar labelling patterns were also observed along the rostral-caudal axis (not shown) of both injections with labelled neurons typically found in deeper layers of V1. It should be noted that we did not observe retrograde labelling in V1 of R878 when CTB was placed in gRSCb (Figure 4.8, bottom row, middle column). The lack of neuronal labelling in R878 could be explain by the slight difference in the location of the injection loci of CTB and/or size of the injection loci (see Table 4.2). Thus, it is plausible that in Lister Hooded rats, unlike Sprague-Dawley rats, V1 projects to both retrosplenial cortex sub-regions.

We next examine for retrograde labelling in the extrastriate V2 cortex. As mentioned, the extrastriate V2 cortex is more complicated than the primary visual cortex and can be divided into multiple smaller regions (Coogan and Burkhalter, 1993). However, for the purpose of this thesis, we divided V2 into V2M (medial; Brodmann area 18b) and V2L (lateral; Brodmann area 18a) as described by Paxinos and Watson (2007). V2M is located more medially and is located between dRSC and primary visual cortex. V2L, in contrast, is located more laterally and is on the lateral end of the primary visual cortex. It should be noted that similar labelling patterns as those shown in the representative images of Figure 4.9 and Figure 4.10 were observed along the entire rostral-caudal axis of V2M and V2L for each animal respectively.

Similar to the retrograde labelling observed in the primary visual cortex, most labelling (except for R878) can be observed in deeper layers of V2M when CTB were placed in dRSC. A similar pattern of labelling was observed when CTB were injected into gRSCb (Figure 4.9), although only in two of the three animals (R682 and R731). The double CTB tracing animal (R878) gave a slightly different labelling pattern with additional labelling in the superficial layer in dRSC injection and no labelling in gRSCb injection. As explained, the inconsistency is likely due to variability in the spread of CTB at the injection sites. In addition, there may be some quantitative

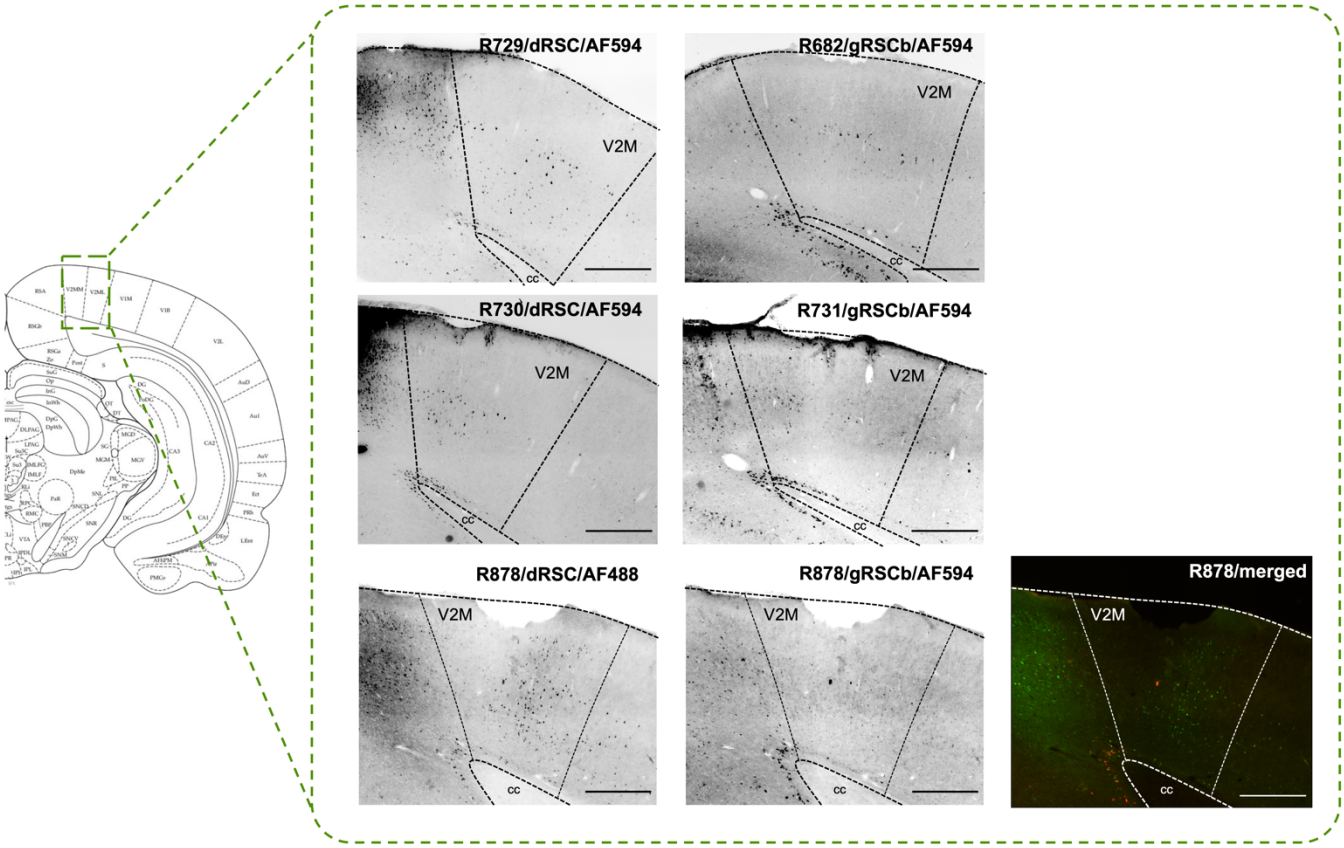

Figure 4.9: Representative images showing retrograde labelling in V2M. Retrograde labelling can be observed in deeper layers of V2M when tracers were placed in dRSC (l*eft most column*). Similarly, retrograde labelling can be observed in deeper layers of the V2M when tracers were placed in gRSCb, but only in two animals (*second column, first two rows; R682 and R731*). No labelling was observed in R878 when CTB was injected into gRSCb, but it is likely a consequence of differentially placed or smaller injection loci leading to insufficient axonal uptake. The animal identity, injection site and tracer used are listed at the top of each image. *AF488 = CTB-AF488; FG = fluorogold; AF594 = CTB-AF594.* Merged images were made by overlaying images pseudo-coloured as c*yan for fluorogold labelling, red for CTB-AF594 labelling and green for CTB-AF488 labelling. Scale bar: 500*μ*m.*

differences in the number of projections, but we could not confirm that in our study as the number of neurons labelled varies a lot even within animals of the same injection status. The variability observed likely reflects variability in the extent of spread around the injection sites and/or limited spread of CTB (also see start of result chapter). Nonetheless, retrograde labelling was typically found in deep layers of V2M when CTB were injected into both retrosplenial sub-regions.

Examination of retrograde labelling in V2L also revealed a similar pattern – retrograde labelling was found predominantly in the deep layers of V2L in both dRSC and gRSCb injections (Figure 4.10). Again, there may be a quantitively difference in the number of projections, but we could not confirm the observation in our study due to the aforementioned reasons. Nonetheless, it is likely that deep layers of V2L project to both retrosplenial sub-regions.

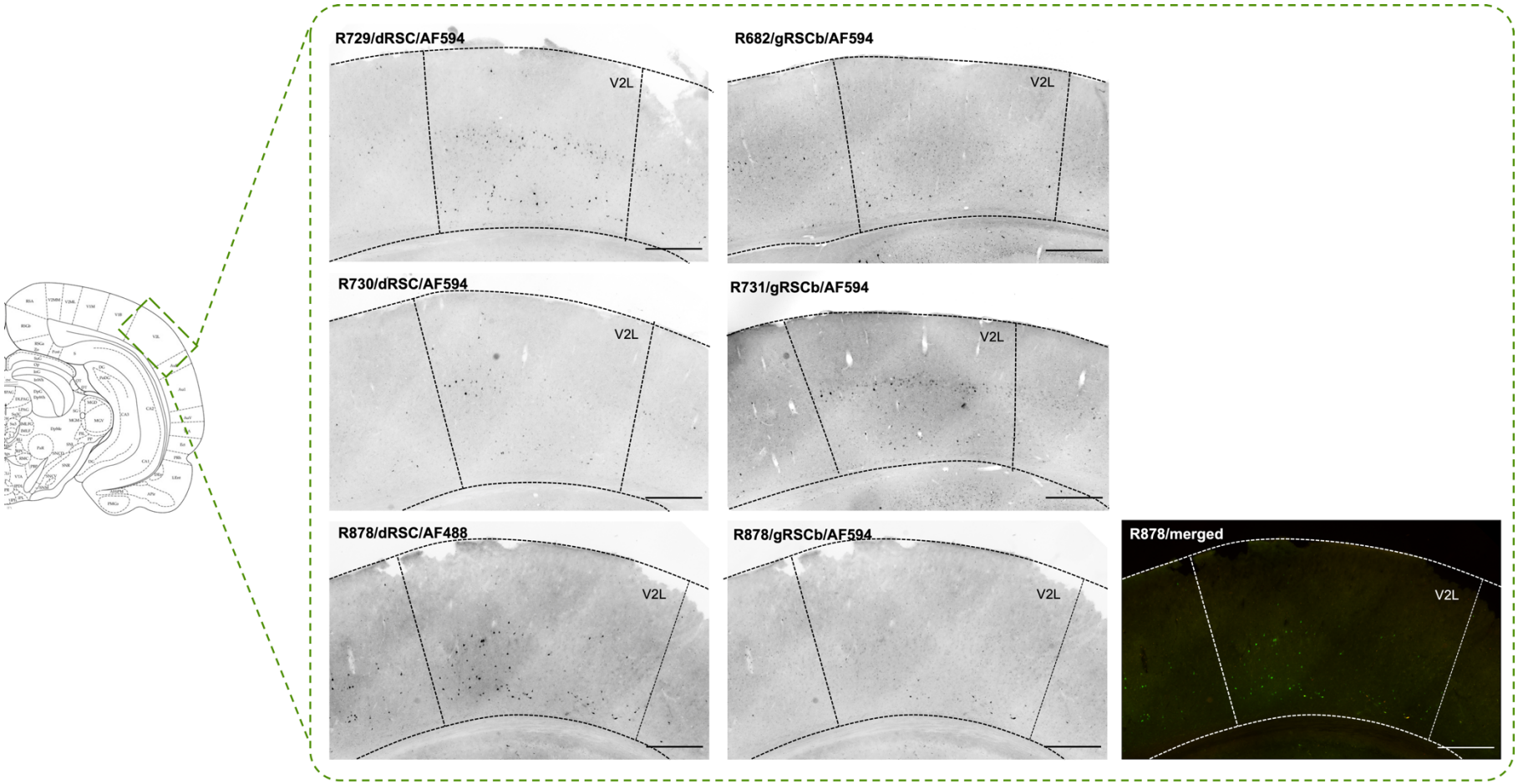

Figure 4.10: Representative images showing retrograde labelling in V2L. Retrograde labelling can be observed in deeper layers of V2L when tracers were placed in dRSC (l*eft most column*). Retrograde labelling can also be observed in deeper layers of the V2L when tracers were placed in gRSCb (*second column, first two rows; R682 and R731*). Very sparse labelling was observed in R878 when CTB was injected into gRSCb and it is likely a consequence of differentially placed or smaller injection loci leading to insufficient axonal uptake. The animal identity, injection site and tracer used are listed at the top of each image. *AF488 = CTB-AF488; FG = fluorogold; AF594 = CTB-AF594.* Merged images were made by overlaying images pseudo-coloured as c*yan for fluorogold labelling, red for CTB-AF594 labelling and green for CTB-AF488 labelling. Scale bar: 500*μ*m.*

To sum up, it is likely that deep layers of the striate and extrastriate visual cortex project to both dRSC and gRSCb in Lister-Hooded rats. Although there may be some quantitative differences (especially in V2M and V2L), it is difficult to confirm the observations in our study. This is because we only examined CTB labelling which generally displayed very limited spread in the brain (see Section 4.2.2). Together with slight variations in the location of the injection sites, this could explain the large variability we observed even among animals with the same injection status. For example, R878 gRSCb injection consistently gave sparse labelling in visual cortical regions that were not observed in R682 or R731. Similarly, for dRSC injections, sparser labelling was observed in R730 as compared to R729 or R878. The differences could be due to CTB not spreading to layers of gRSCb where visual cortical regions project to (and hence are not taken up by the axons), and/or differential spread in the rostral caudal axis. Due to the above reasons, it will be unbefitting to make a quantitative statement (as explained first in the result section). Nonetheless, it should be noted that the lack of labelling in R878 when CTB-AF594 was placed in gRSCb is unlikely to be due to deficit in retrograde transport as we see extensive retrograde labelling from the same animal in other brain regions: anterodorsal thalamus (Figure 4.4) and dorsal subiculum (Figure 4.5).

4.3 Discussion

In this chapter, we have examined the inputs into dRSC and gRSCb by injecting retrograde tracers into the two retrosplenial sub-regions. We showed that gRSCb receives differential inputs from anterodorsal thalamus and exclusive inputs from dorsal subiculum, dorsal hippocampus and lateral entorhinal cortex while both retrosplenial sub-regions receive inputs from postsubiculum and visual cortical areas (Figure 4.11). Most of the findings from our comparative study was similar to those reported by van Groen and Wyss (1992; 2003). Nonetheless, we did observe some differences in projections (e.g. primary visual cortex) that may reflect some fundamental differences in the connectomes between rat strains.

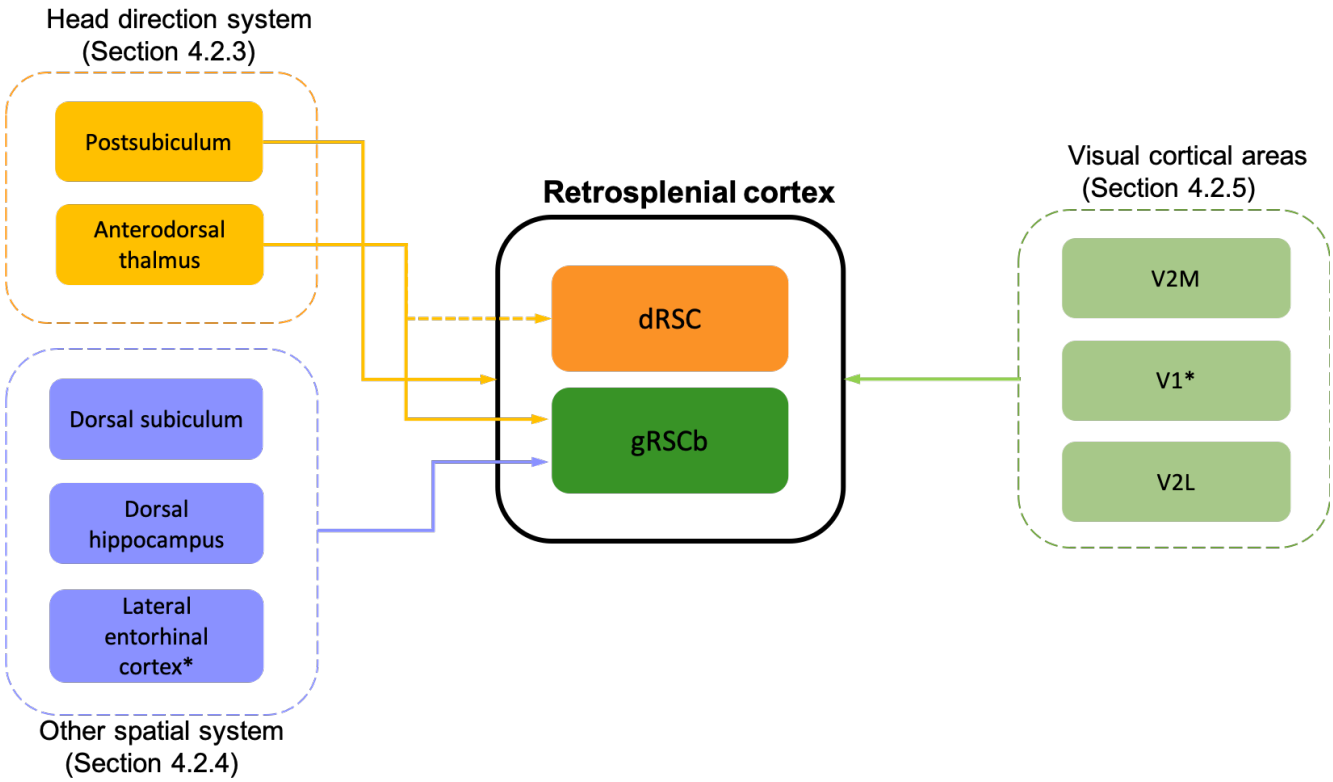

Figure 4.11: Summary diagram of our findings. The head direction system (light orange) was found to project to both retrosplenial sub-regions, although we found a higher number of projections from anterodorsal thalamus to gRSCb. All visual cortical areas (light green) also project to both retrosplenial sub-regions. In contrast, other spatial networks (place and boundary; purple) project only to gRSCb and did not project to dRSC. **Projections not previously described or inconsistent with van Groen and Wyss (1992; 2003).*

4.3.1 Ascending head direction inputs may dominate global directional signals

We first examined inputs from the head direction system. Consistent with van Groen and Wyss (1992; 2003), deep layers of postsubiculum were observed to project to both retrosplenial sub-regions, suggesting that both sub-regions of retrosplenial cortex receive similar inputs from postsubiculum (Figure 4.3). In contrast, a quantitative difference in the number of projections from anterodorsal thalamus to the different sub-regions of retrosplenial cortex was observed with anterodorsal thalamus projecting densely to gRSCb but sparsely to dRSC (Figure 4.4). The anterodorsal thalamus occupies a central position within the head direction network with approximately 60% head direction cells (Taube, 1995). It receives ascending head direction signals from lateral mammillary nuclei (see Section 1.3.2.1), and is critical for propagation of head direction signals to cortical regions as demonstrated by the loss of head direction signals in postsubiculum and medial entorhinal cortex when it is lesioned (Goodridge and Taube, 1997; Winter *et al.*, 2015). The quantitative difference in the number of projections thus suggests that the two retrosplenial sub-regions may receive qualitatively different head direction signals. Specifically, gRSCb may receive more ascending head direction signals from the anterodorsal thalamus (see Figure 1.11; Section 1.3.2.1) while dRSC may receive its head direction inputs primarily from postsubiculum. Like retrosplenial cortex, postsubiculum is hypothesized to be involved in the integration of visual information into the HD network. Lesions of postsubiculum led to decreased landmark control in HD cells recorded in anterodorsal thalamus and lateral mammillary nucleus (Goodridge and Taube, 1997; Yoder *et al.*, 2015). Postsubiculum also projects back to anterodorsal thalamus and lateral mammillary nucleus via two distinct populations of neurons (Yoder and Taube, 2011), through which visual landmark information is hypothesized to be fed back into the head direction network. Taken together, this suggests that dRSC may receive more visual-centric head direction signals from postsubiculum while gRSCb may have access to more vestibular-visual integrated head direction signals from anterodorsal thalamus. The vestibular-visual integrated signal could thus function as a path integrator to inform directional cells in gRSCb of the presence of the two distinct compartments, information which is otherwise not available to directional cells in dRSC. As a result, the vestibular-visual integrated directional signal could stabilize directional coding across the compartments (global directional encoding). In support, recording of head direction cells in anterodorsal thalamus in the two-compartment context box revealed global encoding similar to those seen in gRSCb (see Section 2.3; Figure 2a of Jacob *et al.*, 2017).

4.3.2 Stronger coupling of gRSCb with the hippocampal formation

In addition to quantitative differences from the anterodorsal thalamus, we also observed exclusive inputs from dorsal subiculum (Figure 4.5) and dorsal hippocampus (Figure 4.6) to gRSCb. Dorsal subiculum contains boundary vector cells (Lever *et al.*, 2009) and is the major output structure of dorsal hippocampus (van Strien *et al.*, 2009; O'Mara, 2005), which is where place cells are found (O'Keefe and Dostrovsky, 1971). The hippocampus and place cells are well-known to be involved in contextual coding (Smith and Bulkin, 2014), best exemplified by the study from Anderson and Jeffery (2003). Specifically, the authors demonstrated differential sensitivity of place cells to different features in the environment (odours vs. colour of walls; see Section 1.2.1.3; Figure 1.5). Thus, place cells could provide information about the context (the different odours in the different compartments) to head direction cells in gRSCb either directly (via the CA1 → gRSCb projections) or indirectly (via dorsal subiculum). In agreement with a potential role for the direct projections in propagating contextual information, Yamawaki *et al*. (2019) recently showed that CA1 → gRSC projecting GABAergic neurons may converge with anterior thalamus → gRSC projecting neurons to form a triadic circuit and they may work in tandem to modulate contextual fear memory. The same group also recently showed that the glutamatergic projections from dorsal subiculum to gRSC may modulate contextual fear memory, although the findings of this paper were not as clear because their virus infusions covered the entire dorsal hippocampal formation and not just dorsal subiculum (Yamawaki *et al.*, 2019). Nonetheless, it is probable that contextual information is propagated from dorsal CA1 to gRSCb either directly or indirectly and this information may be privy to global head direction cells such that they can disambiguate the two compartments. However, it should be noted that this hypothesis would suggest that place cells in CA1 could disambiguate the two compartments and would form a global map in the two-compartment context box. It is unclear if place cells do disambiguate the two compartments in the two-compartment context box, and this will be further explored in Chapter 5.

Surprisingly, when we were examining for labelling in the medial entorhinal cortex, we found retrograde neuronal labelling in dorsolateral entorhinal cortex (also generally described as lateral entorhinal cortex) but only when CTB was injected into gRSCb (Figure 4.7). It is unclear why the same retrograde labelling was not observed when fluorogold was injected into gRSCb, but It is unlikely that the differences in labelling observed are a consequence of

differentially placed injection sites as fluorogold was observed to spread more extensively in gRSCb than CTB (Figure 4.2). Instead, it likely reflects differences in the uptake efficacy of fluorogold and CTB in different populations of neurons as a consequence of the different uptake mechanisms utilized by the two tracers. Specifically, CTB is believed to be taken up by axon terminals via GM1 ganglioside (an omnipresent membrane sugar) mediated endocytosis while fluorogold is taken up by fluid phase endocytosis (Saleeba *et al*., 2019). This finding thus further highlights the need to use two different tracers (with different uptake mechanisms) when investigating the inputs into specific brain regions as an absence of labelling using one tracer may not reflect an absence of inputs.

What could be the function of these inputs from the lateral entorhinal cortex? Neurons recorded from the lateral entorhinal cortex are generally less spatially selective than that from medial entorhinal cortex (Hargreaves *et al*., 2005; Yoganarasimha *et al*., 2011), suggesting that lateral entorhinal cortex may not propagate spatial information like medial entorhinal cortex. As such, the lateral entorhinal cortex is often thought to be important for providing non-spatial information (such as information about local cues) to the hippocampus, sub-serving as the 'what' information stream for episodic memory (Knierim *et al.,* 2014). In agreement with a local cue processing role, egocentric bearing neurons that are either responsive to objects in the environment or containing a memory trace of the locations of the objects have been described in lateral entorhinal cortex (Deshmukh and Knierim, 2011; Wang *et al*., 2018; Tsao *et al*., 2013). However, the environment in which bidirectional cells were recorded (see Figure 2.5) did not contain any objects and hence it is unlikely that object and object trace cells are involved. Perhaps more relevant to the discussion at hand is the observation that some neurons recorded from lateral entorhinal cortex were found to display odour-specific firing in an odour-guided delayed nonmatching to sample task. These neurons showed preferential firing to specific odours, suggesting that lateral entorhinal cortex can process odour information (Young *et al*., 1997). The same odour encoding was also observed in the lateral entorhinal cortex of anaesthetised mice (Xu and Wilson, 2012) and hamster (Petrulis *et al*., 2005). It is unlikely that lateral entorhinal cortex is required for recognition of odour information as lesions of lateral entorhinal cortex impaired object-context (visual in this case; Wilson *et al*., 2013) associations without affecting an animal's ability to recognize objects or contexts. Rather, the latter finding would suggest that the lateral entorhinal cortex is important for binding of objects with the context to form a new contextual representation (Wilson *et al*., 2013). In addition, the lateral entorhinal cortex was found to be important for processing information about the local multimodal sensory environment and lateral entorhinal cortex

lesioned animals were impaired in solving an object recognition task that is solvable only by using a local configuration of cues (Kuruvilla and Ainge, 2017). A sensitivity to local multimodal cues was also observed in a cue conflict experiment in which the neural representation in lateral entorhinal cortex preferentially rotates with the local multimodal environment rather than the global environment (Neunuebel *et al*., 2013). Thus, In the two-compartment context box, the lateral entorhinal cortex may help bind the visual cue in each compartment with the information about the odour, thus generating a unique local contextual representation for each compartment. This information could be propagated to gRSCb and be used to disambiguate the compartments, thus stabilizing directional coding across the compartments.

4.3.3 Similar patterns of projections from visual cortical regions

Unexpectedly, in contrast to what was previously described in van Groen and Wyss (1992, 2003), we did not observe exclusive inputs from primary visual cortex to dRSC. Instead, we did not observe any differences in the patterns of projections from the different visual cortical areas to dRSC and gRSCb (Figure 4.8, 4.9 and 4.10). Because retrosplenial cortex is surrounded by multiple visual areas (V2M and superior colliculus), the retrograde labelling observed may reflect contamination of tracers into the surrounding regions. However, this is unlikely as we only examined CTB injected retrograde labelling and the injection sites of CTB were typically smaller and confined to their target structures (Figure 4.2). Instead, the differences between our study and that of van Groen and Wyss (1992, 2003) may reflect differences in projections along the rostral-caudal axis of retrosplenial cortex, with more visual inputs at our coordinates. It could also reflect differences among rat strains as van Groen and Wyss (1992, 2003) used albino Sprague-Dawley rats in their study while we used pigmented Lister-Hooded rats in our study. This is broadly in line with the observation that there are differences in visual acuity between pigmented and albino rats (Prusky *et al*., 2002). Although the study did not compare Lister-Hooded rats with Sprague-Dawley rats directly, Sprague-Dawley rats were reported to have lower visual acuity than pigmented rats (Dark Agouti, Fisher-Norway and Long Evans rats) and may thus have less visual dependency in higher cortical regions including reduced projections from visual cortical regions to higher cortical regions such as gRSCb.

Nonetheless, there is a possibility that extrastriate visual cortical regions (V2M and V2L) have more projections to dRSC than gRSCb (Figure 4.9 and 4.10). However, we think

that it is inappropriate to examine that possibility in our study as large variations in retrograde labelling can be observed even within animals receiving the same injections. This observation also highlights a limitation in our study – that is the placements of injections are extremely important for interpretation, especially when examining retrograde labelling from tracers like CTB that displayed limited spread (also see Section 4.3.5). Slight variations in how the tracers were placed could result in different amount of labelling as a consequence of the tracers not spreading to layers of gRSCb where the brain structure projects to or as a consequence of differential spread in the rostral caudal axis. This limitation is perhaps exaggerated when we examined inputs from visual cortical regions due to our decision to only examine CTB injected samples. Regardless, it can be seen from our data that all areas of visual cortical regions displayed similar projection patterns to both dRSC and gRSCb.

4.3.4 Dysgranular retrosplenial cortex as a visuospatial associative cortical region

Even though dysgranular retrosplenial cortex may not receive unique visual inputs from both striate and extrastriate visual cortical areas (i.e. no exclusive retrograde labelling was found in the different visual cortical regions when tracers were placed in either of the two retrosplenial sub-regions), the disconnect between the dysgranular retrosplenial cortex with the hippocampal formation (except for postsubiculum) nonetheless suggests that dysgranular retrosplenial cortex may be more modulated by visual inputs as compared to gRSCb. Consistent with this finding, dysgranular retrosplenial cortex has been repeatedly implicated in visual processing, and retinotopy and visual responses have been observed in dysgranular retrosplenial cortex (Powell *et al*., 2020; but also see Murakami *et al*., 2015 and Zhuang *et al*., 2017 who reported retinotopy and visual responses in retrosplenial cortex, but did not specify which sub-regions of retrosplenial cortex the studies were conducted in). Taken together, these findings suggest that dysgranular retrosplenial cortex may be more similar functionally to its neighbouring extrastriate V2M as compared to its counterpart (granular retrosplenial cortex), although it should be noted that visual responses in the corresponding granular retrosplenial cortex have not been examined sufficiently. Nonetheless, the bidirectionality observed in dysgranular retrosplenial cortex may (partially) result from sensitivity to the visual features in the two-compartment context box.

Although bidirectional cells may be more visually modulated, it should be noted that these cells are stable in the dark (Jacob *et al*., 2017) and as such, likely receive information

from other sensory modalities. The function of dysgranular retrosplenial cortex may thus lies in associating the sensory information (such as visual information) to form an egocentric representation of the local spatial environment (viewpoint-specific coding of the environment). Particularly, as the rat moves across the two compartments, the viewpoints of the two compartments are similar (but 180° rotated) and as such, lead to a bidirectional tuning curve that 'flips' when the animal crosses the doorway. In agreement with an egocentric representation of the environment, egocentric boundary cells were recently found in the dysgranular retrosplenial cortex (Alexander *et al*., 2020). Together with bidirectional cells, they may represent a functional sub-population of cells in the dysgranular retrosplenial cortex that help to encode the local environment using the local features available to the rats (e.g. visual scene, local borders/boundaries). This information may thus be useful in helping the rats localize itself in multi-compartment spaces. Also consistent with this line of thought, the interconnectedness of the granular retrosplenial cortex with the hippocampal formation would suggests that it may receive more allocentric information (e.g. from place cells) and as such form a global directional representation in the two-compartment context box.

Our study thus further highlights the dissociation *within* the retrosplenial cortex with granular retrosplenial cortex potentially being more implicated in allocentric spatial navigation, while dysgranular retrosplenial cortex being more involved in egocentric visuospatial coding. The connectomic differences seem to be consistent with the cytoarchitectural observation that granular retrosplenial cortex seems to be more similar to the hippocampal archicortex while dysgranular retrosplenial cortex is more similar to the neighbouring neocortex (Miller *et al*., 2014). Given the dissociation in the connectomes and cytoarchitectures between the two sub-regions of retrosplenial cortex and the disconnect of dysgranular retrosplenial cortex from the thalamo-hippocampo-cortical spatial circuit, perhaps it is essential to stop examining and discussing retrosplenial cortex as a single structure (as often does) but instead redefine and separate the retrosplenial cortex into its sub-components: an allocentric spatial retrosplenial sub-region (granular retrosplenial cortex) and an egocentric visual/associative retrosplenial sub-region (dysgranular retrosplenial cortex). This will allow us to discuss the functions of the two retrosplenial sub-regions as its discrete components in the future – a more spatial-related function of granular retrosplenial cortex and a more visuospatial role for dysgranular retrosplenial cortex, a distinction that is currently lacking in the current spatial navigation field but has been highlighted by Miller *et al*. (2014).

4.3.5 Limitations and considerations

Last but not least, although we have extensively discussed the differences in connectivity between the two retrosplenial sub-regions, it is essential for us to be aware of the limitations of this experiment. As pointed out from the get-go, the data presented in this chapter is geared towards qualitative analysis due to the various reasons highlighted. Descriptive qualitative analysis is considerably less informative than quantitative analysis and the lack of reliable quantitative analysis (except for smaller anatomical structure – see anterodorsal thalamus; Figure 4.4) limited the interpretations in this chapter. As a consequence, the conclusions drawn in this chapter are limited to being descriptive in nature – primarily examining the pattern of projections – and this limitation is especially highlighted in the inability to make reliable quantitative statements when retrograde labelling was found in cortical regions (see postsubiculum or visual cortical regions; Figure 4.3 and Section 4.2.6).

Despite this limitation, the data presented in this chapter is still informative. For example, even without quantification, binary outcomes, such as when retrograde labelling were observed in dorsal subiculum, dorsal hippocampus and lateral entorhinal cortex only in gRSCb injections, are indicative of the unique coupling of gRSCb with these structures. This finding further highlights the stronger coupling of gRSCb with the spatial navigation circuit and the disconnect of dRSC with the same structures. In addition, the findings here are presented as an exploratory study, which can be used to guide future inactivation studies either via chemogenetics or optogenetics.

How can we then try to address this limitation? One possibility would be to quantify and model the injection sites in each retrosplenial sub-region as a three-dimensional injection loci and correlate that with the number of cells labelled in each structure. However, this approach might be difficult to implement and/or interpret as interactions between two or more variables (e.g. spread of tracers in the rostral-caudal axis and the types of tracers) will further confound any relationships observed. For example, the types of tracers utilized could potentially affect uptake and subsequent retrograde labelling (see Figure 4.7; lateral entorhinal cortex labelling) and coupled with the different placement of the tracers in the rostral-caudal axis, it will be difficult to determine which factor is actually responsible for the quantitative difference in retrograde labelling (if any) observed. Nonetheless, it may be a useful step towards better understanding the projections observed.

It should also be noted that although a double retrograde labelling approach can enable identifications of axon collaterals, we did not observe significant doubly retrogradely labelled cells in the structures we examined (e.g. postsubiculum, visual cortical areas). This may suggest that non-overlapping populations of cells project to dRSC and gRSCb. Although this is probable, it should also be noted that a lack of doubly labelled cells may result from variations in the location and size of injection sites in the different retrosplenial sub-regions. For instance, one could envision a scenario where the injection sites in the two sub-regions of retrosplenial cortex are of different sizes and locations such that the spread of tracer in one sub-region covers the layers where a particular brain structure projects to but the spread of tracer in the other sub-region did not. Resultantly, the lack of doubly labelled neurons could then be a consequence of insufficient retrograde labelling in the latter sub-region (i.e. underestimating the number of retrogradely labelled neurons from the latter injection). Another possibility is that fluorogold may compete with CTB for uptake and/or transport and as such, leads to an underestimation of axon collaterals. Although fluorogold was not examined with

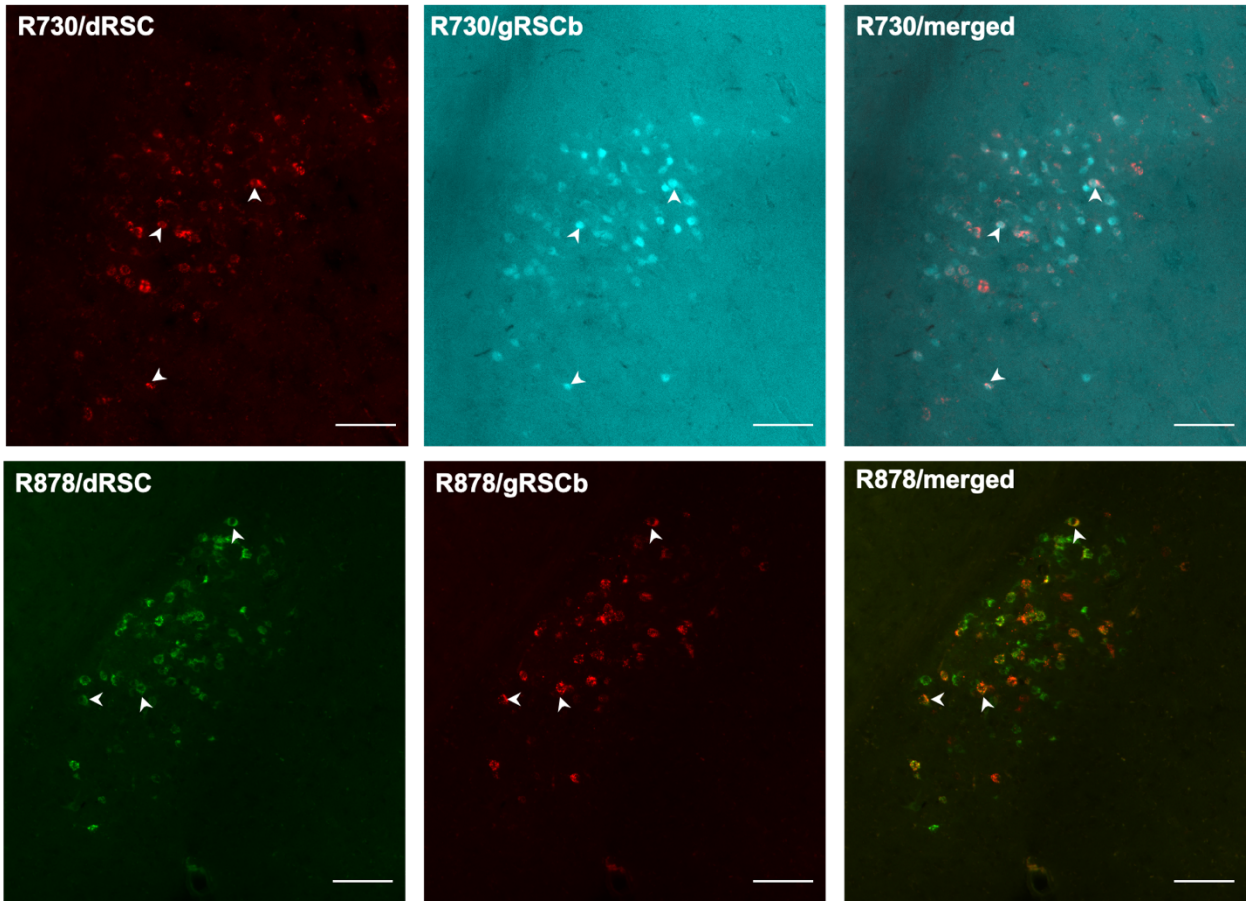

Figure 4.12: Double retrograde labelling in the claustrum. Extensive retrograde labelling in the claustrum was observed regardless of where the tracers were placed in the retrosplenial cortex. In the claustrum, we can easily observe doubly labelled cells (examples indicated by white arrowheads), suggesting that competitions between uptake or transport of tracers cannot fully explain the often sparse and low number of doubly labelled cells seen in postsubiculum and/or visual cortical areas. *Scale bar: 100μm.*

CTB specifically, possible competitions between tracers that impede identifications of axon collaterals have been described (Schofield *et al*., 2007). Nevertheless, we can easily observe doubly labelled cells in structures that project to both retrosplenial sub-regions (e.g. Claustrum; Figure 4.12). Thus, competitions between tracers cannot fully explain the lack of doubly labelled cells in postsubiculum and/or visual cortical areas.

Finally, even though it is well known that structures inform functions, it should be made explicit that the study here is correlative in nature and does not inform us of the functional roles of these projections. It is thus probable that the projections found may not play a role in the reconciliation of local and global reference frames in the brain. For example, recent work by Brennan *et al*. (BioRvix, 2020) suggests that there may be a dissociation in the functions of the projections from claustrum to retrosplenial cortex and the projection from anterior thalamus to retrosplenial cortex, with claustrum → retrosplenial projections mediating fear-related information while anterior thalamus → retrosplenial projections mediating navigation-related information. Thus, even though the claustrum projects to retrosplenial cortex, the inputs may not have a functional role in integrating reference frames, which is generally considered to be a spatial navigation related function. To show causality and a functional role in the integration of reference frames, one would have to inhibit the inputs into the retrosplenial cortex and observed the changes to the downstream spatial signals and/or animals' behaviours. This will be further discussed and explored in Chapter 6.

4.4 Interim conclusion

Taken together, our results suggest that it is more likely that gRSCb receives additional vestibular-visual integrated inputs (via anterodorsal thalamus) and/or contextual inputs (via dorsal subiculum, hippocampus and lateral entorhinal cortex) that allow classical head direction cells to disambiguate the two visually similar, but differentially scented compartments. Consequently, despite the ambiguity in the visual scenes, the directional cells in gRSCb recognize that there are two distinct compartments and can thus maintain their preferred firing directions across the compartments. Bidirectional cells may thus represent a subpopulation of directional cells that do have access to this information. Alternatively, the disconnect of dRSC with the hippocampal formation may suggest that dRSC is functionally distinct from its granular counterpart in spatial navigation and may function predominantly as a visuospatial area (see Section 4.3.4). Bidirectionality may thus represent viewpoint-specific encoding of the local environment.

Nonetheless, the stronger coupling between gRSCb and the hippocampal system would suggest that gRSCb and hippocampus interact with each other so as to ensure that the place signal and the global head direction signal are coherent with each other. This would suggest that the place map in hippocampus is global (that is it can disambiguate the two compartments), but it is currently unclear if the hippocampus encodes the two-compartment context box globally (like global head direction cells) or locally (like bidirectional cells). The next chapter will thus be dedicated to understanding the place representation in the two-compartment context box.

Chapter 5.

Place Cells in a Visually Rotated, Differentially Scented Compartmentalised Environment

As described in the previous chapter, granular retrosplenial cortex was observed to have a stronger coupling with the hippocampal system and receives neuronal inputs from both dorsal subiculum and CA1 subfield of the hippocampus (see Section 4.2.4). Given that subiculum (including dorsal subiculum) is the major output structure of hippocampus (van Strien *et al*., 2009; O'Mara, 2005), it is not inconceivable that granular retrosplenial cortex (and by extension, the head direction system) receives contextual information from hippocampus, either directly via CA1 or indirectly via dorsal subiculum, that enables head direction cells to have stable preferred firing directions across compartments (see Section 4.3). This would suggest that place cells in hippocampus CA1 encode the two-compartment context box globally. However, as mentioned, it is currently unclear if the place map in hippocampus CA1 is global.

This chapter is thus dedicated to investigating the place representation in the two-compartment context box, which has two connected compartments that are differentially scented and have visual cues that are on opposite ends of the compartments (see Figure 3.4B). Given that hippocampal CA1 is more strongly coupled with granular retrosplenial cortex, we hypothesized that the place map in hippocampus CA1 is global in nature and is thus ideal for propagating disambiguating contextual information to the granular retrosplenial cortex. To test this hypothesis, we implanted rats with tetrodes and examined if hippocampal CA1 place cells globally or locally encode the two-compartment context box (see Section 3.3 for a detailed description of the methods).

Before we dive into the nitty-gritty details of the experiments, we would like to take the opportunity to discuss the possible outcomes from the recordings. One can envisage three distinct, but not mutually exclusive, place representations in CA1 (Figure 5.1). First, the place representation can be essentially global in nature – that is place cells have single or independent place fields in the two compartments (Figure 5.1A). This would suggest that place cells could disambiguate the two compartments and form a unified representation of the entire environment (as hypothesized). Alternatively, place cells could represent the two

compartments separately and form a local place representation of each compartment based on features found in each compartment (e.g. visual scene and/or geometry; see Section 1.2.1.2 for a review on sensory influences on place cells). Specifically, place cells can have place fields that occupy the same relative spatial location in each compartment independent of the visual scene ('repetition'; Figure 5.1B), which would indicate place sensitivity to the rectangular geometry of the local compartments. Similarly, because the visual scenes between the compartments have a 180° rotated symmetry, place cells could have place fields that are 180° rotated between the two compartments ('rotation', Figure 5.1B). Such local encoding would reflect a sensitivity to the local visual scene, similar to the bidirectionality of directional cells described in Section 2.3.1. We will examine these possibilities in this chapter, with additional analysis when appropriate to understand how place cells encode the two-compartment context box.

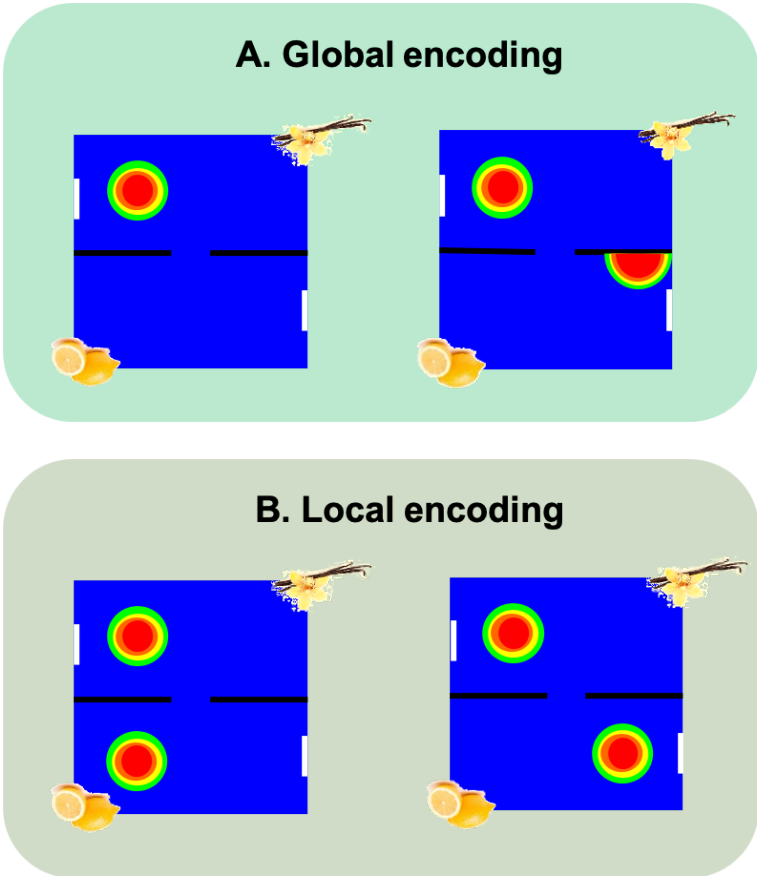

Figure 5.1: Possible place encodings in the two-compartment context box. Schematic rate maps showing how place cells could represent the two-compartment box. The black lines represent the walls dividing the two compartments while the white lines on the two opposite ends of the compartments represent the visual cues used in the two compartments. **(A)** Place cells could represent the two compartments together as a global map, which would suggest disambiguation of the two compartments. Such *global encoding* is evident as place cells having either a single field (left) or spatially independent fields (right) in the two-compartment context box **(B)** Alternatively, the spatial representations in the two compartments may not be random and place cells encode each compartment individually according to the local features. Such local encoding can come in two forms - place cells can be sensitive to the local geometry and have *repeating* fields between the two compartments (left); or place cells could be sensitive to the visual scene and have place fields that are rotated 180° between the two compartments (*rotated* fields).

5.1 Methods

5.1.1 Animals

Three male Lister Hooded rats were used for place cell recordings. Two animals, except for R930, were naïve to the experimental apparatus prior to any recordings. R930 was exposed to the experimental apparatus as part of a behavioural experiment before being enlisted for microdrive implantation. An additional three animals were implanted for this experiment but were unfortunately culled prior to recording due to the pandemic.

The animals were housed individually and maintained on a 12hr/12hr light/dark cycle. A week after surgery and throughout the whole experimental period, all animals were food restricted and their body weight maintained at 90% of their free-feeding body weight. This experiment was done in accordance with the national [Animals (Scientific Procedures) Act, 1986, United Kingdom] and the international [European Communities Council Directive of 24 November 1986 (86/609/EEC)] legislation governing the maintenance of laboratory animals and their use in scientific experiments.

5.1.2 Recording protocol

A week following surgery, the animals were screened for place cells in the screening environment (see Section 3.3.3). If place cells were observed, the animals were first replaced back into the cage and the recording room set up for recording. The arena was first rotated to the appropriate randomised starting baseline orientation and the vanilla and lemon odours were applied onto the floor using a sponge. The lights of the room were then switched off and the halogen lights mounted on the ceiling switched on (see Section 3.3.3). The speaker mounted onto the ceiling was also then switched on to play white noise before the animals

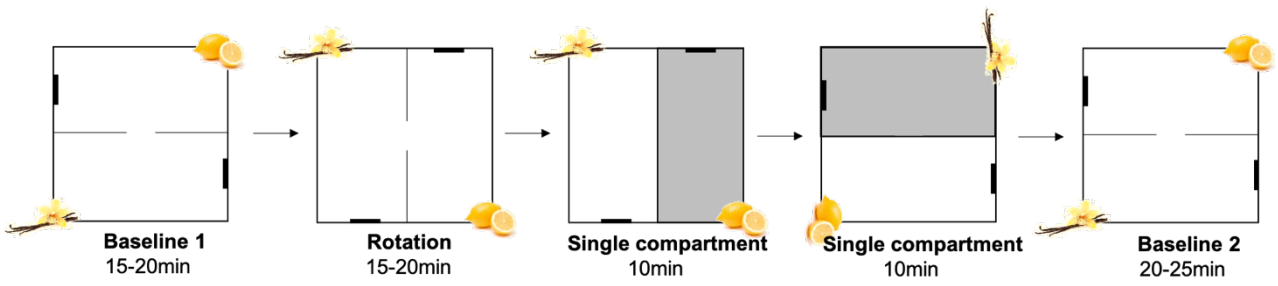

Figure 5.2: A schematic diagram of the recording protocol. A recording session consisted of 5 trials including two baseline trials, a rotation trial and two single-compartment trials. The first baseline trial always starts in a random orientation and between trials, the two-compartment context box was rotated randomly in multiples of 90°.

were transferred to the recording room in a black transport box, the headstage connected and the recording protocol commenced.

A single recording session consisted of five trials in sequence – a baseline trial, a rotation trial, two single-compartment trials, and a second baseline trial (Figure 5.2; Jacob *et al.*, 2017). The two baseline trials were used to examine for the stability of place cells recorded (i.e. check for drifting of tetrodes) while the rotation trial was to ensure that the cells were not anchoring to uncontrolled distal cues outside the black curtains. All two-compartment trials ranged from 15 to 25 min while the single-compartment trials lasted for 10 min each. Rice pops (Waitrose, UK) were thrown into the box from outside the curtain to encourage the animal to explore. Rats were always started in the same compartment. In between trials, the animals were removed from the environment, placed back into black transport box and disoriented. The animals were disoriented by rotating the black transport box in which the animals were in, while walking around the room with the black transport box. The environment was cleaned of any urine or faeces, the odours reapplied, and the box rotated to the appropriate configuration. Rotations of the environment were randomised (except for the final baseline which will be the same as the first baseline orientation) and were done in multiples of 90º between every trial. The order of the single-compartment trials was also randomised across sessions (e.g. lemon single-compartment trial followed by vanilla single-compartment trial in some sessions or vice versa in others). At the end of a recording session, the screw on the microdrive was turned one-eighth of a turn (~25μm) to lower the tetrodes and get new cells for the next recording session. Please read Section 3.3 for a more technical description and understanding of how tetrodes were made and microdrives implanted.

5.1.3 Data analysis

5.1.3.1 Behavioural analysis

A preference index is calculated from the time the animals spent in each compartment so as to examine for any bias in the animals for either compartment. It is calculated as follows:

$$Preference\ Index = \frac{T_V - T_L}{T_V + T_L}$$

where T_V is the time the animals spent in the vanilla compartment, T_L is the time the animals spent in the lemon compartment. A preference index > 0 indicates a preference for the vanilla compartment while a preference index < 0 indicates a preference for the lemon

compartment. A value of 0 will indicate no preferences for either compartment. The preferences for odours were only examined for the two-compartment trials (baseline 1, rotation and baseline 2) and were tested statistically against a preference index of 0 (no preference).

5.1.3.2 Place cell criteria

Data from potential single units were preprocessed and analyzed in Matlab 2019a/b (MathWorks). First, positional data and spikes were speed-filtered. Spikes that occurred when the animals were moving at an instantaneous speed of less than 5 cm/s were removed to exclude non-local spiking (e.g. replay events). Positional data and spikes when the animals were moving with an instantaneous speed more than 100 cm/s were considered to indicate inaccurate tracking and removed. Any out-of-arena positional data and spikes were also removed.

To ensure good unit isolation, any units with more than 0.2% of spikes falling within inter-spike interval < 2s and mean firing rate < 0.1Hz in both baseline trials (trial 1 and trial 5) were excluded. Units were considered to be putative pyramidal cells if the waveform peak to trough > 250 μs and their mean firing rates were between 0.1 Hz to 5 Hz in both baseline trials.

5.1.3.3 Rate maps and place field identification

After identification of putative pyramidal cells, rate maps were constructed to examine for spatial firing. Rate maps were generated in the same manner as described in Leutgeb *et al*. (2005), but with slightly different parameters. Positional data were divided into 3x3 cm bins, and spikes falling within each bin were accumulated accordingly. Positions and spikes were smoothed separately with a gaussian kernel (smoothing factor = 5 cm) centered on the bin. Any bins that were > 9 cm away from the current bin were given a weight of 0. Bins in which the animals spent less than 0.1s were designated as unvisited. The smoothed rate maps were then generated by dividing the smoothed spike maps with the smoothed dwell maps.

Spatial firing was then examined using the smoothed rate maps. A place field is defined as regions of at least 16 contiguous pixels (in all directions) with firing rates more than 40% of the peak firing rate and peak firing of > 1Hz. Putative pyramidal cells with detected fields that have summed pixels more than 50% of the dwell map pixels were considered to be non-spatial and were excluded from further analysis.

For visualization purpose, spikes were also plotted on positional data for each trial (i.e. spike plots). Spikes that fired within the vanilla compartment were coloured brown, and spikes that fired within the lemon compartment were coloured orange.

5.1.3.4 Rate map correlations

To examine how similar or different spatial firing are across trials or compartments, Pearson's correlations were carried out on smoothed rate maps between two trials or two compartments. Before correlation, all rate maps were rotated to the appropriate orientation (either same orientation or 180^{o} rotation). If the rate maps were found to be of different sizes (due to unvisited regions), the smaller rate map was padded to the size of the larger rate map with NaN in all dimensions. The equivalent spatial bins between the two rate maps were then correlated on a bin-by-bin basis. The threshold correlation value for what constitutes a similar spatial map depends on the null distributions generated for each type of comparison (see section 5.1.3.6).

5.1.3.5 Detecting same cells recorded over days

To avoid over- or under-estimating the proportion of place cells that display local or global encoding, place cells that were recorded over multiple days were identified using information about the waveform and the place fields as described below. This method assumed that place cells in the two-compartment context box are stable and do not remap over days.

Place cells that displayed similar spatial firing were first identified by correlating the rate maps of all cells recorded from the same tetrode between consecutive recording sessions. Cell pairs with spatial correlation > 0.375 were then examined for similarities in waveforms using Tolias distances as a measure of waveform similarities (Tolias *et al*., 2007; Duvelle *et al*., 2019). Specifically, the differences in waveforms can be examined using two metrics described by Tolias *et al*. (2007). One of the two waveforms being compared was first scaled by a factor a so as to account for possible changes in waveforms due to tetrode movement across days. After finding the best a fit for each channel, Tolias distance 1 was calculated by looking at the normalized Euclidean distance between the two waveforms. This measure essentially captures the differences in waveform shapes. The second Tolias distance (or Tolias distance 2) examines the differences in amplitudes across the four channels. If the

same cell was recorded over days with minimal changes in the waveforms, both Tolias distances will return small values.

We next sought to determine an objective threshold value that would indicate if two waveforms are similar or different. To do so, we fitted a discriminant analysis classifier using Tolias distances calculated from waveforms of experimentally defined *same cells* or *different cells*. *Same cells* were defined as the Tolias distances obtained by comparing the waveforms of cells determined to be same (via spike sorting) across the different two-compartment trials (baseline 1, rotation and baseline 2) within a recording session. Meanwhile, *different cells* were defined as the Tolias distances obtained by comparing the waveforms of cells recorded in the very first session and the very last session of an animal. Separate discriminant analysis classifiers were generated for each animal (Figure 5.3) under the assumption that each animal (and each microdrive) has its own set of electrical noise during recording.

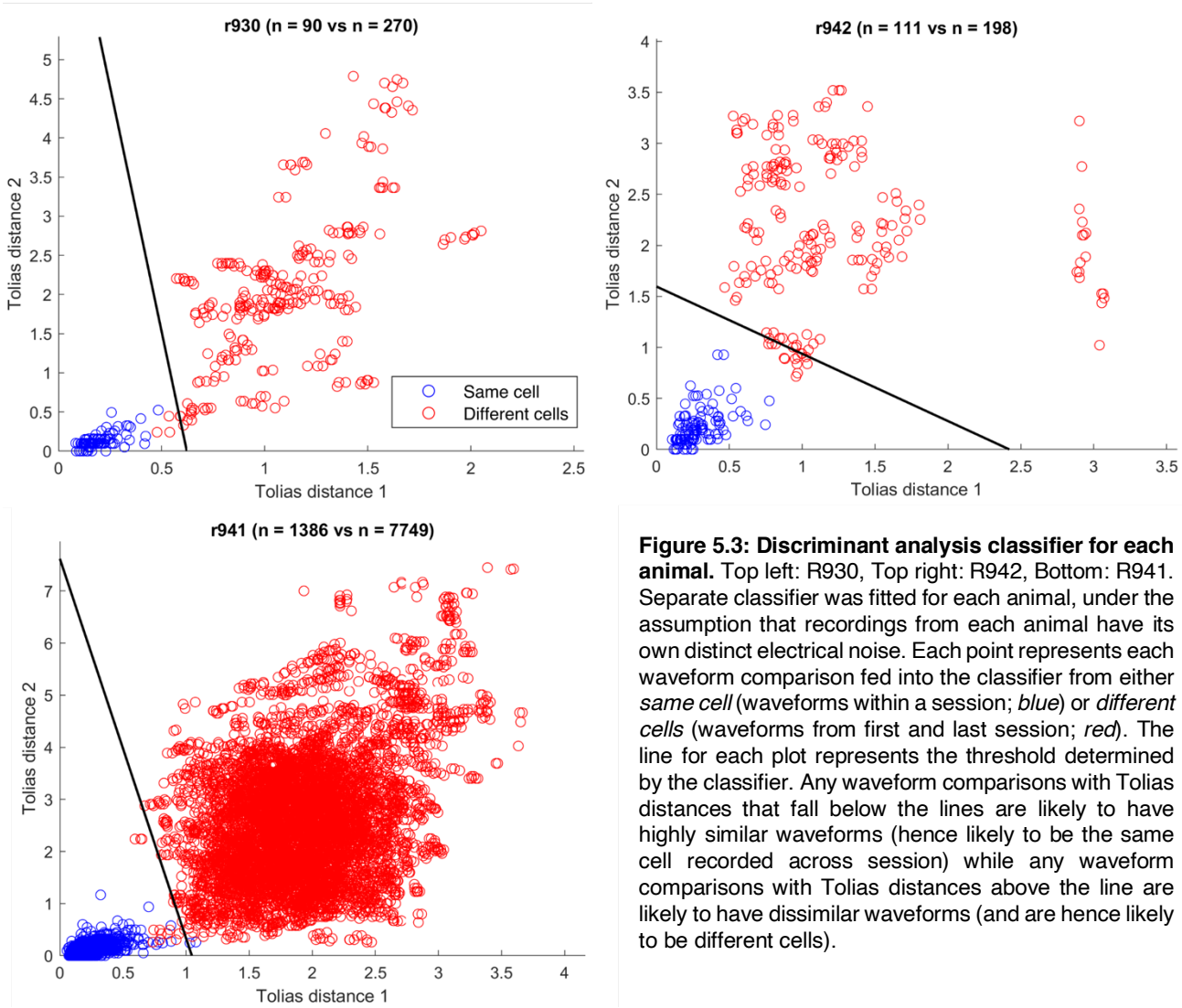

Figure 5.3: Discriminant analysis classifier for each animal. Top left: R930, Top right: R942, Bottom: R941. Separate classifier was fitted for each animal, under the assumption that recordings from each animal have its own distinct electrical noise. Each point represents each waveform comparison fed into the classifier from either *same cell* (waveforms within a session; *blue*) or *different cells* (waveforms from first and last session; *red*). The line for each plot represents the threshold determined by the classifier. Any waveform comparisons with Tolias distances that fall below the lines are likely to have highly similar waveforms (hence likely to be the same cell recorded across session) while any waveform comparisons with Tolias distances above the line are likely to have dissimilar waveforms (and are hence likely to be different cells).

Tolias distances were then systematically calculated for cells recorded on the same tetrode on consecutive sessions (e.g. waveforms of cells recorded on tetrode 1 on session 1 compared to waveforms of cells recorded on tetrode 1 on session 2), and the posterior probability of cell pairs having similar waveform ('*same cell*') is predicted from the trained classifier. Spatially similar cell pairs were considered to be the same if the trained classifier predict a high posterior probability (> 0.5) of it being the same (i.e. similar waveform). Occasionally, two cells recorded in a session can map to a single cell in the next session ('convergence') or a single cell in a session can map to two different cells in the subsequent session ('divergence'). In such scenario, the posterior probabilities of the cell pairs in question were examined. If the absolute difference in the posterior probability between the two cell pairs is > 0.1, the cell pair with the higher posterior probability was considered to be the best matched cell pair. Alternatively, if the difference in the posterior probability is < 0.1, the spatial correlations were considered and the cell pair with the higher spatial correlation was considered to be the best matched cell pair.

5.1.3.6 Null distributions

To determine the chance level for which a place field is in a specific location, null distributions were generated by either pooling all the two-compartment rate maps from baseline one for the two-compartment analysis (see Section 5.2.5) or pooling all the divided compartmental rate maps for the single-compartment correlation analysis (see Section 5.2.6). Pairs of cells were randomly selected from the pool 10,000 times (i.e. cell identity shuffles) with replacement, and the rate maps correlated. The null distributions represent the probability a place cell could have a place field in the exact same location by chance (i.e. the expected distribution if the place representations between the two compartments or trials are completely independent; Skaggs and McNaughton, 1998). The 95th percentile values from these distributions were used as threshold values for the respective comparisons. Correlation values > threshold would indicate similar rate maps while correlation values ≤ threshold suggest dissimilar rate maps.

5.1.3.7 Population vector correlations

Population vectors for each position bin were computed as described by Leutgeb *et al*. (2007). Rate maps of all cells recorded within a session (see Section 5.2.5) or across all session (see Section 5.2.7) were collapsed to form a 3D matrix with the position coordinates in the *X* and *Y* dimension, and the cell identity in the *Z* dimension. A slice through the *Z* axis

gives the population vector (PV) for a specific spatial bin and represents the collective firing activity of all cells within a trial in that particular position. The population vector for a specific spatial bin from a specific trial can then be correlated to the population vector for an equivalent spatial bin from a different trial to examine how similar the collective firing activity is at that specific spatial bin (Figure 5.4).

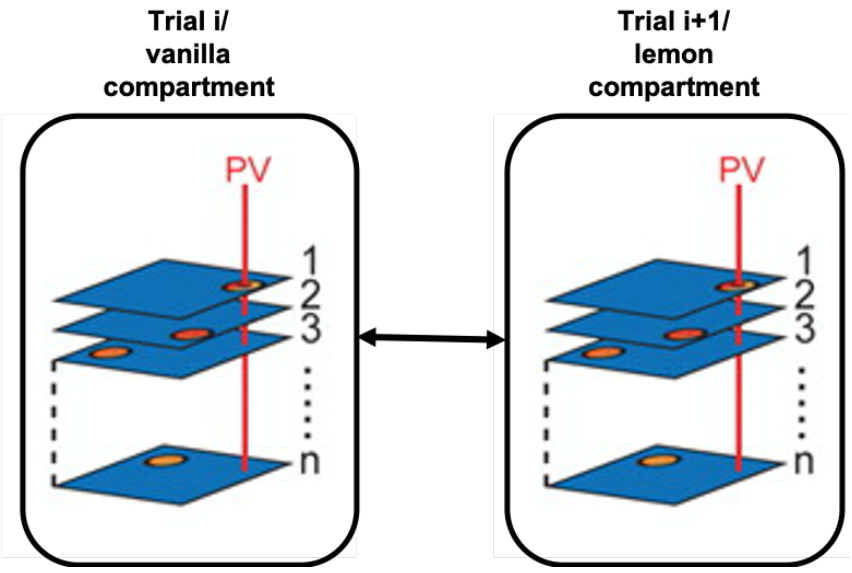

Figure 5.4: Population vector correlation analysis. The population spatial firing activity in a trial can be examined by taking the collective firing activity of all place cells at each position bin, also known as the population vector for the specific bin. Similarity in the spatial activity of the place cell population can then be examined by correlating the population vectors across trials or compartments. *Adapted from Leutgeb et al. (2007)*.

5.1.3.8 Rate remapping analysis

Before we examine for rate remapping (i.e. changes in firing rate in place fields as a consequence of non-spatial features; see Section 1.2.1.3), we must first account for normal fluctuations in firing rate as a consequence of sampling and/or length of recording. We defined such fluctuations in firing rate as 'random fluctuation' and quantify it by examining the changes in the mean firing rate of the same place field in the same scented compartment across all two-compartment trials. We scored the random fluctuations in firing rate as a rate change score (Leutgeb *et al.*, 2005), which can be expressed as follows:

$$Rate\ change\ score_{random\ fluctuation} = \frac{1st\ trial\ mean\ FR\ -\ 2nd\ trial\ mean\ FR}{1st\ trial\ \ mean\ FR\ +\ 2nd\ trial\ mean\ FR}$$

Each place cell with repeating place fields will thus yield six rate change scores for the six possible comparisons within a session: (1) vanilla scented baseline one against vanilla

rotation trial (2) vanilla scented baseline one against vanilla baseline two (3) vanilla scented rotation trial against vanilla baseline two (4) lemon scented baseline one against lemon rotation trial (5) lemon scented baseline one against lemon baseline two (6) lemon scented rotation trial against lemon baseline two. These scores were then averaged to give a single rate change score, which measures the fluctuation in firing rate for that particular cell.

Rate remapping between the two repeating fields was then examined by taking the difference in the mean firing rates between the fields in the vanilla and lemon compartment and calculating a similar rate change score:

$$Rate\ change\ score_{between\ compartment} = \frac{Vanilla\ mean\ FR\ -Lemon\ mean\ FR}{Vanilla\ mean\ FR\ +\ Lemon\ mean\ FR}$$

In this case, each place cell with repeating fields will yield nine rate change score for nine possible comparisons within a session: (1-3) vanilla in baseline one, rotation trial and baseline two against lemon in baseline one, rotation trial and baseline two respectively (4) vanilla scented baseline one against lemon rotation trial (5) vanilla scented baseline one against lemon baseline two (6) vanilla scented rotation trial against lemon baseline one (7) vanilla scented rotation trial against lemon baseline two (8) vanilla scented baseline two against lemon baseline one (9) vanilla scented baseline two against lemon rotation trial. Once again, an average rate change score was obtained for each cell.

The unsigned rate change scores were then used for comparison between the two groups. A minimum value of 0 would suggest no difference in mean firing rates while a maximum value of 1 indicates the largest possible difference in mean firing rates (when one of the mean firing rates is 0).

5.1.3.9 Statistics

We tested the data for normality by using one-sample Kolmogorov-Smirnov test. When the data were normally distributed, we used parametric tests (e.g. one-sample, two-sample t-test) to test for significance. Otherwise, we used non-parametric tests to test for significance (e.g. Wilcoxon signed-rank test). We also used the chi-square goodness-of-fit test when testing the observed number of place cells and place fields in each compartment against an expected equal proportion, or when testing the number of place cells with repeating and rotated place fields against a chance proportion of 0.05. To test the significance between two

cumulative distribution functions, we also employed two-sample Kolmogorov-Smirnov test, in addition to the Wilcoxon signed-rank test.

5.2 Results

5.2.1 Histology

To validate our place cell recordings, we first examined the locations of our tetrodes at the end of the experiments. In all three animals, we observed clear tetrode tracks slightly more anterior than our target implant site (AP: ~-3.5; targeted AP: -4). Nonetheless, we observed tetrode tracks ending past hippocampal CA1 (Figure 5.5), suggesting that the place cells we recorded were indeed CA1 place cells.

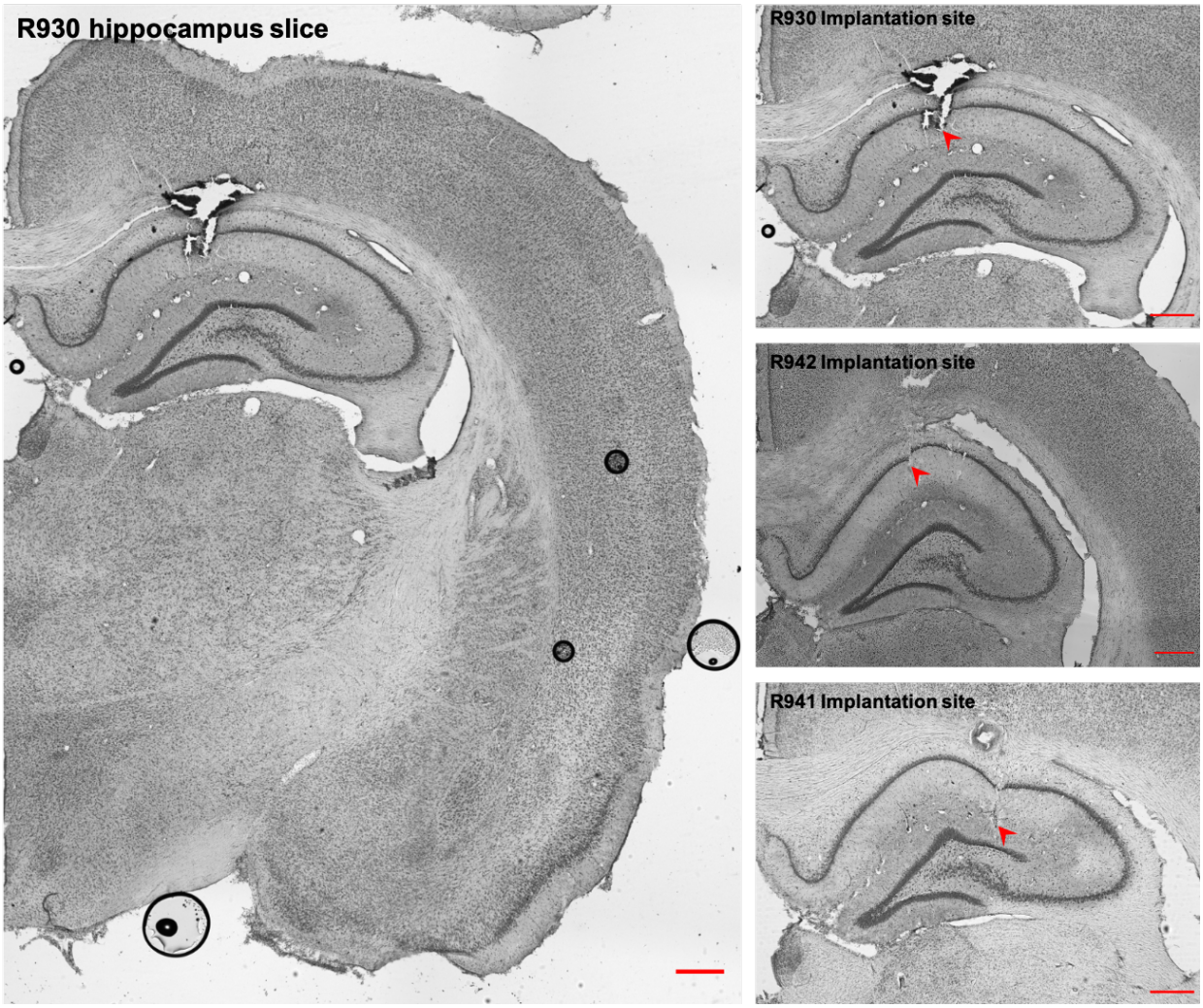

Figure 5.5: Histology slices showing tetrode tracks ending past hippocampus CA1. *Left*, a representative coronal slice from R930 showing the anterior-posterior axis where the tetrode tracks were usually found. *Right,* representative images of hippocampus where the tetrode track was found in R930 (top), R942 (middle) and R941 (bottom). All tetrode tracks were found past CA1 showing that we recorded place cells from CA1. *Red arrowhead indicating the end of the tetrode track. Scale bar: 500μm.*

5.2.2 Summary of recordings

We recorded from the hippocampus of three rats over 24 recording sessions and recorded 597 putative pyramidal cells, among which 529 cells were identified to have place field/s in the environment (see Table 5.1 for more information about the recordings within each animal). The disproportionate number of cells recorded from R941 is a consequence of the higher number of sessions in which cells were retained and the number of tetrodes cells were recorded on (cell signals were found on up to three tetrodes simultaneously).

Table 5.1: Summary of recordings across animals

RATS	HEMI-SPHERE	PRE-EXPOSURE	STARTING COMPARTMENT	NO. SESSIONS	NO. PYRAMIDAL CELLS	NO. PLACE CELLS	NO. UNIQUE PLACE CELLS
R930	Right	Yes	Vanilla	6	39	30	25
R942	Right	No	Lemon	3	41	37	36
R941	Left	No	Lemon	15	517	462	317

Because each animal underwent multiple recording sessions, there is a likelihood that we have recorded the same cell over multiple days despite having lowered the tetrodes. If not taken out of analysis, these cells would ultimately lead to an inappropriate estimation of the number of place cells with repeating or rotated fields, thus undermining our conclusion on place coding in the two-compartment context box. As such, we attempted to identify cells that have been recorded over multiple days systematically and objectively using information about the waveforms and rate maps (see Section 5.1.3.5). This method relies on three assumptions: 1) Place cells are stable and do not remap across days (as in Muller *et al.*, 1987; Thompson and Best, 1990), 2) Cells recorded on the same days across different tetrodes are independent of each other (i.e. not the same cell) and 3) Cells do not appear in one session, disappear on the next and reappear on the subsequent session.

Using this method, 87 place cells were found to be recorded over multiple sessions. 61 place cells were recorded over two consecutive sessions while the remaining 26 place cells were recorded over three to eight sessions. An example cell recorded over 7 sessions is shown in Figure 5.6. For all analyses, we included the cells for when they were first recorded and excluded other instances in which they were recorded. In doing so, we excluded an additional 151 place cells from further analysis, leaving 378 cells in the final analysis.

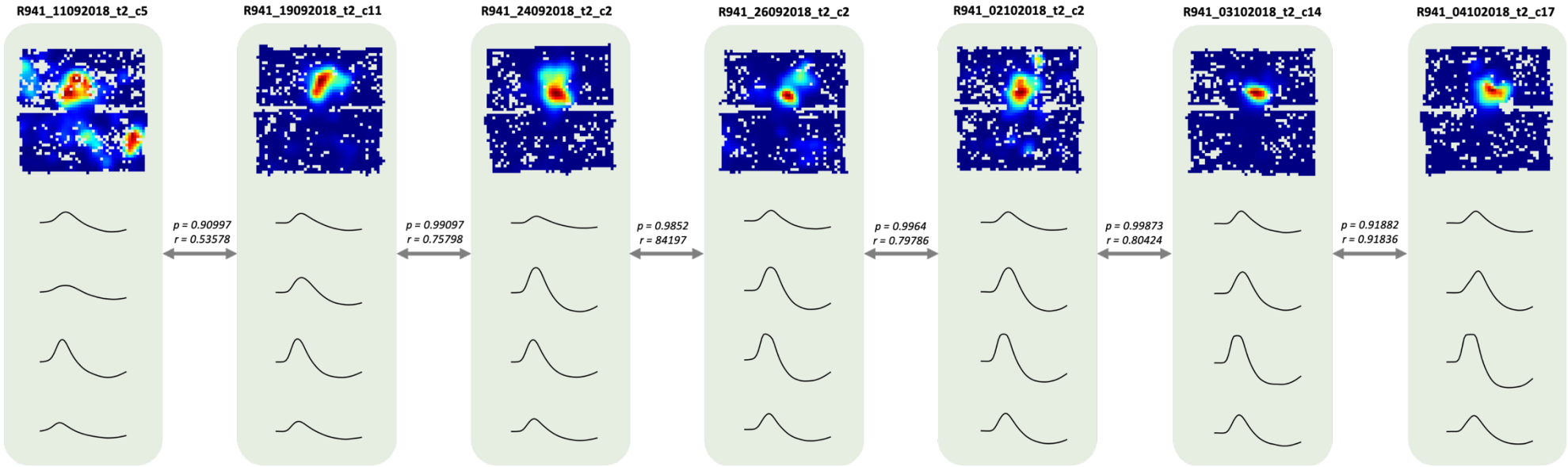

Figure 5.6: Example of an identified cell putatively recorded over days. Because a cell can be recorded over days and could thus lead to an inappropriate estimation of data, we attempted to identify cells recorded over days by using a waveform measure (Tolias distances) to examine for similarity in waveforms and rate map correlations to examine for similarity in place representations (see Section 5.1.3.4). This figure shows an example identified cell recorded over 7 sessions. Each cell recorded in a session is shown with the rate map (*top*) and the waveforms across the four recording channels *(bottom*). Similarity in rate maps is indicated by the correlation values *(r)* while similarity in waveforms across all channels is indicated by the posterior probability *(p)* obtained from the discriminant linear classifiers.

5.2.3 Behaviours differ between the two compartments

We first examine the preference of the three rats for either compartments, which may affect how place cells represent the environment (Mamad *et al.,* 2017). To do so, we examined the time the animals spent in each compartment and expressed it as a preference index (see Section 5.1.3.1).

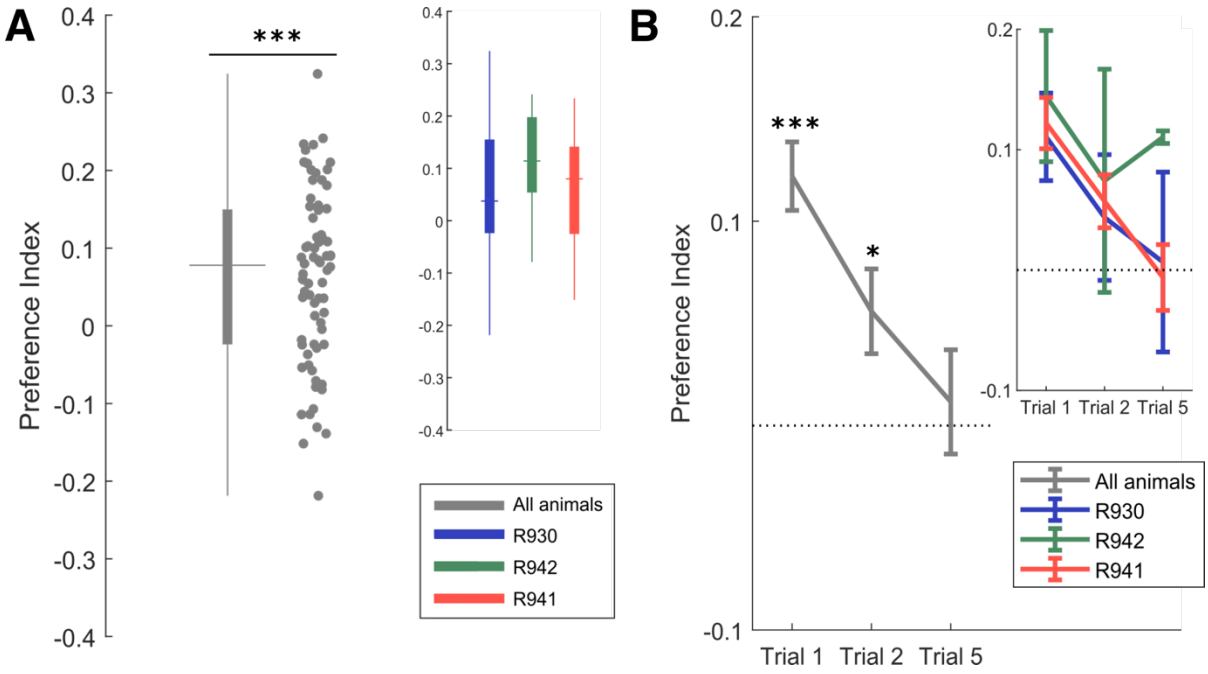

Figure 5.7: Behaviours of animals in the two-compartment context box. (A) Preference index across all animals (grey) and for each animal (inset; coloured box plots). Each marker in grey represents a single two-compartment trial. The preference for the vanilla compartment is evident across all animals. **(B)** Preference index of all animals (grey) and individual animals (inset; coloured line) across trials. The lines represent the mean and standard error of the preference index across sessions. Note how the preference index goes towards 0 in the later trials (except in R942). *** $p < 0.001$. ** $p < 0.01$. * $p < 0.05$.

Surprisingly, we found a consistent preference across animals for the vanilla compartment (Figure 5.7A; one sample t-test $t(71) = 4.76$, $p < 0.001$). The preference for the vanilla compartment slowly diminished over the trials within a session such that usually by the last two-compartment trial, the animals displayed no preference and explored both compartments almost equally (Figure 5.7B, Trial 1 one sample t-test $t(23) = 7.28$, $p < 0.001$; Trial 2 one sample t-test $t(23) = 2.70$, $p = 0.013$; Trial 5 one sample t-test $t(23) = 0.45$, $p = 0.65$).

5.2.4 Place cell properties are similar between the two compartments

Since animals appear to have a preference for the vanilla compartment, we examined place cell and place field properties between the two compartments in the first baseline trial where the bias appears to be the most significant. Most place cells were found to have only one place field in the environment, though multiple place fields were observed (Figure 5.8).

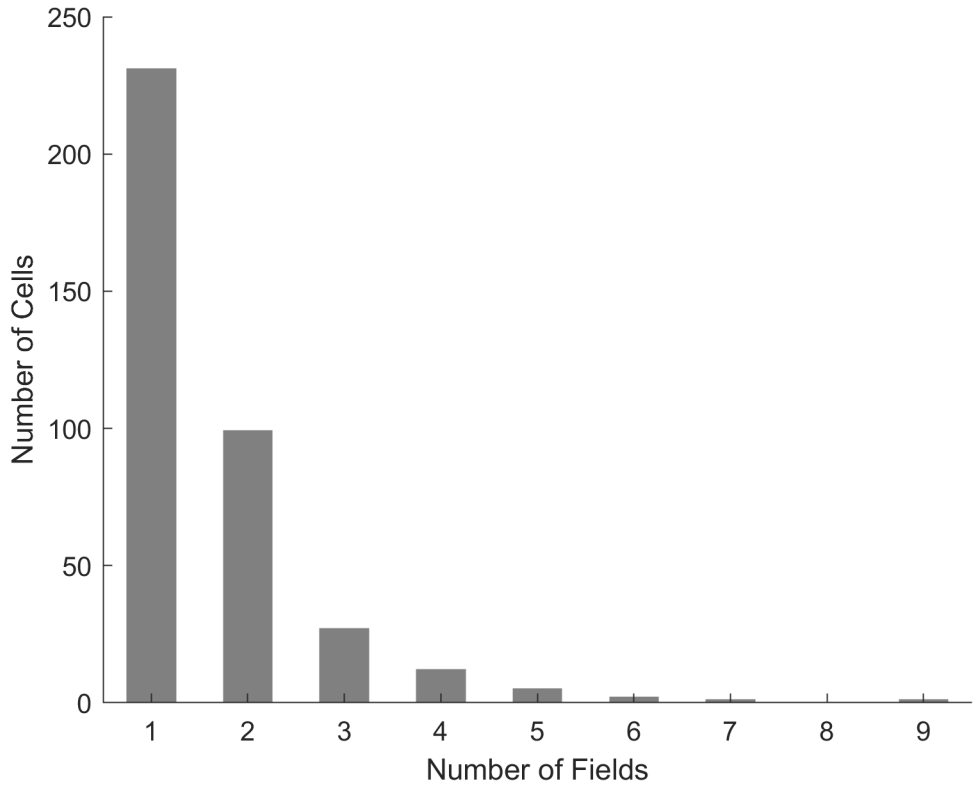

Figure 5.8: Number of place fields each place cell has in the two-compartment context box. Most place cells have one place field in the environment, but about one-third of all place cells have multiple place fields.

We next looked at the properties of place cells between the two compartments by classifying place fields into either lemon or vanilla place field depending on their centroid positions. We found a marginal, but non-significant, higher number of place cells that have place field/s only in the vanilla compartment than place cells that have place field/s only in the lemon compartment (X^2 (1, 278) = 2.43, p = 0.12; Figure 5.9A). This finding suggests that an almost equal number of place cells was recruited for each scented compartment. We went on to examine the absolute number of place fields in each compartment and found an almost equal proportion of vanilla and lemon place fields (X^2 (1, 611) = 0.87, p = 0.35; 317 vanilla

fields and 294 lemon fields; Figure 5.9B) in the two compartments. This thus suggests an approximate equal place representations of both compartments.

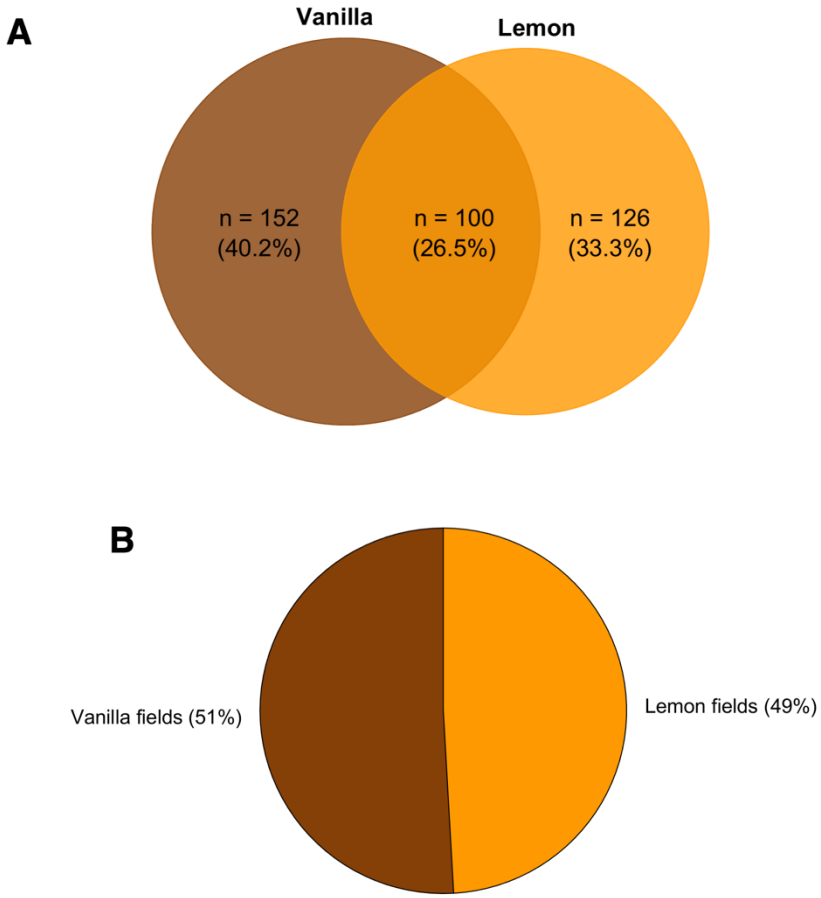

Figure 5.9: Number of place cells and place fields in each compartment. (A) Place cells were examined for the location of their place fields in either the vanilla or lemon compartment and is segregated based on if they have place fields only in the vanilla compartment, in the lemon compartment or in both compartments. There are slightly more place cells that only have place fields in the vanilla compartment, but the observed proportion is not significantly different from an expected equal proportion. **(B)** Similarly, an approximately equal proportion of place fields were observed in both compartments, suggesting an equal place representation of the two compartments.

Similarly, no differences were observed either across or within animals in the peak firing rate (Figure 5.10A; All: two-sample *t* test $t(609) = -0.29$, $p = 0.77$; R930: $t(34) = -0.22$, $p = 0.82$; R942: $t(56) = -0.17$, $p = 0.87$; R941: $t(515) = -0.11$, $p = 0.92$), mean firing rate (Figure 5.10B; All: two-sample *t* test $t(609) = -0.40$, $p = 0.69$; R930: $t(34) = -0.11$, $p = 0.92$; R942: $t(56) = -0.059$, $p = 0.95$; R941: $t(515) = -0.30$, $p = 0.77$) and field area (Figure 5.10C; All: two-sample *t* test $t(609) = 0.14$, $p = 0.88$; R930: $t(34) = -1.38$, $p = 0.18$; R942: $t(56) = 1.43$, $p = 0.16$; R941: $t(515) = 0.0092$, $p = 0.99$) of place fields in the two compartments. Hence, there are no differences in place field properties between the two compartments despite a behavioural preference for the vanilla compartment.

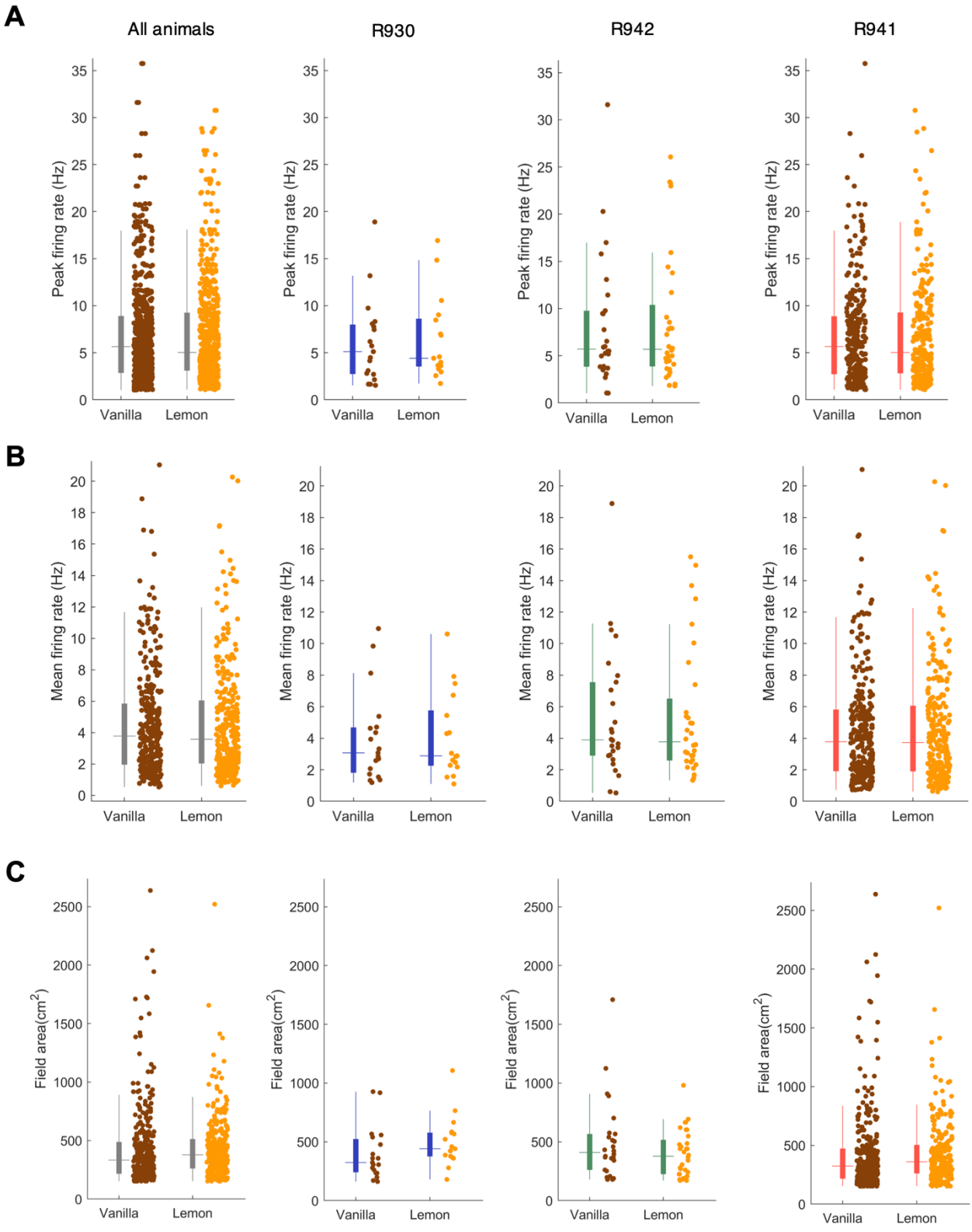

Figure 5.10: Place field properties between the two compartments. Place fields in the two compartments did not differ in **(A)** peak firing rate, **(B)** mean firing rate, and **(C)** field area. No differences can be observed when data are combined (grey) or examined within each animal (blue: R930; green: R942; red: R941). Each marker represents a single place field in either vanilla (brown) or lemon (orange) compartments. Place fields from place cells with multiple place fields were treated as independent sample according to the locations of their centroids.

5.2.5 'Odour-switching' in the environment

Before we start examining the types of encoding place cells exhibit in the compartments (see Figure 5.1), we first examined the place cell maps within a recording session. Surprisingly, we observed that occasionally within a session, the place fields switch their positions between the two compartments – that is a place cell with a place field in the lemon compartment in a trial subsequently fires in the vanilla compartment in the same relative location in the next trial or vice versa. We called this phenomenon 'odour-switching' to indicate the change in the odour relationship of the place fields in the global reference frame.

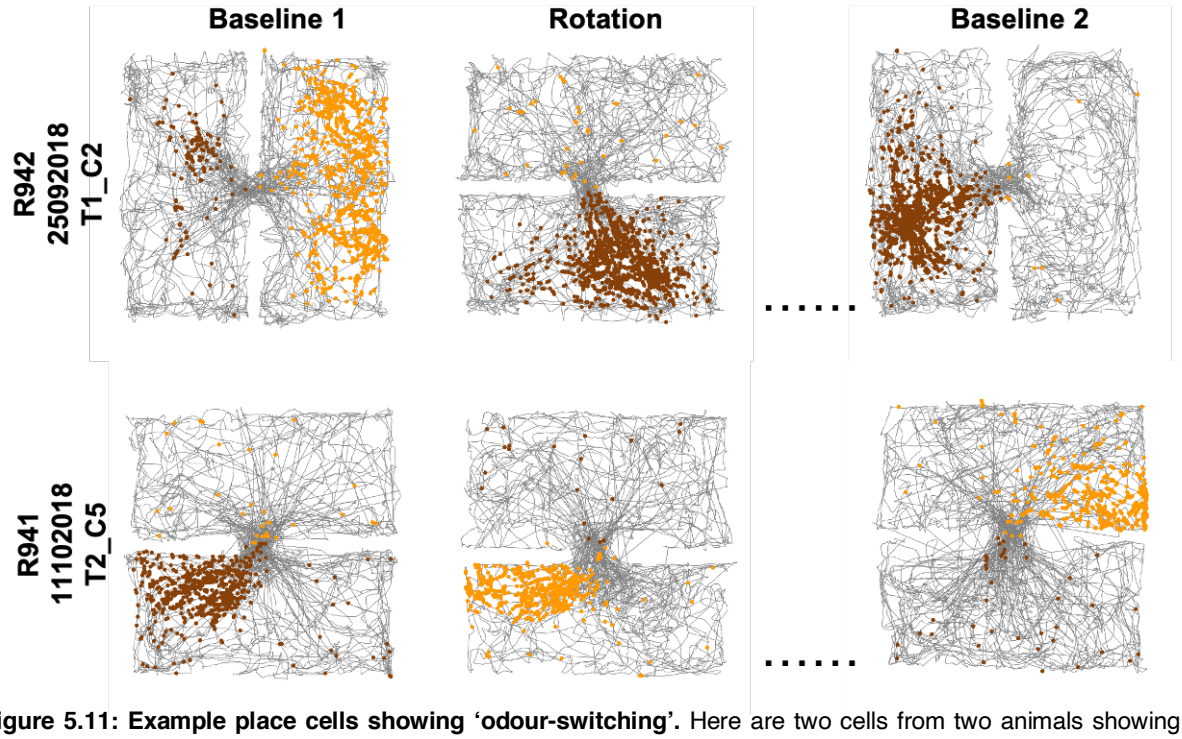

Figure 5.11: Example place cells showing 'odour-switching'. Here are two cells from two animals showing odour-switching in their spiking activity. In the *top row*, a cell originally fires in the lemon compartment but switched to vanilla compartment during the rotation trial. In the *bottom row,* a cell from a different animal and a different session fires in the vanilla compartment originally but switched to the lemon compartment in the rotation trial. *Brown spikes: spikes in the vanilla compartment. Orange spikes: spikes in the lemon compartment. Gray lines: path of animals.*

The observed 'odour-switching' could be due to two possible reasons: 1) the place cells were anchoring to some uncontrolled external cues (such as when the environment was rotated 180° between the baseline and rotation trials; Figure 5.11, bottom cell) or 2) place cells had confused or ignored the two odours and instead guessed which compartments they are in by using the visual cues and/or geometry, which were 180° visually rotated and more salient, to anchor the map. The former reason is highly unlikely as odour-switching can be observed even when the rotations of the environment between the baseline and rotation trials were 90°

and 270º (Figure 5.11, top cell). Place cells were also observed to rotate with the environment at least once even if the environment was rotated by 180º (Figure 5.11, bottom cell, between rotation trial and baseline 2), suggesting that they were anchoring to the local environment and not to some uncontrolled distal cues. In addition, the odour-switching phenomenon was always consistent with the visual/geometry rotational symmetry of the environment and the shifted place fields were always in the relative 180° rotated locations in the global reference frame (see Figure 5.12; i.e. the place fields will be in the same relative location if the environment is rotated by 180°), thus providing support for the latter reason.

We then investigate how often odour-switching occurred. Because odour-switching was always observed as shift in place fields across trials to the relative 180° rotated location in the global reference frame, we correlated the rate maps of every cell across trials, with the

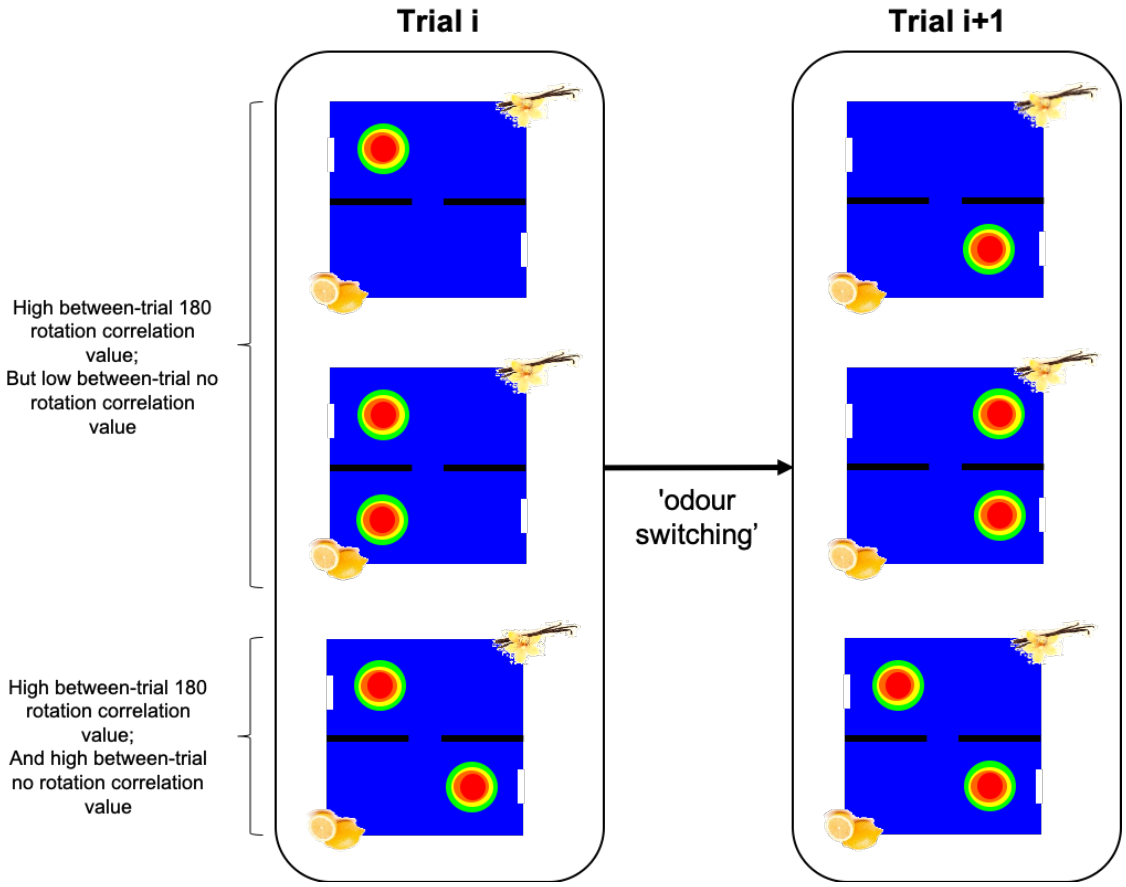

Figure 5.12: Schematic diagram showing odour-switching for the possible types of place encoding. Odour-switching across trials is observed as the shifting of place fields to the equivalent 180° rotated position in the global reference frame such that the place fields are now in the same location relative to the visual cues in the opposing scented compartment. For both global encoding and local repetitive encoding (*first two rows*), the resulting shift can be detected as having high correlation when one of the rate maps is rotated 180° but low correlation when the rate maps from the two trials are not rotated. Odour-switching however cannot be detected in place cells that displayed rotated place fields. In such scenario, rotation of the rate maps 180° in the global reference frame resulted in the same global reference frame place map (*bottom row*). Consequently, high correlation values will be obtained regardless if the rate maps from the two trials were correlated directly or if one of the two rate maps is rotated 180°

trial rate maps in either the same orientation or with one rate map rotated 180° (baseline 1 vs baseline 2; baseline 1 vs rotation trial; rotation trial vs baseline 2; Figure 5.12). This will thus generate a 'no rotation' correlation value and a '180° rotation' correlation value for each comparison for each cell (e.g. baseline 1 vs baseline 2 comparison will give rise to a 'no rotation' correlation value and a '180° rotation' correlation value). Figure 5.12 shows a schematic diagram explaining the odour-switching observed for the possible types of place encoding. It should be noted that if a place cell has place fields in the rotationally equivalent places in the two compartments even within a single trial ('*rotated*' place field; see Figure 5.1), it will be impossible to tell if the place fields odour-switched and the analysis becomes redundant (place cells with rotated place fields will give high correlation values for both no rotation and 180° rotation comparisons). Leaving those instances aside, if odour-switching occurred, the trial pair correlation values will be high for 180° rotation correlations but low for no rotation correlations.

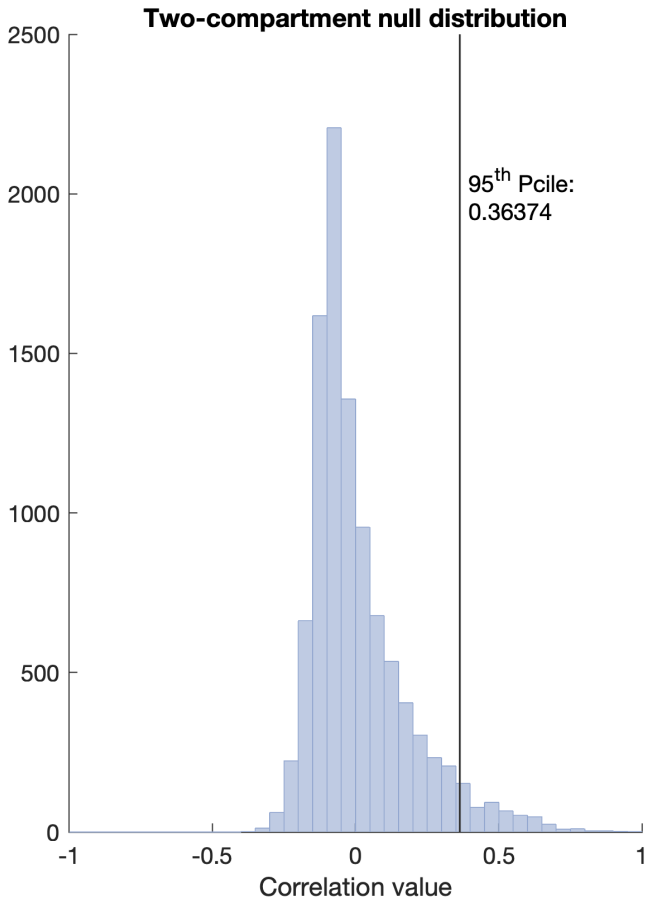

Figure 5.13: Null distribution for two-compartment correlations. Null distribution was generated by shuffling the cell identity. The distribution informs us of the probability of place cells having place field in the same relative location (using correlation values), and the line indicates the threshold chosen (95th percentile of the null distribution).

The obtained correlation values were then compared to the threshold determined by a two-compartment null distribution (see Section 5.1.3.6; Figure 5.13) and only rate map pairs with correlation values that were higher than the 95th percentile of the two-compartment null distribution were considered to be similar (i.e. more likely than chance to have a place field in a specific location; as indicated by the dotted lines in Figure 5.14).

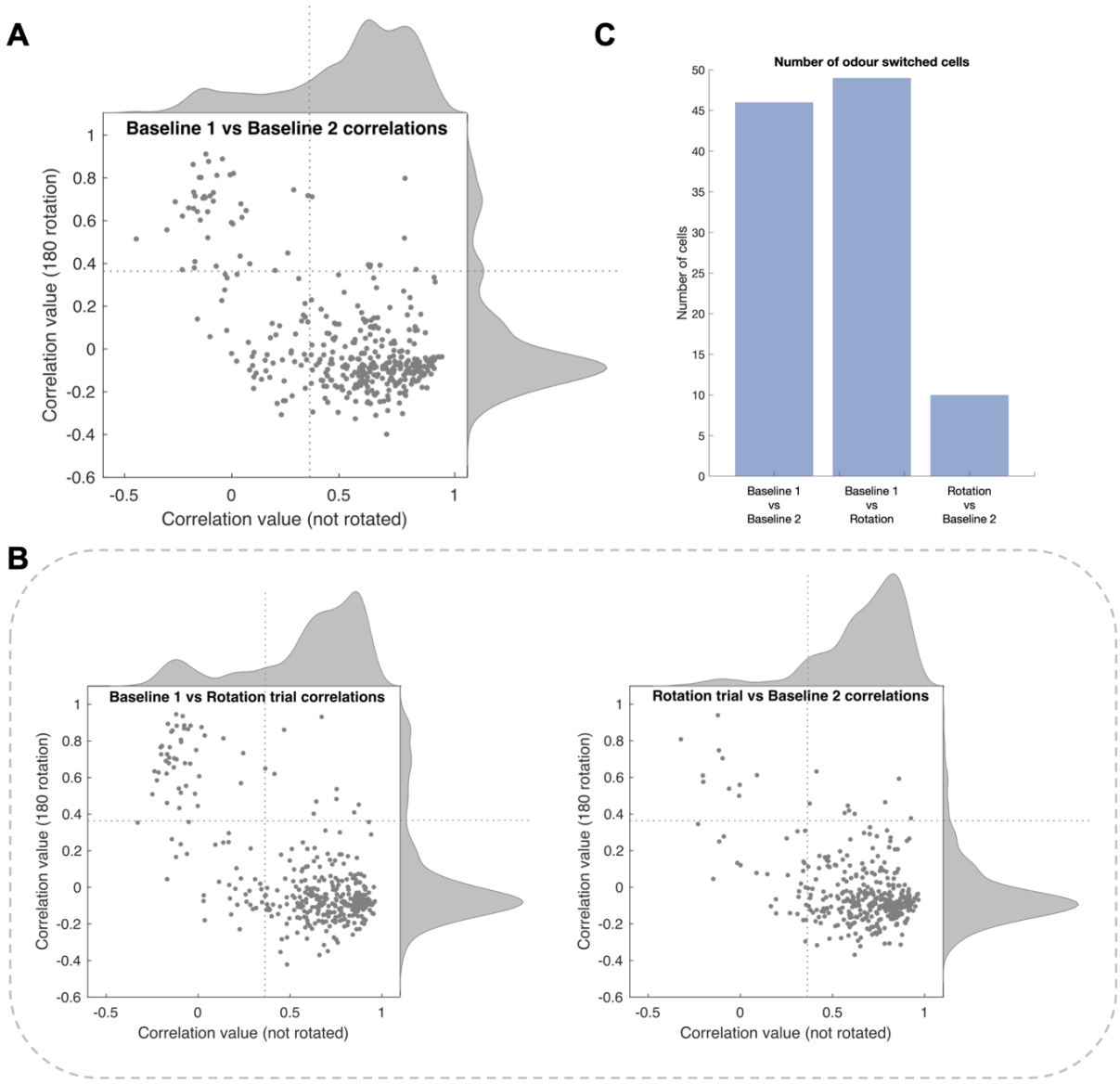

Figure 5.14: Relationships between correlation values of non-rotated and 180° rotated trial pairs. (A) A small proportion of place cells were observed to have similar 180° rotated rate map (top left quadrant) between baseline 1 and baseline 2. Most cells, however, have stable firing patterns (bottom right quadrant). **(B)** The odour-switching phenomenon tend to happen earlier during the recording session as evident by the smaller number of cells that displayed 180° rotated rate maps between baseline 2 and rotation trial (*right*) as compared to baseline 1 and rotation trial (*left).* Each marker represents cell specific, trial-pair rate map correlations. And the dotted lines reflect the threshold as determined by the null distribution (see Figure 5.12) **(C)** Bar plot of the number of cells found in the top left quadrant reflects increased stability in place cells in later trials.

As expected, when we examined the relationship between the correlation values of non-rotated and 180° rotated rate map pairs with each trial pair comparisons, two distinct clusters can be observed: one with high correlation value only when neither rate maps are rotated (bottom right quadrants), and one with high correlation value only when one of the rate maps is rotated 180° (top left quadrants). The odour-switching phenomenon rarely happens, as evidenced by the smaller cluster with high 180° rotated correlation values but low non-rotated correlation values across all trial pair comparisons (top left quadrant, Figure 5.14AB; Baseline 1 vs Baseline 2: 46/378 cells, Baseline 1 vs Rotation trial: 49/378 cells; Rotation trial vs Baseline 2: 10/378 cells). Interestingly, the absolute counts of cells with high 180° rotated but low non-rotated correlation values decrease with time within a recording session (Figure 5.14BC), suggesting that place cells get more stable with trials within a session and maintained the same global reference frame. Also, the low number of cells with high 180° rotated and non-rotated correlation values (top right quadrants) suggests that place cells with rotated place fields rarely occur. This observation will be further explored in Section 5.2.6.

We next asked if the odour-switching phenomenon in place cells happened coherently as a population (as a discrete state attractor network; Wills *et al*., 2005), or if place cells odour-switched independently (as would be if place cells were using different subsets of sensory information). To quantify odour-switching as a population, we limited analyses to sessions with at least 5 co-recorded cells, took the population vector (PV) of each spatial bin across all cells recorded in that session (see Section 5.1.3.7) and correlated the PV in either the same orientation or with one trial rotated 180°. Using this criterion, we removed 4 sessions which had less than 5 co-recorded cells from analysis – 3 from R930 and 1 from R942. The PV correlations were done for consecutive trials: baseline 1 vs rotation trial (Tr1 vs Tr2) and rotation trial vs baseline 2 (Tr2 vs Tr5).

The PV correlation analysis could give rise to three possible outcomes – either place cells remained stable across trials (Figure 5.15A, left), odour-switched independently (Figure 5.15A, middle) or odour-switched coherently as a population (Figure 5.15A, right). Interestingly, if odour-switching happened, the population of co-recorded place cells odour-switched as a whole and behaved like an attractor network with discrete state (Figure 5.15B, right). Statistical analysis between the cumulative distribution functions of the population vectors of non-rotated and 180° rotated trial pairs within each session showed significant differences in all trial pairs, suggesting that all cells within a session tend to either stay stable together or rotate together (Table 5.2). Interestingly, the odour-switching phenomenon did not

only happen in earlier recording sessions (see Table 5.2; R941, session 11102018) and is thus unlikely to be an effect resulting from a lack of experience in the environment.

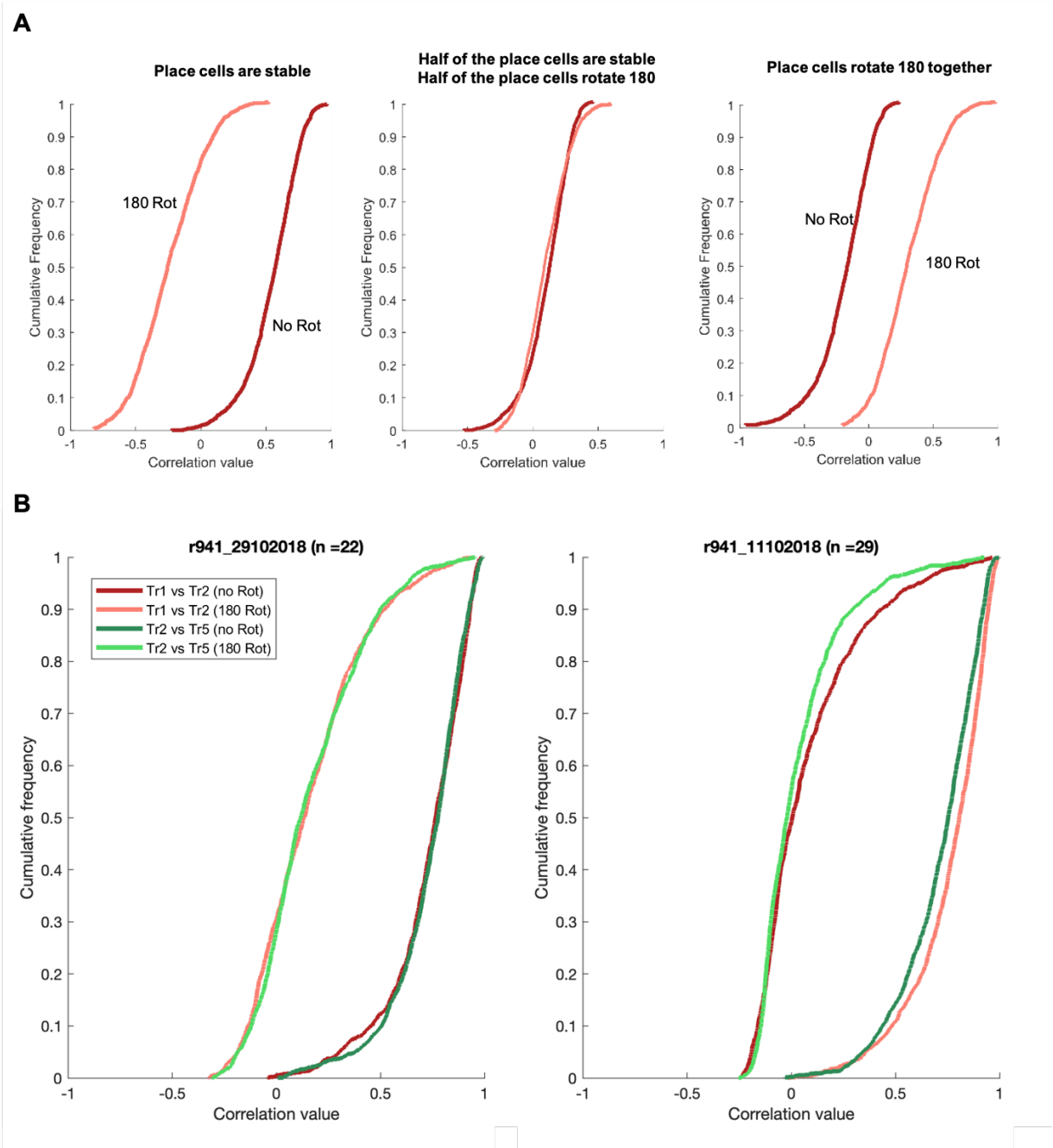

Figure 5.15: Population vector correlation analysis for each session. (A) The population vector correlation analysis can give rise to three possible outcomes. Place cells could remain stable as indicated by the right shifted no rotation PV correlation (*left)*. Place cells could also rotate independently (i.e. some place cells rotate 180° in the global reference frame (i.e. odour-switched), and some do not), which is indicated by the non-significant differences in the PV correlations for non-rotated or 180° rotated comparisons (*middle*). Lastly, place cells could rotate coherently in the global reference frame, as indicated by the right shifted 180° PV correlation (*right*). **(B)** Population vector correlations from two example sessions. Place cells either remained stable (*left*; with non-rotated PV correlations (darker lines) lying to the right of 180° rotated PV correlations (lighter lines)), or rotated coherently as a whole population (*right*; 180° rotated PV correlation for baseline 1 vs rotation trial (pink line) is right shifted compared to the non-rotated PV correlation (red line)).

Table 5.2: Two-tailed two-sample Kolmogorov-Smirnov and Wilcoxon signed-rank test on rotated and non-rotated PV correlations

			Baseline 1 vs Rotation					Rotation vs Baseline 2				
			Kolmogorov-Smirnov		Wilcoxon signed rank		Rotated?[#]	Kolmogorov-Smirnov		Wilcoxon signed rank		Rotated?[#]
Rat	Session	*n* (cells)	*D*	*p*	*Z-val*	*p*		*D**	*p*	*Z-val*	*p*	
930	07082018	6	0.43	< 0.001	-14.93	< 0.001	Yes	0.37	< 0.001	15.12	< 0.001	No
	14082018	5	0.51	< 0.001	-21.92	< 0.001	Yes	0.49	< 0.001	-17.44	< 0.001	Yes
	12092018	5	0.14	< 0.001	-6.09	< 0.001	Yes	0.12	< 0.001	-5.29	< 0.001	Yes
942	03092018	11	0.44	< 0.001	-21.14	< 0.001	Yes	0.48	< 0.001	19.56	< 0.001	No
	18092018	23	0.88	< 0.001	31.15	< 0.001	No	0.85	< 0.001	30.90	< 0.001	No
941	11092018	41	0.89	< 0.001	28.68	< 0.001	No	0.93	< 0.001	30.91	< 0.001	No
	19092018	26	0.85	< 0.001	29.91	< 0.001	No	0.87	< 0.001	30.90	< 0.001	No
	24092018	22	0.73	< 0.001	29.52	< 0.001	No	0.79	< 0.001	31.25	< 0.001	No
	26092018	14	0.53	< 0.001	24.85	< 0.001	No	0.58	< 0.001	25.94	< 0.001	No
	02102018	11	0.46	< 0.001	20.81	< 0.001	No	0.52	< 0.001	25.18	< 0.001	No
	03102018	23	0.83	< 0.001	27.37	< 0.001	No	0.85	< 0.001	30.01	< 0.001	No
	04102018	15	0.57	< 0.001	26.25	< 0.001	No	0.61	< 0.001	28.71	< 0.001	No
	11102018	29	0.83	< 0.001	-26.59	< 0.001	Yes	0.87	< 0.001	29.37	< 0.001	No
	15102018	33	0.92	< 0.001	29.76	< 0.001	No	0.87	< 0.001	30.51	< 0.001	No
	17102018	11	0.61	< 0.001	24.80	< 0.001	No	0.59	< 0.001	25.10	< 0.001	No
	24102018	18	0.79	< 0.001	28.23	< 0.001	No	0.82	< 0.001	29.60	< 0.001	No
	25102018	21	0.86	< 0.001	27.45	< 0.001	No	0.75	< 0.001	27.80	< 0.001	No
	29102018	22	0.77	< 0.001	27.54	< 0.001	No	0.81	< 0.001	28.65	< 0.001	No
	30102018	21	0.81	< 0.001	26.05	< 0.001	No	0.79	< 0.001	27.31	< 0.001	No
	31102018	10	0.59	< 0.001	25.06	< 0.001	No	0.41	< 0.001	20.80	< 0.001	No

[#] Rotated column examined the relationship between non-rotated and 180°-rotated cumulative distribution functions.
Yes = global reference frame rotated; No = place cell ensemble stable

An important thing to note is that some place cells were observed to be unstable within a session (Figure 5.14A; lower left quadrant, rate map pairs with low correlations in both no rotation and 180° rotation comparisons) and/or did not rotate with the local visual scene (Figure 5.14B and Figure 5.14C; lower left quadrant, rate map pairs with low correlations in both no rotation and 180° rotation comparison). Analysis henceforth was done on cells that displayed stable place fields (high baseline trial correlations in both orientations) and anchored to the local visual scene (high baseline/rotation trial correlations in at least one comparison). A total of 311 cells met the criteria and were further analysed.

5.2.6 Global place coding between the two compartments

Do place cells then map the compartments individually or exhibit a global representation of the entire environment (Figure 5.1)? Although most place cells were observed to have only one place field in the environment (see Figure 5.8), this does not necessarily mean that the environment is encoded globally. This is because some place cells may have sparse firing in the opposing compartment (akin to rate remapping) which was not

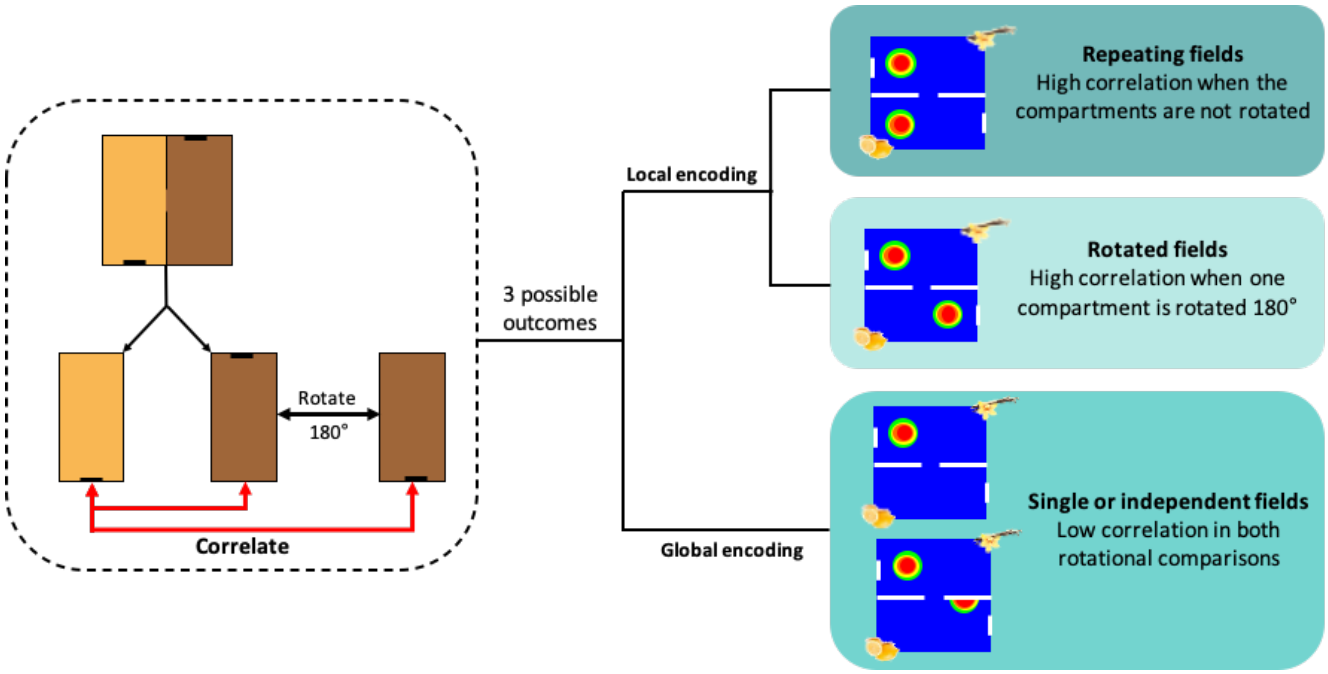

Figure 5.16: Schematic diagram showing how place encoding between compartments were examined. Rate map for each place cell was divided into the compartments and were correlated either directly, or with one compartment rotated 180° such that the visual scene is aligned. A place cell was considered to have repeating place fields if the compartments had high correlation when they were correlated directly without rotation, while a place cell was considered to have rotated fields when high correlation was detected when one compartment was rotated 180°. Place cells were considered to encode the environment globally if low correlation values were observed in both comparisons. *Brown: vanilla compartment; orange: lemon compartment.*

detected as a place field (see Section 5.1.3.3 on place field detection), even though information about the compartments was encoded within its firing.

We thus decided to quantify how often each form of encoding was observed, by correlating the compartmental rate maps of each cell. In this manner, sparse firing in the same relative repeating or rotated position should also give a significant correlation despite the absence of a detected place field. To do so, we systematically separated the rate map of each place cell from baseline trial 1 into the two different scented compartments, thus generating a vanilla rate map and a lemon rate map for each place cell. We then correlated the two compartmental rate maps in their standard (no rotation correlation), or rotated conditions (180° rotation correlation; visual scene aligned). A high correlation when the two rate maps are correlated without any rotation would suggest that the place cells have a repeating firing pattern while a high correlation when one of the two rate maps has been rotated 180° would

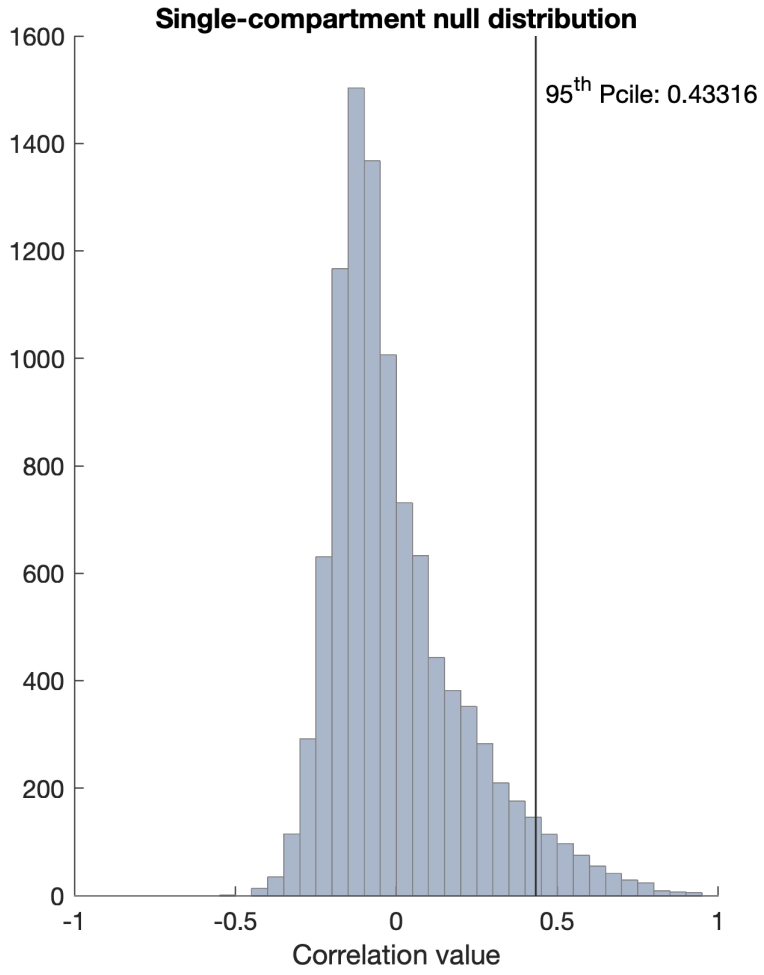

Figure 5.17: Null distribution for single-compartment correlations. Null distribution was generated by shuffling the cell identity. The distribution informs us of the probability of place cells having place fields in the same relative location (using correlation values) within a compartment. The line indicates the threshold chosen (95th percentile of the null distribution).

suggest that the place cells have a rotated firing pattern. Place cells with low correlations in both comparisons are thus considered to have single and/or spatially independent place fields (Figure 5.16). Correlation values were considered to be significant if they were higher than the threshold as determined by the 95th percentile of the single-compartment null distribution (Figure 5.17; see Section 5.1.3.6). The higher threshold observed from the single-compartment null distribution as compared to the threshold derived from the two-compartment null distribution (Figure 5.13) is likely a consequence of the smaller area of the compartment as compared to the entire arena. Thus, it is more likely to have a place field in the same relative location when examining the place maps between the two compartments than between the rate maps of the whole arena between two trials.

Consistent with the findings that most place cells only have one place field (Figure 5.8) and very few cells displayed high 'no-rotation' and '180°-rotation' correlation when the whole map is rotated (top right quadrant; Figure 5.14), most place cells had low between-compartment correlation values. This thus suggests that most place cells globally encode the

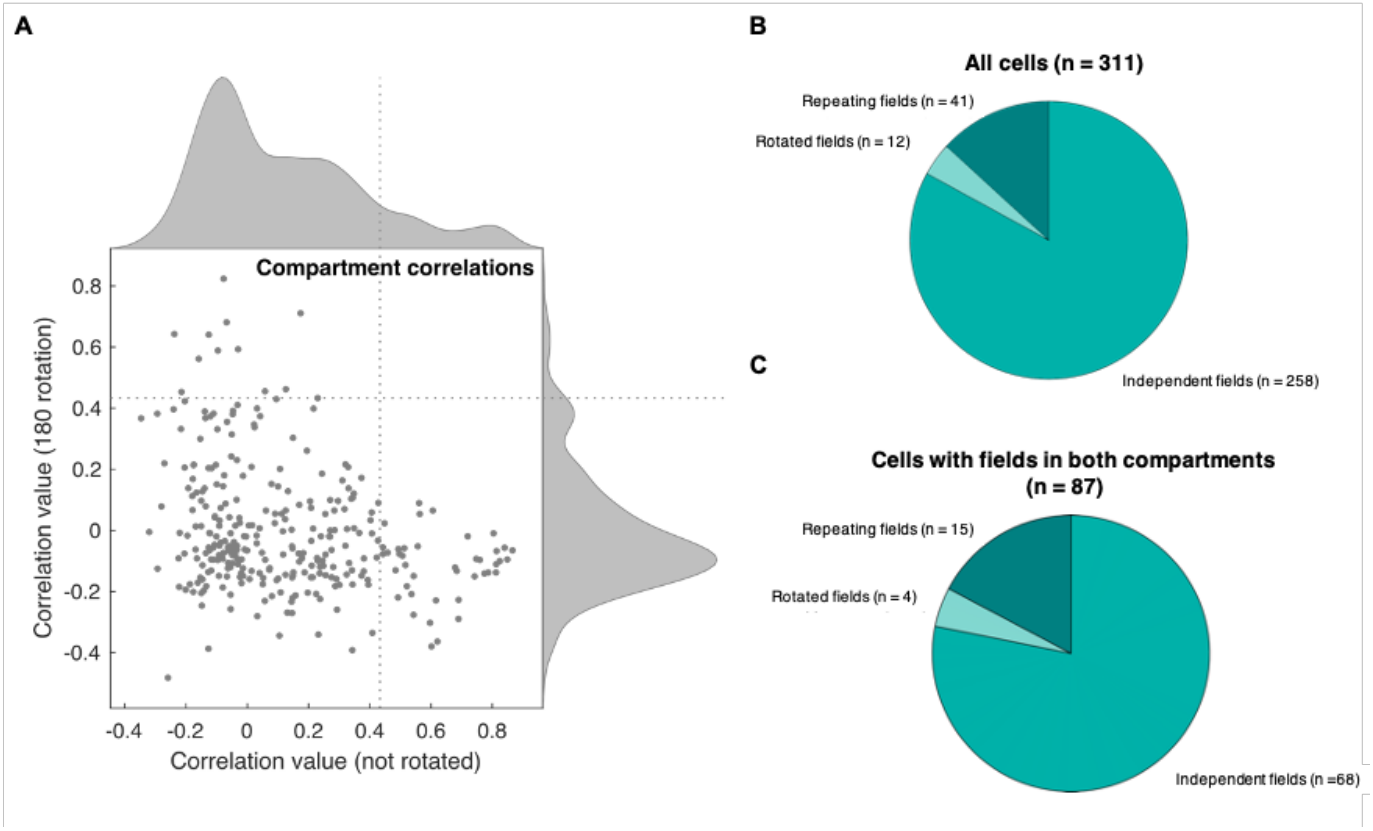

Figure 5.18: Between compartment correlations for baseline trial 1. (A) Scatterplot between non-rotated correlation values and 180° rotated correlation values. Each marker represents a cell and the between-compartment correlations in the two orientation. The dotted lines indicate the threshold for what constitutes similar compartmental rate maps as defined by the null distribution. **(B)** Across all cells, 13% displayed repeating fields while 3.8% displayed rotated fields. **(C)** The same proportion is observed when analysis was done only on cells with place fields in both compartments with 17% of cells found with repeating fields and 4.5% with rotated place fields.

environment. Approximately 13% of place cells exhibited repeating place fields while only 3.8% of place cells exhibited rotated place fields (Figure 5.18B). Given that we set the threshold at 95th percentile for the respective null distributions, it is likely that place cells with rotated place fields would have happened by chance. This was indeed the case with the proportion of place cells with repeating place fields being statistically more likely to happen than chance (X^2 (1, 311) = 43.85, $p < 0.001$) and the proportion of place cells with rotated place fields being not significantly different from chance (X^2 (1, 311) = 0.85, $p = 0.36$). Interestingly, when we restrict the analysis to place cells with detected place fields in both compartments, the same proportion of place cells with repeating (~17%) or rotated (~4%) place fields was found (Figure 5.18D). This suggests that when we detected place fields (see Section 5.1.3.3), there is a thresholded effect that may have hampered detections of cells that have related spatial firing patterns between the two compartments but no detected fields (i.e. these place cells could have similar firing patterns in the same relative location between the two compartments but in one of the compartments, the firing is weaker such that it was not detected as a place field). Nonetheless, the similar proportion of place cells with repeating fields suggests that the range from 13% to 17% likely reflects the true proportion of place cells with repeated fields. Meanwhile, place cells with rotated place fields represented < 5% of the population and could be attributed to chance.

Hence, the place cell system predominantly encodes the two-compartment context box as a global map with most place cells displaying a single field in the environment or spatially independent place fields between the two compartments.

5.2.7 Place cells are able to discriminate compartments based on odours

The previous section showed that most place cells displayed a global map in the two-compartment context box, thus suggesting that most place cells can discriminate the two compartments and 'remap' between the two compartments (N.B.: remapping is used loosely in this context and is use to denote the different maps between the two non-independent connected compartments). To further show that place cells could discriminate between the two compartments, we examined the similarity in place representations between the rotation trials and single-compartment trials (in which the doorway was blocked). Rotation trials were chosen for this analysis as it is the recording trial that happened just before the single-compartment trials (Figure 5.2) and would thus be less likely to display the odour-switching

phenomenon (as evidenced by the low number of cells that showed high 180° correlation values and low no rotation correlation values in the rotation trial vs baseline 2 correlation; Figure 5.14BC).

To that purpose, we divided the rate maps in the rotation trial into the two scented compartments, rotated them appropriately and correlated each compartmental rate map with its respective single-compartment trial rate map (e.g. lemon compartment rate map in rotation

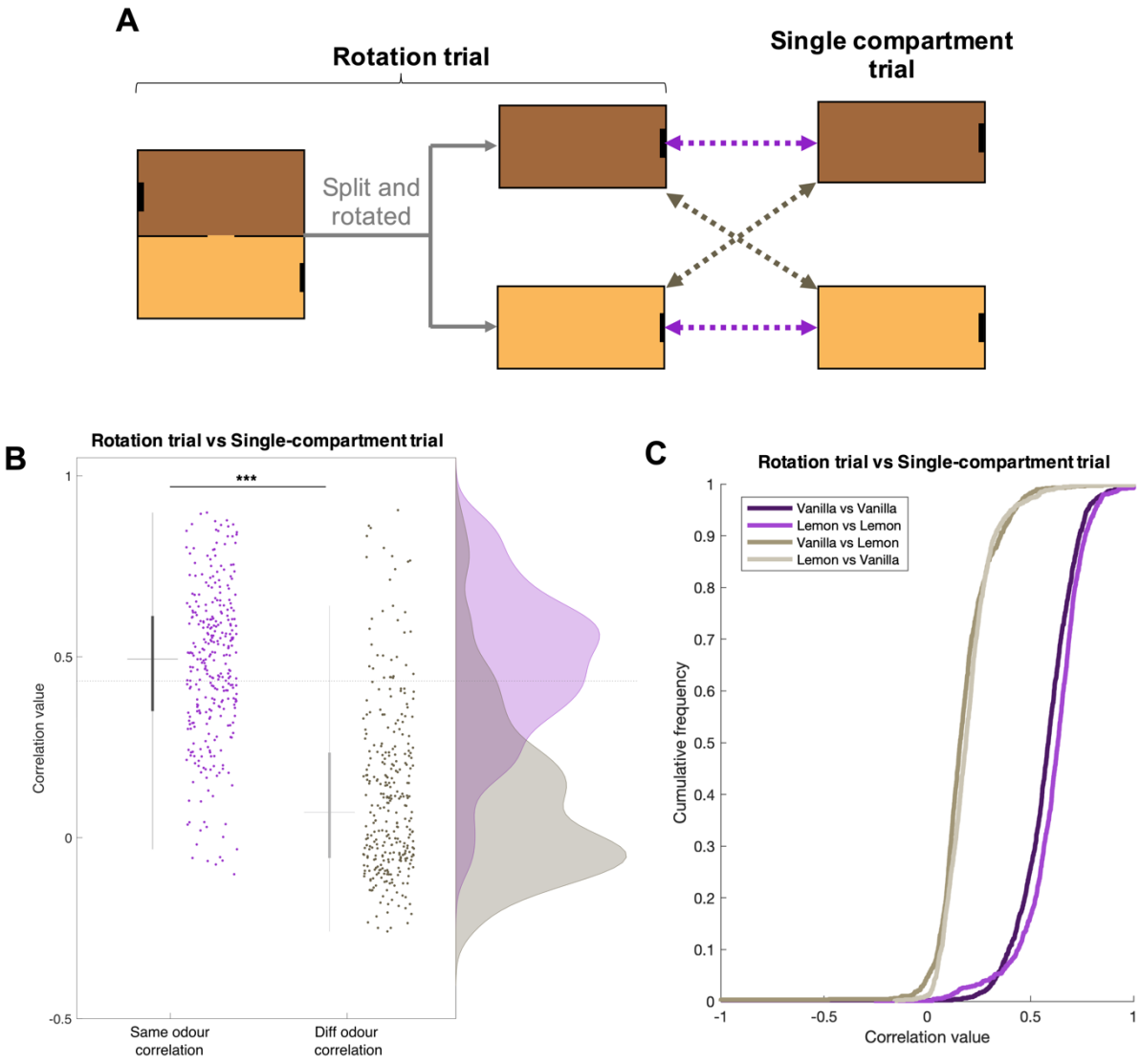

Figure 5.19: Rotation trial versus single-compartment trial correlations. (A) To further show that place cells could discriminate the two compartments, place representations during door-closed single-compartment trials were examined and compared with that of the preceding trial ('rotation trial'). The compartments were separated and rotated as required in the rotation trial and each compartment was correlated with its counterpart in the single-compartment trials (purple arrows) or cross-correlated with the other scented compartment (olive arrows). **(B)** Place cells maintained their place representations in closed-door single-compartment trials as demonstrated by the significantly higher average same odour correlations as compared to that from different odour correlations. Each marker represents each recorded place cell. The dotted line represents the threshold as defined by the single-compartment null distribution. (**C)** When examining the whole population of place cells across each spatial bin via population vector correlations, the same outcome was observed with place cells maintaining its place representation when the doorway is closed.

trial with lemon single-compartment trial; same odour correlations; Figure 5.19A). Additionally, as a control, we correlated the rate maps across odours (e.g. vanilla compartment rate map in rotation trial with lemon single-compartment trial; different odour correlations). The latter correlations examined for similarity in place representations across the different scent compartments, of which high correlation values would otherwise indicate that place cells were unable to discriminate the compartments when the doorway was closed. For instance, if the vanilla rate map in the rotation trial is similar to that of single lemon compartment, it would indicate that the place cells cannot disambiguate the two compartments when the doorway was closed. We also examined the place representations using population vector correlations (see Section 5.1.3.7) which examined the similarity in place representations of the whole place cell populations between equivalent spatial bins across the two trials.

Consistent with a global place representation, place cells were able to discriminate the odours and maintained a similar place representation even when the doorway was closed. Correlation values between rotation trials and single-compartment trials of the same odours were significantly higher than those from different odours (Figure 5.19B, Two-tailed Wilcoxon signed rank test, $Z = 14.68$, $p < 0.001$). Similarly, the same odour correlation values were significantly higher than the threshold as defined by the single-compartment null distribution (Figure 5.17; dotted line in Figure 5.19B; Two-tailed Wilcoxon signed rank test against threshold value of 0.433: $Z = 4.01$; $p < 0.001$) while the different odour correlation values were significantly lower than the threshold (Two-tailed Wilcoxon signed rank test against threshold value of 0.433: $Z = -13.83$; $p < 0.001$). This thus suggests that the place maps between same scent compartments tend to be similar, while the place maps between different scent compartments tend to be different. Interestingly, we also found some cells that displayed high different odour correlation values but low same odour correlation values (as compared to the threshold defined by the single-compartment null distribution; see Figure 5.17), suggesting that some cells may have odour-switched in the single-compartment trials. However, the number of cells that potentially displayed odour-switching was very small (Order of single-compartment trials was randomized; first single-compartment trial: 9/311 cells; second single-compartment trial: 7/311) and is consistent with the suggestion that most cells become more stable across trials within a session (Figure 5.14BC).

Population vector correlation analysis also showed the same effect with same-odour population vector correlations showing a significantly right-shifted distributions (i.e. more similar in their spatial bins) compared to those of different-odour population vector correlations (Figure 5.19C; Two-tailed two-sample Kolmogorov-Smirnov for all comparisons, Vanilla x

Vanilla against Vanilla x Lemon: $D = 0.84$, $p < 0.001$; Vanilla x Vanilla against Lemon x Vanilla: $D = 0.86$, $p < 0.001$; Lemon vs Lemon against Vanilla x Lemon: $D = 0.87$, $p < 0.001$; Lemon vs Lemon against Lemon x Vanilla: $D = 0.87$, $p < 0.001$). Thus, when the doorway was closed, place cells maintained their place representations and were able to discriminate the two scented compartments. This suggests that place cells used odour to discriminate the two compartments and were able to pattern complete based on odour information.

5.2.8 Rate remapping in repeating fields

As described in Section 5.2.6, we found a proportional reduction in the number of place cells with repeating fields when restricting the analysis to place cells with detected fields in both compartments (Figure 5.18C) as compared to when analysis was done on all recorded cells (Figure 5.18B). This finding suggests that some place cells had spatially correlated activity in the two compartments, even when the spiking activity in one of the compartments was insufficient to be detected as a place field. Given that place cells are known to rate remap to non-spatial changes in the environment (Leutgeb *et al.*, 2005), it is thus possible that these cells rate-remap, and encode compartment identity in their firing rates. We thus decided to examine if information about the compartment could be encoded in the firing rates of these repeated fields.

In order to reliably examine for rate-remapping in repeated fields between the two scented compartments, we first have to quantify random fluctuations in firing rates such that the differences in firing activity between fields in both compartments cannot be explained by such random fluctuations. We defined random fluctuations in firing rates as the changes in the compartmental mean firing rates in each repeated field across trials. The differences in mean firing rates between place fields across the two compartments were then compared to these random fluctuations in firing rates. An unsigned rate change score is used to quantify changes in mean firing rates with 0 representing no changes in mean firing rates and 1 indicating the largest possible differences in mean firing rates (when one of the mean firing rates is 0; Leutgeb *et al.*, 2005; see Section 5.1.3.8).

Interestingly, the absolute rate change scores between compartments were significantly higher than that of random fluctuations in firing rates (Figure 5.20A; Wilcoxon signed rank test: $Z = 4.21$, $p < 0.001$), suggesting that there is rate remapping between compartmental place fields in place cells with repeating fields. The variance of the distribution of the rate change scores between compartment was significantly larger than that of random

fluctuations (Figure 5.20; Brown-Forsythe test: $F(1, 80) = 31.29$, $p < 0.001$) and would suggest that some cells rate remapped while others do not. To examine for the proportion of place cells with repeating fields that rate remapped, we defined a cell to have rate remapped if the absolute between-compartment rate change scores exceeded the 95th percentile of that of the random fluctuation distribution (Figure 5.20B). In total, 17 out of 41 place cells with repeating fields (~41%) were found to satisfy the rate remapping criteria, whereby they displayed consistent differences in mean firing rates across trials (vanilla mean firing rate – lemon mean firing rate; Figure 5.20CD). Twelve place cells with repeating fields were observed to have a

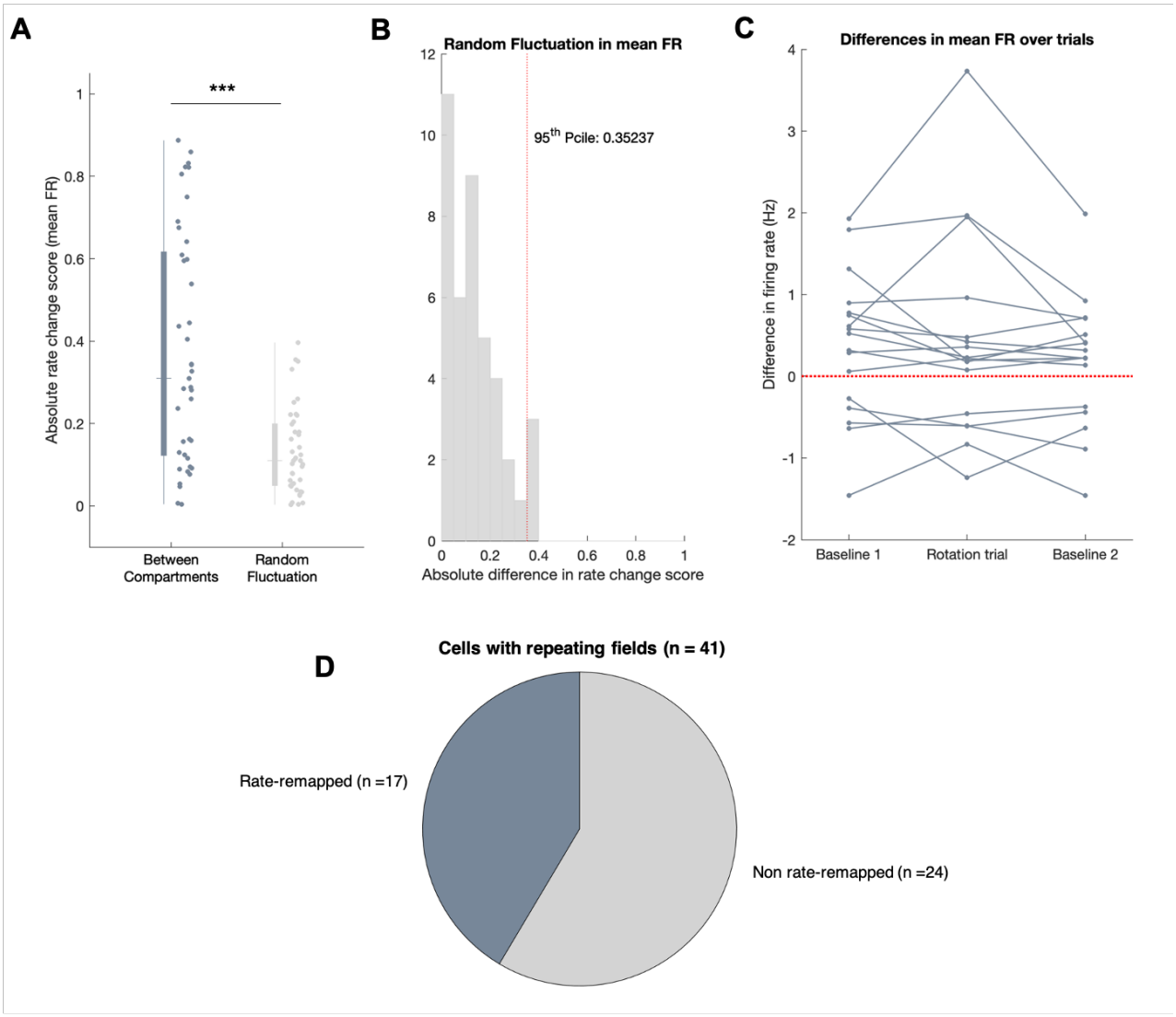

Figure 5.20: Rate remapping in place cells with repeating fields. (A) Examining the absolute rate change scores in cells with repeating fields revealed significantly greater changes in firing rates between the place fields from the two compartments than that explainable by random fluctuations in firing rate. Each marker represents the absolute rate change score of a cell. **(B)** Repeating fields were considered to have significant rate coding between the compartments if the absolute rate change score is more than 95th percentile than that of the random fluctuation distribution. **(C)** Rate remapped place cells consistently have a higher firing rate in one of the two scented compartments with twelve cells showing a higher firing rate in the vanilla compartment (> 0) and five cells showing a higher firing rate in the lemon compartment (< 0). **(D)** Approximately 40% of place cells with repeating fields (17/41) displayed significant rate remapping between the two compartments.

higher mean firing rate in the vanilla compartment (> 0) while five place cells with repeating fields had a higher mean firing rate in the lemon compartment (< 0).

5.3 Discussion

In this chapter, we have examined the place representations in the two-compartment context box. We hypothesized that place cells in hippocampal CA1 encode the two-compartment context box as a whole (global encoding; Figure 5.1) and are hence ideally situated for propagating disambiguating contextual information to granular retrosplenial cortex (see Chapter 4).

5.3.1 Place cells form a global map of the two-compartment context box

Before we explore the types of encoding place cells exhibit, we first examine if there are differences in the behaviours of animals between the two differentially scented compartments, which could affect how place cells represent the environment (Mamad *et al*. 2017). In spite of a preference of the animals for the vanilla compartment (Figure 5.7), we found an approximately equal number of place cells and place fields in the two compartments with no significant differences in their properties (Figure 5.9; 5.10). Thus, unlike Mamad *et al*. (2017), place cells did not over-represent the preferred vanilla compartment. Nonetheless, it should be noted that our task is not goal-directed and the preference for the vanilla scented compartment may not reflect the same saliency and quality of preferences (food reward, ventral tegmental nucleus activation) induced in Mamad *et al*. (2017). Nonetheless, the observation that animals preferred the vanilla scented compartment suggests that the animals could disambiguate the two compartments based on odours.

Could place cells then disambiguate the two compartments? We examine for the types of place encoding by correlating the place maps between the two compartments. In agreement with the behaviours of the animals, most place cells can disambiguate the two compartments and displayed global encoding. These place cells either displayed a single place field in the environment or have spatially independent place fields across the compartments (Figure 5.18). Even though most place cells exhibited global encoding, we did find a significant population of place cells (~15%) that displayed repeating place fields between the two compartments (Figure 5.18). These place cells fire in the same relative locations across the compartments independent of the 180° rotated visual scenes. A small number of place cells that displayed rotated place fields between the compartments was found, but the proportion was not significantly different from chance (i.e. happened to have a place field in the

corresponding rotated location). Our findings thus recapitulate that of Fuhs *et al*. (2005) who also described a small proportions of place cells with repeating place fields between two 180° rotated compartments, in addition to the 'remapping' often seen across the compartments (see Figure 10 of Fuhs *et al*., 2005). Thus, place cells form a global map in the two-compartment context box.

5.3.2 The HD system may help place cells disambiguate the visually rotated compartments

The argument brought forth by Fuhs *et al*. (2005) to explain the 'remapping' observed across 180° visually rotated compartments but not parallel compartments is that differential directional information provided by angular self-motion has a dominant influence on place representations. However, it should be noted that the animals' motions across the compartments were limited in Fuhs *et al.* (2005) and as such, may have increased their dependency on self-motion cues. Nevertheless, several studies have since showed a dominant influence of angular directional information on place representation with place cells displaying less repetition in radially arranged compartments (Grieves *et al*., 2016; Harland *et al*., 2017). Thus, it appears that directional information is sufficient for place cells to disambiguate the compartment. Our results support this notion – that is because animals were moving between the two visually rotated compartments in two distinct heading directions (e.g. east when heading into vanilla but west when heading into lemon), animals were able to use these differential directional cues (provided by angular self-motion) to disambiguate the compartments.

Directional information is often thought to be provided by the head direction system and for directional information to be useful in the disambiguation of the two visually rotated compartments, the head direction signal in the brain will have to ignore the visual cues and be inform by angular self-motion cues. Multiple studies have examined the relative influences of self-motion and visual cues in modulating the PFDs of head direction cells. Consistent with a global encoding, the PFDs of head direction cells tend to remain stable as rats moved across compartmental spaces (see Section 2.3; Taube and Burton, 1995; Dudchenko and Zinyuk, 2005; Whitlock and Derdikman, 2012), thus demonstrating a dominance of self-motion cues in the modulation of PFDs of head direction cell. Similarly, recording of head direction cells from the anterodorsal thalamus and postsubiculum in the two-compartment context box revealed stable PFDs across the two compartments (global encoding; Jacob *et al*., 2017).

Perhaps more conclusively, Harland *et al*. (2017) showed that place cells displayed repeating place fields (i.e. local maps) in radially arranged compartments when lateral mammillary nucleus, a critical head direction node, is lesioned. Taken together, this will suggest that angular direction information, provided by the global head directional signals, is necessary for the disambiguation of visually rotated compartments.

5.3.3 Contextual information is sufficient for disambiguation of visually rotated, differentially scented compartments

However, differential directional information provided by angular self-motion cannot fully explain our results as place cells can also disambiguate the compartments even in single-compartment trials (i.e. when the doorway is closed; Figure 5.19). In the single-compartment trials, angular self-motion cues are not useful, and the animals have to use the context (presumably odours) to disambiguate which compartments they are in. This data thus suggests that place cells receive odour contextual information (in addition to direction information) that is sufficient for disambiguation of the two scented compartments. This finding is in line with Anderson and Jeffery (2003) who showed that place cells receive contextual information, and the contextual inputs to each cell determine how each place cell fires in a specific environment (e.g. environment with white walls and lemon odour vs. environment with white wall and vanilla odour). Thus, in the two-compartment context box, place cells likely receive odour contextual information that determines how they fire even in the absence of reliable angular self-motion cues, and the odour contextual information is sufficient for place cells to disambiguate the two compartments.

Even though contextual information is available to place cells, contextual information may not be needed for the brain to recognize that there are two compartments. Instead, global directional information could be sufficient for the rats to disambiguate the compartments, as evident by the lack of repeating place fields in radially arranged, visually similar *non-scented* compartments (Grieves *et al*., 2016; Harland *et al*., 2017). In the radially arranged environment utilized by Grieves *et al*. (2016) and Harland *et al*. (2017), the compartments are not contextually discriminable (or rather, there are no salient contextual cues) and the only salient cue is the differential directional information provided by the radial arrangement of the compartments. It is nonetheless possible that directional and contextual information have different functional roles in the disambiguation of the two-compartment context box. For instance, the directional signal may help inform the brain of the presence of the two distinct

compartments while contextual information may help identify and recognize the compartments based on the odours.

5.3.4 Distinct functions between geometric information and non-geometric information in place coding

Given that place cells can use the odours to identify the compartments, we were surprised to find that the place maps sometimes displayed 'odour-switching' such that a place cell that has a place field in the vanilla compartment in the first baseline trial switched the location of its place field to the same relative location in the lemon compartment in the next trial (see Section 5.2.5; Figure 5.11). In our experiment, the 'odour-switching' phenomenon was always consistent with the visual/geometry rotational symmetry of the environment such that the shifted place fields were always in the equivalent 180° rotated locations. When odour-switching happened, co-recorded place cells switched as a population (Figure 5.15; Table 5.2) as if the place cells existed in an attractor network with discrete states (Wills *et al*., 2005). Recent work using calcium imaging has also shown coherent rotations of place fields very similar to the odour-switching rotations observed in ours (Keinath *et al*., 2017; Kinsky *et al*., 2018; Sheintuch *et al*., 2020). What is especially interesting is that the rotations observed in these studies were in agreement with the rotational symmetry of the environments (e.g. four-fold rotational probability in a square arena in Keinath *et al*. (2017) and Kinsky *et al*. (2018); two-fold rotational probability in rectangular arena and linear track in Keinath *et al*. (2017) and Sheintuch *et al*. (2020) respectively) despite the presence of polarizing visual cues. As such, they postulated that geometrical cues may play a more important role in anchoring place fields than non-geometric cues (Keinath *et al*., 2017; Kinsky *et al*., 2018). Because both the geometry and the visual scene have a 180° rotational symmetry in our experiment, we cannot conclude if the place maps were anchoring to the geometry or the visual scene when the place cells odour-switched. Nonetheless, the odour-switching phenomenon observed in our setup is likely due to place cells confusing or ignoring the odours in that specific trial. The place cells instead used the visual cues and/or geometry to anchor the place maps. It should be noted that the same observation was also seen in global head direction cells, with global head direction cells in retrosplenial cortex occasionally rotated their PFDs by 180° in the two-compartment context box (see supplementary Figure 2 of Jacob *et al*., 2017). It however remains unclear if place cells and global head direction cells rotate together in the global reference frame in the two-compartment context box, although coherent rotations of place and head direction cells have been reported in other recording apparatus (Knierim *et al*., 1995).

The observation that place cells followed the geometry/visual scene in the odour-switching trials is reminiscent of the geometric module hypothesis (Cheng, 1988; Gallistel, 1990), that is animals (and place cells) tend to use the geometry of the environment to re-orient themselves despite the presence of polarizing and informative non-geometric cues. It is highly unlikely that the non-geometric cues were not processed or perceived by the animals as Julian *et al*. (2015) showed that animals used the polarizing non-geometric cues (visual information in that experiment) to identify which chambers they are in but still ignored them for spatial reorientation. As such, the authors proposed that there are separable systems for place recognition and heading retrieval with non-geometric cues dominating the former and geometric cues dominating the latter. Our findings do corroborate an independence between how geometrical and non-geometric cues are used for localisation in multi-compartment spaces, although there are confounds between visual cues and geometry. Nonetheless, it seems likely that odour information is crucial for telling the place cell system which compartment the animal was in while the environmental layout (geometry and visual information) help align the global place map appropriately. The latter could be mediated via the global head direction signal as the geometry and the visual scene are likely used to help align the global directional signal. As such, when the animals were confused about the odours, the place map did not become random but instead displayed 180° rotational symmetry in the global reference frame. Our data suggest that the brain seemingly has all the information needed to help localisation in compartmentalized spaces. To localise oneself in a multi-compartment environment, one would have to first identify the compartment one is in (i.e. identify the context) before locating (place recognition) and re-orienting oneself within that context (heading retrieval; Julian *et al*., 2018). Specifically, we have shown that place cells can identify the compartment they are in using odour information (Section 5.2.7) and can provide location information by forming a global map (see Section 5.2.6). Together with bidirectional cells, which can provide information about orientation in the local space, this information should in theory be sufficient for an animal to localise itself in multi-compartment spaces.

5.3.5 Boundary vector cell model and contextual gating model can explain for the place coding observed

The most interesting finding, however, is our observation that a substantial population of place cells displayed repeating place fields across the two compartments. The firing patterns of these cells suggest that they are more concerned with the local geometry,

independent of the local visual scene. Among the population of place cells with repeating place fields, a proportion of these cells showed consistent differences in the firing rates of the repeated place fields between the two compartments. This suggests that the identity of the compartments may be encoded within the firing rates of their place fields ('rate remapping'; Figure 5.20). We cannot, however, conclusively show that the non-spatial features encoded in the firing rates are odours, as the visual scene is also different relative to the firing locations of these fields across the two compartments. Nonetheless, it is likely that information about the odours is encoded in the firing rates of these fields, as odours are the most salient discriminating factor between the two compartments. This finding is in line with Leutgeb *et al*. (2005) who showed that non-spatial features of an environment are encoded in the firing rates of place cells. It is also reminiscent of the rate remapping described by Hayman *et al*. (2003) or the rate discriminability between compartments described by Spiers *et al*. (2015).

The firing patterns of these place cells with repeating fields are in agreement with the boundary vector cell model of place cell firing (O'Keefe and Burgess, 1996; Barry *et al*., 2006; Grieves *et al*., 2018) and it is likely that these cells receive the same boundary vector inputs. In particular, the different population of place cells observed in our study can be conceptually explained by a combination of contextual gating and boundary vector cell model. The contextual gating model describes how contextual information regulates and selects metric inputs (grid or boundary inputs) to form place fields while the boundary vector cell model describes how place fields can be formed via a thresholded sum of boundary specific firing. In agreement with the boundary vector cell model, we think that boundary vector cells are the main determinant of how place cells fire in the two-compartment context box, whereby convergence and thresholded sum of these boundary inputs generate place fields. Each place cell could thus receive multiple sets of boundary inputs that determine how the place cell fires in the environment. Contextual inputs (possibly from the lateral entorhinal cortex) however synapse onto and modulate these boundary inputs in a similar way as described by Anderson and Jeffery (2003). Most place cells could thus receive unique drive from one of the two odour contexts and generating a single place field in the environment (Figure 5.21A). Place cells with spatially independent place fields in the two compartments could then be generated by the odour contexts driving distinct sets of boundary inputs in the two compartments (Figure 5.21B). Place cells with repeating place fields could arise from one set of boundary inputs receiving inputs from both or neither odour contexts. This would therefore generate similar

firing patterns between the two compartments (Figure 5.21C; Latter not shown in Figure 5.21). Last but not least, rate remapping in place cells with repeating fields could reflect cells that receive the same boundary inputs, but the strengths of the odour contextual drives are different (Figure 5.21D).

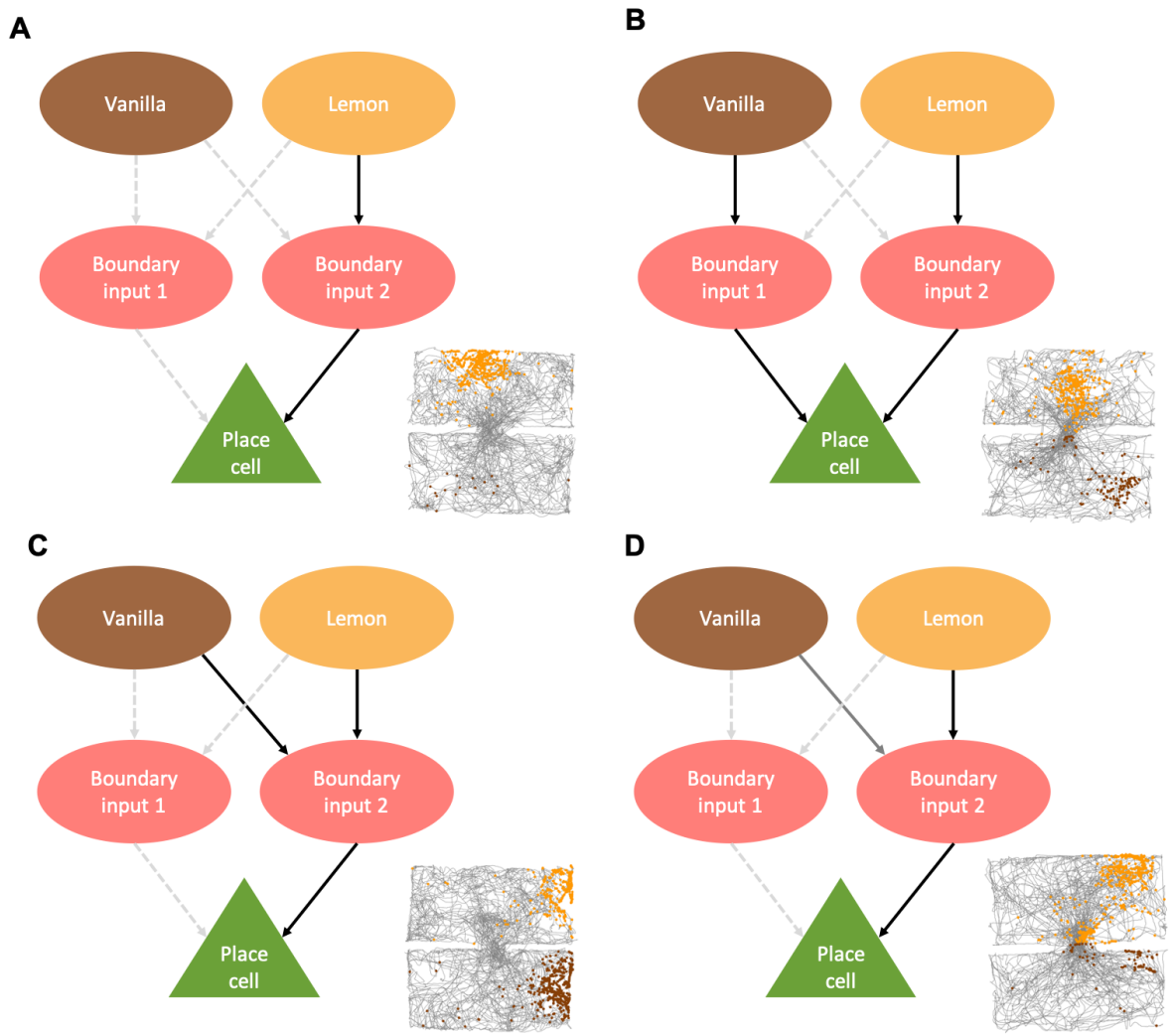

Figure 5.21: Conceptual model to explain for the types of encoding observed. Our data can be conceptually explained by a combination of boundary vector cell model (O'Keefe and Burgess, 1996; Barry *et al.*, 2006) and contextual gating model (Anderson and Jeffery, 2003; Jeffery, 2007; Hayman and Jeffery, 2008; Jeffery, 2011). Specifically, each place cell could receive multiple sets of boundary inputs which determine how it fires in the two-compartment context box. **(A)** A place cell could thus have a single field in the environment by having only one odour context driving one set of boundary input. **(B)** Spatially independent place fields could thus be explained by each odour context driving distinct sets of boundary inputs. **(C)** Place cells with repeating fields can be envisaged as the two odour contexts driving the same set of boundary inputs into the place cells but could also be explained by a set of boundary inputs that do not receive any odour contextual inputs. **(D)** Rate remapping in place cells with repeating fields could thus be explained by the boundary inputs receiving different strengths of drives from the different odour context. It should be noted that different strengths of visual information (resulting from the distinct visual scene from the same relative location in the two compartments) could also explain for rate remapping in repeating fields. However, odours were the most salient cues, and it is more likely that odour information is encoded within the firing rates. *Solid black lines*: *active connections; Dotted grey lines: inactive connections; Solid grey lines (in D): weak connections.*

What do these findings mean in the context of local and global directional firing? The hippocampus and the granular retrosplenial cortex are bidirectionally connected: that is both sub-regions of retrosplenial cortex project to the hippocampus (via postsubiculum and medial entorhinal cortex; see Section 1.3.2.1) and the hippocampus feeds back to granular retrosplenial cortex (either directly via CA1 or indirectly via dorsal subiculum; see Chapter 4). The presence of a global map in hippocampus CA1 thus suggests that (i) it is plausible that CA1 propagates disambiguating contextual information to granular retrosplenial cortex which helps to inform global directional cells of the presence of two distinct compartments (as per our hypothesis) and (ii) the global directional signal and the more visually modulated local bidirectional signal are resolved before being passed on to hippocampal CA1. The latter is supported by our observation, or rather lack of observation, of visually sensitive local place cells, which suggests that the visual information is resolved upstream of CA1. This is broadly in line with the model by Li *et al*. (2020) who suggest that visual place cells exist in CA3 and the visual information is integrated with self-motion cues derived from motion-based place cells to form conjunctive place cells in CA1. Consequently, place cells in CA1 conjunctively encode self-motion cues and visual information and this could explain the lack of visual sensitivity observed in CA1 place cells (i.e. no place cells that just showed sensitivity to the local visual scene). The implications of these findings will be further discussed in the next chapter (see Section 6.2).

5.3.6 Limitations and considerations

Although we have drawn several conclusions from the analysis in this chapter, it should be noted that the work in this chapters is not perfect and have several caveats – most prominently the sampling from a relatively small number of animals and an over-sampling of cells from one rat which contributed extensively to the data in this thesis. These caveats may have weakened the conclusion of our data (e.g. imagine a scenario where repetitive cells are only found in one animal) and/or the statistical power of our analysis. Although so, it should be pointed out that findings from three animals have been published previously (Fuhs *et al*., 2005). Additionally, our main research question is centred around the types of place encoding observed in the visually rotated, two-compartment context box and cells with repeated fields across the two compartments were found across all animals, suggesting that the phenomenon is unlikely to be an artifact resulting from bias sampling in one animal.

We can nonetheless try to alleviate the problem with unequal samplings possibly by conducting a monte carlos simulation and probabilistically solve the question at hand by either

randomly selecting a session from each animal or randomly selecting a fixed number of cells recorded across sessions from each animal for each loop of the simulation. Cells that are selected can then be correlating in the same way as in Section 5.2.6 and the proportion of cells with repetitive fields from each loop of the simulation recorded. This proportion can then be compared with an expected proportion of 0.05 (see Section 5.2.6).

Alternatively, we could sub-sample the data across animals such that each animal contributed a similar sample (see Grieves *et al*, 2020). For example, we could examine the session with the greatest number of cells co-recorded from each animal and examine the proportion of place cell with repetitive fields found within these sessions. Although this may be useful, it should also be noted that the low number of cells recorded from some animals (e.g. highest number of cells co-recorded within a session from R930 is 6) would imply that place cells with repetitive fields may not be observed in these session due to insufficient sampling and may thus lead to an underestimation in the proportion of repeating place cells.

Last but not least, it should be noted that although cells recorded across sessions and across animals are combined and treated as independent sample in this thesis (as well as often within the spatial navigation field), place cells co-recorded within each session and each animal are not independent. Hence, data segregated according to animals and/or sessions should be shown whenever statistically appropriate (i.e. when there is sufficient sampling; Figure 5.7 and Figure 5.10).

5.4 Interim conclusion

The main finding of this chapter is the observation that most place cells can disambiguate the two compartments by using the odours and/or rotated visual scenes, thus displaying global encoding. A small population of place cells displayed local encoding where they repeated their place fields between the two compartments independent of the local visual scene. A proportion of these place cells with repeating place fields could also disambiguate the compartments, by having differential firing rates across the compartments. Particularly, an insignificant proportion of place cells displayed rotated place fields, suggesting that there are no place cells in CA1 that are only modulated by the local visual scene. Therefore, these findings suggest that hippocampal CA1 can disambiguate the two compartments and could provide contextual information back to the global head direction system in granular retrosplenial cortex. The next chapter will focus on bringing our results from the two chapters together and we will consider how the two directional signals interact in the brain.

Chapter 6.
General Discussion

The work done in this thesis is inspired by the study from Jacob *et al*. (2017), who found bidirectional cells in dRSC as animals traverse between two visually rotated, differentially scented compartments (see Section 2.3.1). These bidirectional cells are believed to encode information about the local visual environment, which is distinct from the global directional information provided by head direction cells found in all sub-regions of retrosplenial cortex (see Section 2.3; Chen *et al*., 1994; Cho and Sharp, 2001; Jacob *et al*., 2017). In this thesis, we further showed that the bidirectionality in dRSC likely arises as a consequence of dRSC sitting partly outside a thalamo-hippocampo-cortical spatial circuit that gRSC is a part of. We also provided evidence for a global map in dorsal CA1 that is consistent with its interactions with gRSC. In this chapter, we will summarize the results and then consider the results within the context of local visual and global directional information integration.

6.1 A spatial granular retrosplenial cortex vs. a visuospatial dysgranular retrosplenial cortex

In the first experiment, we replicated and extended previous studies by van Groen and Wyss (1992; 2003) showing that gRSCb (and by extension, the global head direction system) receives more inputs from the anterodorsal thalamus (Figure 4.4). gRSCb also receive exclusive inputs from several spatial memory relevant brain structures such as dorsal CA1 (Figure 4.6), dorsal subiculum (Figure 4.5) and lateral entorhinal cortex (Figure 4.7). On the contrary, the dRSC is disconnected from these spatially relevant structures. These findings thus suggest that dRSC and gRSC may be functionally distinct with gRSC being more involved in spatial navigation and memory while dRSC being predominantly dominated by its connections with visual cortical area.

How can these differing connections then give rise to the different directionality observed in the different retrosplenial sub-regions? Firstly, dRSC may function as a visuospatial area and help to associate sensory information in the local environment to form an egocentric viewpoint-specific encoding of the environment. As such, when the rats move across the two compartments, cells in the dRSC generate bidirectional tuning curves due to the visually rotated and ambiguous sensory information found in the two compartments (see

Section 4.3.4). Alternatively, directional cells in gRSCb may receive additional vestibular-visual integrated information from anterodorsal thalamus (see Section 1.11; Section 4.2.3) and contextual information from dorsal hippocampus (either directly or indirectly via dorsal subiculum) and lateral entorhinal cortex (see Section 4.2.4), which can help inform the directional cells in gRSCb of the presence of two distinct compartments and thus stabilise directional firing across the compartments. Bidirectional cells may thus arise in dRSC as they represent a subpopulation of directional cells that do not have access to this information and thus do not know that there are two distinct compartments.

Although we have two alternative explanations for how bidirectionality may arise, it should be noted that these possibilities may not be mutually exclusive – that is bidirectional cells may represent directional cells that do not have access to self-motion and contextual inputs but yet, also egocentrically encode information about the local sensory information. Nonetheless, these hypotheses on how bidirectionality can arise would imply that the directional signal in dRSC is more visually modulated while the global directional signal in gRSCb is more multi-modal in nature (receiving self-motion cues and contextual odour cues). It also further highlights the dissociation within the retrosplenial cortex into an allocentric spatial granular retrosplenial cortex and an egocentric visuospatial dysgranular retrosplenial cortex. This distinction is in line with the hypothesis of retrosplenial cortex being a transformation circuit that mediates between allocentric and egocentric representation (Bryne *et al*., 2007).

6.2 Bidirectional interactions between retrosplenial cortex and hippocampus

Nonetheless, the stronger coupling of gRSC with anterodorsal thalamus and the hippocampal formation suggests that these structures may help disambiguate the two compartments. If anterodorsal thalamus and dorsal hippocampus are truly involved in the disambiguation of the two compartments, the directional and spatial signals within these structures might themselves be able to disambiguate the compartments (Page and Jeffery, 2018). In agreement, head direction cells in anterodorsal thalamus globally encode the two-compartment context box (Jacob *et al*., 2017). Likewise, given the stronger coupling between dorsal hippocampus and gRSCb, we predicted that place cells would be able to disambiguate the two compartments and encode the environment as a whole. To test that hypothesis, we went on to record place cells in CA1. In agreement with a global encoding mechanism, most

place cells were found to display either one place field in the two-compartment context box or spatially unrelated place fields between the two compartments. No place cells were found to exhibit rotated place fields (see Figure 5.1; Section 5.2.6), which would otherwise suggest sensitivity to the local visual scenes. As directional information from retrosplenial cortex is also believed to be propagated to place cells in hippocampus (Cooper and Mizumori, 2001), the bidirectional interactions between granular retrosplenial cortex and hippocampus thus suggest a complex interaction between the two structures. Specifically, the conclusion from this finding is twofold: (i) the bidirectional signals and global direction signals are resolved upstream of CA1 such that a coherent global directional signal is available to place cells and (ii) CA1 place cells could disambiguate the two compartments and are thus capable of propagating contextual information to gRSCb (see Chapter 4)

The non-significant number of visual place cells found supported the former conclusion and would suggest that the visual bidirectional signal and the global directional signal are integrated and resolved before they reach the place cells in the hippocampus (via medial entorhinal cortex or postsubiculum). As such, the place cells in CA1 receive a resolved and coherent global directional signal that likely helps place cells disambiguate the two differentially scented compartments (see Section 5.3.3) and compute relevant contextual information. Because dorsal CA1 also project back to granular retrosplenial cortex, it would suggest that the contextual information may be fed back to the granular retrosplenial cortex, which may in turn help compute global head direction signal. This is supported by evidence showing that place cells in hippocampus can readily distinguish between different contexts, including but not limited to colours and odours (Anderson and Jeffery, 2003). Thus, it seems likely that dorsal CA1 and granular retrosplenial cortex consistently communicate with each other to ensure that that the neural representation of the global environment is coherent with each other (e.g. global directional signal and CA1 place signal).

6.3 The two-streams model of retrosplenial cortex

The first conclusion then raises the question – where in the brain *do* the local visual bidirectional signal and the global multimodal directional signals get resolved? Visual information is often thought to enter the head direction network and other spatial systems via retrosplenial cortex and postsubiculum (see Section 1.3.2.1 and Section 1.3.2.2; Goodridge and Taube, 1997; Clark *et al.*, 2010; Yoder *et al.*, 2015; Calton *et al.*, 2003; Winter *et al.*, 2015; Cooper and Mizumori, 2001) but it remains unclear where the information gets integrated.

The discovery of the visually modulated bidirectional cells in retrosplenial cortex thus suggests that retrosplenial cortex may be critically involved in the integration of visual information into the HD network. This is further bolstered by the presence of directional cells that displayed bidirectional tuning curves within each compartment ('within-compartment bidirectional cells'; Jacob *et al*., 2017). These within-compartment bidirectional cells have asymmetrical tuning curves that reversed between compartments and are thus believed to represent steps in the integration of HD and visual information (Page and Jeffery, 2018). Particularly interesting, the within-compartment bidirectional cells were also only found in the dRSC, thus suggesting that visual integration may predominantly take place in the dRSC. This further corroborate the visuospatial associative role of dRSC, with visual information and spatial information possibly being integrated within the sub-region.

Although visual integration could happen at the level of retrosplenial cortex, visually sensitive directional cells have also been found downstream of retrosplenial cortex in the parasubiculum and medial entorhinal cortex (see Section 2.3.1; Kornienko *et al*., 2018). Thus, it is possible that the local visual directional signal is propagated downstream from dysgranular retrosplenial cortex to medial entorhinal cortex. Considering our connectivity study (together with other studies) within the context of visual integration, we proposed that a parallel stream of local visual information and multi-modal sensory information exists in the different sub-regions of retrosplenial cortex (dRSC and gRSCb respectively; Figure 6.1). The two streams of information appear to persist downstream considering that distinct populations of visually modulated directional cells and global head direction cells have also been found in parasubiculum and medial entorhinal cortex (Kornienko *et al*., 2018). However, when we examine place cells in CA1, the two different directional signals – the local visually modulated directional signal and the global multimodal directional signal – have been integrated, as indicated by the lack of place cells with rotated place fields. Taken together, these findings would suggest that the local visual directional signal is integrated with the global multimodal directional signal downstream of medial entorhinal cortex but upstream of CA1, possibly in dentate gyrus or CA3. It is however unlikely that dentate gyrus plays such an integrative role as genetic disruption of dentate gyrus was shown to largely maintain spatially constrained firing in place cells, although the place fields of these place cells drift over time in the light (Lee *et al*., 2012). This finding suggests that genetic ablation of dentate gyrus preferentially affects visual inputs but spares self-motion inputs. This result is thus inconsistent with what would be expected (i.e. place fields would be disrupted) if the two types of information are integrated in dentate gyrus. Thus, it is more likely that the information is integrated in CA3 or in the inputs

from CA3 to CA1. Particularly, in a model describing how self-motion information could be integrated with visual information to represent multi-compartment spaces, Li *et al.* (2020) speculated that visual place cells may be present in CA3 and the integration may happen via convergence of inputs onto CA1 neurons such that CA1 place cells are conjunctive place cells. If that was the case, recording of place cells in hippocampal CA3 may reveal a sub-population of place cells with rotated place fields (i.e. visual place cells).

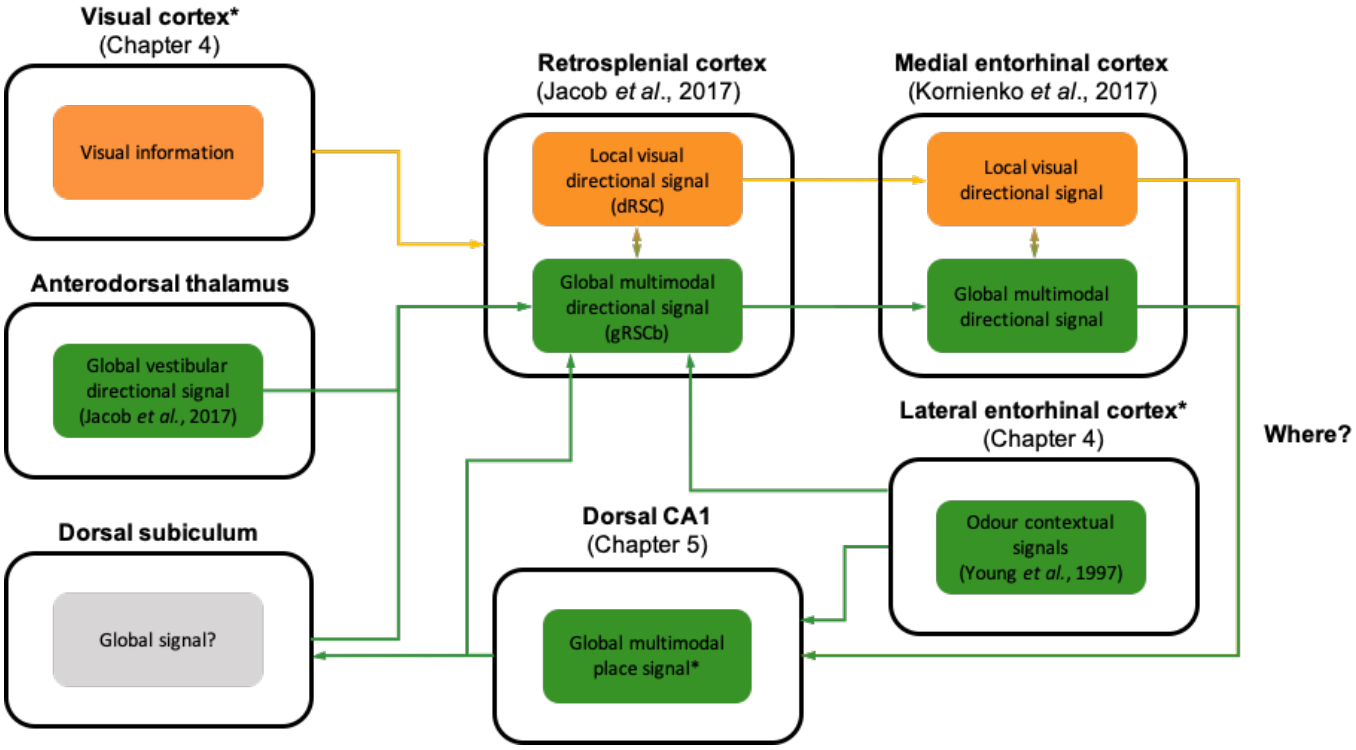

Figure 6.1: Summary diagram showing the two-stream model of retrosplenial cortex based on our findings and that of others. In chapter 4, we investigated the inputs into the retrosplenial cortex showing that most global encoding structures are interconnected with each other. In chapter 5, we provided evidence that dorsal CA1 also provide a global map of the environment. Taken together, we proposed a two-streams model of retrosplenial cortex where local visual directional information exists in a parallel stream to that of global multimodal directional signal. Presently, we are unaware if the spatial signal in dorsal subiculum is global or where in the spatial network the local and global signals are integrated and/or resolved. **indicate novel findings* from the work done in this thesis.

Even though we described the information propagated as two parallel streams of information – the local visual bidirectional signal and the global multimodal directional signal, it is likely that there is extensive cross-talk between the two signals even in the retrosplenial cortex such that the visual bidirectional signal has access to self-motion information and vice versa (denoted by the bidirectional arrows in retrosplenial cortex and medial entorhinal cortex in Figure 6.1). For instance, bidirectional cells were found to be stable in the dark, suggesting that they have access to information from other sensory modalities. In addition, within-compartment bidirectional cells (subpopulation of bidirectional cells that have two PFDs within each compartment) have also been described in Jacob *et al.* (2017) and they are believed to

be generated via an interaction between visual inputs and global head direction inputs (as previously discussed, Page and Jeffery, 2018). Even though the projections are sparser, anterodorsal thalamus also projects to dRSC (and by extension, the bidirectional signal; Figure 4.4; van Groen and Wyss, 1992), suggesting that the bidirectional signals may also receive ascending vestibular information from dorsal tegmental nucleus (see Section 1.3.2.1). Consistent with this, two photon calcium imaging in dysgranular retrosplenial cortex revealed sensitivity of dRSC neurons to locomotion in the dark (i.e. self-motion cues; Powell *et al.*, 2020). It is however unclear if these neurons are part of the same population of bidirectional neurons or if they coincide with the global head directional cells that are also found in dRSC (Figure 2.6; Jacob *et al.*, 2017).

Regardless of where in the brain the local visual bidirectional signal and the global multimodal directional signal are integrated and resolved, it is likely that place cells in dorsal CA1 receive a resolved global head direction signal and they can use this signal to help compute contextual information, which is then fed back to the granular retrosplenial cortex to help compute global head direction.

6.4 Future works

This thesis had bridged some gaps in knowledge of how the local directional signals could fit in the framework of spatial navigation (Figure 6.1). Taking our results together in the context of integration of local and global reference frames, it is clear that global encoding is prevalent in many of the main spatial regions (including CA1; Chapter 5) and the global encoding observed in gRSCb is likely a consequence of its stronger coupling with vestibular-directional thalamic nuclei and the hippocampal system ('thalamo-hippocampo-cortical spatial circuit'). It should also be highlighted that there is a feedback route from CA1 to gRSCb (either directly or indirectly via dorsal subiculum) that may play a big role in ensuring coherent spatial coding across all spatial systems. Meanwhile, the local directional signal in dysgranular retrosplenial cortex likely arises as a result of its dissociation from the global multimodal directional network and may reflect the visuospatial associative role of dysgranular retrosplenial cortex.

Although the data appear to fit together, it should be noted that the data described in this thesis are correlative in nature and future work can focus on teasing out the circuit in a causative manner by either activating or inactivating some of the inputs to retrosplenial cortex and observing the effects on the downstream directional or place signals (e.g. recording in retrosplenial cortex or dorsal hippocampus). However, the crucial question is which inputs

should we start examining? Our findings from Chapter 4 provided an exploratory framework to guide such causative experiments. For example, the author of this thesis was working on temporarily inactivating anterodorsal thalamus inputs (using muscimol) while recording from CA1, but the work was unfortunately disrupted due to the pandemic. The rationale of the experiment was to investigate if the vestibular directional signal from anterodorsal thalamus was important for maintaining global encoding, and if this was the case, a reversal of the place cell signal from global encoding to local visual encoding would be expected (also see Harland *et al.*, 2017 who demonstrated a reversal of the place code from a non-repetitive global code to a repetitive place code in radially arranged compartments when lateral mammillary nucleus was lesioned). The use of reversible inactivation techniques offers the advantage of within-animals experimental design and one could also utilize other reversible inactivation protocols such as optogenetic or chemogenetic, which are temporally and spatially more precise, to manipulate the inputs. Thus, future experiments involving reversible manipulations of these inputs could lead to a better understanding of the interactions between the local visual directional signal and the global multimodal directional signal. In addition, recordings can be carried out in dentate gyrus and CA3 (see Section 6.1) to determine if visually sensitive place cells could be found in these regions, so as to get a better understanding of where the local and global directional signals get resolved.

As retrosplenial cortex is believed to conjunctively encode local and global spaces, future work can also be directed towards examining the reference frame integrative function of retrosplenial cortex by testing retrosplenial cortex lesioned animals on a behavioural task in the two-compartment context box that is only solvable if the animals use both information in the local compartmental space and information in the global space. For example, one could train rats to recognize which compartment it is in using a constellation of distal cues and local contextual cues, and subsequently scramble these cues in both control and retrosplenial lesioned animals and observe the subsequent behavioural changes. The separate roles of the different sub-regions of retrosplenial cortex and their respective inputs can then also be examined in the same task by either lesioning the different sub-regions of the retrosplenial cortex or inactivating the different inputs into the different retrosplenial sub-regions (e.g. inactivating dorsal subiculum inputs into gRSCb).

In conclusion, this thesis has explored how the cognitive map represents a visually rotated, two-compartment context box. The work presented here is meant to examine the spatial signals underlying navigation in compartmental spaces, complex spaces that humans and animals often have to navigate, in light of the recent findings that retrosplenial cortex

displayed distinct directional signals in a visually rotated, differentially scented two-compartment context box. We have demonstrated that the local visual directional encoding likely arises as a consequence of dysgranular retrosplenial cortex sitting partly outside a thalamo-hippocampo-cortical spatial circuit that granular retrosplenial cortex is a part of. In addition, we showed that there is a global map in dorsal CA1 that is consistent with its interactions with granular retrosplenial cortex. Future work can be directed towards further understanding the functional roles of the inputs into the different retrosplenial sub-regions as well as demonstrating a behavioural correlate of the same spatial signal.

References

Alexander, A.S., Carstensen, L.C., Hinman, J.R., Raudies, F., Chapman, G.W. and Hasselmo, M.E. (2020). Egocentric boundary vector tuning of retrosplenial cortex. *Science Advances*, 6(8): eaaz2322.

Allen, G.V. and Hopkins, D.A. (1989). Mammillary body in the rat: Topography and synaptology of projections from the subicular complex, prefrontal cortex and midbrain tegmentum. *Journal of Comparative Neurology*, 286: 311-336.

Alme, C.B., Miao, C., Jezek, K., Treves, A., Moser, E.I. and Moser, M.B. (2014). Place cells in the hippocampus: Eleven maps for eleven rooms. *Proceedings of the National Academy of Sciences*, 111(52): 18428-18435.

Alvernhe, A., Save, E. and Poucet, B. (2011). Local remapping of place cell firing in the Tolman detour task. *European Journal of Neuroscience*, 33: 1696-1705.

Alvernhe, A., Van Cauter, T., Save, E. and Poucet, B. (2008). Different CA1 and CA3 representations of novel routes in a shortcut situation. *Journal of Neuroscience*, 28(29): 7324-7333.

Andersen, P., Bliss, T.V.P and Skrede, K.K. (1971). Lamellar organization of hippocampal excitatory pathways. *Experimental Brain Research*, 13: 222-238.

Anderson, M.I. and Jeffery, K.J. (2003). Heterogeneous modulation of place cell firing by changes in context. *Journal of Neuroscience*, 23(26): 8827-8835.

Aparicio, M.A. and Saldana, E. (2014). The dorsal tectal longitudinal column (TLCd): A second longitudinal column in the paramedian region of the midbrain tectum. *Brain Structure and Function*, 219(2): 607-630.

Barry, C., Ginzberg, L.L., O'Keefe, J. and Burgess, N. (2012). Grid cell firing patterns signal environmental novelty by expansion. *Proceedings of the National Academy of Sciences*, 109(43): 17687-17692.

Barry, C., Hayman, R., Burgess, N. and Jeffery, K.J. (2007). Experience-dependent rescaling of entorhinal grids. *Nature Neuroscience*, 10(6): 682-684.

Barry, C., Lever., C., Hayman, R., Hartley, T., Burton, S., O'Keefe, J., Jeffery, K. and Burgess, N. (2006). The boundary vector cell model of place cell firing and spatial memory. *Reviews in the Neurosciences*, 17(1-2): 71-97.

Bassett, J.P. and Taube, J.S. (2001). Neural correlates for angular head velocity in the rat dorsal tegmental nucleus. *Journal of Neuroscience*, 21(15): 5740-5751.

Bassett, J.P., Tullman, M.L. and Taube, J.S. (2007). Lesions of the tegmentomammilary circuit in the head direction system disrupt the head direction signal in the anterior thalamus. *Journal of Neuroscience*, 27(28): 7564-7577.

Behrens, T.E.J., Muller, T.H., Whittington, J.C.R., Mark, S., Baram., A.B., Stachenfeld, K.L. and Kurth-Nelson, Z. (2018). What is a cognitive map? Organizing knowledge for flexible bahavior. *Neuron*, 100(2): 490-509.

Bennett, A.T.D (1996). Do animals have cognitive maps? *The Journal of Experimental Biology*, 199: 219-224.

Best, P.J. and Thompson, L.T. (1989). Persistence, reticence, and opportunism of place-field activity in hippocampal neurons. *Psychobiology*, 17(3): 236-246.

Biazoli Jr., C.E., Goto, M., Campos, A.M.P. and Canteras, N.S. (2006). The supragenual nucleus: A putative relay station for ascending vestibular signs to head direction cells. *Brain Research*, 1094: 138-148.

Blair, H.T., Cho, J. and Sharp, P.E. (1998). Role of the lateral mammillary nucleus in the rat head direction circuit: A combined single unit recording and lesion study. *Neuron*, 21: 1387-1397.

Blair, H.T., Cho, J. and Sharp, P.E. (1999). The anterior thalamic head-direction signal is abolished by bilateral but not unilateral lesions of the lateral mammillary nucleus. *Journal of Neuroscience,* 19(15): 6673-6683.

Blair, H.T., Lipscomb, B.W. and Sharp, P.E. (1997). Anticipatory time intervals of head-direction cells in the anterior thalamus of the rat: Implications for path integration in the head direction circuit. *Journal of Neurophysiology*, 78: 145-159.

Blair, H.T. and Sharp, P.E. (1995). Anticipatory head direction signals in anterior thalamus: Evidence for a thalamocortical circuit that integrates angular head motion to compute head direction. *Journal of Neuroscience*, 15(9): 6260-6270.

Bonnevie, T., Dunn, B., Fyhn, M., Hafting, T., Derdikman, D., Kubie, J.L., Roudi, Y., Moser, E.I. and Moser, M.B. (2013). Grid cells require excitatory drive from the hippocampus. *Nature Neuroscience*, 16(3): 309-317.

Brennan, E.K.W., Jedrasiak-Cape, I., Kailasa, S., Rice, S.P., Sudhakar, S.K. and Ahmed, O.J. (2020). Thalamus and claustrum control parallel layer I circuits in retrosplenial cortex. *BioRxiv*: 300863.

Brun, V.H., Leutgeb, S., Wu, H.Q., Schwarcz, R., Witter, M.P., Moser, E.I. and Moser, M.B. (2008). Impaired spatial representation in CA1 after lesion of direct input from entorhinal cortex. *Neuron*, 57: 290-302.

Brun, V.H., Otnæss, M.K., Molden, S., Steffenach, H.A., Witter, M.P., Moser, M.B. and Moser, E.I. (2002). Place cells and place recognition maintained by direct entorhinal-hippocampal circuitry. *Science*, 296(5576): 2243-2246.

Bryne, P., Becker, S. and Burgess, N. (2007). Remembering the past and imagining the future: a neural model of spatial memory and imagery. *Psychological Review,* 114(2): 340-375.

Buffenstein, R., Park, T., Hanes, M. and Artwohl, J.E. (2012). Naked Mole Rat. *The Laboratory Rabbit, Guinea Pig, Hamster, and Other Rodents*: 1055-1074.

Bush, D., Barry, C. and Burgess, N. (2014). What do grid cells contribute to place cell firing? *Trends in Neurosciences*, 37(3): 136-145.

Butler, W.N, and Taube, J.S. (2015). The nucleus prepositus hypoglossi contributes to head direction cell stability in rats. *Journal of Neuroscience*, 35(6): 2547-2558.

Caballero-Bleda, M. and Witter, M.P. (1993). Regional and laminar organization of projections from the presubiculum and parasubiculum to the entorhinal cortex: An anterograde tracing study in the rat. *Journal of Comparative Neurology*, 328: 115-129.

Cain, D.P., Humpartzoomian, R. and Boon, F. (2006). Retrosplenial cortex lesions impair water maze strategies learning or spatial place learning depending on prior experience of the rat. *Behavioural Brain Research*, 170: 316-325.

Calton, J.L., Stackman, R.W., Goodridge, J.P., Archey, W.B., Dudchenko, P.A. and Taube, J.S. (2003). Hippocampal place cell instability after lesions of the head direction cell network. *Journal of Neuroscience*, 23(3): 9719-9731.

Carpenter, F., Manson, D., Jeffery, K., Burgess, N. and Barry, C. (2015). Grid cells form a global representation of connected environment. *Current Biology*, 25: 1176-1182.

Catapano, L.A., Magavi, S.S. and Macklis, J.D. (2008). Neuroanatomical tracing of neuronal projections with Fluoro-Gold. *Methods in Molecular Biology*, 438: 353-359.

Cenquizca, L.A. and Swanson, L.W. (2007). Spatial organization of direct hippocampal field CA1 axonal projections to the rest of the cerebral cortex. *Brain Research Reviews*, 56: 1-26.

Chen, L.L., Lin, L.H., Green, E.J., Barnes, C.A. and McNaughton, B.L. (1994). Head-direction cells in the rat posterior cortex. I. anatomical distribution and behavioural modulation. *Experimental Brain Research*, 101: 8-23.

Cheng, Ken. (1986). A purely geometric module in the rat's spatial representation. *Cognition*, 23: 149-178.

Cho, J. and Sharp, P.E. (2001). Head direction, place, and movement correlates for cells in the rat retrosplenial cortex. *Behavioral Neuroscience*, 115(1): 3-25.

Clark, B.J., Bassett, J.P., Wang, S.S. and Taube, J.S. (2010). Impaired head direction cell representation in the anterodorsal thalamus after lesions of the retrosplenial cortex. *Journal of Neuroscience*, 30(15): 5289-5302.

Clark, B.J., Brown, J.E. and Taube, J.S. (2012). Head direction cell activity in the anterodorsal thalamus requires intact supragenual nuclei. *Journal of Neurophysiology*, 108: 2767-2784.

Clark, B.J., Harris, M.J. and Taube, J.S. (2010). Control of anterodorsal thalamic head direction cells by environmental boundaries: comparison with conflicting distal landmarks. *Hippocampus*, 22(2): 172-187.

Clark, B.J., Sarma, A. and Taube, J.S. (2009). Head direction cell instability in the anterior dorsal thalamus after lesions of the interpeduncular nucleus. *Journal of Neuroscience*, 29(2): 493-507.

Clark, B.J. and Taube, J.S. (2011). Intact landmark control and angular path integration by head direction cells in the anterodorsal thalamus after lesions of the medial entorhinal cortex. *Hippocampus*, 21(7): 767-782.

Conte, W.L., Kamishina, H. and Reep, R.L. (2009). The efficacy of the fluorescent conjugates of cholera toxin subunit B for multiple retrograde tract tracing in the central nervous system. *Brain Structure and Function*, 213(4): 367-373.

Contestabile, A. and Flumerfelt, B.A. (1981). Afferent connections of the interpeduncular nucleus and the topographic organization of the habenulo-interpeduncular pathway: An HRP study in the rat. *Journal of Comparative Neurology*, 196: 253-270.

Coogan, T.A. and Burkhalter, A. (1993). Hierarchical organization of areas in rat visual cortex. *Journal of Neuroscience*, 13(9): 3749-3772.

Cooper, B.G. and Mizumori, S.J.Y. (1999). Retrosplenial cortex inactivation selectively impairs navigation in darkness. *NeuroReport*, 10: 625-630.

Cooper, B.G. and Mizumori, S.J.Y. (2001). Temporary inactivation of the retrosplenial cortex causes a transient reorganization of spatial coding in the hippocampus. *Journal of Neuroscience*, 21(11): 3986-4001.

Derdikman, D., Whitlock, J.R., Tsao, A., Fyhn, M., Hafting, T., Moser, M.B. and Moser, E.I. (2009). Fragmentation of grid cell maps in a multicompartment environment. *Nature Neuroscience*, 12(10): 1325-1332.

Deshmukh, S.S. and Knierim, J.J. (2011). Representation of non-spatial and spatial information in the lateral entorhinal cortex. *Frontiers in Behavioural Neuroscience*, 5: 69.

Dombeck, D.A., Harvey, C.D., Tian, L., Looger, L.L. and Tank, D.W. (2010). Functional imaging of hippocampal place cells at cellular resolution during virtual navigation. *Nature Neuroscience*, 13(11): 1433-1440.

Dudchenko, P.A. and Zinyuk, L.E. (2005). The formation of cognitive maps of adjacent environments: Evidence from the head direction cell system. *Behavioral Neuroscience*, 119(6): 1511-1523.

Duvelle, É, Grieves, R.M., Hok, V., Poucet, B., Arleo, A., Jeffery, K.J. and Save, E. (2019). Insensitivity of place cells to the value of spatial goals in a two-choice flexible navigation task. *Journal of Neuroscience*, 39(13): 2522-2541.

Eichenbaum, H., Wiener, S.I., Shapiro, M.L. and Cohen, N.J. (1989). The organization of spatial coding in the hippocampus: a study of neural ensemble activity. *Journal of Neuroscience*, 9(8), 2764-2775.

Elduayen, C. and Save, E. (2014). The retrosplenial cortex is necessary for path integration in the dark. *Behavioural Brain Research*, 272: 303-307.

Ettienne, A.S. and Jeffery, K.J. (2004). Path integration in mammals. *Hippocampus*, 14: 180-192.

Fenton, A.A., Csizmadia, G. and Muller, R.U. (2000). Conjoint control of hippocampal place cell firing by two visual stimuli I. The effects of moving the stimuli on firing field positions. *Journal of General Physiology*, 116(2): 191-210.

Fenton, A.A., Kao, H.Y., Neymotin, S.A., Olypher, A., Vayntrub, Y., Lytton, W.W. and Ludvig, N. (2008). Unmasking the CA1 ensemble place code by exposures to small and large environment: more place cells and multiple, irregularly arranged, and expanded place fields in the large space. *Journal of Neuroscience*, 28(44): 11250-11262.

Fischer, L.F., Soto-Albors, R.M., Buck, F. and Harnett, M.T. (2020). Representation of visual landmarks in retrosplenial cortex. *eLife*, 9: e51458.

Fox, S.E. and Ranck Jr, J.B. (1975). Localization and anatomical identification of theta and complex spike cells in dorsal hippocampal formation of rats. *Experimental Neurology*, 49: 299-313.

Fuhs, M.C., VanRhoads, S.R., Casale, A.E., McNaughton, B. and Touretzky, D.S. (2005). Influence of path integration versus environmental orientation on place cell remapping between visually identical environment. *Journal of Neurophysiology*, 94: 2603-2616.

Fyhn, M., Hafting, T., Treves, A., Moser, M.B. and Moser, E.I. (2007). Hippocampal remapping and grid realignment in entorhinal cortex. *Nature*, 446(7132): 190-194.

Fyhn, M., Molden, S., Witter, M.P., Moser, E.I. and Moser, M.B. (2004). Spatial representation in the entorhinal cortex. *Science*, 305 (5688): 1258-1264.

Gallistel, C.R. (1990). The organization of learning. *MIT Press, Cambridge, MA*.

Gentry, G., Brown, W.L. and Kaplan, S.J. (1947). An experimental analysis of the spatial location hypothesis in learning. *Journal of Comparative and Physiological Psychology*, 40(5): 309-322.

Gil, M., Ancau, M., Schlesiger, M.I., Neitz, A., Allen, K., De Marco, R.J. and Monyer, H. (2018). Impaired path integration in mice with disrupted grid cell firing. *Nature Neuroscience*, 21: 81-91.

Giocomo, L.M., Stensola, T., Bonnevie, T., Van Cauter, T., Moser, M.B. and Moser, E.I. Topography of head direction cells in medial entorhinal cortex. *Current Biology*, 24: 252-262.

Golob, E.J. and Taube, J.S. (1997). Head direction cells and episodic spatial information in rats without a hippocampus. *Proceedings of the National Academy of Sciences*, 94: 7645-7650.

Golob, E.J. and Taube, J.S. (1999). Head direction cells in rats with hippocampal or overlying neocortical lesions: Evidence for impaired angular path integration. *Journal of Neuroscience*, 19(16): 7198-7211.

Golob, E.J., Wolk, D.A. and Taube, J.S. (1998). Recordings of postsubiculum head direction cells following lesions of the laterodorsal thalamic nucleus. *Brain Research*, 780: 9-19.

Goodridge, J.P., Dudchenko, P.A., Worboys, K.A., Golob, E.J. and Taube, J.S. (1998). Cue control and head direction cells. *Behavioral Neuroscience*, 112(4): 749-761.

Goodridge, J.P. and Taube, J.S. (1995). Preferential use of the landmark navigational system by head direction cells in rats. *Behavioral Neuroscience*, 109(1): 49-61.

Goodridge, J.P. and Taube, J.S. (1997). Interaction between the postsubiculum and anterior thalamus in the generation of head direction cell activity. *Journal of Neuroscience*, 17(23): 9315-9330.

Goodridge, J.P. and Touretzky, D.S. (2000). Modeling attractor deformation in the rodent head direction system. *Journal of Neurophysiology*, 83(6): 3402-3410.

Grieves, R.M. and Dudchenko, P.A. (2013). Cognitive maps and spatial inference in animals: Rats fail to take a novel shortcut, but can take a previously experienced one. *Learning and Motivation*, 44: 81-92.

Grieves, R.M., Duvelle, É. And Dudchenko, P.A. (2018). A boundary vector cell model of place field repetition. *Spatial Cognition and Computation*, 18(3): 217-256.

Grieves, R.M., Duvelle, É., Wood, E.R. and Dudchenko, P.A. (2017). Field repetition and local mapping in the hippocampus and the medial entorhinal cortex. *Journal of Neurophysiology*, 118: 2378-2388.

Grieves, R.M. and Jeffery, K.J. (2017). The representation of space in the brain. *Behavioural Processes*, 135: 113-131.

Grieves, R.M., Jedidi-Ayoub, S., Mishchanchuk, K., Liu, A., Renaudineau, S. and Jeffery, K.J. (2020). The place-cell representation of volumetric space. *Nature Communication*, 11: 789.

Grieves, R.M., Jenkins, B.W., Harland, B.C., Wood, E.R. and Dudchenko, P.A. (2016). Place field repetition and spatial learning in a multicompartment environment. *Hippocampus*, 26: 118-134.

Hafting, T., Fyhn, M., Molden, S., Moser, M.B. and Moser, E.I. (2005). Microstructure of a spatial map in the entorhinal cortex. *Nature*, 436(7052): 801-806.

Hales, J.B., Schlesiger, M.I., Leutgeb, J.K., Squire, L.R., Leutgeb, S. and Clark, R.E. (2014). Medial entorhinal cortex lesions only partially disrupt hippocampal place cells and hippocampus-dependent place memory. *Cell Reports*, 9: 893-901.

Hampson, R.E., Simeral, J.D. and Deadwyler, S.A. (1999). Distribution of spatial and nonspatial information in dorsal hippocampus. *Nature*, 402: 610-614.

Hargreaves, E.L., Rao, G., Lee, I. and Knierim, J.J. (2005). Major dissociation between medial and lateral entorhinal input to dorsal hippocampus. *Science*, 308(5729): 1792-1794.

Harker, K.T. and Whishaw, I.Q. (2004). Impaired place navigation in place and matching-to-place swimming pool tasks follows both retrosplenial cortex lesions and cingulum bundle lesions in rats. *Hippocampus*, 14: 224-231.

Harland, B., Grieves, R.M., Bett, D., Stentiford, R., Wood, E.R. and Dudchenko, P.A. (2017). Lesions of the head direction cell system increase hippocampal place field repetition. *Current Biology*, 27: 2706-2712.

Harris, K.D., Henze, D.A., Csicsvari, J., Hirase, H. and Buzsáki, G. (2000). Accuracy of tetrode spike separation as determined by simultaneous intracellular and extracellular measurements. *Journal of Neurophysiology*, 84(1): 401-414.

Hayakawa, T. and Zyo, K. (1990). Fine structure of the lateral mammillary projection to the dorsal tegmental nucleus of Gudden in the rat. *Journal of Comparative Neurology*, 298: 224-236.

Hayman, R.M.A., Chakraborty, S., Anderson, M.I. and Jeffery, K.J. (2003). Context-specific acquisition of location discrimination by hippocampal place cells. European Journal of Neuroscience, 18: 2825-2834.

Hayman, R.M. and Jeffery, K.J. (2008). How heterogeneous place cell responding arises from homogenous grids – a contextual gating hypothesis. Hippocampus, 18:1301-1313.

Hetherington, P.A. and Shapiro, M.L. (1997). Hippocampal place fields are altered by the removal of single visual cues in a distance-dependent manner. *Behavioral Neuroscience*, 111(1): 20-34.

Hill, A.J. and Best, P.J. (1981). Effects of deafness and blindless on the spatial correlates of hippocampal unit activity in the rat. Experimental Neurology, 74, 204-217.

Hindley, E.L., Nelson, A.J.D., Aggleton, J.P. and Vann, S.D. (2014). The rat retrosplenial cortex is required when visual cues are used flexibly to determine location. *Behavioural Brain Research*, 263: 98-107.

Hinman, J.R., Chapman, G.W. and Hasselmo, M.E. (2019). Neuronal representation of environmental boundaries in egocentric coordinates. *Nature communication*, 10: 2772.

Huang, L.W., Simonnet, J., Nassar, M., Richevaux, L., Lofredi, R. and Fricker, D. (2017). Laminar localization and projection-specific properties of presubicular neurons targeting the lateral mammillary nucleus, thalamus, or medial entorhinal cortex. eNeuro, 4(2): e0370-16.2017.

Iwasaki, H., Kani, K. and Maeda, T. (1999). Neural connections of the pontine reticular formation, which connects reciprocally with the nucleus prepositus hypoglossi in the rat. *Neuroscience*, 93(1): 195-208.

Jacob, P.V., Casali, G., Spieser, L., Page, H., Overington, D. and Jeffery, K.J. (2017). An independent, landmark-dominated head direction signal in dysgranular retrosplenial cortex. *Nature Neuroscience*, 20(2): 173-175.

Jayakumar, R.P., Madhav, M.S., Savelli, F., Blair, H.T., Cowan, N.J. and Knierim, J.J. (2019). Recalibration of path integration in hippocampal place cells. *Nature*, 566(7745): 533-537.

Jeffery, K.J. (2007). Integration of the sensory inputs to place cells: What, where, why, and how? *Hippocampus*, 17: 775-785.

Jeffery, K.J. (2011). Place cells, grid cells, attractors, and remapping. *Neural Plasticity*, 2011: 182602.

Jeffery, K.J., Donnett, J.G., Burgess, N. and O'Keefe, J.M. (1997). Directional control of hippocampal place fields. *Experimental Brain Research*, 117: 131-142.

Jeffery, K.J., Grieves, R.M. and Donnett, J. (2018). Recording the spatial mapping cells: Place, head direction, and grid cells. *Handbook of Behavioral Neuroscience*, 28(Chapter 5): 95-121.

Jeffery, K.J. and O'Keefe, J.M. (1999). Learned interaction of visual and idiothetic cues in the control of place field orientation. *Experimental Brain Research*, 127: 151-161.

Jinno, S., Klausberger, T., Marton, L.F., Dalezios, Y., Roberts, J.D.B., Fuentealba, P., Bushong, E.A., Henze, D., Buzsáki, G. and Somoygyi, P. (2007). Neuronal diversity in GABAergic long-range projections from the hippocampus. *Journal of Neuroscience*, 27(33): 8790 -8804.

Jovalekic, A., Hayman, R., Becares, N., Reid, H., Thomas, G., Wilson, J. and Jeffery, K. (2011). Horizontal biases in rats' use of three-dimensional space, *Behavioural Brain Research*, 222: 279-288.

Julian, J.B., Keinath, A.T., Marchette, S.A. and Epstein, R.A. (2018). The neurocognitive basis of spatial reorientation. *Current Biology*, 28: R1059-R1073.

Julian, J.B., Keinath, A.T., Muzzio, I.A. and Epstein, R.A. (2015). Place recognition and heading retrieval are mediated by dissociable cognitive systems in mice. *Proceedings of the National Academy of Sciences*, 112(20): 6503-6508.

Jung, M.W. and McNaughton, B.L. (1993). Spatial selectivity of unit activity in the hippocampal granular layer. *Hippocampus*, 3(2): 165-182.

Jung, M.W., Wiener, S.I. and McNaughton, B.L. (1994). Comparison of spatial firing characteristics of units in dorsal and ventral hippocampus of the rat. *Journal of Neuroscience*, 14(12): 7347-7356.

Juszczak, G.R. and Miller, M. (2016). Detour behaviour of mice trained with transparent, semitransparent and opaque barriers. *PloS One*, 11(9): e0162018.

Kadir, S.N., Goodman, D.F.M. and Harris, K.D. (2014). High-dimensional cluster analysis with the masked EM algorithm. *Neural Computation*, 26(11): 2379-2394.

Keene, C.S. and Bucci, D.J. (2009). Damage to the retrosplenial cortex produces specific impairments in spatial working memory. *Neurobiology of Learning and Memory*, 91: 408-414.

Keinath, A.T., Julian, J.B., Epstein, R. and Muzzio, I.A. (2017). Environmental geometry aligns the hippocampal map during spatial reorientation. *Current Biology*, 27: 309-317.

Khan, S. and Chang, R. (2013). Anatomy of the vestibular system: A review. *NeuroRehabilitation*, 2013: 437-443.

Kinsky, N.R., Sullivan, D.W., Mau, W., Hasselmo, M.E. and Eichenbaum, H.B. (2018). Hippocampal place fields maintain a coherent and flexible map across long timescales. *Current Biology*, 28: 3578-3588.

Kjelstrup, K.B., Solstad, T., Brun, V.H., Hafting, T., Leutgeb, S., Witter, M.P., Moser, E.I. and Moser, M.B. (2008). Finite scale of spatial representation in the hippocampus. *Science*, 321(5885): 140-143.

Knierim, J.J. (2002). Dynamic interactions between local surface cues, distal landmarks, and intrinsic circuitry in hippocampal place cells. *Journal of Neuroscience*, 22(14): 6254-6264.

Knierim, J.J. (2015). The hippocampus. *Current Biology*, 25(23): R1116-R1121.

Knierim, J.J., Kudrimoti, H.S. and McNaughton, B.L. (1995). Place cells, head direction cells, and the learning of landmark stability. *Journal of Neuroscience*, 15(3): 1648-1659.

Knierim, J.J., Neunuebel, J.P. and Deshmukh, S.S. (2014). Functional correlates of the lateral and medial entorhinal cortex: Objects, path integration and local-global reference frames. *Philosophical Transactions of the Royal Society of London. Series B, Biological Sciences*, 369: 20130369.

Knierim, J.J. and Zhang, K. (2012). Attractor dynamics of spatially correlated neural activity in the limbic system. *Annual Review of Neuroscience*, 35: 267-285.

Knight, R., Hayman, R., Ginzberg, L.L. and Jeffery, K. (2011). Geometric cues influence head direction cells only weakly in nondisoriented rats. *Journal of Neuroscience*, 31(44): 15681-15692.

Kononenko, N.L. and Witter, M.P. (2012). Presubiculum layer III conveys retrosplenial input to the medial entorhinal cortex. *Hippocampus*, 22: 881-895.

Kornienko, O., Latuske, P., Bassler, M., Kohler, L. and Allen, K. (2018). Non-rhythmic head-direction cells in the parahippocampal region are not constrained by attractor network dynamics. *eLife*, 7: e35949.

Kuruvilla, M.V. and Ainge, J.A. (2017). Lateral entorhinal cortex lesions impair local spatial frameworks. *Frontiers in System Neuroscience*, 11: 30.

LaChance, P.A., Todd, T.P. and Taube, J.S. (2019). A sense of space in postrhinal cortex. *Science*, 365(6449): eaax4192.

Lanciego, J.L. and Wouterlood, F.G. (2020). Neuroanatomical tract-tracing techniques that did go viral. *Brain Structure and Function*, 225: 1193-1224.

Lee, D., Lin, B.J. and Lee, A.K. (2012). Hippocampal place fields emerge upon single-cell manipulation of excitability during behavior. *Science*, 337 (6096): 849-853.

Lee, I., Yoganarashimha, D., Rao, G. and Knierim, J.J. (2004). Comparison of population coherenece of place cells in hippocampal subfields CA1 and CA3. *Nature*, 430: 456-459.

Lee, J.W., Kim, W.R., Sun, W. and Jung, M.W. (2012). Disruption of dentate gyrus blocks effect of visual input on spatial firing of CA1 neurons. *Journal of Neuroscience*, 32(38): 12999-13003.

Leutgeb, J.K., Leutgeb, S., Moser, M.B. and Moser, E.I. (2007). Pattern separation in the dentate gyrus and CA3 of the hippocampus. *Science*, 315(5814): 961-966.

Leutgeb, J.K., Leutgeb, S., Treves, A., Meyer, R., Barnes, C.A., McNaughton, B.L., Moser, M.B. and Moser, E.I. (2005). Progressive transformation of hippocampal neuronal representations in “morphed” environments. *Neuron*, 48(2): 345-358.

Leutgeb, S., Leutgeb, J.K., Barnes, C.A., Moser, E.I., McNaughton, B.L. and Moser, M.B. (2005). Independent codes for spatial and episodic memory in hippocampal neuronal ensembles. *Science*, 309 (5734): 619-623.

Leutgeb, S., Leutgeb, J.K., Treves, A., Moser, M.B. and Moser, E.I. (2004). Distinct ensemble codes in hippocampal areas CA3 and CA1. *Science*, 305(5688): 1295-1298.

Lever, C., Burton, S., Jeewajee, A., O’Keefe, J. and Burgess, N. (2009). Boundary vector cells in the subiculum of the hippocampal formation. *Journal of Neuroscience,* 29(31): 9771-9777.

Li, T., Arleo, A. and Sheynikhovich, D. (2020). Modeling place cells and grid cells in multi-compartment environments: Entorhinal-hippocampal loop as a multisensory integration circuit. *Neural Networks*, 121: 37-51.

Li, X.G., Somogyi, P., Ylinen, A. and Buzsaki, G. (1994). The hippocampal CA3 network: An in vivo intracellular labelling study. *Journal of Comparative Neurology*, 339: 181-208.

Ling, C., Hendrickson, M.L. and Kalil, R.E. (2012). Resolving the detailed structure of cortical and thalamic neurons in the adult rat brain with refined biotinylated dextran amine labelling. *PLoS One*, 7(11): se45886

Liu, R., Chang, L. and Wickern, G. (1984). The dorsal tegmental nucleus: An axoplasmic transport study. *Brain Research*, 310: 123-132.

Lozano, Y.R., Page, H., Jacob, P.Y., Lomi, E., Street, J. and Jeffery, K. (2017). Retrosplenial and postsubicular head direction cells compared during visual landmark discrimination. Brain and Neuroscience Advances, 1: 1-17.

Lucas, J., Calef, B. and Knox, K. (2013). Image enhancement for astronomical scenes. *Proceedings of SPIE – The International Society for Optical Engineering*, 8856: 885603.

Malinowska, M., Niewiadomska, M. and Wesierka, M. (2016). Spatial memory formation differentially affects c-Fos expression in retrosplenial areas during place avoidance training in rats. *Acta Neurobiologiae Experimentalis*, 76(3): 244-265.

Mamad, O., Stumpp, L., McNamara, H.M., Ramakrishnan, C., Deisseroth, K., Reilly, R.B. and Tsanov, M. (2017). Place field assembly distribution encodes preferred locations. *PloS Biology*, 15(9): e2202365.

Mankin, E.A., Diehl, G.W., Sparks, F.T., Leutgeb, S. and Leutgeb, J.K. (2015). Hippocampal CA2 activity patterns change over time to a larger extent between spatial contexts. *Neuron*, 85(1): 190-201.

Marchette, S.A., Vass, L.K., Ryan, J. and Epstein, R.A. (2014). Anchoring the neural compass: Coding of local spatial reference frames in human media parietal lobe. *Nature Neuroscience*, 17(11): 1598-1606.

Marozzi, E., Ginzberg, L.L., Alenda, A. and Jeffery, K.J. (2015). Purely translational realignment in grid cell firing patterns following nonmetric context change. *Cerebral Cortex*, 25: 4619-4627.

Marozzi, E. and Jeffery, K.J. (2012). Place, space and memory cells. *Current Biology*, 22(22): R939-R942.

McKenzie, S., Huszar, R., English, D.F., Kim, K., Yoon, E. and Buzsáki, G. (2019). Preexisting hippocampal network dynamics constrain optogenetically induced place fields. *BioRxiv*: 803577.

McNaughton, B.L., Barnes, C.A., Meltzer, J. and Sutherland, R.J. (1989). Hippocampal granule cells are necessary for normal spatial learning but not for spatially-selective pyramidal cell discharge. *Experimental Brain Research*, 76: 485-496.

McNaughton, B.L., Battaglia, F.P., Jensen, O., Moser, E.I. and Moser, M.B. (2006). Path integration and the neural basis of the 'cognitive map'. *Nature reviews. Neuroscience.* 7(8): 663-678.

Miao, C., Cao, Q., Ito, H.T., Yamahachi, H., Witter, M.P., Moser, M.B. and Moser, E.I. (2015). Hippocampal remapping after partial inactivation of the medial entorhinal cortex. *Neuron*, 88: 590-603.

Miller, A.M.P., Vedder, L.C., Law, L.M. and Smith, D.M. (2014). Cues, context, and long-term memory: the role of the retrosplenial cortex in spatial cognition. *Frontiers in Human Neuroscience*, 8: 586.

Miller, V.M. and Best, P.J. (1980). Spatial correlates of hippocampal unit activity are altered by lesions of the fornix and entorhinal cortex. *Brain Research*, 194: 311-323.

Mitchell, A.S., Czajkowski, R., Zhang, N., Jeffery, K. and Nelson, A.J.D. (2018). Retrosplenial cortex and its role in spatial cognition. *Brain and Neuroscience Advances*, 2: 1-13.

Mittelstaedt, M.L. and Mittelstaedt, H. (1980). Homing by path integration in a mammal. *Naturwissenschaften*, 67: 566-567.

Miyashita, T. and Rockland, K.S. (2007). GABAergic projections from the hippocampus to the retrosplenial cortex in the rat. *European Journal of Neuroscience*, 26: 1193-1204.

Mizumori, S.J.Y. and Williams, J.D. (1993). Directionally selective mnemonic properties of neurons in the lateral dorsal nucleus of the thalamus of rats. *Journal of Neuroscience,* 13(9): 4015-4028.

Moser, E.I. (2011). The multi-laned hippocampus. *Nature Neuroscience*, 14(4): 407-408.

Moser, E.I., Roudi, Y., Witter, M.P., Kentros, C., Bonhoeffer, T. and Moser, M.B. (2014). Grid cells and cortical representation. *Nature Reviews. Neuroscience.* 15: 466-481.

Muir, G.M. and Taub, J.S. (2004). Head direction cell activity and behavior in a navigation task requiring a cognitive mapping strategy. *Behavioural Brain Research*, 153: 249-253.

Muller, R.U. and Kubie, J.L. (1987). The effects of changes in the environment on the spatial firing of hippocampal complex-spikes cells. *Journal of Neuroscience*, 7(7): 1951-1968.

Muller, R.U., Kubie, J.L. and Ranck Jr, J.B. (1987). Spatial firing patterns of hippocampal complex-spike cells in a fixed environment. *Journal of Neuroscience*, 7(7): 1935-1950.

Murakami, T., Yoshida, T., Matsui, T. and Ohki, K. (2015). Wide-field Ca^{2+} imaging reveals visually evoked activity in the retrosplenial area. *Frontier in Molecular Neuroscience*, 8: 20.

Nakamura, N.H., Fukunaga, M., Akama, K.T., Soga, T., Ogawa, S. and Pavlides, C. (2010). Hippocampal cells encode places by forming small anatomical clusters. *Neuroscience*, 166: 994-1007.

Navawongse, R. and Eichenbaum, H. (2013). Distinct pathways for rule-based retrieval and spatial mapping of memory representations in hippocampal neurons. *Journal of Neuroscience*, 33(3): 1002-1013.

Nelson, A.B. and Kreitzer, A.C. (2014). Reassessing models of basal ganglia function and dysfunction. *Annual Review of Neuroscience*, 37: 117-135.

Neunuebel, J.P., Yoganarasimha, D., Rao, G. and Knierim, J.J. (2013). Conflicts between local and global spatial frameworks dissociate neural representations of the lateral and medial entorhinal cortex. *Journal of Neuroscience*, 33(22): 9246-9258.

O'Keefe, J. (1976). Place units in the hippocampus of the freely moving rat. *Experimental Neurology*, 51: 78-109.

O'Keefe, J. and Burgess, N. (1996). Geometric determinants of the place fields of hippocampal neurons. *Nature*, 381(6581): 425-428.

O'Keefe, J., Burgess, N., Donnett, J.G., Jeffery, K.J. and Maguire, E.A. (1998). Place cells, navigational accuracy, and the human hippocampus. *Philosophical Transactions of the Royal Society of London. Series B, Biological Sciences*, 353(1373): 1333-1340.

O'Keefe, J. and Conway, D.H. Hippocampal place units in the freely moving rat: Why they fire where they fire. *Experimental Brain Research*, 31: 573-590.

O'Keefe, J. and Dostrovsky, J. (1971). The hippocampus as a spatial map. Preliminary evidence from unit activity in the freely-moving rat. *Brain Research*, 34(1): 171-175.

O'Keefe, J. and Nadel, L. (1978). The hippocampus as a cognitive map. *Oxford Unversity Press*.

O'Keefe, J. and Speakman, A. (1987). Single unit activity in the rat hippocampus during a spatial memory task. *Experimental Brain Research*, 68(1): 1-27.

O'Mara, S. (2005). The subiculum: what it does, what it might do, and what neuroanatomy has yet to tell us. *Journal of Anatomy*, 207: 271-282.

Ormond, J. and McNaughton, B.L. (2015). Place field expansion after focal MEC inactivations is consistent with loss of Fourier components and path integrator gain reduction. *Proceedings of the National Academy of Sciences*, 112(13): 4116-4121.

Page, H.J.I. and Jeffery, K.J. (2018). Landmark-based updating of the head direction system by retrosplenial cortex: A computational model. *Frontiers in Cellular Neuroscience*, 12: 191.

Park, E., Dvorak, D. and Fenton, A.A. (2011). Ensemble place codes in hippocampus: CA1, CA3, and dentate gyrus place cells have multiple place fields in large environments. *PloS One*, 6(7): e22349.

Parron, C. and Save, E. (2004). Comparison of the effects of entorhinal and retrosplenial cortical lesions on habituation, reaction to spatial and non-spatial changes during object exploration in the rat. *Neurobiology of Learning and Memory*, 82: 1-11.

Paxinos, G. and Watson, C. (2007). The rat brain in stereotaxic coordinates: 6th edition. *Amsterdam; Boston: Academic Press/Elsevier*.

Petrulis, A., Alvarez, P. and Eichenbaum, H. (2005). Neural correlates of social odor recognition and the representation of individual distinctive social odors within entorhinal cortex and ventral subiculum. *Neuroscience*, 130: 259-274,

Plitt, M.H. and Giocomo, L.M. (2019). Experience dependent contextual codes in the hippocampus. *bioRvix*: 864090.

Pothuizen, H.H.J., Aggleton, J.P. and Vann, S.D. (2008). Do rats with retrosplenial cortex lesions lack direction? *European Journal of Neuroscience*, 28: 2486-2498.

Pothuizen, H.H.J., Davies, M., Albasser, M.M., Aggleton, J.P. and Vann, S.D. (2009). Granular and dysgranular retrosplenial cortices provide qualitatively different contributions to spatial working memory: Evidence from immediate-early gene imaging in rats. *European Journal of Neuroscience*, 30: 877-888.

Pothuizen, H.H.J., Davies, M., Aggleton, J.P. and Vann, S.D. (2010). Effects of selective granular retrosplenial cortex lesions on spatial working memory in rats. *Behavioural Brain Research*, 208: 566-575.

Poucet, B. (1993). Spatial cognitive maps in animals: New hypotheses on their structure and neural mechanisms. *Psychological Review*, 100(2): 163-182.

Powell, A., Connelly, W.M., Vasalauskaite, A., Nelson, A.J.D., Vann, S.D., Aggleton, J.P., Sengpiel, F. and Ranson, A. (2020). Stable encoding of visual cues in the mouse retrosplenial cortex. *Cerebral Cortex*, 30: 4424-4437.

Preston-Ferrer, P., Coletta, S., Frey, M. and Burgalossi. (2016). Anatomical organization of presubicular head-direction circuits. *eLife*, 5: e14592.

Prusky, G.T., Harker, K.T., Douglas, R.M. and Whishaw, I.Q. (2002). Variation in visual acuity within pigmented, and between pigmented and albino rat strains. *Behavioural Brain Research*, 136: 339-348.

Quirk, G.J., Muller, R.U. and Kubie, J.L. (1990). The firing of hippocampal place cells in the dark depends on the rat's recent experience. *Journal of Neuroscience*, 10(6): 2008-2017.

Redish, A.D., Battaglia, F.P., Chawla, M.K., Ekstrom, A.D., Gerrard, J.L., Lipa, P., Rosenzweig, E.S., Worley, P.F., Guzowski, J.F., McNaughton, B.L. and Barnes, C.A. (2001). Independence of firing correlates of anatomically proximate hippocampal pyramidal cells. *Journal of Neuroscience*, 21: RC134(1-6).

Redish, A.D., Elga, A.N. and Touretzky, D.S. (1996). A coupled attractor model of the rodent head direction system. *Network*: *Computation in Neural Systems*, 7: 671-685.

Renaudineau, S., Poucet, B. and Save, E. (2007). Flexible use of proximal objects and distal cues by hippocampal place cells. *Hippocampus*, 17: 381-395.

Rich, P.D., Liaw, H.P. and Lee, A.K. (2014). Large environments reveal the statistical structure governing hippocampal representations. *Science*, 345(6198): 814-817.

Roberts, W.A., Cruz, C. and Tremblay, J. (2007). Rats take correct novel routes and shortcuts in an enclosed maze. *Journal of Experimental Psychology: Animal Behavior Processes*, 33(2): 79-91.

Roy, D.S., Kitamura, T., Okuyama, T., Ogawa, S.K., Sun, C., Obata, Y., Yoshiki, A. and Tonegawa, S. (2017). Distinct neural circuits for the formation and retrieval of episodic memories. *Cell*, 170: 1000-1012

Rueckemann, J.W., DiMauro, A.J., Rangel, L.M., Han, X., Boyden, E.S. and Eichenbaum, H. (2016). Transient optogenetic inactivation of the medial entorhinal cortex biases the active population of hippocampal neurons. *Hippocampus*, 26: 246-260.

Russell, N.A., Horii, A., Smith, P.F., Darlington, C.L. and Bilkey, D.K. (2003). Long-term effects of permanent vestibular lesions on hippocampal spatial firing. *Journal of Neuroscience*, 23(16): 6490-6498.

Saleeba, C., Dempsey, B., Le, S., Goodchild, A. and McMullan, S. (2019). A student's guide to neural circuit tracing. *Frontiers in Neuroscience*, 13: 897.

Sargolini, F., Fyhn, M., Hafting, T., McNaughton, B.L., Witter, M.P., Moser, M.B. and Moser, E.I. (2006). Conjunctive representation of position, direction, and velocity in the entorhinal cortex. *Science*, 312(5774): 758-762.

Save, E., Cressant, A., Thinus-Blanc, C. and Poucet, B. (1998). Spatial firing of hippocampal place cells in blind rats. *Journal of Neuroscience*, 18(5): 1818-1826.

Scaplen, K.M., Gulati, A.A., Heimer-McGinn, V.L. and Burwell, R.D. (2014). Objects and landmarks: Hippocampal place cells respond differently to manipulations of visual cues depending on size, perspective, and experience. *Hippocampus*, 24: 1287-1299.

Scharfman, H.E. (1994). EPSPs of dentate gyrus granule cells during epileptiform bursts of dentate hilar "mossy" cells and area CA3 pyramidal cells in disinhibited rat hippocampal slices. *Journal of Neuroscience*, 14(10): 6041-6057.

Schofield, B.R., Schofield, R.M., Sorensen, K.A. and Motts, S.D. (2007). On the use of retrograde tracers for identification of axon collaterals with multiple fluorescent retrograde tracers. *Neuroscience*, 146: 773-783.

Scoville, W.B. and Milner, B. (1957). Loss of recent memory after bilateral hippocampal lesions. *Journal of Neurology, Neurosurgery, and Psychiatry*, 20: 11-21.

Seelig, J.D. and Jayaraman, V. (2015). Neural dynamics for landmark orientation and angular path integration. *Nature*, 521(7551): 186-191.

Shapiro, M.L., Tanila, H. and Eichenbaum, H. (1997). Cues that hippocampal place cells encode: Dynamic and hierarchical representation of local and distal stimuli. *Hippocampus*, 7: 624-642.

Sharp, P.E. and Koester, K. (2008). Lesions of the mammillary body region severely disrupt cortical head direction, but not place cell signal. *Hippocampus*, 18: 766-784.

Sharp, P.E., Tinkelman, A. and Cho, J. (2001). Angular velocity and head direction signals recorded from the dorsal tegmental nucleus of gudden in the rat: Implications for path integration in the head direction cell circuit. *Behavioural Neuroscience*, 115(3): 571-588.

Sheintuch, L., Geva, N., BBaumer, H., Rechavi, Y., Rubin, A. and Ziv, Y. (2020). Multiple maps of the same spatial context can stably coexist in the mouse hippocampus. *Current Biology*, 30: 1467-1476.

Shibata, H. (1989). Descending projections to the mammillary nuclei in the rat, as studied by retrograde and anterograde transport of agglutinin-horseradish peroxidase. *Journal of Comparative Neurology*, 285: 436-452.

Shibata, H. (1992). Topographic organization of subcortical projections to the anterior thalamic nuclei in the rat. *Journal of Comparative Neurology*, 323: 117-127.

Shinder, M.E. and Taube, J.S. (2011). Active and passive movement are encoded equally by head direction cells in the anterodorsal thalamus. *Journal of Neurophysiology*, 106: 788-800.

Sik, A., Penttonen, M., Ylinen, A. and Buzsaki, G. (1995). Hippocampal CA1 interneurons: An *in vivo* intracellular labelling study. *Journal of Neuroscience*, 15(1): 6651-6665.

Sik, A., Ylinen, A., Penttonen, M. and Buzsaki, G. (1994). Inhibitory CA1-CA3-hilar region feedback in the hippocampus. *Science*, 265(5179): 1722-1724.

Singer, A.C., Karlsson, M.P., Nathe, A.R., Carr, M.F. and Frank, L.M. (2010). Experience-dependent development of coordinated hippocampal spatial activity representing the similarity of related locations. *Journal of Neuroscience*, 30(35): 11586-11604.

Singer, R.A., Abroms, B.D. and Zentall, T.R. (2006). Formation of a simple cognitive map by rats. *International Journal of Comparative Psychology*, 19: 417-425.

Skaggs, W.E., Knierim, J.J., Kudrimoti, H.S. and McNaughton, B.L. (1995). A model of the neural basis of the rat's sense of direction. *Advances in Neural information Processing Systems*, 7: 173-180.

Skaggs, W.E. and McNaughton, B.L. (1998). Spatial firing properties of hippocampal CA1 populations in an environment containing two visually identical regions. *Journal of Neuroscience*, 18(20): 8455-8466.

Smith, A.E., Cheek, O.A., Sweet, E.L.C., Dudchenko, P.A. and Wood, E.R. (2019). Lesions of the head direction cell system impair direction discrimination. *Behavioral Neuroscience*, 133(6): 602-613.

Smith, D.M. and Bulkin, D.A. (2014). The form and function of hippocampal context representations. *Neuroscience and Biobehavioral Reviews*, 40: 52-61.

Solstad, T., Boccara, C.N., Kropff, E., Moser, M.B. and Moser, E.I. (2008). Representation of geometric borders in the entorhinal cortex. *Science*, 322(5909): 1865-1868.

Solstad, T., Moser, E.I. and Einevoll, G.T. (2006). From grid cells to place cells: A mathematical model. *Hippocampus*, 16: 1026-1031.

Song, P. and Wang, X.J. (2005). Angular path integration by moving 'hill of activity': A spiking neuron model without recurrent excitation of the head-direction system. *Journal of Neuroscience*, 25(4): 1002-1004.

Spiers, H.J., Hayman, R.M.A., Jovalekic, A., Marozzi, E. and Jeffery, K.J. (2015). Place field repetition and purely local remapping in a multicompartment environment. *Cerebral Cortex*, 25: 10-25.

Sripanidkulchai, K. and Wyss, J.M. (1986). Thalamic projections to retrosplenial cortex in the rat. *Journal of Comparative Neurology*, 254: 143-165.

Stackman, R.W., Clark, A.S. and Taube, J.S. (2002). Hippocampal spatial representations require vestibular input. *Hippocampus*, 12: 291-303.

Stackman, R.W., Golob, E.J., Bassett, J.P. and Taube, J.S. (2003). Passive transport disrupts directional path integration by rat head direction cells. *Journal of Neurophysiology*, 90: 2862-2874.

Stackman, R.W. and Taube, J.S. (1997). Firing properties of head direction cells in the rat anterior thalamic nucleus: Dependence on vestibular input. *Journal of Neuroscience*, 17(11): 4349-4358.

Stackman, R.W. and Taube, J.S. (1998). Firing properties of rat lateral mammillary single units: Head direction, head pitch, and angular head velocity. *Journal of Neuroscience*, 18(21): 9020-9037.

Stensola, H., Stensola, T., Solstad, T., Frøland, K., Moser, M.B. and Moser, E.I. (2012). The entorhinal grid map is discretized. *Nature*, 492: 72-78.

Stewart, S., Jeewajee, A., Wills, T.J., Burgess, N. and Lever, C. (2014). Boundary coding in the rat subiculum. *Philosophical Transactions of the Royal Society of London. Series B, Biological Sciences*, 369: 20120514.

Sun, Y., Jin, S., Lin, X., Chen, L., Qiao, X., Jiang, L., Zhou, P., Johnston, K.G., Golshani, P., Nie, Q., Holmes, T.C., Nitz, D.A. and Xu, X. (2019). CA1- projecting subiculum neurons facilitate object-place learning. *Nature Neuroscience*, 22: 1857-1870.

Sun, Y., Nguyen, A.Q., Nguyen, J.P., Le, L., Saur, D., Choi, J., Callaway, E.M. and Xu, X. (2014). Cell-type-specific circuit connectivity of hippocampal CA1 revealed through Cre-dependent rabies tracing. *Cell Reports*, 7(1): 269-280.

Sun, Y., Nitz, D.A., Holmes, T.C. and Xu, X. (2018). Opposing and complementary topographic connectivity gradients revealed by quantitative analysis of canonical and noncanonical hippocampal CA1 inputs. *eNeuro*, 5(1): e0322-17.2018.

Sutherland, R.J., Whishaw, I.Q. and Kolb, B. (1988). Contributions of cingulate cortex to two forms of spatial learning and memory. *Journal of Neuroscience*, 8(6): 1863-1872.

Tanila, H. (1999). Hippocampal place cells can develop distinct representations of two visually identical environments. *Hippocampus*, 9: 235-246.

Tanila, H., Shapiro, M.L. and Eichenbaum, H. (1997). Discordance of spatial representation in ensembles of hippocampal place cells. *Hippocampus*, 7: 613-623.

Taube, J.S. (1995). Head direction cells recorded in the anterior thalamic nuclei of freely moving rats. *Journal of Neuroscience*, 15(1): 70-86.

Taube, J.S. (2007). The head direction signal: Origins and sensory-motor integration. *Annual Review of Neuroscience*, 30: 181-207.

Taube, J.S. and Burton, H.L. (1995). Head direction cell activity monitored in a novel environment and during a cue conflict situation. *Journal of Neurophysiology*, 74(5): 1953-1971.

Taube, J.S. and Muller, R.U. (1998). Comparisons of head direction cell activity in the postsubiculum and anterior thalamus of freely moving rats. *Hippocampus*, 8:87-108.

Taube, J.S., Muller, R.U. and Ranck Jr, J.B. (1990a). Head-direction cells recorded from the postsubiculum in freely moving rats. I. Description and quantitative analysis. *Journal of Neuroscience*, 10(2): 420-435.

Taube, J.S., Muller, R.U. and Ranck Jr, J.B. (1990b). Head-direction cells recorded from the postsubiculum in freely moving rats. II. Effects of environmental manipulations. *Journal of Neuroscience*, 10(2): 420-435.

Temido-Ferreira, M., Coelho, J.E., Pousinha, P.A. and Lopes, L.V. (2019). Novel players in the aging synapse: Impact on cognition. *Journal of Caffeine and Adenosine Research*, 9(3): 104-127.

Thompson, L.T. and Best, P.J. (1990). Long-term stability of the place-field activity of single units recorded from the dorsal hippocampus of freely behaving rats. *Brain Research*, 509(2): 299-308.

Thorndike, E.L. (1898). Animal intelligence: An experimental study of the associative processes in animals. *Psychological Review: Monograph Supplements*, 2(4): i-109.

Toates, F. (1998). The interaction of cognitive and stimulus-response processes in the control of behaviour. *Neuroscience and Biobehavioral Reviews*, 22(1): 59-83.

Tolias, A.S., Ecker, A.S., Siapas, A.G., Hoenselaar, A., Keliris, G.A. and Logothetis, N.K. (2007). Recording chronically from the same neurons in awake, behaving primates. *Journal of Neurophysiology*, 98(6): 3780-3790.

Tolman, E.C. (1948). Cognitive maps in rats and men. *Psychological Review*, 55(4): 189-208.

Tolman, E.C., Ritchie, B.F. and Kalish, D. (1946). Studies in spatial learning. I. Orientation and the short-cut. *Journal of Experimental Psychology*, 36:13-24.

Tsao, A., Moser, M.B. and Moser, E.I. (2013). Traces of experience in the lateral entorhinal cortex. *Current Biology*, 23: 399-405.

van Buren, J.M. and Borke, R.C. (1972). Variations and connections of the human thalamus. Springer-Verlag Berlin Heidelberg.

van Cauter, T., Poucet, B. and Save, E. (2008). Unstable CA1 place cell representation in rats with entorhinal cortex lesions. *European Journal of Neuroscience*, 27: 1933-1946.

van der Kooy, D. and Carter, D.A. (1981). The organization of the efferent projections and striatal afferents of the entopeduncular nucleus and adjacent areas in the rat. *Brain Research*, 211: 15-36.

van Groen, T. and Wyss, J.M. (1990a). Connections of the retrosplenial granular a cortex in the rat. *Journal of Comparative Neurology*, 300: 593-606.

van Groen, T. and Wyss, J.M. (1990b). The postsubicular cortex in the rat: Characterization of the fourth region of the subicular cortex and its connections. *Brain Research*, 529: 165-177.

van Groen, T. and Wyss, J.M. (1990c). Extrinsic projections from area CA1 of the rat hippocampus: Olfactory, cortical, subcortical, and bilateral hippocampal formation projections. *Journal of Comparative Neurology*, 302: 512-528.

van Groen, T. and Wyss, J.M. (1992). Connections of the retrosplenial dysgranular cortex in the rat. *Journal of Comparative Neurology*, 315: 200-216.

van Groen, T. and Wyss, J.M. (1995). Projections from the anterodorsal and anteroventral nucleus of the thalamus to the limbic cortex in the rat. *Journal of Comparative Neurology*, 358: 584-604.

van Groen, T. and Wyss, J.M. (2003). Connections of the retrosplenial granular b cortex in the rat. *Journal of Comparative Neurology*, 463: 249-263.

van Strien, N.M., Cappaert, N.L.M. and Witter, M.P. (2009). The anatomy of memory: an interactive overview of the parahippocampal-hippocampal network. *Nature Reviews Neuroscience*, 10: 272-282.

Valerio, S. and Taube, J.S. (2016). Head direction cell activity is absent in mice without the horizontal semicircular canals. *Journal of Neuroscience*, 36(3): 741-754.

Vann, S.D. and Aggleton, J.P. (2002). Extensive cytotoxic lesions of the rat retrosplenial cortex reveal consistent deficits on tasks that tax allocentric spatial memory. *Behavioral Neuroscience*, 116(1): 85-94.

Vann, S.D. and Aggleton, J.P. (2005). Selective dysgranular retrosplenial cortex lesions in rats disrupt allocentric performance of the radial-arm maze task. *Behavioral Neuroscience*, 119(6): 1682-1686.

Vann, S.D. and Aggleton, J.P. (2004). Testing the importance of the retrosplenial guidance system: Effects of different sized retrosplenial cortex lesions on heading direction and spatial working memory. *Behavioural Brain Research*, 155: 97-108.

Vann, S.D., Aggleton, J.P. and Maguire, E.A. (2009). What does the retrosplenial cortex do? *Nature Reviews Neuroscience*, 10: 792-802.

Vann, S.D., Kristina Wilton, L.A., Muir, J.L. and Aggleton, J.P. (2003). Testing the importance of the caudal retrosplenial cortex for spatial memory in rats. *Behavioural Brain Research*, 140: 107-118.

Vogt, B.A. and Miller, M.W. (1983). Cortical connections between rat cingulate cortex and visual, motor, and postsubicular cortices. *Journal of Comparative Neurology*, 216: 192-210.

Vogt, B.A. and Peters, A. (1981). Form and distribution of neurons in rat cingulate cortex: Areas 32, 24, and 29. *Journal of Comparative Neurology*, 195: 603-625.

Wallace, M.L., Saunders, A., Huang, K.W., Philson, A.C., Goldman, M., Macosko, E.Z., McCarroll, S.A. and Sabatini, B.L. (2017). Genetically distinct parallel pathways in the entopeduncular nucleus for limbic and sensorimotor output of the basal ganglia. *Neuron*, 94(1): 138-152.

Wang, C., Chen, X., Lee, H., Deshmukh, S.S., Yoganarasimha, D., Savelli, F. and Knierim, J.J. (2018). Egocentric coding of external items in the lateral entorhinal cortex. *Science*, 362: 945-949.

Wesierska, M., Adamska, I. and Malinowska, M. (2009). Retrosplenial cortex lesion affected segregation of spatial information in place avoidance task in the rat. *Neurobiology of Learning and Memory*, 91: 41-49.

Whishaw, I.Q., Masswinkel, H., Gonzalez, C.L.R. and Kolb. (2001). Deficits in allothetic and idiothetic spatial behaviour in rats with posterior cingulate cortex lesions. *Behavioural Brain Research*, 118: 67-76.

Whitlock, J.R. and Derdikman, D. (2012). Head direction maps remain stable despite grid map fragmentation. *Frontiers in Neural Circuits*, 6(9): 1-10.

Wills, T.J., Lever, C., Cacucci, F., Burgess, N. and O'Keefe, J. (2005). Attractor dynamics in the hippocampal representation of the local environment. *Science*, 308(5723): 873-876.

Wilson, D.I.G., Langston, R.F., Schlesiger, M.I., Wagner, M., Watanabe, S. and Ainge, J.A. (2013). Lateral entorhinal cortex is critical for novel object-context recognition. *Hippocampus*, 23: 352-366.

Winter, S.S., Clark, B.J. and Taube, J.S. (2015). Disruption of the head direction cell network impairs the parahippocampal grid cell signal. *Science*, 347(6224): 870-874.

Wirtshafter, D. and Stratford, T.R. (1993). Evidence for GABAergic projections from the tegmental nuclei of Gudden to the mammillary body in the rat. *Brain Research*, 630: 188-194.

Witter, M.P., Canto, C.B., Couey, J.J., Koganezawa, N. and O'Reilly, K.C. (2014). Architecture of spatial circuits in the hippocampal region. *Philosophical Transactions of the Royal Society of London. Series B. Biological Sciences*, 369(1635): 20120515.

Wright, N.F., Erichsen, J.T., Vann, S.D., O'Mara, S.M. and Aggleton, J.P. (2010). Parallel but separate inputs from limbic cortices to the mammillary bodies and anterior thalamic nuclei in the rat. *Journal of Comparative Neurology*, 518: 2334-2354.

Xu, W. and Wilson, D.A. (2012). Odor-evoked activity in the mouse lateral entorhinal cortex. *Neuroscience*, 223: 12-20.

Yamawaki, N., Corcoran, K.A., Guedea, A.L., Shepherd, G.M.G. and Radulovic, J. (2019). Differential contributions of glutamatergic hippocampal → retrosplenial cortical projections to the formation and persistence of context memories. *Cerebral Cortex*, 29: 2728-2736.

Yamawaki, N., Li, X., Lambot, L., Ren, L.Y., Radulovic, J. and Shepherd, G.M.G. (2019). Long-range inhibitory intersection of a retrosplenial thalamocortical circuit by apical tuft-targeting CA1 neurons. *Nature Neuroscience*, 22: 618-626.

Yao, F., Zhang, E., Gao, Z., Ji, H., Marmouri, M. and Xia, X (2018). Did you choose appropriate tracer for retrograde tracing of retinal ganglion cells? The differences between cholera toxin subunit B and Fluorogold. *PloS ONE*, 13(10): e0205133.

Yoder, R.M., Peck, J.R. and Taube, J.S. (2015). Visual landmark information gains control of the head direction signal at the lateral mammillary nuclei. *Journal of Neuroscience*, 35(4): 1354-1367.

Yoder, R.M. and Taube, J.S. (2011). Projections to the anterodorsal thalamus and lateral mammillary nuclei arise from different cell populations within the postsubiculum: Implications for the control of head direction cells. *Hippocampus*, 21: 1062-1073.

Yoganarasimha, D., Rao, G. and Knierim, J.J. (2011). Lateral entorhinal neurons are not spatially selective in cue-rich environments. *Hippocampus*, 21: 1363-1374.

Yoganarasimha, D., Yu, X. and Knierim, J.J. (2006). Head direction cell representations maintain internal coherence during conflicting proximal and distal cue rotations: comparison with hippocampal place cells. *Journal of Neuroscience*, 26(2): 622-631.

Young, B.J., Otto, T., Fox, G.D. and Eichenbaum, H. (1997). Memory representation within the parahippocampal region. *Journal of Neuroscience*, 17(13): 5183-5195.

Zhang, K. (1995). Representation of spatial orientation by the intrinsic dynamics of the head-direction cell ensemble: A theory. *Journal of Neuroscience*, 16(6): 2112-2126.

Zhou, N., Maire, P.S., Masterson, S.P. and Bickford, M.E. (2017). The mouse pulvinar nucleus: organization of the tectorecipient zones. *Visual Neuroscience*, 34: E011.

Zhuang, J., Ng, L., Williams, D., Valley, M., Li, Y., Garrett, M. and Waters, J. (2017). An extended retinotopic map of mouse cortex. *eLife*, 6:e18372.

Ziv, Y., Burns, L.D., Cocker, E.D., Hamel, E.O., Ghosh, K.K., Kitch, A.J. Gamal, A.E. and Schnitzer, M.J. (2013). Long-term dynamics of CA1 hippocampal place codes. *Nature Neuroscience*, 16(3): 264-266.

Zugaro, M.B., Berthoz, A. and Wiener, S.I. (2001). Background, but not foreground, spatial cues are taken as references for head direction responses by rat anterodorsal thalamus neurons. *Journal of Neuroscience*, 21: RC154.

Zugaro, M.B., Tabuchi, E., Fouquier, C., Berthoz, A. and Wiener, S.I. (2001). Active locomotion increases peak firing rates of anterodorsal thalamic head direction cells. *Journal of Neurophysiology*, 86: 692-702.